ZooKeys 1138: 1–27 (2023)
doi: 10.3897/zookeys.1138.95968
https://zookeys.pensoft.net

RESEARCH ARTICLE

A peer-reviewed open-access journal
ZooKeys
Launched to accelerate biodiversity research

Taxonomic revision of the genus *Phylacastus* Fairmaire (Tenebrionidae, Eurynotina): shortfalls of anatomical nomenclature with notes on aedeagal homology

Ryan Lumen[1], Marcin Jan Kamiński[1,2]

1 *Zoological Museum, Museum and Institute of Zoology, Polish Academy of Sciences, Warsaw, Poland*
2 *Department of Entomology, Purdue University, West Lafayette, Indiana, USA*

Corresponding author: Ryan Lumen (rplumen@gmail.com)

Academic editor: Patrice Bouchard | Received 4 October 2022 | Accepted 29 November 2022 | Published 5 January 2023

https://zoobank.org/94AF8515-FC53-4C7E-B08A-646F2D64355F

Citation: Lumen R, Kamiński MJ (2023) Taxonomic revision of the genus *Phylacastus* Fairmaire (Tenebrionidae, Eurynotina): shortfalls of anatomical nomenclature with notes on aedeagal homology. ZooKeys 1138: 1–27. https://doi.org/10.3897/zookeys.1138.95968

Abstract
The genus *Phylacastus* Fairmaire (Tenebrionidae, Blaptinae, Platynotini, Eurynotina) is revised. Two new species and one new synonymy are presented along with new diagnoses, descriptions, a distribution map, and key to species. The resulting species of *Phylacastus* are: *P. ancoralium* **sp. nov.**, *P. crypticoides* Koch (= *P. pretoriensis* Koch **syn. nov.**), *P. makskacymirowi* **sp. nov.**, *P. rhodesianus* Koch, and *P. striolatus* Fairmaire. Lectotypes are designated for the type species, *P. striolatus*, to fix the taxonomic status of the species and genus. As a result of examination and subsequent description of *P. ancoralium* **sp. nov.**, a brief review and treatment of aedeagal morphology is presented. The nomenclature ("clavae" versus "laciniae") and phylogenetic occurrence of accessory structures of the paramere-median lobe area within Blaptinae Leach and Adelinina LeConte (Diaperinae, Diaperini) are discussed. New descriptive terminology (i.e., ancora [singular] and ancorae [plural]) is proposed for these aedeagal structures in Blaptinae to clarify their function and resolve past ambiguities. The morphology within representatives of *Adelina* Dejean, *Alphitophagus* Stephens, *Gnatocerus* Thunberg, and *Sitophagus* Mulsant is also briefly contrasted and outlined.

Keywords
Amphidorini, clavae, Dendarini, laciniae, median lobe, parameres, Pedinini, South Africa

Introduction

Eurynotina Mulsant & Rey is a subtribe of darkling beetles from Southern Africa within the tribe Platynotini Mulsant & Rey and subfamily Blaptinae Leach (Koch 1954a; Bouchard et al. 2021; Kamiński et al. 2021a). Platynotini are distinguished via the presence of a stridulatory file on the gula (synapomorphy for the tribe; see Koch 1954a, b, 1956). Eurynotina are further diagnosable via their aedeagi, which lack additional "styles", "clavae", or "lacinia" (Antoine 1930; Koch 1954a, b; Lindroth and Palmen 1956) and have a strongly sclerotized medial lobe with reduced basal apophyses (Iwan 2001). Eurynotina has been supported as molecularly distinct by Kamiński et al. (2019, 2021a); however, the taxa included were not fully sufficient to test the monophyly of the group. This paper is the first of a series dedicated to revising subtribe Eurynotina as a part of the first author's Ph.D. dissertation.

Platynotini has received attention from many generations of entomologists (Fairmaire 1897; Gebien 1904, 1910; Reichardt 1936; Español 1945; Koch 1956, 1958; Kaszab 1975; Iwan 1995, 2002, 2006; Endrödy-Younga 2000; Kamiński and Raś 2011; Iwan and Kamiński 2012, 2014; Kamiński 2013, 2015a); however, most contributions concern the subtribe Platynotina Mulsant & Rey. Only a handful of papers concern Eurynotina (Koch 1954a, b, 1955, 1956; Kamiński 2016). For example, *Phylacastus* was erected in Opatrini Brullé by Fairmaire (1897) with a single new species (*P. striolatus* Fairmaire) and remained unstudied for nearly 60 years. In 1954a, Koch described three additional species and assigned the genus to his recently installed subtribe Oncotina Koch, now interpreted as a synonym of Eurynotina (see Kamiński 2016). He hypothesized a relationship between *Phylacastus* and *Eurynotus* Kirby through the following characters: horizontally produced prosternal apophysis, median emargination of epistoma, sharp and rectangular posterior angles of pronotum, and closely jointed prothorax and mesothorax. Prior to the study presented here, the only count of *Phylacastus* specimens was provided by Koch's (1954a) work (34 specimens, 25 of which belonged to one of his new species *P. pretoriensis*, and two syntypes of *P. striolatus*).

After queries to several entomological collections (see list in Materials and Methods) we identified new specimens and species of the genus. These materials provided the opportunity to test the taxonomic concepts of *Phylacastus* and its species. Furthermore, as one of the newly discovered species challenges Koch's (1954a, b) subtribal definition of Eurynotina, male terminalia morphology within subfamily Blaptinae is discussed based on dissected specimens, alongside previous literature (e.g. Koch 1956; Iwan 2001, 2004). Consequently, new terminology is proposed in light of previous application of the terms "clavae" and "laciniae" in the context of their meaning and priority within Blaptinae. They are also briefly contrasted with representatives of Diaperinae Latreille to better describe function, homology, and resolve some ambiguities.

Materials and methods

Revision of genus *Phylacastus*

Pinned material for morphological examination of *Phylacastus* and other taxa was borrowed from the following institutional insect collections: **MNHN** – Muséum national d'Histoire naturelle; Paris, France; and **TMNH** – Ditsong National Museum of Natural History; Pretoria, South Africa. Additional comparative material for redefining the genus and investigating aedeagal morphology was obtained from: **MIIZPAN** – Muzeum i Instytut Zoologii, Polska Akademia Nauk; Warsaw, Poland; **SANC** – South African National Collection of Insects; Pretoria, South Africa. While specimens of Eurynotina are relatively uncommon, the holdings of the aforementioned collections are the most comprehensive for the subtribe, accounting for both the majority of type material, and additional specimens for examination. As a result of specimen loans and contact with collections presented here, all 16 genera and over 90% of the species of Eurynotina are represented by type material and photographs for reference for this project and continued revision of the subtribe.

Original label data for specimens are given in quotation marks and separated by a comma. Morphological terminology follows that of Matthews at al. (2010), with additional specialized terms used for the female terminalia following Kamiński et al. (2022). Dissections were performed following methodology illustrated by Kamiński (2021); specimens were soaked in 10% KOH solution for dissection of genitalia before staining with chlorazol black. Images were taken using a Canon 1000D body with extension rings and a Canon EF 100 mm macro lens, a Nikon D3500 body with adapter for a Nikon SMZ800N microscope, and with a Hitachi S-3400N SEM in MIZ PAS. A species distribution map was produced using QGIS v. 3.16, with vector layers downloaded from the Natural Earth web page (www.naturalearthdata.com). Photographs as well as distribution map figures were edited in Photoshop v. 23.5.1. A table of all localities is presented in Appendix 1.

Male terminalia analysis

Revelation of new structures on the aedeagus of *Phylacastus ancoralium* sp. nov. necessitated a review of aedeagal morphology to confirm its affiliation. To this end, we performed a historical literature review, and assessed aedeagal terminology and morphology (Antoine 1930; Español 1945; Koch 1954a, b; Lindroth and Palmen 1956; Doyen and Tschinkel 1982; Doyen 1984; Iwan 2001, 2004; Kamiński 2014, 2015b). Taxon selection mainly focused on Blaptinae, as various subgroups have historically been defined by the presence or absence of additional structures of the parameres/median lobes (e.g. Platynotina and Eurynotina, Opatrini); however other groups of Tenebrionidae Latreille with structures described as "clavae", "lacinia", "struts", or "styles" were also sampled for morphological study and comparison. Taxa were also chosen for potential homology and concurrent terminology based on literature descriptions. Taxa selected were: Blaptinae: *Amatodes* Dejean (Pedinini: Helopinina), *Anomalipus* Guérin-Méneville (Platynotini: Platynotina), *Eleodes* Eschscholtz (Amphidorini), *Heliopates* Dejean (Pedinini: Dendarina), *Trigonopus* Mulsant & Rey (Platynotini: Platynotina), and Diaperinae (Diaperini: Adelinina): *Adelina* Dejean, *Alphitophagus* Stephens, *Gnatocerus* Thunberg, and *Sitophagus* Mulsant.

Taxonomy

Genus *Phylacastus* Fairmaire

Phylacastus Fairmaire, 1897: 116. Koch 1954a: 275; 1954b: 2; 1956: 27; Kamiński 2016: 245.

Type species. *Phylacastus striolatus* Fairmaire; by monotypy.

Diagnosis. Within Eurynotina, *Phylacastus* largely resembles *Eurynotus* and *Capidium* Koch. All three have relatively sharp basal pronotal angles, rather than broadly rounded as is the case in the rest of Eurynotina (Kamiński 2016: fig. 2). The only other exception is *Oncotus* Solier which, while some representatives have basal angles of the pronotum similarly shaped, is separable by prosternal process shape (rounded rather than angular in lateral view (Kamiński 2016), body shape (much rounder/transverse than *Phylacastus*), tibial morphology (foretibia greatly expanded apically and with a sharp lateral projection; Kamiński 2016), and coloration (species may be bicolored and/or very pale or testaceous in color). *Phylacastus* can be easily separated from all other subtribal representatives by the presence of (at most) weak tubercles on the apical declivity of the elytra (Figs 1, 2), the form of the prosternal process which is angular rather than rounded in lateral view (Kamiński 2016: fig. 2D), and the pronotum with basal angles present rather than absent/rounded) (Kamiński 2016: fig. 2J).

Eurynotus, the most closely affiliated genus according to Koch (1954a), can be separated from *Phylacastus* by body size (*Eurynotus* ~9–20 mm long and ~5–12 mm wide, versus *Phylacastus* 4–8 mm long and ~2.75–4 mm wide (Koch 1954a; Kamiński 2016); pronotal hind angles (*Eurynotus* prominently produced often rearward projecting; less prominent and not rearwardly projected in *Phylacastus*; Kamiński 2016), tibial morphology (*Eurynotus* with slender/narrow tibiae lacking coarse spines on ventral surface of foretibia; dorsoventrally flattened and apically expanded tibiae with coarse spines on the underside of the foretibia in *Phylacastus* (Kamiński 2016), elytral sculpturing (*Eurynotus* with coarse or well-defined tubercles in most species; while most species of *Phylacastus* lack well-defined tubercles (Kamiński 2016). Finally, *Eurynotus* lacks a subapical sulcus on abdominal ventrite V, which is present in all *Phylacastus* species (Fig. 3F, G).

Capidium can be separated from *Phylacastus* most reliably via the structure of the prosternal process and abdominal ventrite V (prosternal process rounded and not produced in *Capidium*, angular and produced in *Phylacastus* (Kamiński 2016), and subapical sulcus absent in *Capidium* (present in *Phylacastus*); additionally, although *Capidium* also is defined by angular basal angles of the pronotum (Kamiński 2016), the angles are usually more produced. Finally, the elytral sculpturing and tuberculation of representatives of *Capidium* (when present) are stronger than in *Phylacastus*.

Genus redescription. Length 4–8 mm. Shining to dull; colored tenebrous; reddish to dark brown/black. ***Head*:** epistoma with well-defined median notch. Transition between clypeus and frons gradual and smooth along lateral edge, or with slight depression. Coarsely punctate, punctures large and closely spaced, separated by ≤ 1 feature diameter. Mentum with enlarged, ventrally projecting middle portion parallel-sided to slightly narrowing apically with reduced/slightly hidden lateral wings. Gula with stridulatory file. Eye constricted in middle and reniform, with strong to weakly impressed sulcus situated around posterior perimeter of dorsal lobe. Antennae with 11 antennomeres, terminal members forming weak club. ***Prothorax*:** pronotum base straight, with basal angles roundly produced. Without lateral depression or flattening along margins. Hypomeron at most only finely sculptured and finely punctured, dull to shining. Prosternal process angulate in lateral view, weakly produced or rounded at apex, with clear sulcus running perimeter, projecting at most only weakly toward midcoxae. ***Pterothorax*:** scutellar shield small and transversely triangular. Elytra not costate, with or without shallow or weakly defined punctate striae. Intervals punctate, without microtubercles; weak to well-defined tubercles (when present) only on apical declivity. Interval X terminating before reaching elytra base. Epipleura without microtubercules, broad basally, narrowing apically. Apterous. ***Abdomen*:** punctate. Ventrite V with sulcus running parallel to apical perimeter. ***Legs*:** femora slightly curved and expanded toward apex. Tibiae dorsoventrally compressed. Meso- and metatibia slightly curved. Foretibia dilated triangularly toward apex with coarse spines underneath. ***Male terminalia*:** tegmen bipartite with or without ancorae (small ancorae present in one species); basal portion membranous ventrally; dorsally with small, triangular membranous field at base of apical portion. Parameres fused dorsally at base, apical opening (in dorsal view) small or broad (Fig. 4). In lateral view, parameres flattened toward apex, with or without slight curvature. ***Female terminalia*:** paraprocts nearly as long or slightly longer than coxites I–IV, coxite IV reflected dorsally with gonostyli present (Fig. 5); bursa copulatrix divided into two sections by median constriction (bilobate) or not (Fig. 6), with or without additional "accessory pouch" situated near to spermatheca and accessory glands.

Species included (5). *Phylacastus ancoralium* sp. nov., *P. crypticoides*, *P. makskacymirowi* sp. nov., *P. rhodesianus*, *P. striolatus*.

Distribution. Southern Africa (Lesotho, South Africa, Zimbabwe) (Fig. 7).

Key to the species of the genus *Phylacastus*

1	Well-defined tubercles present on apical declivity of elytra (Fig. 2D) **2**
–	Well-defined tubercles absent on apical declivity of elytra (Fig. 2B) **3**
2	Male parameres widely spaced with large dorsal opening exposing median lobe (Fig. 4C); mentum parallel-sided and broad (Fig. 3C); elytral intervals densely punctate; generally larger (6–8 mm) .... ***P. rhodesianus* Fairmaire**
–	Male parameres not widely spaced, with small dorsal opening exposing at most only the tip of the median lobe (Fig. 4D); elytral intervals less densely punctate; mentum narrowing apically (Fig. 3B); generally smaller (4–6 mm) .... ***P. makskacymirowi* sp. nov.**
3	Aedeagus with ancorae (Fig. 4G); Ratio of ovipositor coxites I–IV to paraprocts nearly 1:1 (Fig. 5); elytra with at most weakly impressed striae on elytral disc, absent stria on apical declivity (Figs 2A, B) .... ***P. ancoralium* sp. nov.**
–	Aedeagus lacking ancorae (Fig. 4); Ratio of ovipositor coxites I–IV to paraprocts distinctly < 1:1 (Fig. 5); more clearly impressed elytral striae (Figs 2E, F) **4**
4	Mentum with narrow carina/keel running up median (Fig. 3A); 5th abdominal sulcus narrowly separated from apex (Fig. 3F) .... ***P. crypticoides* Koch**
–	Mentum lacking narrow carina/keel running up median; 5th abdominal sulcus widely separated from apex (Fig. 3G) .... ***P. striolatus* Fairmaire**

***Phylacastus ancoralium* sp. nov.**

https://zoobank.org/FDB06FBF-4FCA-4888-B36A-9E9724BDA235

Figs 1A, 2A, B, 3F, 4B, G, 5, 6C

Material examined (data represents single specimens unless otherwise noted). ***Holotype*** (TMNH): "S.Afr.;E. Lesotho Hodson's Peak 300 m 29.37°S, 29.17°E; 11.3.1976;E-Y:1069 fr.und.stones, 3150 m leg. Endrödy-Younga." With an additional label on red paper: "Holotype: *Phylacastus ancoralium* Lumen & Kaminski".

Paratypes (*n* = 11) (TMNH and MIIZPAN): Two specimens with same data as Holotype (MIIZPAN). "S.Afr.Basutoland Makheke Mnts 15 miles ENE Mokhotlong. 8.IV.51 No. 268;Swedish South Africa Expedition 1950–1951; red label." (MIIZPAN), "S.Afr., Lesotho Drakensbg,Black Mt. 29.31°S, 29.12°E; 9.3.1976;E-Y:1060 from under stones leg. Endrödy-Younga.", "S.Afr.;E. Lesotho Hodson's Peak 300 m 29.37°S, 29.17°E; 11.3.1976;E-Y:1067 from under stones leg. Endrödy-Younga" (five specimens)., "S.Afr., E.Lesotho Sani Pass Valley 29.39°S, 29.12°E; 10.3.1976; E-Y:1066 from under stones leg. Endrödy-Younga" (two specimens).

Diagnosis. *Phylacastus ancoralium* is highly modified compared with its congeners. In addition to its wide geographic separation from other species (Lesotho), it can be separated from all other species of *Phylacastus* via the elytra (with extremely weak to absent elytral striae), prosternum (weakly produced between forecoxae, rather

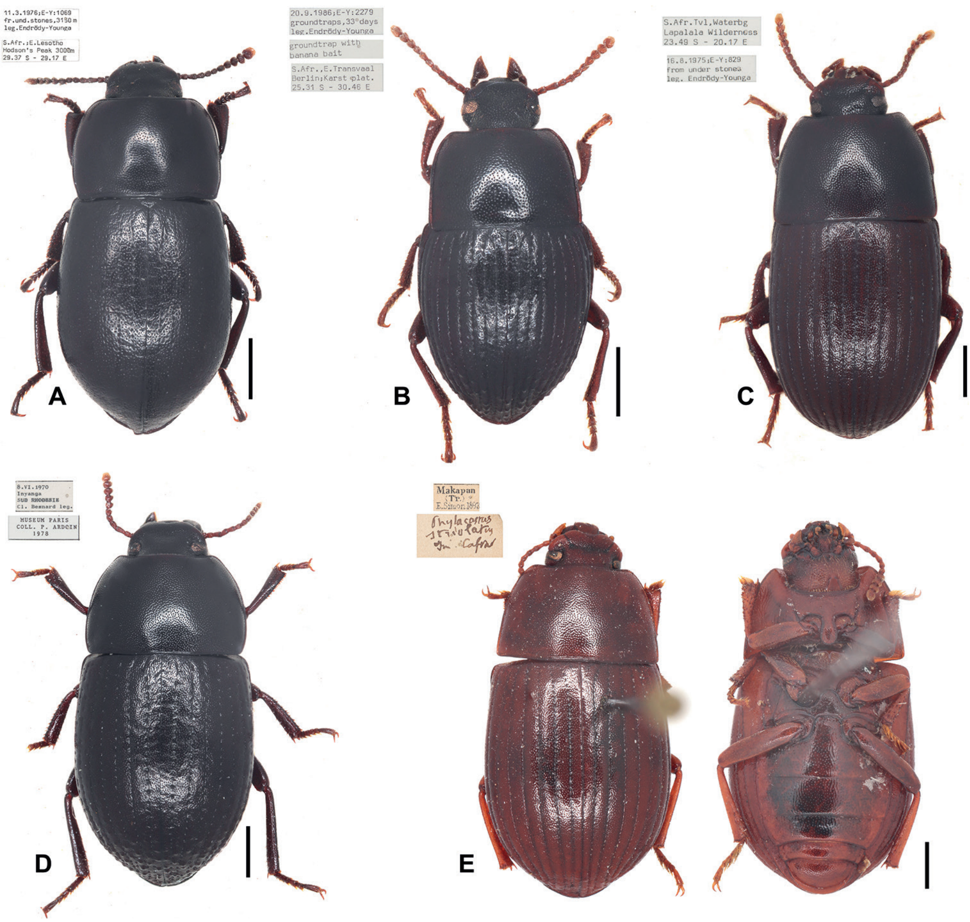

Figure 1. Dorsal habitus of *Phylacastus* species **A** *Phylacastus ancoralium* sp. nov. holotype **B** *Phylacastus makskacymirowi* sp. nov. **C** *Phylacastus crypticoides* **D** *Phylacastus rhodesianus* **E** *Phylacastus striolatus* lectotype. Scale bars: 1 mm.

than projecting more strongly beyond (Fig. 3E)), aedeagus with ancorae on the ventral surface of the parameres (Fig. 4G), and ovipositor relatively short compared to other species (ratio of ovipositor coxites I–IV to paraprocts nearly 1:1, rather than more distinctly < 1:1) (Fig. 5).

Etymology. This species is named for the ancorae of the male aedeagus, which in Blaptinae are hypothesized to anchor the male genitalia during copulation. To date, this is the only species within the subtribe Eurynotina with ancorae.

Description. Length 6–7 mm. ***Head*:** punctures separated by ~1 feature diameter. Mentum midportion slightly narrowing apically, exposing lateral wings, midportion without distinct median carina. ***Prothorax*:** pronotum finely punctate, punctures widely spaced, separated by > 1 feature diameter. Hypomeron lightly wrinkled and finely punctate. Prosternal process weakly produced between forecoxae. ***Pterothorax*:**

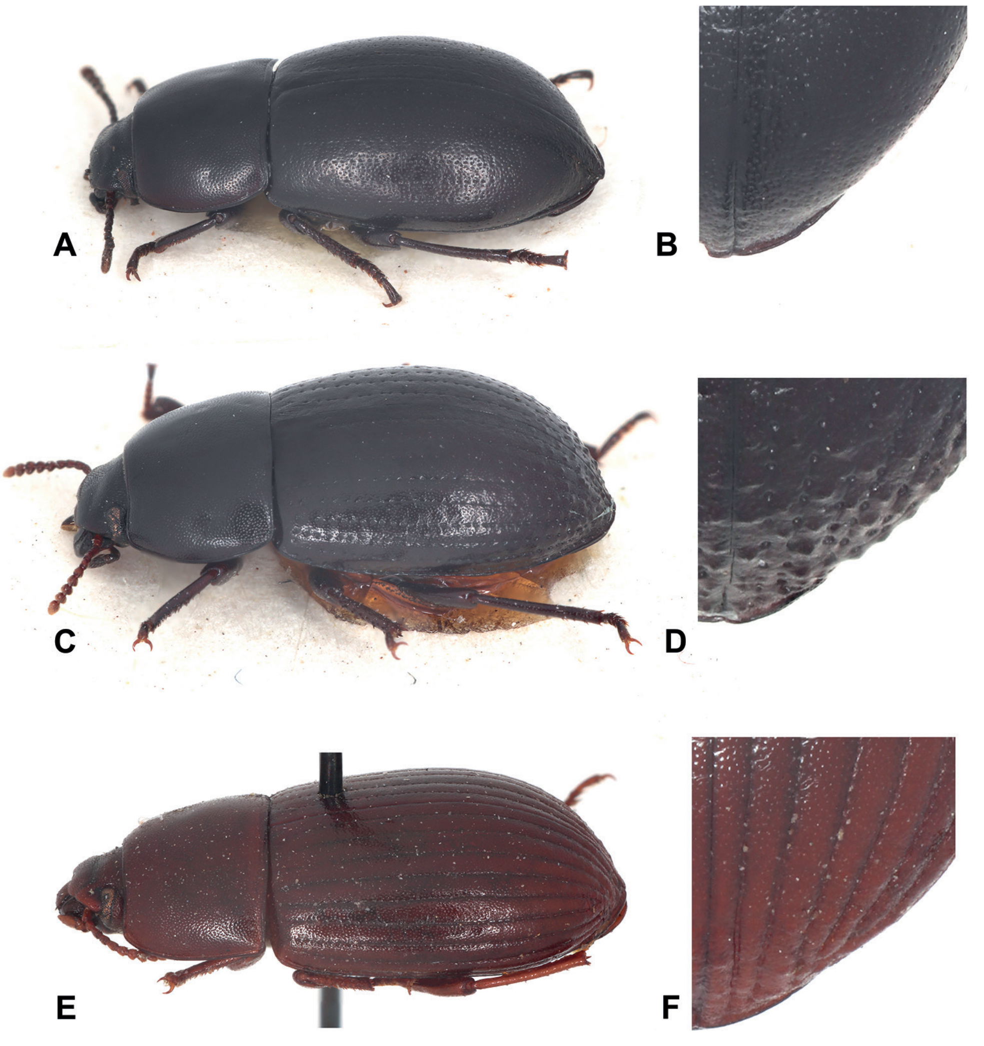

Figure 2. *Phylacastus* lateral aspect photographs and close-up of apical elytral tubercles and striae **A** *Phylacastus ancoralium* lateral angle **B** *P. ancoralium* close-up of elytra apical declivity **C** *P. rhodesianus* lateral angle **D** *P. rhodesianus* close-up of elytra apical declivity **E** *P. striolatus* lateral angle **F** *P. striolatus* close-up of elytra apical declivity.

elytra width about equal to pronotal width. Elytral striae and intervals punctate; striae very weakly impressed or absent. Interval punctures fine and widely spaced (>1 feature diameter), distinctly smaller than strial punctures. Elytral tubercles absent. ***Abdomen*:** ventrite V sulcus narrowly separated from apical border. ***Terminalia*:** male: parameres tapering apically, fused basally with narrow opening at apex exposing median lobe. Each paramere bearing a small, ventral medial ancora. Female: Ratio of ovipositor coxites I–IV to paraprocts nearly 1:1. Bursa copulatrix not bilobate, accessory gland present near-to spermatheca, accessory pouch present.

Distribution. Lesotho.

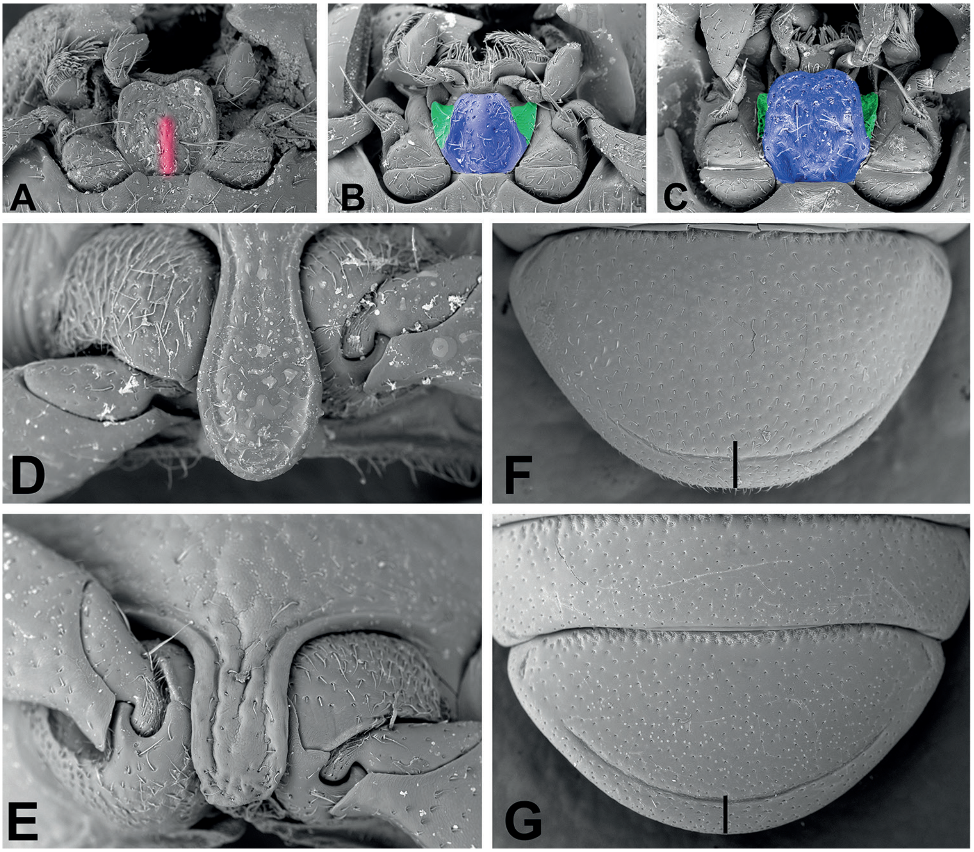

Figure 3. Diagnostic features of *Phylacastus* species **A–C** mentum (Median keel red, middle portion and lateral wings blue and green respectively) **D–E** prosternal process **F–G** abdominal ventrite V **A, D, F** *Phylacastus crypticoides* **B** *P. makskacymirowi* **C** *P. rhodesianus* **E** *P. ancoralium* **G** *P. striolatus*. Scale bars: 0.1 mm

Phylacastus crypticoides **Koch**
Figs 1C, 3A, D, F, 4E, 5, 6B, 8B

Phylacastus crypticoides Koch, 1954a: 286. Kamiński 2016: 245.
= *Phylacastus pretoriensis* Koch, 1954a: 285, syn. nov. Kamiński 2016: 245.

Material examined (data represents single specimens unless otherwise noted). ***Holotype*** (TMNH): "Lydenburg Distr. 1896 P.A. Krantz; Phylacastus crypticoides DET.C.KOCH 1953; Holotype No: 1873 Phylacastus crypticoides KOCH; crypticoides Koch; Eurynotus? sp.."

Additional material examined (TMNH). "S.Afr.,N.Transvaal Nylsvley Met.Sta. 24.40°S, 28.42°E; 285.1975; E-Y:1160 humus, Berlese, open leg. Endrödy-Younga.", "S.Afr.,N.Transvaal Nylsvley, Smith frm 24.40°S, 24.42°E 15.11.1975; E-Y: 952 cattle dung leg. Endrödy-Younga; trench; rep: 5 cage mesh 9 mm 7 day aft.sett."*, "S.Afr.,N.Transvaal Nylsvley Met.Sta. 24.40°S, 28.42°E; 29.3.1976; E-Y:1112 sifted

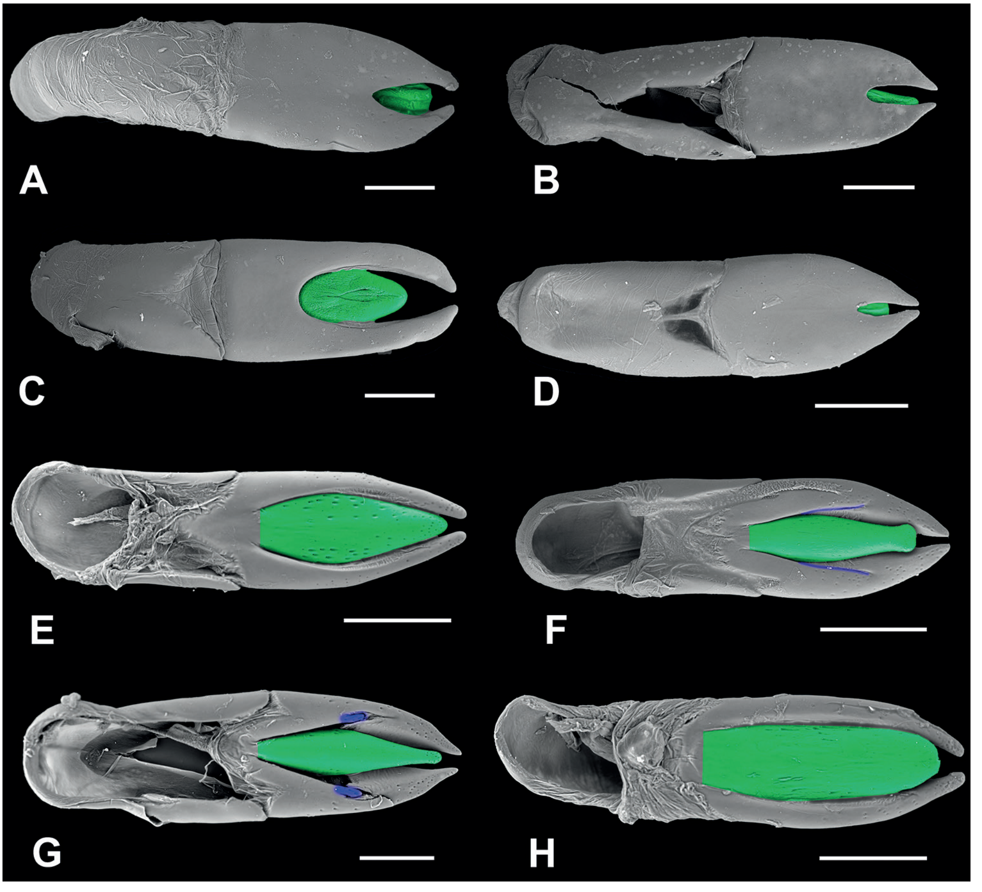

Figure 4. *Phylacastus speciesspp.* aedeagi **A–D** aedeagus dorsal view **E, F** aedeagus Ventral view **A, H** *Phylacastus striolatus* **B, G** *P. ancoralium* (ancorae highlighted blue) **C** *P. rhodesianus* **E** *P. crypticoides* **D, F** *P. makskacymirowi* (subapical sutures highlighted blue). Median lobes highlighted green. Scale bars: 0.2 mm.

litter, open leg. Endrödy-Younga.", "S.Afr.;Limpopo Prov. Lindani Nat Res 1336 m 24.02°S, 28.23°E; 8.12.2005; E-Y:3687 single, bushveld leg.Gusmann, Müller.", "S.Afr.,N.Transvaal Nylsvley, Smith frm 24.40°S, 24.42°E 8.1.1976; E-Y: 990 sifted litter. Endrödy-Younga"*, "S.Afr.Tvl.Waterbg Lapalala Wilderness 23.49°S, 20.17°E; 16.8.1975; E-Y:829 from under stones leg. Endrödy-Younga" (seven specimens)[1].

Notes. Koch described both *Phylacastus crypticoides* and *P. pretoriensis* (1954a), differentiating them from the already described *P. striolatus* and his additional species *P. rhodesianus* based on the following: *P. pretoriensis* with a basal pronotal margin that

1 Some collecting events are likely erroneous in their coordinates (24.40°S, 24.42°E and 23.49°S, 20.17°E). These localities should be represented in northeastern South Africa (circa 24.40°S, 28.42°E); however, the coordinates as written on the labels refer to far-off localities in Botswana. As such, while the labels are recorded here, these points are omitted from the species' range map.

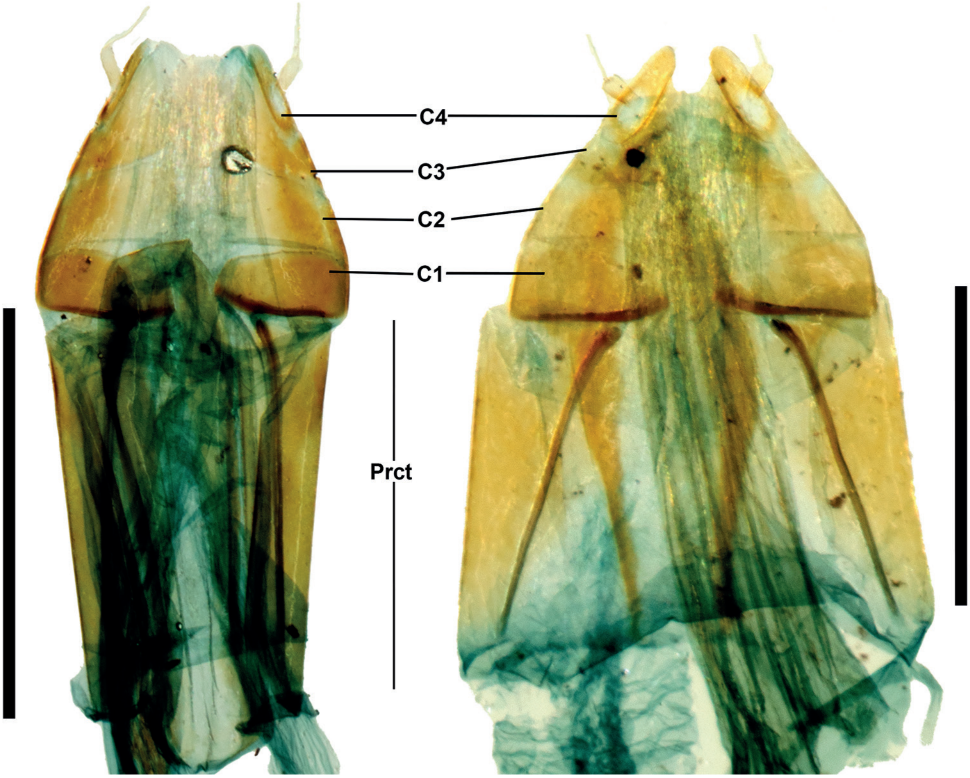

Figure 5. *Phylacastus* ovipositor (dorsal). **Right** *Phylacastus ancoralium* **Left** *P. crypticoides*. Abbreviations: C – Coxae (1–4); Prct – Paraprocts. Scale bars: 1 mm.

is reduced medially, and *P. crypticoides* with a cariniform structure of the mentum and a more apically positioned sulcus on abdominal ventrite V. Upon investigation here, the margination of the pronotal base, while variable, appears to be consistently present in all species with no uniform reduction in restricted populations or collection events examined here. The sulcus of abdominal ventrite V is also consistent between specimens of both of Koch's species. Furthermore, *P. crypticoides* and *P. pretoriensis* specimens compared with his type material bear the carina attributed to *P. crypticoides*. As such, we have decided here to synonymize the two species under *P. crypticoides*.

Redescription. Length 6–7 mm. ***Head*:** punctures separated by < 1 diameter. Mentum broad, lateral wings concealed, midportion with thin, distinct medial carina. ***Prothorax*:** pronotum punctate, punctures closely spaced, separated by ≤ 1 diameter. Hypomeron lightly wrinkled to rugose. Prosternal process produced between forecoxae (Fig. 3D). ***Pterothorax*:** elytra width about equal to pronotal width. Elytral striae, intervals punctate; striae clearly impressed. Interval punctures closely spaced (≤1 diameter), slightly smaller than strial punctures. Elytral tubercles absent; apical declivity with at most weak bumps or callosities (Figs 1C, 2E, F). ***Abdomen*:** ventrite V sulcus narrowly separated from apical border. ***Terminalia*:** male: parameres tapering apically,

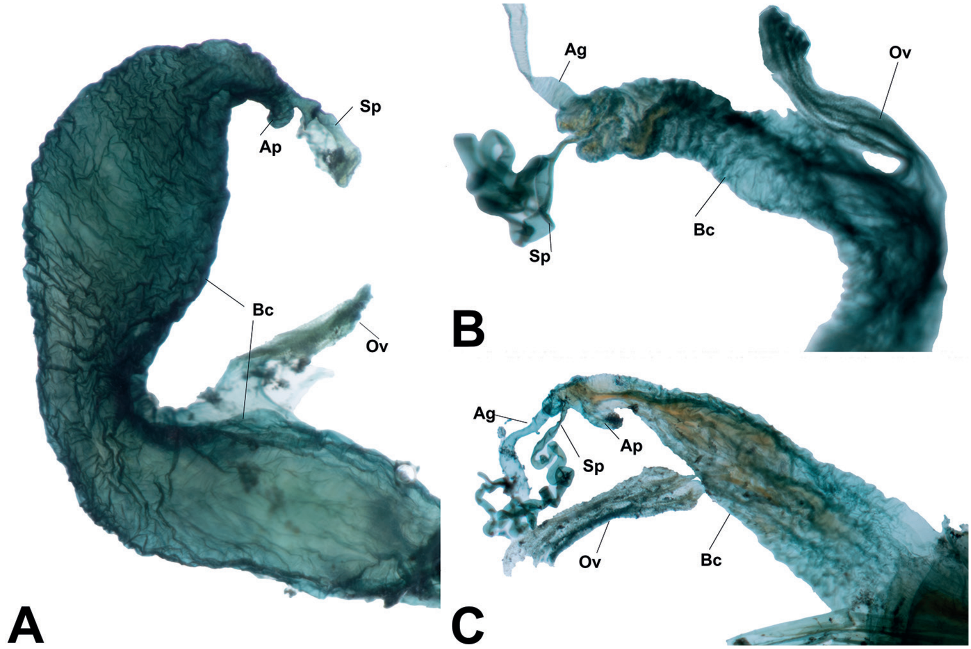

Figure 6. *Phylacastus* internal female structures **A** *Phylacastus striolatus* **B** *P. crypticoides* **C** *P. ancoralium*. Abbreviations: Ag - Accessory gland, Ap - Accessory pouch, Bc - Bursa copulatrix, Ov - Oviduct, *Sp* - Spermatheca.

fused basally with narrow opening at apex exposing median lobe. Female: ovipositor slightly elongate (ratio of ovipositor coxites I–IV to paraprocts < 1:1). Bursa copulatrix not bilobate, accessory gland present near-to spermatheca, accessory pouch absent.

Distribution. South Africa.

Phylacastus makskacymirowi **sp. nov.**

https://zoobank.org/D45D3B72-5E44-451F-96B1-35D28A05E555

Figs 1B, 3B, 4D, F

Material examined (data represents single specimens unless otherwise noted). ***Holotype*** (TMNH): "S.Afr.,E.Transvaal Berlin;Karst plat. 25.31°S, 30.46°E; 20.9.1986; E-Y:2279 groundtraps, 33 days leg. Endrödy-Younga; ground trap with meat bait." With an additional label on red paper: "Holotype: *Phylacastus makskacymirowi* Lumen & Kaminski"

Paratypes (*n* = 11) (TMNH and MIIZPAN): Three additional specimens with same data as holotype (MIIZPAN). "S.Afr.,E.Transvaal Berlin;Karst plat. 25.31°S, 30.46°E; 23.10.1986; E-Y:2001 groundtraps, 42 days leg. Endrödy-Younga; ground trap with meat bait.", "S.Afr.,E.Transvaal Berlin;Karst plat. 25.31°S, 30.46°E; 4.2.1986 E-Y:2414 under fungous logs leg. Endrödy-Younga.", "S.Afr.; Mpumalanga

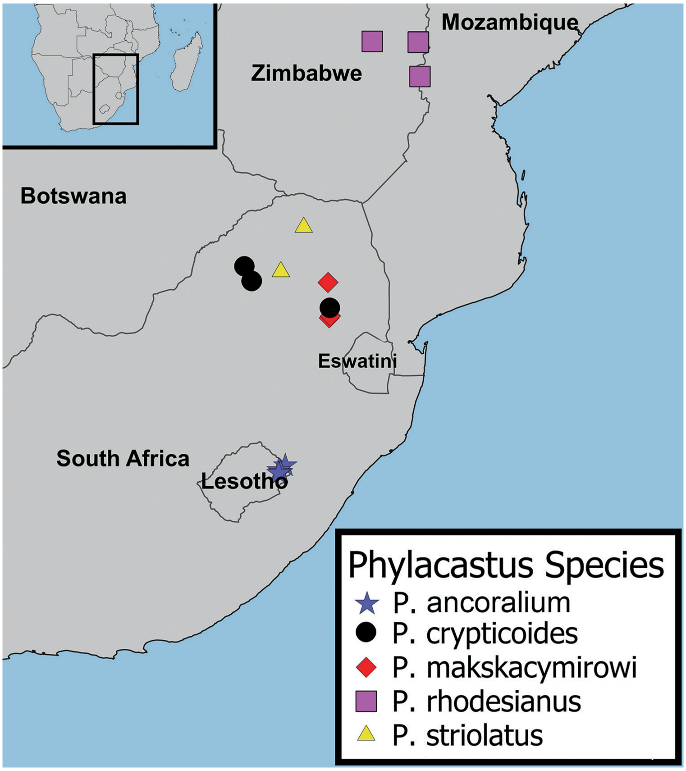

Figure 7. *Phylacastus* species distribution map. *P. ancoralium* (blue star), *Phylacastus crypticoides* (black circle), *P. makskacymirowi* (red diamond), *P. rhodesianus* (pink square), *P. striolatus* (yellow triangle).

10 km E Kaapsehoop 25.36°S, 30.43°E; 4–6.1.2014: E-Y:3943 sifting; indigenous forest leg. Ruth Müller.", "S.Afr.;Mpumalanga Sjonajona, Badplaas 24.44°S, 30.40°E; 11.11.2002; E-Y:3565 general collect. 1410 m leg. TMSA staff" (four specimens), "S.Afr.,E.Transvaal Berlin;Karst plat. 25.31°S, 30.46°E; 8.12.1986 E-Y:2363 fungous Pinus logs leg. Endrödy-Younga."

Diagnosis. As of this revision, this is the smallest species of the genus (4–6 mm). In addition to its size, this species is further defined by the presence of well-defined tubercles on the apical declivity of the elytra—a trait shared only by *P. rhodesianus*, which is larger and can be further differentiated by 1) punctures on elytral intervals (more numerous and dense in *P. rhodesianus*); 2) the shape of the mentum is broad, not tapered, further concealing the lateral wings in *P. rhodesianus* (Fig. 3C), tapers apically, exposing lateral wings in *P. makskacymirowi* (Fig. 3B); 3) aedeagus with a wide space between parameres, exposing large portion of median lobe in P. rhodesianus (Fig. 4C), narrow exposing only the tip of the median lobe in *P. makskacymirowi* (Fig. 4D).

Etymology. Named after young bug enthusiast Maksymilian Jan Kacymirow (born on December 17, 2014 in Warsaw, Poland).

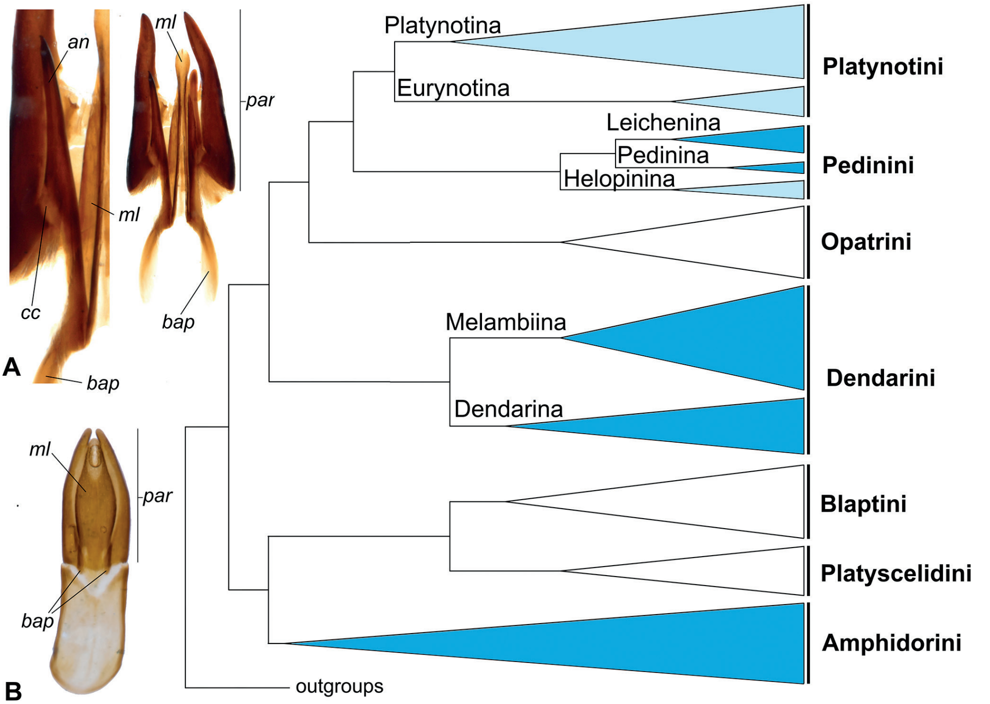

Figure 8. Distribution of *ancorae* in Blaptinae (displayed on Bayesian molecular topology from Kamiński et al. 2021a) **A** *Heliopates ibericus* Mulsant & Rey (Dendarina) apical aedeagus **B** *Phylacastus crypticoides* aedeagus. Dark blue clades = all representatives have ancorae. Light blue clades = exceptions (with or without ancorae). White clades = no ancorae. Abbreviations: an - ancora, bap - basal apophysis, cc - sclerotized connection to parameres, ml - median lobe, par - parameres.

Description. Length 4–6 mm. ***Head***: punctures separated by < 1 diameter. Mentum midportion medially raised but without distinct median carina, laterally tapering slightly toward apex, lateral wings exposed. ***Prothorax***: pronotum finely punctate, punctures smaller and widely spaced, separated by > 1 diameter. Hypomeron very finely punctate and lightly sculptured/wrinkled. Prosternal process produced between forecoxae. ***Pterothorax***: elytra wider than pronotal width. Elytral striae and intervals punctate; striae clearly impressed. Interval punctures fine, widely spaced (>1 diameter), distinctly smaller than strial punctures. Elytra distinctly tuberculate on apical declivity. ***Abdomen***: ventrite V sulcus narrowly separated from apical border. ***Terminalia***: male: parameres tapering apically, fused basally with narrow opening at apex exposing median lobe. Each paramere bearing a small, weak, subapical suture (Fig. 4F). Female: ovipositor slightly elongate (ratio of ovipositor coxites I–IV to paraprocts < 1:1). Bursa copulatrix not bilobate, accessory gland present near-to spermatheca, accessory pouch absent.

Distribution. South Africa.

Phylacastus rhodesianus **Koch**

Figs 1D, 2C, D, 3C, 4C

Phylacastus rhodesianus Koch, 1954a: 287. Kamiński 2016: 245.

Material examined (data represents single specimens unless otherwise noted). ***Holotype*** (TMNH): "Marandella Mashld XI.97 GKMarshall; Holotype No: 1877 Phylacastus rhodesianus KOCH; Phylacastus rhodesianus Koch DET.C.KOCH; rhodesianus Koch."

Additional material examined (MNHN). "9.VI.1970 Vumba SUD RHODESIE Cl. Besnard leg. 8.VI.1970 Inyanga SUD RHODESIE Cl. Besnard leg." (10 specimens).

Redescription. Length 6–8 mm. ***Head*:** punctures separated by ≤ 1 diameter. Mentum midportion broad, concealing lateral wings, midportion without distinct median carina. ***Prothorax*:** pronotum punctate, punctures closely spaced, separated by ~1 diameter. Hypomeron very lightly textured, without clear punctation. Prosternal process produced between forecoxae. ***Pterothorax*:** elytra width about equal to pronotal width. Elytral striae and intervals punctate; striae impressed. Interval punctures fine, closely spaced (~1 diameter), distinctly smaller than strial punctures. Elytral tubercles present on apical declivity. ***Abdomen*:** ventrite V sulcus narrowly separated from apical border. ***Terminalia*:** male: parameres converging apically, fused basally with deep and wide opening at apex exposing median lobe (Fig. 4C). Female: ovipositor slightly elongate (ratio of ovipositor coxites I–IV to paraprocts < 1:1). Bursa copulatrix bilobate, accessory gland present near-to spermatheca, accessory pouch absent.

Distribution. Zimbabwe.

Phylacastus striolatus **Fairmaire**

Figs 1E, 2E, F, 3G, 4A, H, 6A

Phylacastus striolatus Fairmaire, 1897: 117. Koch 1954a: 287; 1954b: 2; Kamiński 2016: 245.

Material examined (data represents single specimens unless otherwise noted). Lectotype (MNHN) here designated: "Makapan (TR.) E. Simon 1893; Phylacastus striolatus ? Cafrar?". With an additional label on red paper: "Lectotype: *Phylacastus striolatus* Fairmaire" Paralectotype (MNHN): single specimen with same data as lectotype.

Additional material examined (MIIZPAN). "Transvaal Soutpansberg Mphome Magd Knothe S" (two specimens).

Redescription. Length 8 mm. ***Head*:** punctures separated by < 1 diameter. Mentum midportion broad, concealing lateral wings, midportion without distinct median carina. ***Prothorax*:** pronotum punctate, punctures closely spaced, separated by ≤ 1 diameter. Hypomeron lightly wrinkled. Prosternal process produced between forecoxae. ***Pterothorax*:** elytra width slightly greater than pronotal width. Elytral striae and intervals punctate; striae impressed. Interval punctures closely spaced (~1 diameter), smaller than strial punctures. Elytral tubercles absent; apical declivity with at most weak bumps or callosities. ***Abdomen*:** ventrite V sulcus widely separated from apical border. ***Terminalia*:** male: parameres converging apically, fused basally with small opening at apex exposing median lobe. Female: ovipositor slightly elongate (ratio of ovipositor coxites I–IV to paraprocts < 1:1). Bursa copulatrix bilobate, accessory gland present near-to spermatheca, accessory pouch present.

Distribution. South Africa.

Note. While Fairmaire did not specify the number of specimens he examined in his original description, he did make mention of the collector (E. Simon) and locality, making specimens of his syntype series identifiable. Two specimens from MNHN are here designated as the lectotypes to fix the taxonomic status of the species.

Discussion

Revision of genus *Phylacastus*

Overall, there were relatively few specimens available for study (n = 45), which may represent restricted ranges or collecting bias, although the collections we sampled represent older historical collections of their range. Despite the number of specimens, we borrowed and examined all of the type material, as well as additional representatives of all species. As of this revision, many of the traits that Koch (1954a) used to diagnose *Phylacastus* are still supported; however, some characters (e.g. the joining of the pronotum and elytra and the dilated male protarsi) were difficult to reliably confirm in the material gathered for this study. We interpret Koch's (1954a) species *P. crypticoides* and *P. pretoriensis* as synonymous, as the traits used to differentiate them (mentum with sharp median carina in *P. crypticoides* and lack of basal pronotal margination in *P. pretoriensis*) were actually congruent between Koch's type material for both species in the case of the mentum, and inconsistent throughout all the available material in the case of the pronotal margins. As to Koch's (1954a) asserted relationship between *Phylacastus* and *Eurynotus*, additional phylogenetic study using morphological and/or molecular data will be required (Lumen and Kaminski in prep.). Currently, as of this revision their affiliation is not rejected—both genera have angled basal margins of the pronotum, angular prosternal processes, and tubercles on the apical declivity of the elytra (though often reduced in *Phylacastus*). The ovipositor of *Phylacastus* is only diagnostic for one species (*P. ancoralium*), and the genus appears to be overall congruent with other representatives of the subtribe (e.g. *Oncotus*), while also differing from *Eurynotus*, which has extremely long paraprocts (Iwan 2000; Banaszkiewicz 2006). There is some variation in the construction of the internal female anatomy of *Phylacastus*. In particular, *P. striolatus* and *P. rhodesianus* have a bursa copulatrix which is divided into two "lobes" by a median constriction (Fig. 6A), and there is an additional pouch situated near the spermatheca and accessory glands in *P. striolatus* and *P. ancoralium* (Fig. 6A, C). While the function of these structures is unclear at present, there may be similar structures in other representatives of the subtribe (e.g. *Eurynotus capensis* (Fabricius) appears to have a similarly divided bursa copulatrix; Tschinkel 1978: fig. 1), which may be helpful for diagnosing groups or for phylogenetic inference. Additionally, there were some accessory structures on the aedeagi of *P. ancoralium* and *P. makskacymirowi*. Namely, the former possesses structures historically referred to as "lacinia" or "clavae", and *P. makskacymirowi* has small, preapical sutures or grooves on the ventral side of the parameres. While the case of *P. ancoralium* is discussed in the below section, it is possible that the structures in *P. makskacymirowi* offer additional flexibility in the parameres.

Male terminalia analyses

Our discovery of accessory structures on the parameres of *P. ancoralium* (Fig. 4G) raise questions not only on the phylogenetic placement of the species, but on the concept of Eurynotina and the way such structures have been defined historically in Tenebrionidae (e.g. Koch 1954a, b, 1955, 1956; Iwan 2001, 2002, 2004). The revelation of these structures highlights the necessity of investigating Eurynotina, as well as other enigmatic and poorly understood groups. One such subtribe, Helopinina Lacordaire (Pedinini Eschscholtz), is morphologically similar to Eurynotina, despite molecular evidence separating them (Kamiński et al 2021a, b; Fig. 8). In the case of Helopinina, there is also a marked reduction in accessory structures (similar to Eurynotina), though they can be differentiated in other ways (e.g. scale-like setation, non-reduced or elongate basal apophyses, basal versus apical tegmen length ratio, lack of stridulatory gula). A literary review revealed a myriad of terms used to refer to accessory structures associated with the median lobe, parameres, and tegmen (Antoine 1930; Español 1945; Doyen and Tschinkel 1982; Doyen 1984; Iwan 2001, 2002, 2004; Kamiński et al. 2019). Terms which have garnered the most use historically and recently are "clavae" and "lacinia." Unfortunately, they have not been used uniformly, nor explicitly/formally defined in a way that is easily traceable or consistent. In fact, the two most used terms appear to follow authorship in North America ("clavae"—see Doyen and Tschinkel 1982; Doyen 1984; Aalbu et al. 2012; Johnston 2019) versus elsewhere ("lacinia"—see Español 1945; Iwan 2001). Thus far, the terms appear to have been used in an effort to qualitatively describe their shape. However, "clavae" is misleading in this regard and is much more widely used to refer to antennae (e.g. clava in Hymenoptera, Yoder et al. 2010). Additionally, while lacinia may adequately describe the form in some taxa, it misses the mark in others (e.g. *Anomalipus* spp.) and overlaps with much more widely used anatomical features (lacinia of the maxillary mouthparts of insects; Lawrence et al. 2011). Iwan (2004) gave a definition using the term lacinia (accessory spike- or hook-like structures which connect the median lobe with the inflexed alae of the apical piece), while also outlining their potential function (a means for the male to anchor itself internally during copulation as they extend/evert)—as well as the change in aedeagal function in groups which lacked them, such as Eurynotina (switching from lateral movement of "lacini" to a dorsoventral motion with a sclerotized median lobe and flexible parameres).

The aforementioned accessory structures to the median lobe and parameres have been recorded in two subfamilies and appear to be uncommon within Tenebrionidae. The first subfamily, Blaptinae, has several tribes (Amphidorini LeConte, Dendarini Mulsant & Rey, Pedinini, and Platynotini), and the second, Diaperinae, has one subtribe (Adelinina LeConte) that seem to have evolved variations of this characteristic morphology (Doyen 1984; Kamiński 2015b; Johnston 2019; Kamiński et al. 2021a). As a result of their unique and varied appearance, "clavae" or "lacinia" have been used to diagnose many tribes and subtribes (see Koch 1958; Doyen 1984; Iwan 2001); though in the case of some subtribes there are representatives that stand out contrastingly with their cohort as either having these structures (e.g. *Phylacastus ancoralium*, unusual in Eurynotina; Fig. 4G) or lacking them (e.g. *Anomalipus heraldicus* Gerstaecker and *Anchophthalmus* spp. of Platynotina or *Amatodes* Dejean (Fig. 9A), *Ametrocera* Fåhraeus, and *Oncopteryx* Gebien of Helopinina).

We examined published records and dissected representatives of Blaptinae (e.g. *Anomalipus* and *Eleodes*) (Fig. 9C, D) to first solidify an anatomical definition for our accessory aedeagal structures of interest. Our dissections reveal these structures always mediate the connection between the parameres and median lobe in some capacity, though the diversity of morphological structures may obfuscate connecting points, giving the illusion they are linked only to the median lobe (Figs 8, 9). Additionally, even in less-closely related taxa, the conglomerate structure of the parameres and median lobe (plus accouterments) possess a median extension connected/merged with the basal apophyses (Fig. 9B–D), giving evidence for homology. To make referring to these structures more uniform, while also making their function more apparent, we propose naming these structures ancorae (singular: ancora) from the Latin *ancor*—in reference to the organ's apparent reproductive function in anchoring the male to the female. We also hope that coining a new name for this feature will provide a means to better investigate homology, evolutionary strategies, and phylogeny. Our definition aims to unify the terminology and enable verification of homology in problematic cases. For example, some species of *Anomalipus* are known to possess several appendages of the tegmen (Endrödy-Younga 1988). Dissections of *Anomalipus mastodon* Fåhraeus (Fig. 9D) revealed most of these appendages are not linked to the median lobe or parameres; therefore, they cannot be regarded as ancorae. All of the extra appendages originate either from the basal piece of the tegmen (Fig. 9D, *pan3*) or are loosely attached by connecting membranes (Fig. 9D, *pan1* and *pan2*). Using the following criterion: connection to the parameres and the median lobe and linkage to the basal apopyses, we conclude that *A. mastodon* possesses only one pair of ancorae homological with the structures in other Platynotina (e.g. Fig. 9B). In another case, the subtribe Adelinina (Diaperinae: Diaperini) is defined by structures coined by Doyen (1984) as "clavae." To test our definition, we also dissected representatives of *Adelina*, *Alphitophagus*, *Gnatocerus*, and

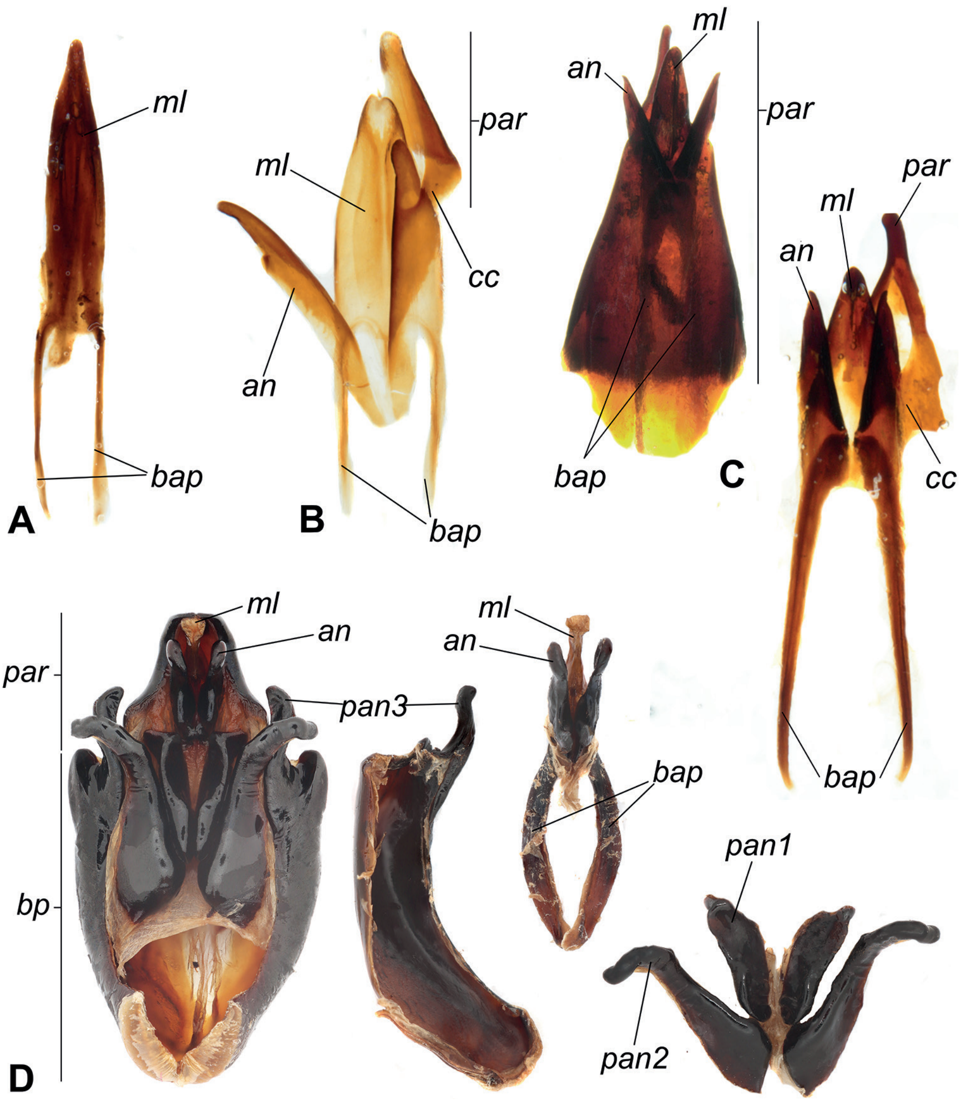

Figure 9. Dissections of ancorae variation and aedeagal morphology from Blaptinae **A** *Amatodes* Dejean (Pedinini, Helopinina) median lobe with basal apophyses **B** *Trigonopus similis* Iwan (Platynotini, Platynotina) parameres, median lobe, and ancorae **C** *Eleodes obscura* (Say) (Amphidorini) intact and extracted parameres, median lobe, and ancorae **D** *Anomalipus mastodon* Fåhraeus, 1870 (Platynotini, Platynotina). Abbreviations: an - ancorae, bap - basal aphophyses, bp - basal portion of tegmen, cc - cuticular connection of ancorae to parameres, ml - median lobe, pan 1–3 - pseudo ancorae, par - parameres.

Sitophagus. While all three possess accessory structures related to the median lobe and apex (parameres) of the aedeagus, there are several differences in comparison with what we observe in Blaptinae: 1) the median lobe is divided into two halves (Fig. 10), rather than fused as in Blaptinae (Figs 4, 8, 9); 2) the "clavae" are strongly connected with

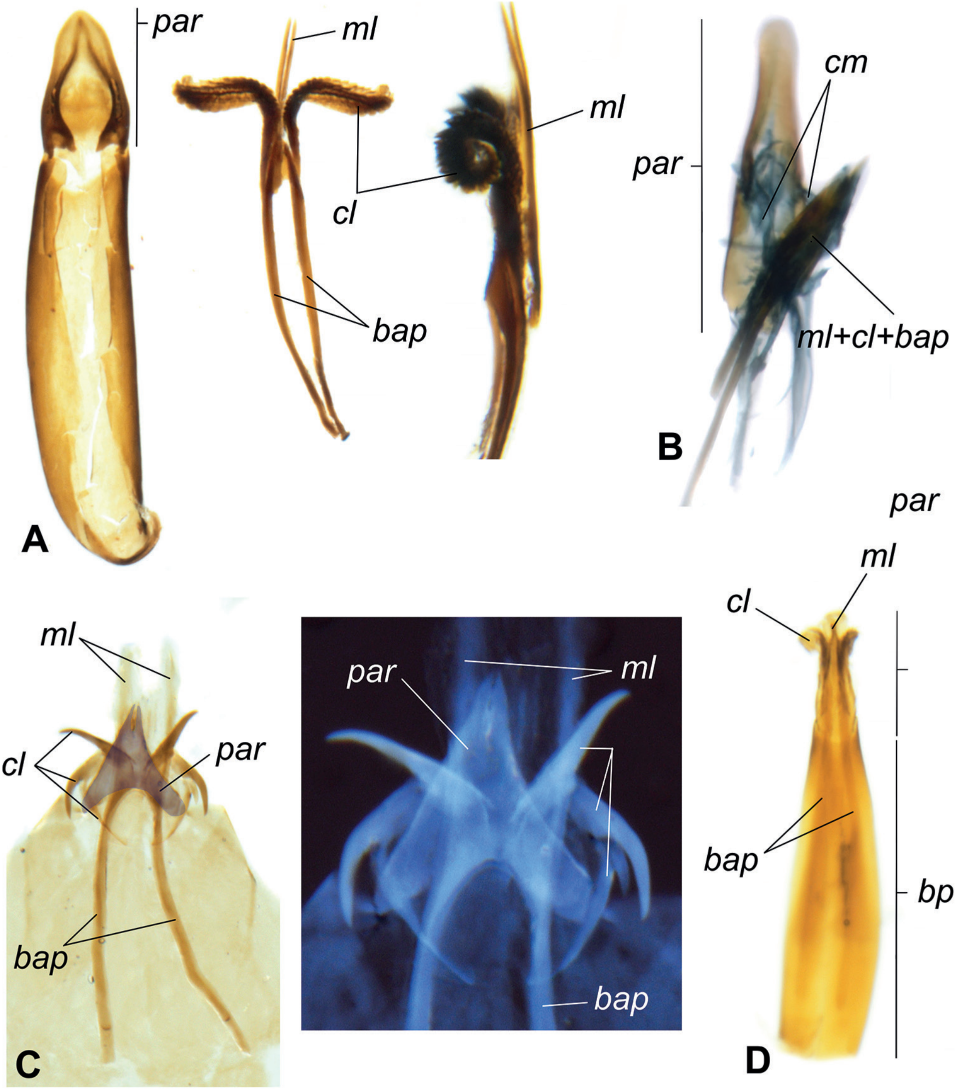

Figure 10. Sampled Adelenina (Diaperinae: Diaperini: Adelinina) aedeagi **A** *Sitophagus hololeptoides* (Laporte) **B** *Adelina plana* (Fabricius) **C** *Alphitophagus bifasciatus* (Say) **D** *Gnatocerus cornutus* (Fabricius) Abbreviations: *bap* - basal apophyses, *cl* - "clavae", *ml* - median lobe, *par* - parameres, *bp* - basal portion of aedeagus, *cm* - connective membrane.

the basal aphophyses, which were long in all dissected specimens, but very weakly attached/associated with the median lobe (Fig. 10A); in Blaptinae all three structures are strongly associated/fused into a conglomerate structure (Figs 4, 8, 9); 3) the connection of the "clavae" to the parameres appears to be mediated by membranous structures (Fig. 10B). All the Blaptinae we observed have a much more strongly sclerotized connection (Fig. 9B, C). As a result, we propose that while these structures may be similar in form and operate in similar function(s), they do not fit our definition of ancorae focused on Blaptinae in particular. Diaperini Latreille as a tribe is very distantly related to Blaptinae phylogenetically (Kergoat et al. 2014; Kamiński et al. 2021a), and so these structures are likely not homologous, and likely would require additional examination in the future, and potential new terminology of their own. As such, we leave further investigation to other researchers focused on this and other more closely related groups.

Acknowledgements

We thank Ruth Müller (TMNH), Antoine Mantilleri (MNHM), Riaan Stals (SANC), and other museum workers for their hospitality, access to material, and invaluable assistance (reference photographs, locating specimens, etc.). We also thank Magdalena Kowalewska at MIIZ PAN for SEM photographs. This research was funded by the OPUS 19 Project (number 2020/37/B/NZ8/02496) from the National Science Centre, Poland.

References

Aalbu RL, Smith AD, Triplehorn CA (2012) A revision of the *Eleodes* (subgenus *Caverneleodes*) with new species and notes on cave breeding *Eleodes*. Annales Zoologici 62(2): 199–216. https://doi.org/10.3161/000345412X652729

Antoine M (1930) Étude des espèces appartenant au genre *Litoborus* Mulsant et Rey (Col. Tenebrionidae). Bulletin de la Société des Sciences Naturelles du Maroc 10: 175–209.

Banaszkiewicz M (2006) Comparative study of female genitalia in Pedinini *sensu* Iwan 2004 (Coleoptera: Tenebrionidae: Pedinini), with notes on the classification. Annales Zoologici 56: 59–77.

Bouchard P, Bousquet Y, Aalbu RL, Alonso-Zarazaga MAO, Merkl O, Davies AE (2021) Review of genus-group names in the family Tenebrionidae (Insecta, Coleoptera). ZooKeys 1050: 1–633. https://doi.org/10.3897/zookeys.1050.64217

Doyen JT (1984) Reconstitution of the Diaperini of North America, with new species of *Adelina* and *Sitophagus* (Coleoptera: Tenebrionidae). Proceedings of the Entomological Society of Washington 86(4): 777–789.

Doyen JT, Tschinkel WR (1982) Phenetic and cladistic relationships among tenebrionid beetles (Coleoptera). Systematic Entomology 7(2): 127–183. https://doi.org/10.1111/j.1365-3113.1982.tb00129.x

Endrödy-Younga S (1988) Revision of the genus *Anomalipus* Latreille, 1846 (Coleoptera: Tenebrionidae: Platynotini). Transvaal Museum Monograph 6: 1–129.

Endrödy-Younga S (2000) Revision of the subtribe Gonopina (Coleoptera: Tenebriondae, Opatrinae, Platynotini). Annals of the Transvaal Museum 37: 1–54.

Español F (1945) Nuevos comentarios sistemáticos sobre ls subfamilia Opatrinae Reitt. con la descriptón de un nuevo representante del Sáhara Espańol (Col. Tenebrionidae). Eos, Revista Española de Entomología [1944] 20(3–4): 213–232. [pls xii–xvii]

Fairmaire L (1897) Coléoptères nouveaux de l'Afrique intertropicale et australe. Annales de la Société Entomologique de France 66: 109–155. https://doi.org/10.5962/bhl.part.29501

Gebien H (1904) Beiträge zur Kenntnis der Insektenfauna von Kamerun. No 28. Verzeichnis der von Professor Dr. Yngve Sjöstedt in Kamerun gesa mmelten Tenebrioniden. Arkiv för Zoologi 2: 1–31. https://doi.org/10.5962/bhl.part.4542

Gebien H (1910) Coleoptera. Tenebrionidae. Sjöstedts Kilimandjaro–Meru und Massaisteppen Expedition 1905–1906(7): 363–396.

Iwan D (1995) A revision of the genus *Zidalus* Mulsant et Rey, 1853 (Coleoptera: Tenebrionidae, Platynotini). Genus 6(3–4): 359–400.

Iwan D (2001) Comparative study of male genitalia in Opatrinae sensu Medvedev (1968) (Coleoptera: Tenebrionidae), with notes on the tribal classification. Part I. Annales Zoologici 51: 351–390.

Iwan D (2000) Ovoviviparity in tenebrionid beetles of the melanocratoid Platynotina (Coleoptera: Tenebrionidae: Platynotini) from Madagascar, with notes on the viviparous beetles. Annales Zoologici 50: 15–25.

Iwan D (2002) Generic classification of the tribe Platynotini (Coleoptera: Tenebrionidae), with notes on phylogeny. Annales Zoologici 52: 1–149.

Iwan D (2004) A comparative study of male genitalia in Opatrinae sensu Medvedev (1968) (Coleoptera: Tenebrionidae), with notes on the reinterpreted tribal classification. Part II. Annales Zoologici 54: 735–765.

Iwan D (2006) Revision of African *Ectateus* group (Coleoptera: Tenebrionidae: Platynotina). Part IV. *Quadrideres luigii*, new species from Kenya. Annales Zoologici 56: 79–84.

Iwan D, Kamiński MJ (2012) Revision of the Malagasy genus *Lechius* Iwan, 1995 (Coleoptera: Tenebrionidae: Pedinini). Zootaxa 3399(1): 23–34. https://doi.org/10.11646/zootaxa.3399.1.2

Iwan D, Kamiński MJ (2014) Taxonomy of the genus *Schelodontes* Koch, 1956 with a key to species (Coleoptera: Tenebrionidae: Platynotina). Insect Systematics & Evolution 45(2): 159–179. https://doi.org/10.1163/1876312X-00002092

Johnston MA (2019) Phylogenetic revision of the psammophilic *Trogloderus* LeConte (Coleoptera: Tenebrionidae), with biogeographic implications for the Intermountain Region. Peerj 7: e8039 https://doi.org/10.7717/peerj.8039

Kamiński MJ (2013) Two new species of the Afrotropical genus *Quadrideres K*och, 1956 (Coleoptera: Tenebrionidae: Pedinini), with notes on the *interioris* species-group. Annales Zoologici 63(1): 85–94. https://doi.org/10.3161/000345413X666129

Kamiński MJ (2014) A cladistically based reinterpretation of the taxonomy of two Afrotropical tenebrionid genera *Ectateus* Koch, 1956 and *Selinus* Mulsant & Rey, 1853 (Coleoptera, Tenebrionidae, Platynotina). ZooKeys 415: 81–132. https://doi.org/10.3897/zookeys.415.6406

Kamiński MJ (2015a) Phylogenetic reassessment and biogeography of the *Ectateus* generic group (Coleoptera: Tenebrionidae: Platynotina). Zoological Journal of the Linnean Society 175(1): 73–106. https://doi.org/10.1111/zoj.12263

Kamiński MJ (2015b) Afrotropical Melambiina: four new species of *Zadenos* (Tenebrionidae: Pedinini), with notes on related taxa. Annales Zoologici 65(4): 531–550. https://doi.org/10.3161/00034541ANZ2015.65.4.002

Kamiński MJ (2016) Catalogue and distribution of the subtribe Eurynotina (Coleoptera: Tenebrionidae: Pedinini). Annales Zoologici 66(2): 227–266. https://doi.org/10.3161/00034541ANZ2016.66.2.006

Kamiński MJ (2021) Techniques for dissecting adult darkling beetles. Harvard Dataverse. https://doi.org/10.7910/dvn/8zqvyw

Kamiński MJ, Raś M (2011) New status of the genus *Ectateus* Koch, 1956 with taxonomic notes on the *Ectateus* generic group (Coleoptera: Tenebrionidae: Platynotina). Annales Zoologici 61(4): 647–655. https://doi.org/10.3161/000345411X622507

Kamiński MJ, Kanda K, Lumen R, Smith AD, Iwan D (2019) Molecular phylogeny of Pedinini (Coleoptera, Tenebrionidae) and its implications for higher-level classification. Zoological Journal of the Linnean Society 185: 77–97. https://doi.org/10.1093/zoolinnean/zly033

Kamiński MJ, Lumen R, Kanda K, Iwan D, Johnston MA, Kergoat G, Bouchard P, Bai X-L, Li X-M, Ren G-D, Smith AD (2021a) Reevaluation of Blapimorpha and Opatrinae: addressing a major phylogeny-classification gap in darkling beetles (Coleoptera: Tenebrionidae: Blaptinae). Systematic Entomology 46(1): 140–156. https://doi.org/10.1111/syen.12453

Kamiński MJ, Lumen R, Müller R, Kanda K, Robiche G, Smith AD (2021b) Illustrated catalog of the subtribe Helopinina Latreille (Coleoptera: Tenebrionidae: Blaptinae). Coleopterists Bulletin 75(3): 537–578. https://doi.org/10.1649/0010-065X-75.3.537

Kamiński MJ, Gearner OM, Raś M, Hunsinger ET, Smith AL, Mas-Peinado P, Girón JC, Bilska AG, Strümpher WP, Wirth CC, Kanda K, Swichtenberg K, Iwan D, Smith AD (2022) Female terminalia morphology and cladistic relations among Tok-Tok beetles (Tenebrionidae: Sepidiini). Cladistics 38(6): 623–648. https://doi.org/10.1111/cla.12510

Kaszab Z (1975) Revision der Asiatischen Platynotinen (Coleoptera: Tenebrionidae). Acta Zoologica Academiae Scientiarum Hungaricae 21(3–4): 277–367.

Kergoat GJ, Soldati L, Clamens A-L, Jourdan H, Jabbour-Zahab R, Genson G, Bouchard P, Condamine FL (2014) Higher level molecular phylogeny of darkling beetles (Coleoptera: Tenebrionidae). Systematic Entomology 39: 486–499. https://doi.org/10.1111/syen.12065

Koch C (1954a) The Tenebrionidae of Southern Africa. XXIV. New Portuguese East African Species collected by Dr. A. J. Barbosa. Revista da Faculdade de Ciências, C-Ciências Naturais, Vol. III – Fasc. 2. Biblioteca da Faculdade de Ciências, Rua da Escola Politécnica, Lisboa, 239–310.

Koch C (1954b) Die Tenebrioniden des südlichen Afrikas XV. Revisioin der Oncotini nov. trib. Opatrinae (Psectropini Kaszab p.p.). Arkiv Zoologi (Stockholm) 7: 1–96.

Koch C (1955) The Tenebrionidae of Southern Africa. XXV. New, forgotten or Palearctic genera and species of Opatrinae. Annals of the Transvaal Museum 22: 419–476.

Koch C (1956) Exploration du Parc National de l'Upemba. II. Tenebrionidae (Coleoptera, Polyphaga), Opatrinae, first part: Platynotini, Litoborini and Loensini. Institut des Parcs nationaux du Congo Belge, Bruxelles, 472 pp.

Koch C (1958) Tenebrionidae of Angola. Publicacões Culturais da Companhia de Diamantes de Angola 39: 11–231.

Lawrence JF, Ślipiński A, Seago AE, Thayer MK, Newton AF, Marvaldi AE (2011) Phylogeny of the Coleoptera based on morphological characters of adults and larvae. Annales Zoologici 61(1): 1–217. https://doi.org/10.3161/000345411X576725

Lindroth CH, Palmen E (1956) Coleoptera. In: Tuxen SL (Ed.) Taxonomist's Glossary of Genitalia in Insects, 2nd Edn. Monksgaard, Copenhagen, 80–88.

Matthews EG, Lawrence JF, Bouchard P, Steiner WE, Ślipiński SA (2010) Tenebrionidae Latreille, 1802. In: Leschen RAB, Beutel RG, Lawrence JF (Eds) Handbook of Zoology: A Natural History of the Phyla of the Animal Kingdom. Vol. IV – Arthropoda: Insecta. Part 38. Coleoptera, Beetles. Vol. 2: Systematics. Walter de Gruyter, Berlin, 574–659. https://doi.org/10.1515/9783110911213.574

Reichardt AN (1936) Darkling beetles of the tribe Opatrini (Coleoptera Tenebrionidae) of the Palearctic Region. Keys to the fauna of the USSR. 19: 1–224. Zoological Institute of the Russian Academy of Sciences, Moscow.

Tschinkel WR (1978) Ovoviviparity in some tenebrionid beetles. Coleopterists Bulletin 32(4): 315–317.

Yoder MJ, Mikó I, Seltmann KC, Bertone MA, Deans AR (2010) A gross anatomy ontology for Hymenoptera. PLoS ONE 5(12): e15991. https://doi.org/10.1371/journal.pone.0015991

Appendix 1

Table of *Phylacastus* distributional data in .csv format.

Genus, Species,Verbatim Label, date (d.m.y), Determined Lat, Determined Long, note(s)

Phylacastus, *striolatus*, Makapan (TR.) E. Simon 1893; *Phylacastus striolatus* ? Cafrar; , 1893, -24.1586, 29.1769, Type Locality; Point based on Makapan valley archeological site near to Mokopan.

Phylacastus, *striolatus*, Makapan (TR.) E. Simon 1893, 1893, -24.1586, 29.1769, Point based on Makapan valley archeological site near to Mokopan.

Phylacastus, *striolatus*, Transvaal Soutpansberg Mphome Magd Knothe S, -,-23.0084, 29.7690, point based on Soutpansberg Mountain.

Phylacastus, *striolatus*, Transvaal Soutpansberg Mphome Magd Knothe S, -,-23.0084, 29.7690, point based on Soutpansberg Mountain.

Phylacastus, *rhodesianus*, Marandella Mashld XI.97 GKMarshall; Holotype No: 1877 *Phylacastus rhodesianus* KOCH; *Phylacastus rhodesianus* Koch DET.C.KOCH; *rhodesianus* Koch, 11.1897, -18.1897, 31.5467, Type locality; Marondera (Marandella synonym).

Phylacastus, *rhodesianus*, 9.VI.1970 Vumba SUD RHODESIE Cl. Besnard leg.,9.VI.1970, -19.1000, 32.7833, Point based on Bvumba Mts.

Phylacastus, *rhodesianus*, 8.VI.1970 Inyanga SUD RHODESIE Cl. Besnard leg.,8.VI.1970, -18.2100, 32.7400,"Point based on Nyanga, Zimbabwe".

Phylacastus, *rhodesianus*, 8.VI.1970 Inyanga SUD RHODESIE Cl. Besnard leg.,8.VI.1970, -18.2100, 32.7400,"Point based on Nyanga, Zimbabwe".

Phylacastus, *rhodesianus*, 8.VI.1970 Inyanga SUD RHODESIE Cl. Besnard leg.,8.VI.1970, -18.2100, 32.7400,"Point based on Nyanga, Zimbabwe".

Phylacastus, *rhodesianus*, 8.VI.1970 Inyanga SUD RHODESIE Cl. Besnard leg.,8.VI.1970, -18.2100, 32.7400,"Point based on Nyanga, Zimbabwe".

Phylacastus, *rhodesianus*, 8.VI.1970 Inyanga SUD RHODESIE Cl. Besnard leg.,8. VI.1970, -18.2100, 32.7400,"Point based on Nyanga, Zimbabwe".
Phylacastus, *rhodesianus*, 8.VI.1970 Inyanga SUD RHODESIE Cl. Besnard leg.,8. VI.1970, -18.2100, 32.7400,"Point based on Nyanga, Zimbabwe".
Phylacastus, *rhodesianus*, 8.VI.1970 Inyanga SUD RHODESIE Cl. Besnard leg.,8. VI.1970, -18.2100, 32.7400,"Point based on Nyanga, Zimbabwe".
Phylacastus, *rhodesianus*, 8.VI.1970 Inyanga SUD RHODESIE Cl. Besnard leg.,8. VI.1970, -18.2100, 32.7400,"Point based on Nyanga, Zimbabwe".
Phylacastus, *rhodesianus*, 8.VI.1970 Inyanga SUD RHODESIE Cl. Besnard leg.,8. VI.1970, -18.2100, 32.7400,"Point based on Nyanga, Zimbabwe".
Phylacastus, *rhodesianus*, 8.VI.1970 Inyanga SUD RHODESIE Cl. Besnard leg.,8. VI.1970, -18.2100, 32.7400,"Point based on Nyanga, Zimbabwe".
Phylacastus, *makskacymirowi*, "S.Afr.,E.Transvaal Berlin;Karst plat. 25.31 S - 30.46 E; 23.10.1986; E-Y:2001 groundtraps, 42 days leg. Endrödy-Younga; ground trap with meat bait",23.10.1986, -25.52, 30.77.
Phylacastus, *makskacymirowi*, "S.Afr.,E.Transvaal Berlin;Karst plat. 25.31 S - 30.46 E; 20.9.1986; E-Y:2279 groundtraps, 33 days leg. Endrödy-Younga; ground trap with meat bait",20.8.1986, -25.52, 30.77, Type locality.
Phylacastus, *makskacymirowi*, "S.Afr.,E.Transvaal Berlin;Karst plat. 25.31 S - 30.46 E; 20.9.1986; E-Y:2279 groundtraps, 33 days leg. Endrödy-Younga; ground trap with meat bait",20.8.1986, -25.52, 30.77.
Phylacastus, *makskacymirowi*, "S.Afr.,E.Transvaal Berlin;Karst plat. 25.31 S - 30.46 E; 20.9.1986; E-Y:2279 groundtraps, 33 days leg. Endrödy-Younga; ground trap with meat bait",20.8.1986, -25.52, 30.77.
Phylacastus, *makskacymirowi*, "S.Afr.,E.Transvaal Berlin;Karst plat. 25.31 S - 30.46 E; 20.9.1986; E-Y:2279 groundtraps, 33 days leg. Endrödy-Younga; ground trap with meat bait",20.8.1986, -25.52, 30.77.
Phylacastus, *makskacymirowi*, "S.Afr.,E.Transvaal Berlin;Karst plat. 25.31 S - 30.46 E; 4.2.1986 E-Y:2414 under fungous logs leg. Endrödy-Younga",4.2.1986, -25.52, 30.77.
Phylacastus, *makskacymirowi*, "S.Afr.,E.Transvaal Berlin;Karst plat. 25.31 S - 30.46 E; 8.12.1986 E-Y:2363 fungous Pinus logs leg. Endrödy-Younga",8.12.1986, -25.52, 30.77.
Phylacastus, *makskacymirowi*, S.Afr.;Mpumalanga 10km E Kaapsehoop 25.36 S - 30.43 E; 4-6.1.2014: E-Y:3943 sifting; indigenous forest leg. Ruth Müller, 4-6.1.2014, -25.60, 30.72.
Phylacastus, *makskacymirowi*, "S.Afr.;Mpumalanga Sjonajona, Badplaas 24.44 S - 30.40 E; 11.11.2002; E-Y:3565 general collect. 1410m leg. TMSA staff",11.11.2002, -25.73, 30.67.
Phylacastus, *makskacymirowi*, "S.Afr.;Mpumalanga Sjonajona, Badplaas 24.44 S - 30.40 E; 11.11.2002; E-Y:3565 general collect. 1410m leg. TMSA staff",11.11.2002, -25.73, 30.67.

Phylacastus, *makskacymirowi*, "S.Afr.;Mpumalanga Sjonajona, Badplaas 24.44 S - 30.40 E; 11.11.2002; E-Y:3565 general collect. 1410m leg. TMSA staff",11.11.2002, -25.73, 30.67.

Phylacastus, *makskacymirowi*, "S.Afr.;Mpumalanga Sjonajona, Badplaas 24.44 S - 30.40 E; 11.11.2002; E-Y:3565 general collect. 1410m leg. TMSA staff",11.11.2002, -25.73, 30.67.

Phylacastus, *crypticoides*, Lydenburg Distr. 1896 P.A. Krantz; *Phylacastus crypticoides* DET.C.KOCH 1953; Holotype No: 1873 *Phylacastus crypticoides* KOCH; *crypticoides* Koch; Eurynotus? sp.,1896, -25.0960, 30.4460, Approximated in Google Earth.

Phylacastus, *crypticoides*, "S.Afr.,N.Transvaal Nylsvley Met.Sta. 24.40 S - 28.42 E; 285.1975; E-Y:1160 humus, Berlese, open leg. Endrödy-Younga",28.5.1975, -25.67, 28.70.

Phylacastus, *crypticoides*, "S.Afr.,N.Transvaal Nylsvley, Smith frm 24.40S-24.42E 15.11.1975; E-Y: 952 cattle dung leg. Endrödy-Younga; trench; rep: 5 cage mesh 9mm 7 day aft.sett.",15.11.1975, -25.67, 28.70.

Phylacastus, *crypticoides*, "S.Afr.,N.Transvaal Nylsvley Met.Sta. 24.40 S - 28.42 E; 29.3.1976; E-Y:1112 sifted litter, open leg. Endrödy-Younga",29.3.1976, -25.67, 28.70.

Phylacastus, *crypticoides*, "S.Afr.;Limpopo Prov. Lindani Nat Res 1336m 24.02 S - 28.23 E; 8.12.2005; E-Y:3687 single, bushveld leg.Gusmann, Müller",8.12.2005, -24.03, 28.38.

Phylacastus, *crypticoides*, "S.Afr.,N.Transvaal Nylsvley, Smith frm 24.40S-24.42E 8.1.1976; E-Y: 990 sifted litter. Endrödy-Younga",8.1.1976, -25.67, 28.70.

Phylacastus, *crypticoides*, S.Afr.Tvl.Waterbg Lapalala Wilderness 23.49 S- 20.17 E; 16.8.1975; E-Y:829 from under stones leg. Endrödy-Younga, 16.8.1975, -23.82, 20.28.

Phylacastus, *crypticoides*, S.Afr.Tvl.Waterbg Lapalala Wilderness 23.49 S- 20.17 E; 16.8.1975; E-Y:829 from under stones leg. Endrödy-Younga, 16.8.1975, -23.82, 20.28.

Phylacastus, *crypticoides*, S.Afr.Tvl.Waterbg Lapalala Wilderness 23.49 S- 20.17 E; 16.8.1975; E-Y:829 from under stones leg. Endrödy-Younga, 16.8.1975, -23.82, 20.28.

Phylacastus, *crypticoides*, S.Afr.Tvl.Waterbg Lapalala Wilderness 23.49 S- 20.17 E; 16.8.1975; E-Y:829 from under stones leg. Endrödy-Younga, 16.8.1975, -23.82, 20.28.

Phylacastus, *crypticoides*, S.Afr.Tvl.Waterbg Lapalala Wilderness 23.49 S- 20.17 E; 16.8.1975; E-Y:829 from under stones leg. Endrödy-Younga, 16.8.1975, -23.82, 20.28.

Phylacastus, *crypticoides*, S.Afr.Tvl.Waterbg Lapalala Wilderness 23.49 S- 20.17 E; 16.8.1975; E-Y:829 from under stones leg. Endrödy-Younga, 16.8.1975, -23.82, 20.28.

Phylacastus, *crypticoides*, S.Afr.Tvl.Waterbg Lapalala Wilderness 23.49 S- 20.17 E; 16.8.1975; E-Y:829 from under stones leg. Endrödy-Younga, 16.8.1975, -23.82, 20.28.

Phylacastus, *pseudoclavum*, S.Afr.Basutoland Makheke Mnts 15 miles ENE Mokhotlong. 8.IV.51 No. 268;Swedish South Africa Expedition 1950-1951; red label, 8.IV.1951, -29.19, 29.29, Approximated in Google Earth.

Phylacastus, *pseudoclavum*, "S.Afr.;E. Lesotho Hodson's Peak 300m 29.37S - 29.17 E; 11.3.1976;E-Y:1069 fr.und.stones, 3150m leg. Endrödy-Younga",11.3.1976, -29.62, 29.28, Type locality.

Phylacastus, *pseudoclavum*, "S.Afr.;E. Lesotho Hodson's Peak 300m 29.37S - 29.17 E; 11.3.1976;E-Y:1069 fr.und.stones, 3150m leg. Endrödy-Younga",11.3.1976, -29.62, 29.28.

Phylacastus, *pseudoclavum*, "S.Afr.;E. Lesotho Hodson's Peak 300m 29.37S - 29.17 E; 11.3.1976;E-Y:1069 fr.und.stones, 3150m leg. Endrödy-Younga",11.3.1976, -29.62, 29.28.

Phylacastus, *pseudoclavum*, S.Afr.;E. Lesotho Hodson's Peak 300m 29.37S - 29.17 E; 11.3.1976;E-Y:1067 from under stones leg. Endrödy-Younga, 11.3.1976, -29.62, 29.28.

Phylacastus, *pseudoclavum*, S.Afr.;E. Lesotho Hodson's Peak 300m 29.37S - 29.17 E; 11.3.1976;E-Y:1067 from under stones leg. Endrödy-Younga, 11.3.1976, -29.62, 29.28.

Phylacastus, *pseudoclavum*, S.Afr.;E. Lesotho Hodson's Peak 300m 29.37S - 29.17 E; 11.3.1976;E-Y:1067 from under stones leg. Endrödy-Younga, 11.3.1976, -29.62, 29.28.

Phylacastus, *pseudoclavum*, S.Afr.;E. Lesotho Hodson's Peak 300m 29.37S - 29.17 E; 11.3.1976;E-Y:1067 from under stones leg. Endrödy-Younga, 11.3.1976, -29.62, 29.28.

Phylacastus, *pseudoclavum*, S.Afr.;E. Lesotho Hodson's Peak 300m 29.37S - 29.17 E; 11.3.1976;E-Y:1067 from under stones leg. Endrödy-Younga, 11.3.1976, -29.62, 29.28.

Phylacastus, *pseudoclavum*, "S.Afr., Lesotho Drakensbg, Black Mt. 29.31 S - 29.12 E; 9.3.1976;E-Y:1060 from under stones leg. Endrödy-Younga",9.3.1976, -29.52, 29.20.

Phylacastus, *pseudoclavum*, "S.Afr., E.Lesotho Sani Pass Valley 29.39 S - 29.12 E; 10.3.1976; E-Y:1066 from under stones leg. Endrödy-Younga",10.3.1976, -29.52, 29.20.

Phylacastus, *pseudoclavum*, "S.Afr., E.Lesotho Sani Pass Valley 29.39 S - 29.12 E; 10.3.1976; E-Y:1066 from under stones leg. Endrödy-Younga",10.3.1976, -29.52, 29.20.

ZooKeys 1138: 29–48 (2023)
doi: 10.3897/zookeys.1138.95626
https://zookeys.pensoft.net

RESEARCH ARTICLE

A peer-reviewed open-access journal
ZooKeys
Launched to accelerate biodiversity research

Comparative mitogenomics and phylogenetic analyses of the genus *Menida* (Hemiptera, Heteroptera, Pentatomidae)

Xiaofei Ding[1*], Chao Chen[1*], Jiufeng Wei[1], Xiaoyun Gao[1], Hufang Zhang[2], Qing Zhao[1]

1 *College of Plant Protection, Shanxi Agricultural University, Taigu 030801, Shanxi, China* **2** *Department of Biology, Xinzhou Teachers University, Xinzhou 034000, Shanxi, China*

Corresponding author: Qing Zhao (zhaoqing86623@163.com)

Academic editor: Jader Oliveira | Received 25 September 2022 | Accepted 12 December 2022 | Published 5 January 2023

https://zoobank.org/5D29FD5C-1FC7-4D9D-A4FB-04BBB6709C41

Citation: Ding X, Chen C, Wei J, Gao X, Zhang H, Zhao Q (2023) Comparative mitogenomics and phylogenetic analyses of the genus *Menida* (Hemiptera, Heteroptera, Pentatomidae). ZooKeys 1138: 29–48. https://doi.org/10.3897/zookeys.1138.95626

Abstract

In order to explore the genetic diversity and phylogenetic relationship of the genus *Menida* Motschulsky, 1861 and reveal the molecular evolution of the family Pentatomidae, subfamily Pentatominae, complete mitochondrial genomes of three species of *Menida* were sequenced, and the phylogenetic relationships of tribes within the subfamily Pentatominae were studied based on these results. The mitochondrial genomes of *Menida musiva* (Jakovlev, 1876), *M. lata* Yang, 1934, and *M. metallica* Hsiao & Cheng, 1977 were 16,663 bp, 16,463 bp, and 16,418 bp, respectively, encoding 37 genes and including 13 protein-coding genes (PCGs), two rRNA genes, 22 tRNA genes, and a control region. The mitochondrial genome characteristics of *Menida* were compared and analyzed, and the phylogenetic tree of the Pentatominae was constructed based on the mitochondrial genome datasets using Bayesian inference (BI) and maximum likelihood (MI) methods. The results showed that gene arrangements, nucleotide composition, codon preference, gene overlaps, and RNA secondary structures were highly conserved within the *Menida* and had more similar characteristics in Pentatominae. The phylogenetic analysis shows a highly consistent topological structure based on BI and ML methods, which supported that the genus *Menida* belongs to the Pentatominae and is closely related to Hoplistoderini. The examined East Asian species of *Menida* form a monophyletic group with the internal relationships: (*M. musiva* + (*M. lata* + (*M. violacea* + *M. metallica*))).

* These authors contributed equally to this work.

In addition, these results support the monophyly of Eysarcorini and Strachiini. *Placosternum* and Cappaeini are stable sister groups in the evolutionary branch of Pentatominae. The results of this study enrich the mitochondrial genome databases of Pentatominae and have significance for further elucidation of the phylogenetic relationships within the Pentatominae.

Keywords
Menida, mitochondrial genomesm Pentatominae, phylogenetic relationship

Introduction

Mitochondrial genomes are one of the most widely used molecular markers in evolutionary studies due to their small size, stable genetic composition, relatively conserved gene sequence, rapid rate of evolution, and relatively complete molecular information (Wolstenholme 1992; Chen et al. 2020a). In recent years, with the development of sequencing technology, more and more insect mitochondrial genomes have been sequenced, covering almost all insect orders. A typical insect mitochondrial genome comprises circular double-stranded molecules 15–20 kb in size that usually code for 37 genes: 13 protein-coding genes (PCGs), two ribosomal RNA genes (rRNAs), 22 transfer RNA genes (tRNAs), and a control region (also known as AT-rich region) (Boore 1999). The structure of insect mitochondrial genomes is compact, the overlap region and spacing region of adjacent genes are very short, and there are no introns (Zink 2005). Insect mitochondrial genomes are widely used in molecular evolution, phylogenetic and population genetic structure analyses, and biogeographic studies (Simon and Hadrys 2013; Yuan and Guo 2016; Wang et al. 2017; Wang et al. 2020; Zheng et al. 2021).

Pentatominae is the largest subfamily of Pentatomidae, which is composed of at least 3484 species belonging to 660 genera in 43 tribes (Rider et al. 2018). Species feed on the liquid flowing in the host plant's vegetative organs using piercing-sucking mouthparts; they suck up nutrients in the host plant and make it shrink and dry. They cause great losses to crops, vegetables, fruit trees, and forests, and, as such, are important agricultural pests (Mi et al. 2020). The lack of unique diagnostic characteristics hampers the identification of this subfamily, making it difficult to construct criteria for practical and reliable classification. Most previous studies have focused on the high-level relationships within Pentatomoidea, while the phylogenetic relationships of tribes within Pentatominae remain controversial. Liu et al. (2019) reconstructed the phylogeny of Pentatomomorpha based on the PCGrRNA dataset under the Bayesian site-heterogeneous mixture model, and they examined the evolutionary history of the group through a fossil-calibrated divergence dating analysis, confirming the monophyly of Pentatomoidea and its sister relationship with Eutrichophora. Ye et al. (2022) also presented a phylogenetic analysis. Yuan et al. (2015) constructed the phylogenetic tree of Pentatomoidea based on mitochondrial genome data, which strongly supported the monophyly of Pentatomoidea. The data produced by Zhao et al. (2019b) strongly supported *Eurydema* Laporte, 1833 within the tribe Strachiini and as a sister group with *Nezara viridula* (Linnaeus, 1758). Genevcius et al. (2021) confirmed that the currently recognized Neotropical tribe Chlorocorini is not monophyletic based on DNA and morphological data. Roca-Cusachs et al. (2022) rejected the currently accepted monophyletic nature of Pentatomidae, confirming that Serbaninae are a sister lineage of all remaining Pentatomidae, rather than members of Phloeidae as previously assumed. Li et al. (2021) studied the phylogenetic relationships among the groups of Pentatominae and supported the placement of *Eysarcoris* Hahn, 1834 and *Carbula* Stål, 1864 in Eysarcorini.

The genus *Menida* Motschulsky, 1861 is distributed worldwide, but most species are distributed in Afrotropical and Oriental regions (Li 2015). Species of the genus *Menida* pierce the surface of the host plant and sucks the liquid in the plant using piercing-sucking mouthparts. This destroys the plant's tissue and causes loss of water, thus causing the plant to suffer from such diseases as withering spot and decay. Examples are *Menida versicolor* (Gmelin, 1790) feeding on and damaging rice and *Menida pinicola* Zheng & Liu, 1987 feeding on and damaging pine trees. The body shape of *Menida* species is oval, and the surface is often with a metallic luster and color spots. However, the body color is variable and some species have a large range of variation (Li 2015), which can cause difficulties in identifications. Most of the research on the genus has focused on morphology or biology and less on the mitochondrial genome (Dai and Zheng 2005; Li et al. 2015; Markova et al. 2020).

In this study, we newly sequenced the complete mitochondrial genomes of three species of *Menida* based on high-throughput sequencing, analyzed the characteristics of the mitochondrial genome in detail and drew the secondary structure of RNA. By comparing and analyzing the characteristics of mitochondrial genome sizes, nucleotide composition, codon preference, RNA structure, and evolutionary rates among *Menida* species, we explore the phylogenetic position of *Menida* in Pentatominae, as well as the relationship of tribes within the subfamily Pentatominae. The new data will provide a reference for the phylogenetic analysis and identification of Pentatomidae.

Materials and methods

Sample collection and DNA extraction

Adult specimens of *Menida musiva* (Jakovlev, 1876) were collected from Gaoleshan National Nature Reserve (32°39.90'N, 113°37.37'E), Tongbai County, Nanyang City, Henan Province, China, in August 2019. Adult specimens of *M. lata* Yang, 1934 were collected from Buddhist College of Tongbo County (32°21'N, 113°23'E), Nanyang City, Henan Province, China, in August 2019. Adult specimens of *M. metallica* Hsiao & Cheng, 1977 were collected from Wuli Village (30°52'N, 103°35'E), Qingchengshan Town, Dujiangyan City, Sichuan Province, China, in September 2020. All samples were immediately placed in absolute ethanol and stored in a freezer at –20 °C until DNA extraction. The total DNA was extracted from thoracic tissue using the HiPure Universal DNA Kit (Jisi Huiyuan biotechnology, Nanjing, China).

Sequencing, assembly, annotation, and bioinformatics analyses

The complete mitochondrial genomes of the three species were sequenced on Illumina Novaseq 6000 Sequencing System with a read length of PE150. Fastp (Chen et al. 2018) software was used to filter the original data and remove the joint sequences and low-quality reads to obtain high-quality, clean data. Three mitochondrial genomes were assembled using SPAdes v. 3.10.1 (Bankevich et al. 2012), and the assembly of the genomes did not depend on the reference genome. After assembly, the complete mitogenomes were manually annotated using Geneious v. 11.0 (Kearse et al. 2012) software. A reference sequence of *M. violacea* for annotation was obtained from the basic local alignment search tool (BLAST) in the NCBI database. PCGs were identified by open reading frame (ORF) Finder (http://www.ncbi.nlm.nih.gov/gorf/gorf.html) implemented through the NCBI website using invertebrate mitochondrial genetic codes. The position and structure of 22 tRNAs were predicted using the MITOS Web Server (http://mitos.bioinf.uni-leipzig.de/index.py/) (Bernt et al. 2013). The exact locations of rRNA adjacent genes and the control regions were determined by confirming the boundary between them. In addition, tandem repeats of the control region were identified with the Tandem Repeats Finder server (http://tandem.bu.edu/trf/trf.html) (Benson 1999).

The circular maps of mitogenomes were produced by the CGView Server (Grant and Stothard 2008). Nucleotide composition and codon usage were analyzed with MEGA v. 11 (Tamura et al. 2021). To investigate the evolutionary patterns among the mitochondrial PCGs in Pentatominae species, DnaSP5 software (Librado and Rozas 2009) was used to count the non-synonymous substitutions (Ka) and synonymous substitutions (Ks) of 13 PCGs of Pentatominae, and to calculate the Ka/Ks values. The skew of the nucleotide composition was calculated with the formulas: AT-skew = (A – T) / (A + T) and GC-skew = (G – C) / (G + C) (Perna and Kocher 1995).

Phylogenetic analysis

We selected three newly sequenced species of *Menida* and 37 available mitogenomes of related taxa (including all available Pentatominae sequences and two Acanthosomatidae sequences as outgroups) from GenBank to determine the phylogenetic status of *Menida* and to discuss the phylogenetic relationships of tribes within the subfamily Pentatominae (Table 1). The phylogenetic relationships were reconstructed based on two datasets: (1) 13 PCGs + 2 rRNAs (PR) and (2) 13 PCGs + 2 rRNAs + 22 tRNAs (PRT). The two data sets represent relatively complete genetic evolution information of mitochondrial genomes.

The nucleic acid sequences of the PCGs and RNA genes were extracted using Geneious v. 11.0 and aligned using the MUSCLE strategy in MEGA v. 11. Multiple sequences for each species were then connected using SequenceMatrix v. 1.7.8 (Vaidya et al. 2011), protein-coding genes were optimized using MACSE (Ranwez et al. 2011), ambiguous loci were deleted using Gblocks (Talavera and Castresana 2007), and converted into Nexus and Phylip formats in Mesquite v. 3.7 (Maddison 2008). To determine the best model for partitioning, four datasets were analyzed us-

Table 1. List of sequences used to reconstruct the phylogenetic relationships within Pentatominae.

Family	Subfamily	Tribe	Species	GenBank number	Reference
Pentatomidae	Pentatominae	Antestiini	*Anaxilaus musgravei*	MW679031	Unpublished
		Antestiini	*Plautia crossota*	NC_057080	(Wang et al. 2019)
		Antestiini	*Plautia fimbriata*	NC_042813	(Liu et al. 2019)
		Antestiini	*Plautia lushanica*	NC_058973	(Xu et al. 2021)
		Cappaeini	*Halyomorpha halys*	NC_013272	(Lee et al. 2009)
		Carpocorini	*Dolycoris baccarum*	NC_020373	(Zhang et al. 2013)
		Catacanthini	*Catacanthus incarnatus*	NC_042804	(Liu et al. 2019)
		Caystrini	*Caystrus obscurus*	NC_042805	(Liu et al. 2019)
		Caystrini	*Hippotiscus dorsalis*	NC_058969	(Xu et al. 2021)
		Eysarcorini	*Carbula sinica*	NC_037741	(Jiang 2017)
		Eysarcorini	*Eysarcoris aeneus*	MK841489	(Zhao et al. 2019a)
		Eysarcorini	*Eysarcoris annamita*	MW852483	(Li et al. 2021)
		Eysarcorini	*Stagonomus gibbosus*	MW846868	(Li et al. 2021)
		Eysarcorini	*Eysarcoris guttigerus*	NC_047222	(Chen et al. 2020b)
		Eysarcorini	*Eysarcoris montivagus*	MW846867	(Li et al. 2021)
		Eysarcorini	*Eysarcoris rosaceus*	MT165687	(Li et al. 2021)
		Halyini	*Dalpada cinctipes*	NC_058967	(Xu et al. 2021)
		Halyini	*Erthesina fullo*	NC_042202	(Ji et al. 2019)
		Hoplistoderini	*Hoplistodera incisa*	NC_042799	(Liu et al. 2019)
		Menidini	*Menida musiva*	OP066239	This study
		Menidini	*Menida metallica*	OP066240	This study
		Menidini	*Menida lata*	OP066241	This study
		Menidini	*Menida violacea*	NC_042818	(Liu et al. 2019)
		Nezarini	*Glaucias dorsalis*	NC_058968	(Xu et al. 2021)
		Nezarini	*Nezara viridula*	NC_011755	(Hua et al. 2008)
		Nezarini	*Palomena viridissima*	NC_050166	(Chen et al. 2021)
		Pentatomini	*Neojurtina typica*	NC_058971	(Xu et al. 2021)
		Pentatomini	*Pentatoma metallifera*	NC_058972	(Xu et al. 2021)
		Pentatomini	*Pentatoma rufipes*	MT861131	(Zhao et al 2021)
		Pentatomini	*Pentatoma semiannulata*	NC_053653	(Wang et al. 2021)
		Pentatomini	*Placosternum urus*	NC_042812	(Liu et al. 2019)
		Sephelini	*Brachymna tenuis*	NC_042802	(Liu et al. 2019)
		Strachiini	*Eurydema dominulus*	NC_044762	(Zhao et al. 2019b)
		Strachiini	*Eurydema gebleri*	NC_027489	(Yuan et al. 2015)
		Strachiini	*Eurydema liturifera*	NC_044763	(Zhao et al. 2019b)
		Strachiini	*Eurydema maracandica*	NC_037042	(Zhao et al. 2017)
		Strachiini	*Eurydema oleracea*	NC_044764	(Zhao et al. 2019b)
		Strachiini	*Eurydema qinlingensis*	NC_044765	(Zhao et al. 2019b)
Acanthosomatidae	Acanthosomatinae		*Anaxandra taurina*	NC_042801	(Liu et al. 2019)
			Sastragala esakii	NC_058975	(Xu et al. 2021)

ing PartitionFinder v. 2.1.1 (Lanfear et al. 2017). The maximum likelihood (ML) and Bayesian inference (BI) methods were used for phylogenetic analysis based on two datasets. The ML trees were constructed by IQ-TREE v. 2.2.0 (Minh et al. 2020), and the support value for each node was evaluated by the standard bootstrap (BS) algorithm, which was tested 500,000 times. The Bayesian inference (BI) method was used for phylogenetic analysis based on four datasets. The BI tree was constructed by

MrBayes v. 3.2.7 (Ronquist et al. 2012). Two independent runs were run for 10 million generations, and samples were taken every 1000 generations. Four independent Markov Chains (including three heated chains and a cold chain) were run. A consensus tree was obtained from all the trees after the initial 25% of trees from each MCMC run were discarded as burn-in, with the chain convergence assumed after the average standard deviation of split frequencies fell below 0.01.

Results

Mitochondrial genomic structure

We studied the relationship among four species of *Menida* (three newly sequenced species and one species downloaded from NCBI). All four mitogenomes are double-strand circular DNA molecules. The total lengths of the mitogenomes of *M. musiva*, *M. lata*, *M. metallica*, and *M. violacea* are 16,663bp, 16,463bp, 16,418bp, and 15,379bp, respectively. The mitogenomes of the four species each contain 37 genes (13 protein-coding genes (PCGs), 22 tRNA genes, and 2 rRNA genes) and a control region (Fig. 1), with 23 genes located on the J-strand and 14 genes on the N-strand.

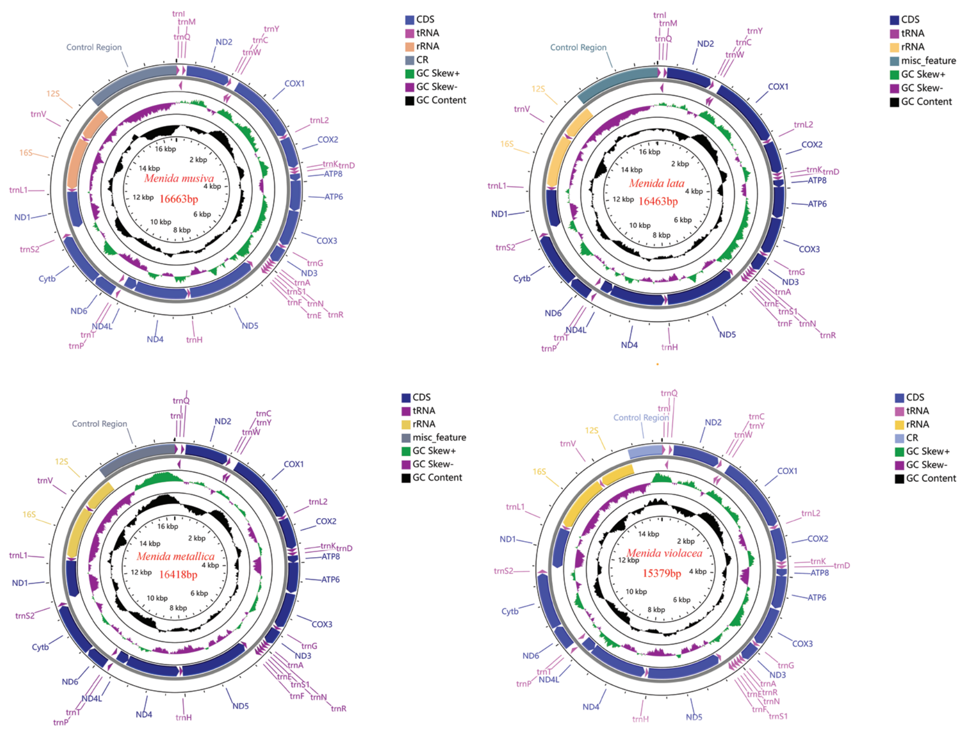

Figure 1. Gene arrangements of the four complete mitochondrial genomes.

The sequence of genes was consistent with the original gene arrangement of *Drosophila yakuba* Burla, 1954 (Clary and Wolstenholme 1985; Hua et al. 2008) without rearrangement. Nucleotide composition of the complete mitogenome of *M. musiva*: A 42.51%, T 33.70%, C 14.18%, G 9.60%; nucleotide composition of the complete mitogenome of *M. lata*: A 41.95%, T 32.92%, C 15.08%, G 10.05%; nucleotide composition of the complete mitogenome of *M. metallica*: A 41.39%, T 33.51%, C 13.77%, G 11.33%; nucleotide composition of the complete mitogenome of *M. violacea*: A: 42.19%, T: 33.32%, C: 13.86%, G: 11.33%. The four species show similar nucleotide composition (Suppl. material 1: table S1). All the mitogenomes exhibit a strong base composition bias toward AT, ranging from 74.86% to 76.22% in the four species (mean value = 75.37%). Moreover, all mitogenomes have a slightly positive AT-skew (ranging from 0.11 to 0.12, mean = 0.11) and a negative GC-skew (ranging from 0.20 to –0.10, mean = –0.16) (Suppl. material 1: table S1).

The four mitogenomes have similar overlapping regions and gene spacers. The longest intergenic region (31–34bp) of the four species of the genus *Menida* appeared between *trnS2* and *nad1*, and there were mainly three conserved overlaps, with a 8 bp overlap between *trnC*/*trnW* (AAGCTTTA) and a 7 bp overlap between *atp8*/*atp6* and *nad4*/*nad4L* (ATGATAA) (Suppl. material 1: table S2).

Protein-coding genes

For the four studied species, nine PCGs (*nad2*, *cox1*, *cox2*, *atp8*, *atp6*, *cox3*, *nad3*, *nad6*, and *cytb*) were found to be coded on the majority strand (J-strand) and four PCGs (*nad5*, *nad4*, *nad4L*, and *nad1*), on the minority strand (N-strand). The longest PCG is *nad5* (1707–1710 bp), while the shortest is *atp8* (159 bp). Five PCGs (*cox1*, *cox2*, *atp8*, *atp6*, and *nad3*) did not vary in length among the four species. Most of the PCGs use ATN (ATT/ATA/ATG/ATC) as initiation codon. TTG was the second most used initiation codon, and was found in *cox1*, *atp8*, *nad1*, and *nad6* (except in *M. musiva*). The coding region of most PCGs ends with the complete termination codon TAA, except *cox1*, *cox2*, and *nad3*, which ended with the incomplete stop codon T (Suppl. material 1: table S2).

Statistics on the relative synonymous codon usage (RSCU) of the four species showed distinct bias and similar codon usage patterns. The most frequently used codons are UUA (Leu2), while the least commonly used codons are AAC (Asn), GAC (Asp), UGC (Cys), CAC (His), AUC (Ile), UUC (Phe), and UAC (Tyr) (Fig. 2). These results indicate that the codons of the mitochondrial protein-coding genes of *Menida* prefer the codon ending with A/T.

To further investigate the codon usage bias among Pentatominae species, we analyzed the correlations between ENC (effective number of codons), the GC content of all codons, and the GC content of the third codon positions. We found a positive correlation between ENC and GC content for all codons (R^2 = 0.9199) and the third codon positions (R^2 = 0.959) (Fig. 3). These results are consistent with prevailing neutral mutational theories, in which genomic GC content is the most significant factor in determining codon bias among organisms.

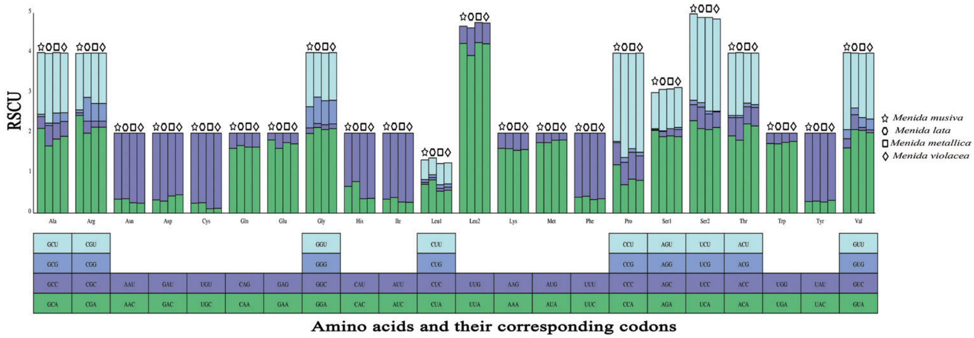

Figure 2. Relative synonymous codon usage (RSCU) in the mitogenomes of four *Menida* species.

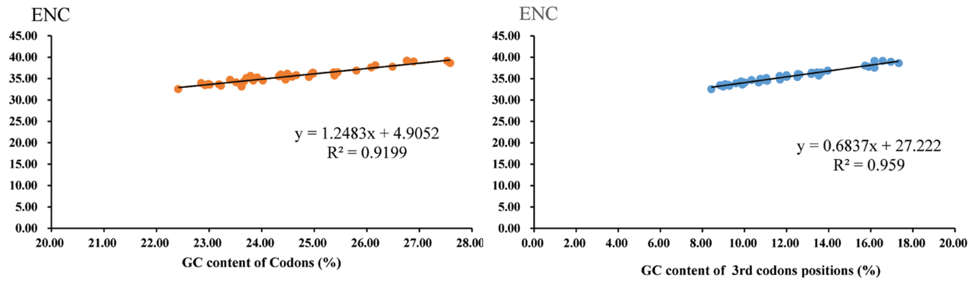

Figure 3. Evaluation of codon bias in the mitochondrial genomes of 40 Pentatominae species.

The values of Ka (the number of non-synonymous substitutions per nonsynonymous site), Ks (the number of synonymous substitutions per synonymous site), and Ka/Ks were calculated for each PCG, respectively (Fig. 3). The Ka/Ks ratio for all 13 PCGs were below 1.0, indicating evolution under purifying selection. The Ka/Ks ratio of *atp8* was the highest, while that of *cox1* was the lowest. We also observed lower Ka/Ks ratios in the genes that are usually used as a barcode, such as *cox2*, *cox3*, and *cytb*; it is showed that at the nucleotide and amino acid levels, these four genes had the lowest evolutionary rates (Fig. 4).

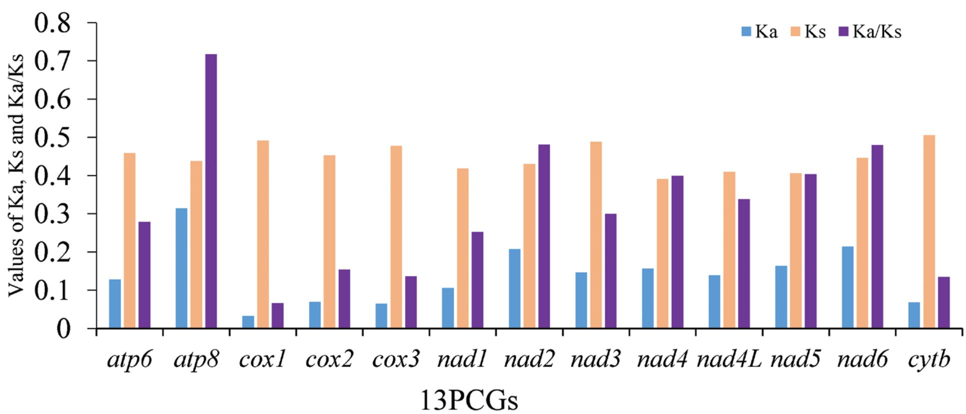

Figure 4. The Ka, Ks, and Ka/Ks values of protein-coding genes within Pentatominae.

Transfer and ribosomal RNAs

The total lengths of the 22 tRNAs of the four species range between 1464 bp (*M. musiva*) and 1484 bp (*M. metallica*), and the length of 22 tRNA genes ranged from 63 to 72 bp. Fourteen tRNA genes (*trnI*, *trnM*, *trnW*, *trnL2*, *trnK*, *trnD*, *trnG*, *trnA*, *trnR*, *trnN*, *trnS1*, *trnE*, *trnT*, *trnS2*) are coded on the J-strand and eight (*trnQ*, *trnC*, *trnY*, *trnF*, *trnH*, *trnP*, *trnL1*, *trnV*) on the N-strand. We found that only *trn S1* lacked the dihydrouridine (DHU) arm, and the remaining 21 tRNA genes can form a typical cloverleaf structure in the four species. All tRNAs in the four mitogenomes use the standard anticodon. Among all the tRNAs of the four species in *Menida*, *trnH* has the weakest conservatism compared with other genes. In addition, 16 wobble G-U pairs were found in 22 tRNAs of *Menida* (Fig. 5), which usually need three-dimensional structure to stabilize.

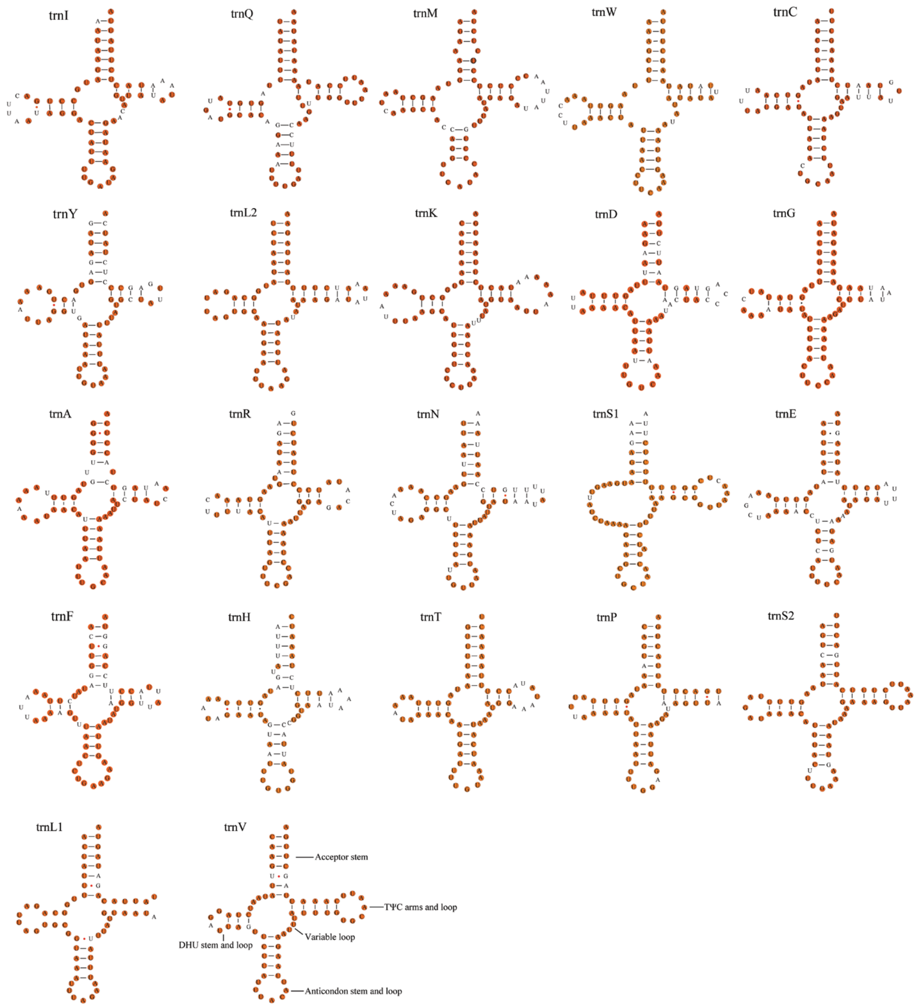

Figure 5. Potential secondary structure of tRNA in *Menida musiva*. The conserved sites within *Menida* were marked in orange.

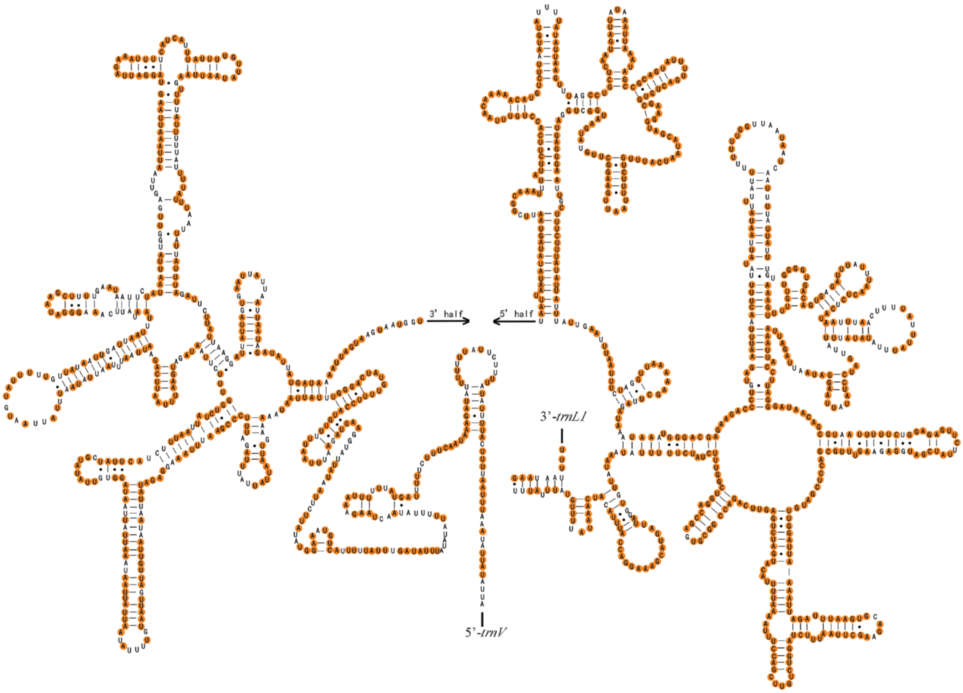

Figure 6. Potential secondary structure of *16S* rRNA in *Menida musiva*. The conserved sites within *Menida* were marked in orange.

The two rRNA genes (*12S* rRNA and *16S* rRNA) are encoded on the N-strand in these species. The *16S* rRNA gene, ranging from 1277 to 1285 bp in size, is located at a conserved position between *trnL1* and *trnV*. The *12S* rRNA (795–804 bp) was found between *trnV* and the control region. The complete secondary structures of the *12S* rRNA and *16S* rRNA genes are shown in Figs 6, 7, respectively. In *Menida*, *16S* rRNA contained 78.49% conserved sites and *12S* rRNA contained 78.17% conserved sites.

Control region

The control regions located between *12S* rRNA and *trnI* of the four species showed more variation in length, and the length ranged from 686 to 2,002 bp. This variation leads to the difference in the total length of its mitochondrial genome. The AT content in the control area of *M. musiva* (82.82%) was significantly higher than that of the other three species. The longest repeating unit length (284 bp) was found in *M. metallica*. However, no tandem repeats were detected in *M. violacea* (Fig. 8).

Phylogenetic relationships

Before constructing the phylogenetic tree, we performed saturation and heterogeneity analysis on two data sets. Saturation analysis showed that the sequence was not saturated (*Iss* < *Iss.c*, and $p < 0.05$) (Suppl. material 1: fig. S1). Heterogeneity analysis of the two data sets shows that the composition of the sequence has low heterogeneity (Fig. 9). These two data sets are suitable for further phylogenetic studies.

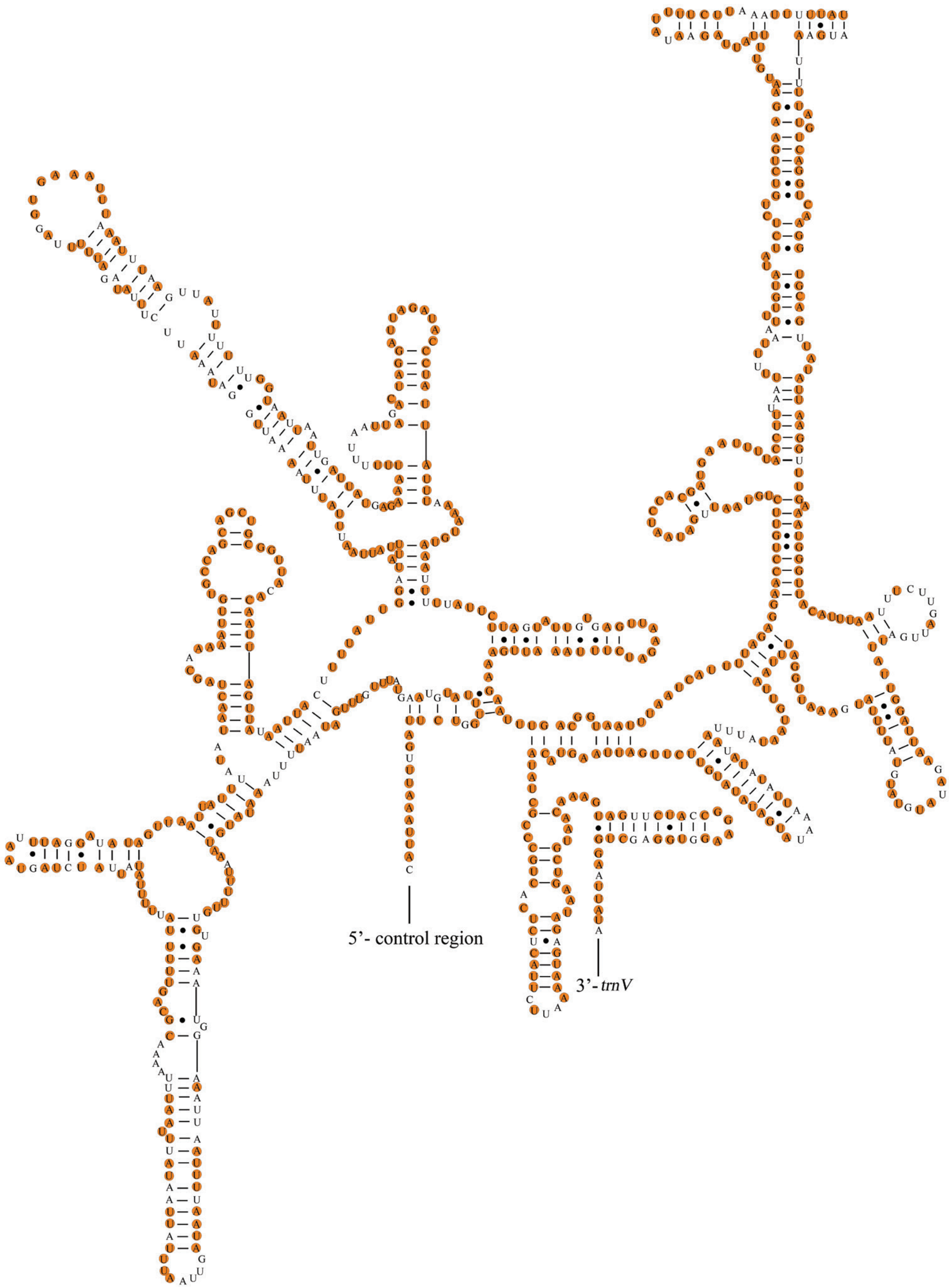

Figure 7. Potential secondary structure of *12S* rRNA in *Menida musiva*. The conserved sites within *Menida* were marked in orange.

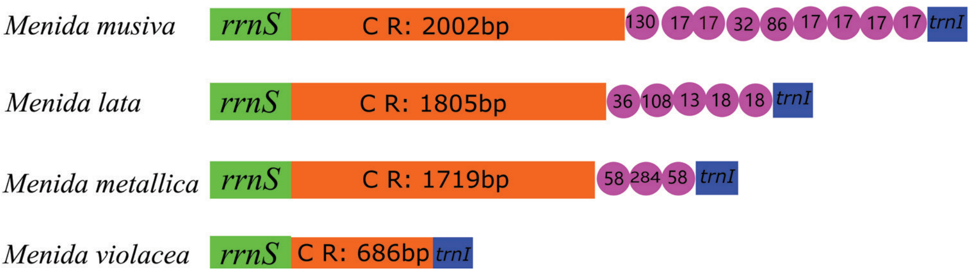

Figure 8. Organization of the control region in the four mitochondrial genomes. The tandem repeats are showed by the magenta circle with repeat length inside. The orange boxes indicate the length of the sequence of the control region.

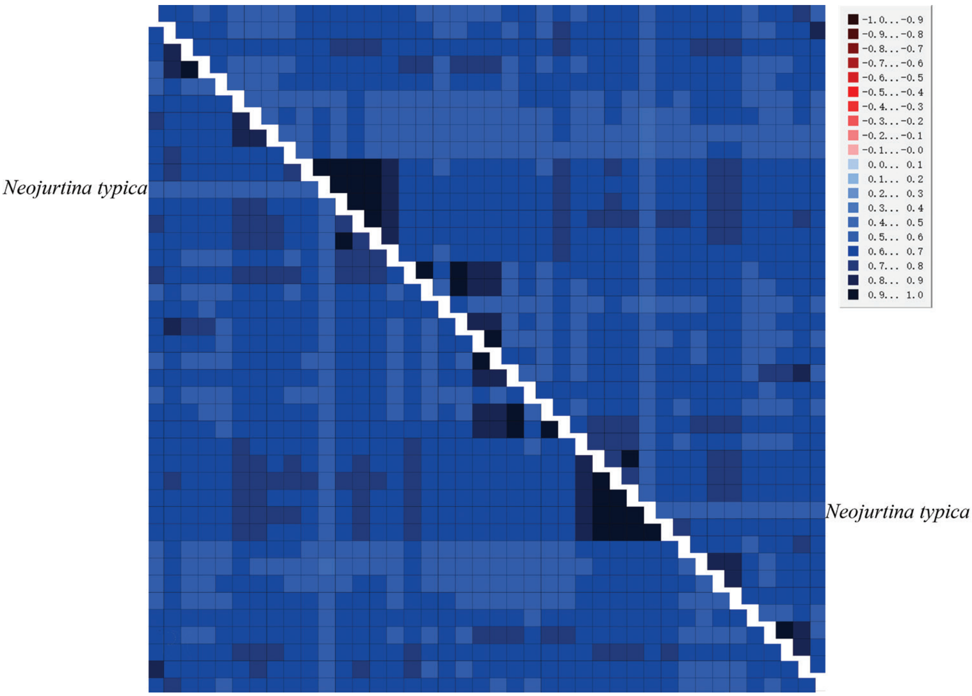

Figure 9. Analysis of heterogeneity of sequence divergence for two datasets (PRT and PR). The heterogeneity of the corresponding sequence relative to other sequences increases as the indicated color becomes lighter. The species with relatively higher sequence heterogeneity are shown.

We constructed phylogenetic trees of Pentatominae based on the two data sets using BI and ML (Fig. 10). The topological structure of the four trees was highly consistent, and most clades had high posterior probabilities. The phylogenetic positions of the Pentatominae are as follows: (*Neojurtina* + ((Caystrini + Halyini) + (Eysarcorini + (Carpocorini + ((*Palomena* + *Nezara*) + (*Anaxilaus* + (*Glaucias* + *Plautia*))))) + ((*Placosternum* + Cappaeini) + (Sephelini + ((Catacanthini + Strachiini) + (*Pentatoma* +

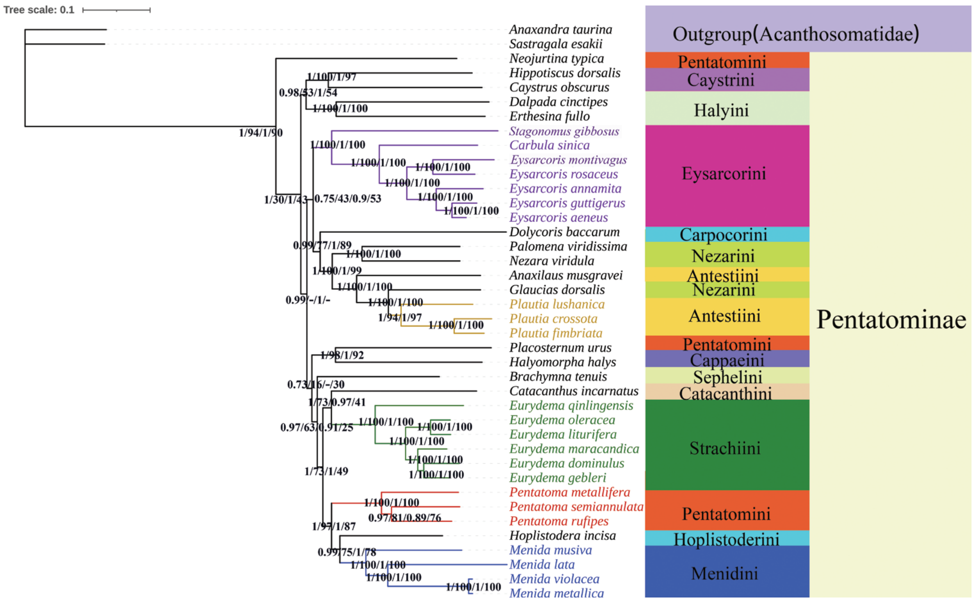

Figure 10. Phylogenetic relationships inferred by the BI and ML method based on the PRT and PR datasets. Numbers on nodes are the posterior probabilities (PP).

(Hoplistoderini + Menidini))))))). The species *Neojurtina typica* Distant, 1921 was the earliest diverged lineage within Pentatominae. Other species of Pentatominae were scattered in the phylogenetic tree. *Placosternum* and Cappaeini form a sister-group relationship, and the phylogenetic tree also strongly supports the monophyly of *Pentatoma*. Caystrini and Halyini form a sister group relationship. At the same time, our phylogenetic relationship also shows that the genus *Menida* and Hoplistoderini are closely related within Pentatominae. The four *Menida* species are well grouped; *M. metallica* and *M. violacea* are closely related, and *M. lata* has the longest differentiation time compared to the other species.

Discussion and conclusions

In this study, we sequenced the complete mitochondrial genomes of *M. musiva*, *M. lata*, and *M. metallica* based on high-throughput sequencing. Compared with other species of *Menida* with published genomes, no gene rearrangement occurred in the four mitochondrial genomes, and the gene arrangements are conserved, which are consistent with other published mitochondrial genomes of Hemiptera (Lee et al. 2009; Li et al. 2013; Zhang et al. 2013; Wang et al. 2018; Zhao et al. 2018). The size of the complete mitochondrial genome sequence of *Menida* varies greatly, ranging from 15,379 bp in *M. violacea* to 16,663 bp in *M. musiva* (Suppl. material 1: table S2), mainly due to the significant size change of the control region. Previous studies have reported different sizes and different tandem repeats in other Pentatomidae species (Yuan et al. 2015; Zhao et al. 2020; Li et al. 2021). The nucleotide composition of *Menida* is extremely unbalanced (A > T>C > G), showing a strong AT preference. In addition, our analysis of relative synonymous codon usage showed that the codon of protein-coding genes preferred to end with A/T, which was common in all sequenced Pentatomidae (Yuan and Guo 2016). This preference for nucleotide composition is generally thought to be caused by mutational pressures and natural selection (Hassanin et al. 2005).

Most PCGs of mitochondrial genomes of *Menida* use ATN as the initiation codon. TTG is another commonly used start codon and is commonly found in the protein-coding genes (*cox1*, *atp8*, *nad1*, and *nad6*), which is similar to most mitochondrial genomes of Pentatomidae. We found that the stop codon of most PCGs ends with TAA or TAG, while *cox1* and *cox2* end with incomplete stop codon T, which is more conservative in Pentatomidae (Yuan et al. 2015; Zhao et al. 2019b). In addition, most species of Hemiptera also show these three kinds of overlaps, mainly including *trnC*/*trnW* overlap of 8 bp (AAGCTTTA), *atp8*/*atp6* and *nad4*/*nad4l* overlap of 7 bp (ATGATAA) (Zhang et al. 2019).

In the genus *Menida*, tRNAs (except *trnS1*) have a typical shamrock secondary structure and are highly conserved. *TrnS1* lacks DHU arms and only has a ring structure, which is common in many other insect groups. In addition to typical Watson-Crick pairings (G-C and A-U), there are also some atypical pairings such as G-U pairings, and these non-Watson-Crick pairings can be transformed into fully functional proteins by post-transcriptional mechanisms (Chao et al. 2008; Pons et al. 2014).

We obtained highly similar topology based on two different methods of two datasets. Our results are basically consistent with the traditional morphological classification and recent molecular studies (Rider et al. 2018; Chen et al. 2021; Genevcius et al. 2021). Eysarcorini and Strachiini are highly supported as monophyletic (1/100/1/100). We provide support for Roca-Cusachs and Jung's (2019) suggestion to transfer *E. gibbosus* Jakovlev, 1904 to the genus *Stagonomus* Gorski, 1852. In previous studies, Zhao et al. (2019b) showed that species of *Eurydema* Laporte, 1833 form a sister group with *N. viridula* (Linnaeus, 1758). However, in our study, Catacanthini and Strachiini formed a sister group relationship, and this is also different from the results of Li et al. (2021); more species may be required to support this relationship. Rider et al. (2018) temporarily placed *Plautia* (Stål, 1865) in Antestiini, and our phylogenetic results supported this morphology-based view. Both Antestiini and Nezarini are found non-monophyletic, but combined they form a monophyletic group. At the same time, our phylogenetic analysis also strongly supports the monophyly of the examined species of the genus *Menida*, and the internal relationship of the genus *Menida*: (*M. musiva* + (*M. lata* + (*M. violacea* + *M. metallica*))). However, because there are too few species in this study, the monophyly of the genus *Menida* cannot be well determined, and it is expected to be supplemented by subsequent studies. In addition, in view of the richness of species, it is necessary to analyze more groups, and then clarify the taxonomic status of subfamilies or tribes in Pentatomidae by combining morphological and molecular data.

In the present study, three mitochondrial genomes from the Pentatomidae were analyzed, and the monophyly of some genus has been supported. Due to the richness and diversity of the genus *Menida*, some species within the genus have great morphological variation, so it will be difficult to morphologically identify these species. The addition of these three mitochondrial sequences can provide some data support for the identification of *Menida* species. However, more insect mitochondrial genomes need to be sequenced, which is of great significance for understanding the evolution of mitochondrial genomes and for clarifying the phylogenetic relationship of Pentatomidae.

Acknowledgements

This research was funded by the National Science Foundation Project of China (no. 31872272); the Research Project Supported by Shanxi Scholarship Council of China (no. 2020-064 and no. 2020-065), Natural Science Research General Project of Shanxi Province (no. 202103021224331 and 202103021224132).

References

Bankevich A, Nurk S, Antipov D, Gurevich AA, Dvorkin M, Kulikov AS, Lesin VM, Nikolenko SI, Pham S, Prjibelski AD, Pyshkin AV, Sirotkin AV, Vyahhi N, Tesler G, Alekseyev MA, Pevzner PA (2012) SPAdes: A new genome assembly algorithm and its applications to single-cell sequencing. Journal of Computational Biology 19(5): 455–477. https://doi.org/10.1089/cmb.2012.0021

Benson G (1999) Tandem repeats finder: A program to analyze DNA sequences. Nucleic Acids Research 27(2): 573–580. https://doi.org/10.1093/nar/27.2.573

Bernt M, Donath A, Juhling F, Externbrink F, Florentz C, Fritzsch G, Putz J, Middendorf M, Stadler PF (2013) MITOS: Improved de novo metazoan mitochondrial genome annotation. Molecular Phylogenetics and Evolution 69(2): 313–319. https://doi.org/10.1016/j.ympev.2012.08.023

Boore JL (1999) Animal mitochondrial genomes. Nucleic Acids Research 27(8): 1767–1780. https://doi.org/10.1093/nar/27.8.1767

Chao JA, Patskovsky Y, Almo SC, Singer RH (2008) Structural basis for the coevolution of a viral RNA-protein complex. Nature Structural & Molecular Biology 15(1): 103–105. https://doi.org/10.1038/nsmb1327

Chen S, Zhou Y, Chen Y, Gu J (2018) fastp: An ultra-fast all-in-one FASTQ preprocessor. Bioinformatics (Oxford, England) 34(17): i884–i890. https://doi.org/10.1093/bioinformatics/bty560

Chen LP, Zheng FY, Bai J, Wang JM, Lv CY, Li X, Zhi YC, Li XJ (2020a) Comparative analysis of mitogenomes among six species of grasshoppers (Orthoptera: Acridoidea: Catantopidae) and their phylogenetic implications in wing-type evolution. International Journal of Biological Macromolecules 159: 1062–1072. https://doi.org/10.1016/j.ijbiomac.2020.05.058

Chen Q, Niu X, Fang Z, Weng Q (2020b) The complete mitochondrial genome of *Eysarcoris guttigerus* (Hemiptera: Pentatomidae). Mitochondrial DNA. Part B, Resources 5(1): 687–688. https://doi.org/10.1080/23802359.2020.1714498

Chen WT, Zhang LJ, Cao Y, Yuan ML (2021) The complete mitochondrial genome of *Palomena viridissima* (Hemiptera: Pentatomidae) and phylogenetic analysis. Mitochondrial DNA, Part B, Resources 6(4): 1326–1327. https://doi.org/10.1080/23802359.2021.1909442

Clary DO, Wolstenholme DR (1985) The mitochondrial DNA molecule of *Drosophila yakuba*: Nucleotide sequence, gene organization, and genetic code. Journal of Molecular Evolution 22(3): 252–271. https://doi.org/10.1007/BF02099755

Dai JX, Zheng ZM (2005) Phylogenetic relationships of eleven species of Pentatominae based on sequences of cytochrome b gene. Yingyong Kunchong Xuebao 42: 395–399.

Genevcius BC, Greve C, Koehler S, Simmons RB, Rider DA, Grazia J, Schwertner CF (2021) Phylogeny of the stink bug tribe Chlorocorini (Heteroptera, Pentatomidae) based on DNA and morphological data: The evolution of key phenotypic traits. Systematic Entomology 46(2): 327–338. https://doi.org/10.1111/syen.12464

Grant JR, Stothard P (2008) The CGView Server: A comparative genomics tool for circular genomes. Nucleic Acids Research 36(Web Server): W181–W184. https://doi.org/10.1093/nar/gkn179

Hassanin A, Leger N, Deutsch J (2005) Evidence for multiple reversals of asymmetric mutational constraints during the evolution of the mitochondrial genome of Metazoa, and consequences for phylogenetic inferences. Systems Biology 54(2): 277–298. https://doi.org/10.1080/10635150590947843

Hua J, Li M, Dong P, Cui Y, Xie Q, Bu W (2008) Comparative and phylogenomic studies on the mitochondrial genomes of Pentatomomorpha (Insecta: Hemiptera: Heteroptera). BMC Genomics 9(1): 610. https://doi.org/10.1186/1471-2164-9-610

Ji H, Xu X, Jin X, Yin H, Luo J, Liu G, Zhao Q, Chen Z, Bu W, Gao S (2019) Using high-resolution annotation of insect mitochondrial DNA to decipher tandem repeats in the control region. RNA Biology 16(6): 830–837. https://doi.org/10.1080/15476286.2019.1591035

Jiang P (2017) Studies on the comparative mitochondrial genomics and phylogeny of Heteroptera (Insecta: Hemiptera). PhD, China Agricultural University, Beijing.

Kearse M, Moir R, Wilson A, Stones-Havas S, Cheung M, Sturrock S, Buxton S, Cooper A, Markowitz S, Duran C, Thierer T, Ashton B, Meintjes P, Drummond A (2012) Geneious Basic: An integrated and extendable desktop software platform for the organization and analysis of sequence data. Bioinformatics 28(12): 1647–1649. https://doi.org/10.1093/bioinformatics/bts199

Lanfear R, Frandsen PB, Wright AM, Senfeld T, Calcott B (2017) PartitionFinder 2: New methods for selecting partitioned models of evolution for molecular and morphological phylogenetic analyses. Molecular Biology and Evolution 34: 772–773. https://doi.org/10.1093/molbev/msw260

Lee W, Kang J, Jung C, Hoelmer K, Lee SH, Lee S (2009) Complete mitochondrial genome of brown marmorated stink bug *Halyomorpha halys* (Hemiptera: Pentatomidae), and phylogenetic relationships of hemipteran suborders. Molecules and Cells 28(3): 155–165. https://doi.org/10.1007/s10059-009-0125-9

Li XR (2015) A study of the genus *Menida* Motschulsky from China (Hemiptera: Heteroptera: Pentatomidae). PhD thesis, Nankai University, Tianjin.

Li T, Gao C, Cui Y, Xie Q, Bu W (2013) The complete mitochondrial genome of the stalk-eyed bug *Chauliops fallax* Scott, and the monophyly of Malcidae (Hemiptera: Heteroptera). PLoS ONE 8(2): e55381. https://doi.org/10.1371/journal.pone.0055381

Li XR, Fan ZH, Liu GQ (2015) Note on genus *Menida* Motschulsky from China (Hemiptera: Pentatomidae). Journal of Tianjin Normal University 35(03): 12–22. [Natural Science Edition]

Li R, Li M, Yan J, Bai M, Zhang H (2021) Five mitochondrial genomes of the genus *Eysarcoris Hahn*, 1834 with phylogenetic implications for the Pentatominae (Hemiptera: Pentatomidae). Insects 12(7): 597. https://doi.org/10.3390/insects12070597

Librado P, Rozas J (2009) DnaSP v5: A software for comprehensive analysis of DNA polymorphism data. Bioinformatics (Oxford, England) 25(11): 1451–1452. https://doi.org/10.1093/bioinformatics/btp187

Liu Y, Li H, Song F, Zhao Y, Wilson JJ, Cai W (2019) Higher-level phylogeny and evolutionary history of Pentatomomorpha (Hemiptera: Heteroptera) inferred from mitochondrial genome sequences. Systematic Entomology 44(4): 810–819. https://doi.org/10.1111/syen.12357

Maddison WP (2008) Mesquite: A modular system for evolutionary analysis. Evolution 62: 1103–1118. https://doi.org/10.1111/j.1558-5646.2008.00349.x

Markova TO, Kanyukova EV, Maslov MV (2020) On the ecology of the shield bug *Menida violacea* Motschulsky, 1861 (Heteroptera, Pentatomidae), host of parasitic dipterans (Diptera, Tachinidae) in the south of Primorskii Territory (Russia). Entomological Review 100(4): 466–472. https://doi.org/10.1134/S0013873820040053

Mi Q, Zhang J, Gould E, Chen J, Sun Z, Zhang F (2020) Biology, ecology, and management of *Erthesina fullo* (Hemiptera: Pentatomidae): a review. Insects 11(6): 346. https://doi.org/10.3390/insects11060346

Minh BQ, Schmidt HA, Chernomor O, Schrempf D, Woodhams MD, Von Haeseler A, Lanfear R (2020) IQ-TREE 2: new models and efficient methods for phylogenetic inference in the genomic era. Molecular biology and evolution 37(5): 1530–1534. https://doi.org/10.1093/molbev/msaa015

Perna NT, Kocher TD (1995) Patterns of nucleotide composition at fourfold degenerate sites of animal mitochondrial genomes. Journal of Molecular Evolution 41(3): 353–358. https://doi.org/10.1007/BF01215182

Pons J, Bauzà-Ribot MM, Jaume D, Juan C (2014) Next-generation sequencing, phylogenetic signal and comparative mitogenomic analyses in Metacrangonyctidae (Amphipoda: Crustacea). BioMed Central 15(1): e566. https://doi.org/10.1186/1471-2164-15-566

Ranwez V, Harispe S, Delsuc F, Douzery EJ (2011) MACSE: Multiple Alignment of Coding SEquences accounting for frameshifts and stop codons. PLoS ONE 6(9): e22594. https://doi.org/10.1371/journal.pone.0022594

Rider DA, Schwertner CF, Vilímová J, Rédei D, Kment P, Thomas DB (2018) Higher systematics of the Pentatomoidea. In: McPherson JE (Ed.) Invasive Stink Bugs and Related Species (Pentatomoidea): Biology, Higher Systematics, Semiochemistry, and Management. CRC Press, Boca Raton, 25–204. https://doi.org/10.1201/9781315371221-2

Roca-Cusachs M, Jung S (2019) Redefining *Stagonomus* Gorski based on morphological and molecular data (Pentatomidae: Eysarcorini). Zootaxa 4658: 368–374. https://doi.org/10.11646/zootaxa.4658.2.10

Roca-Cusachs M, Schwertner CF, Kim J, Eger J, Grazia J, Jung S (2022) Opening Pandora's box: molecular phylogeny of the stink bugs (Hemiptera: Heteroptera: Pentatomidae) reveals great incongruences in the current classification. Systematic Entomology 47(1): 36–51. https://doi.org/10.1111/syen.12514

Ronquist F, Teslenko M, van der Mark P, Ayres DL, Darling A, Hohna S, Larget B, Liu L, Suchard MA, Huelsenbeck JP (2012) MrBayes 3.2: Efficient Bayesian phylogenetic inference and model choice across a large model space. Systematic Biology 61(3): 539–542. https://doi.org/10.1093/sysbio/sys029

Simon S, Hadrys H (2013) A comparative analysis of complete mitochondrial genomes among Hexapoda. Molecular Phylogenetics and Evolution 69(2): 393–403. https://doi.org/10.1016/j.ympev.2013.03.033

Talavera G, Castresana J (2007) Improvement of phylogenies after removing divergent and ambiguously aligned blocks from protein sequence alignments. Systematic Biology 56(4): 564–577. https://doi.org/10.1080/10635150701472164

Tamura K, Stecher G, Kumar S (2021) MEGA11: Molecular Evolutionary Genetics Analysis version 11. Molecular Biology and Evolution 38(7): 3022–3027. https://doi.org/10.1093/molbev/msab120

Vaidya G, Lohman DJ, Meier R (2011) SequenceMatrix: Concatenation software for the fast assembly of multi-gene datasets with character set and codon information. Cladistics 27(2): 171–180. https://doi.org/10.1111/j.1096-0031.2010.00329.x

Wang J, Zhang L, Zhang QL, Zhou MQ, Wang XT, Yang XZ, Yuan ML (2017) Comparative mitogenomic analysis of mirid bugs (Hemiptera: Miridae) and evaluation of potential DNA barcoding markers. PeerJ 5: e3661. https://doi.org/10.7717/peerj.3661

Wang JJ, Yang MF, Dai RH, Li H, Wang XY (2018) Characterization and phylogenetic implications of the complete mitochondrial genome of Idiocerinae (Hemiptera: Cicadellidae). International Journal of Biological Macromolecules 120: 2366–2372. https://doi.org/10.1016/j.ijbiomac.2018.08.191

Wang Y, Duan Y, Yang X (2019) The complete mitochondrial genome of *Plautia crossota* (Hemiptera: Pentatomidae). Mitochondrial DNA. Part B, Resources 4(2): 2281–2282. https://doi.org/10.1080/23802359.2019.1627924

Wang J, Wu Y, Dai R, Yang M (2020) Comparative mitogenomes of six species in the subfamily Iassinae (Hemiptera: Cicadellidae) and phylogenetic analysis. International Journal of Biological Macromolecules 149: 1294–1303. https://doi.org/10.1016/j.ijbiomac.2020.01.270

Wang J, Ji Y, Li H, Song F, Zhang L, Wang M (2021) Characterization of the complete mitochondrial genome of *Pentatoma semiannulata* (Hemiptera: Pentatomidae). Mitochondrial DNA, Part B, Resources 6(3): 750–752. https://doi.org/10.1080/23802359.2021.1875912

Wolstenholme DR (1992) Animal mitochondrial DNA: Structure and Evolution. International Review of Cytology 141: 173–216. https://doi.org/10.1016/S0074-7696(08)62066-5

Xu S, Wu Y, Liu Y, Zhao P, Chen Z, Song F, Li H, Cai W (2021) Comparative mitogenomics and phylogenetic analyses of Pentatomoidea (Hemiptera: Heteroptera). Genes 12(9): 1306. https://doi.org/10.3390/genes12091306

Ye F, Kment P, Rédei D, Luo J, Wang Y, Kuechler S, Zhang W, Chen P, Wu H, Wu Y, Sun X, Ding L, Wang Y, Xie Q (2022) Diversification of the phytophagous lineages of true bugs (Insecta: Hemiptera: Heteroptera) shortly after that of the flowering plants. Cladistics 38(4): 403–428. https://doi.org/10.1111/cla.12501

Yuan M, Guo Z (2016) Research progress of mitochondrial genomes of Hemiptera insects. Scientia Sinica Vitae 46(2): 151–166. https://doi.org/10.1360/N052015-00229

Yuan ML, Zhang QL, Guo ZL, Wang J, Shen YY (2015) Comparative mitogenomic analysis of the superfamily Pentatomoidea (Insecta: Hemiptera: Heteroptera) and phylogenetic implications. BMC Genomics 16(1): 460. https://doi.org/10.1186/s12864-015-1679-x

Zhang QL, Yuan ML, Shen YY (2013) The complete mitochondrial genome of *Dolycoris baccarum* (Insecta: Hemiptera: Pentatomidae). Mitochondrial DNA 24(5): 469–471. https://doi.org/10.3109/19401736.2013.766182

Zhang DL, Gao J, Li M, Yuan J, Liang J, Yang H, Bu W (2019) The complete mitochondrial genome of *Tetraphleps aterrimus* (Hemiptera: Anthocoridae): genomic comparisons and phylogenetic analysis of Cimicomorpha. International Journal of Biological Macromolecules 130: 369–377. https://doi.org/10.1016/j.ijbiomac.2019.02.130

Zhao WQ, Zhao Q, Li M, Wei JF, Zhang XH, Zhang HF (2017) Characterization of the complete mitochondrial genome and phylogenetic implications for *Eurydema maracandica* (Hemiptera: Pentatomidae). Mitochondrial DNA. Part B, Resources 2(2): 550–551. https://doi.org/10.1080/23802359.2017.1365649

Zhao Q, Wang J, Wang MQ, Cai B, Zhang HF, Wei JF (2018) Complete mitochondrial genome of *Dinorhynchus dybowskyi* (Hemiptera: Pentatomidae: Asopinae) and phylogenetic analysis of Pentatomomorpha species. Journal of Insect Science 18(2): e44. https://doi.org/10.1093/jisesa/iey031

Zhao Q, Chen C, Liu J, Wei JF (2019a) Characterization of the complete mitochondrial genome of *Eysarcoris aeneus* (Heteroptera: Pentatomidae), with its phylogenetic analysis. Mitochondrial DNA, Part B, Resources 4(2): 2096–2097. https://doi.org/10.1080/23802359.2019.1622465

Zhao WQ, Zhao Q, Li M, Wei JF, Zhang XH, Zhang HF (2019b) Comparative mitogenomic analysis of the *Eurydema* genus in the context of representative Pentatomidae (Hemiptera: Heteroptera) Taxa. Journal of Insect Science 19(6): 1–12. https://doi.org/10.1093/jisesa/iez122

Zhao Q, Cassis G, Zhao L, He Y, Zhang HF, Wei JF (2020) The complete mitochondrial genome of *Zicrona caerulea* (Linnaeus) (Hemiptera: Pentatomidae: Asopinae) and its phylogenetic implications. Zootaxa 4747(3): 547–561. https://doi.org/10.11646/zootaxa.4747.3.8

Zhao L, Wei JF, Zhao WQ, Chen C, Gao XY, Zhao Q (2021) The complete mitochondrial genome of *Pentatoma rufipes* (Hemiptera, Pentatomidae) and its phylogenetic implications. ZooKeys 1042: 51–72. https://doi.org/10.3897/zookeys.1042.62302

Zheng XY, Cao LJ, Chen PY, Chen XX, van Achterberg K, Hoffmann AA, Li-u JX, Wei SJ (2021) Comparative mitogenomics and phylogenetics of the stinging wasps (Hymenoptera: Aculeata). Molecular Phylogenetics and Evolution 159: 107119. https://doi.org/10.1016/j.ympev.2021.107119

Zink RM (2005) Natural selection on mitochondrial DNA in Parus and its relevance for phylogeographic studies. Proceedings. Biological Sciences 272(1558): 71–78. https://doi.org/10.1098/rspb.2004.2908

Supplementary material 1

Supplementary information

Authors: Xiaofei Ding

Data type: Phylogenetic (2 files in zip archive).

Explanation note: In order to explore the genetic diversity and phylogenetic relationship of *Menida* and reveal the molecular evolution of Pentatominae, three complete mitochondrial genomes of *Menida* were sequenced, and the phylogenetic relationships of tribes within the subfamily Pentatominae were studied based on mitochondrial genomes. The mitochondrial genomes of three species (*Menida musiva*, *M. lata* and *M. metallica*) were 16,663bp, 16,463bp and 16,418 bp, respectively, encoded 37 genes, including 13 protein-coding genes (PCGs), two rRNA genes, 22 tRNA genes and a control region. We compared and analyzed the mitochondrial genomes characteristics of *Menida*, and constructed the phylogenetic tree of Pentatominae based on the mitochondrial genomes datasets by Bayesian method. The results showed that gene arrangements, nucleotide composition, codon preference, gene overlaps and RNA secondary structures were highly conserved within the *Menida*, and had more similar characteristics in Pentatominae. Phylogenetic analysis showed highly consistent topological structures based on BI methods, which strongly supported that the genus *Menida* belongs to the Pentatominae and is the earliest branch of the sequenced pentatominae species. In addition, (Pentatomini+Strachiini) and (Nezarini+Antestiini) were found to be stable sister groups in the evolutionary branch of Pentatominae. The results of this study enrich the mitochondrial genomes databases of Pentatominae, and have important significance for further elucidate the phylogenetic relationship of Pentatominae.

Link: https://doi.org/10.3897/zookeys.1138.95626.suppl1

ZooKeys 1138: 49–88 (2023)
doi: 10.3897/zookeys.1138.94580
https://zookeys.pensoft.net

RESEARCH ARTICLE

A peer-reviewed open-access journal
ZooKeys
Launched to accelerate biodiversity research

New descriptions and new records of the braconid parasitoids subfamilies Doryctinae and Rhyssalinae (Hymenoptera, Braconidae) in the fauna of South Korea

Sergey A. Belokobylskij[1], Deokseo Ku[2]

1 *Zoological Institute, Russian Academy of Sciences, St Petersburg 199034, Russia* **2** *The Science Museum of Natural Enemies, Geochang 50147, Republic of Korea*

Corresponding author: Sergey A. Belokobylskij (doryctes@gmail.com)

Academic editor: K. van Achterberg | Received 7 September 2022 | Accepted 4 December 2022 | Published 5 January 2023

https://zoobank.org/623D6500-707D-47F6-9C5B-2E601837C36C

Citation: Belokobylskij SA, Ku D (2023) New descriptions and new records of the braconid parasitoids subfamilies Doryctinae and Rhyssalinae (Hymenoptera, Braconidae) in the fauna of South Korea. ZooKeys 1138: 49–88. https://doi.org/10.3897/zookeys.1138.94580

Abstract

Five doryctine species, *Aivalykus kseniae* **sp. nov.**, *Dendrosotinus gajwadongus* **sp. nov.**, *Doryctes* (*Plyctes*) *jinjuensis* **sp. nov.**, *Neoheterospilus* (*Neoheterospilus*) *geochangus* **sp. nov.**, and *Spathius fumipennis* **sp. nov.**, are described as new for sciences from South Korea. Five doryctine genera, *Aivalykus* Nixon, *Dendrosoter* Wesmael, *Dendrosotinus* Telenga, *Guaygata* Marsh and *Pareucorystes* Tobias, and fifteen species are recorded in the fauna of the Korean Peninsula for the first time. Additionally, two genera from the subfamily Rhyssalinae, *Proacrisis* Tobias and *Histeromerus* Wesmael, and two species, *Proacrisis orientalis* Tobias, 1983 and *Histeromerus orientalis* Chou & Chou, 1991, are recorded in the fauna of Korea for the first time.

Keywords

Descriptions, diagnoses, Ichneumonoidea, new records, new species, parasitoid

Introduction

The fauna of the parasitoid family Braconidae of the Eastern Palaearctic is considerably diverse and abundant with numerous taxa penetrating here from the Oriental region. Despite the number of publications dedicated to the braconid subfamily Doryctinae for this zoogeographic region (e.g., Belokobylskij 1996; Belokobylskij and Maetô 2009; Belokobylskij et al. 2013; Tang et al. 2013, 2015; Belokobylskij and Ku 2021, etc.), the number of new records and species for this group continues increasing every year.

Information about the Doryctinae from the Korean Peninsula has been published in several survey and faunistic articles (Papp 1984; Belokobylskij 1998; Ku et al. 2001; Lee et al. 2020; Belokobylskij and Ku 2021, etc.).

In this article, five new doryctine species are described from Korea, seven genera and 17 species from subfamilies Doryctinae and Rhyssalinae are recorded for the first time for the Korean Peninsula.

Materials and methods

The terminology employed for the morphological features, sculpture, and body measurements follows Belokobylskij and Maetô (2009). The wing venation nomenclature follows Belokobylskij and Maetô (2009), with the terminology of van Achterberg (1993) shown in parentheses. The new distribution records presented in this paper are marked with an asterisk (*).

The specimens were examined using an Olympus SZ51 stereomicroscope. Photographs were taken with an Olympus OM-D E-M1 digital camera mounted on an Olympus SZX10 microscope (Zoological Institute of the Russian Academy of Sciences, St Petersburg, Russia). Image stacking was performed using Helicon Focus 8.0. The figures were produced using the Adobe Photoshop CS6 program.

The specimens examined in this study were deposited in the collections of the National Institute of Biological Resources (Incheon, Republic of Korea; **NIBR**), the Science Museum of Natural Enemies (Geochang, Republic of Korea; **SMNE**), and the Zoological Institute of the Russian Academy of Sciences (St Petersburg, Russia; **ZISP**).

Taxonomic account

Class Hexapoda Blainville, 1816
Order Hymenoptera Linnaeus, 1758
Family Braconidae Nees, 1811
Subfamily Doryctinae Foerster, 1863

Species from the Korean Peninsula new for science

Genus *Aivalykus* Nixon, 1938

Type species. *Aivalykus eclectus* Nixon, 1938.

Notes. The genus *Aivalykus* Nixon from the tribe Ecphylini is recorded in the fauna of Korea for the first time. This genus is unknown yet in southern regions of the Russian Far East and Japan (Belokobylskij 1996, 1998; Belokobylskij and Maetô 2009), though it has been found in the south of China (Belokobylskij and Chen 2002).

Aivalykus kseniae sp. nov.

https://zoobank.org/659BD181-E950-4827-BAB4-3D11FD877281
Figs 1, 2

Type material. ***Holotype*:** female, "Korea (GB), Ian yeomul san [Ian-myeon, Yeomulri San] 39–4, Sangji-[shi], 36°32'46.9"N, 128°07'46.6"E, 2020.V.24–VI.12, Coll. S.S. Kim, The 5th National Ecosystem Survey" (NIBR).

***Paratype*:** 1 female, "Korea (GB), Cheonbu3-gil, Buk-myeon, Ulleung-gun, V.23–VI.7.2017 (Malaise trap), Ku Deokseo" (SMNE).

Comparative diagnosis. This new species is similar to *Aivalykus nitidus* Belokobylskij & Chen, 2002 (Belokobylskij and Chen 2002), but differs by having the vertex with a distinct aciculation (very finely aciculate in *A. nitidus*), five carinae on the prescutellar depression (only a single median carina in *A. nitidus*), second medial abscissa (2-SR+M) short, recurrent vein (m-cu) weakly antefurcal, ~ 8.0× longer than second medial abscissa (2-SR+M) (long, strongly antefurcal, in 1.6–2.0× longer in *A. nitidus*), brachial cell closed weakly before recurrent vein (distinctly before it in *A. nitidus*), setae on the dorsal margin of the hind tibia short, 0.3–0.5× as long as the maximum width of the tibia (long, 0.7–0.8× as long as the width of the tibia in *A. nitidus*), and apical segments of antenna dark brown to black (three apical segments white in *A. nitidus*).

Description. Female. Body length 2.2–2.5 mm; fore wing length 2.0–2.2 mm; ovipositor sheath length 1.7–2.0 mm.

Head. Head width (dorsal view) 1.5–1.6× its median length, 1.1× width of mesoscutum. Head behind eye (dorsal view) weakly convex or subparallel in anterior 1/2, roundly narrowed in posterior 1/2; transverse diameter of eye 1.6–1.8× length of temple. Ocelli small, arranged in equilateral triangle with base 1.1–1.2× its sides. POL 1.1–1.2× Od, 0.5–0.6× OOL. Eye glabrous, 1.1–1.2× as high as broad. Malar space 0.4–0.5× height of eye, almost equal to basal width of mandible. Face width 0.9–1.0× height of eye and almost equal to height of face and clypeus combined. Malar suture absent. Clypeus high, 1.0–1.2× as wide as high. Clypeal suture shallow, distinct laterally and almost absent upper medially. Hypoclypeal depression round, its trans-

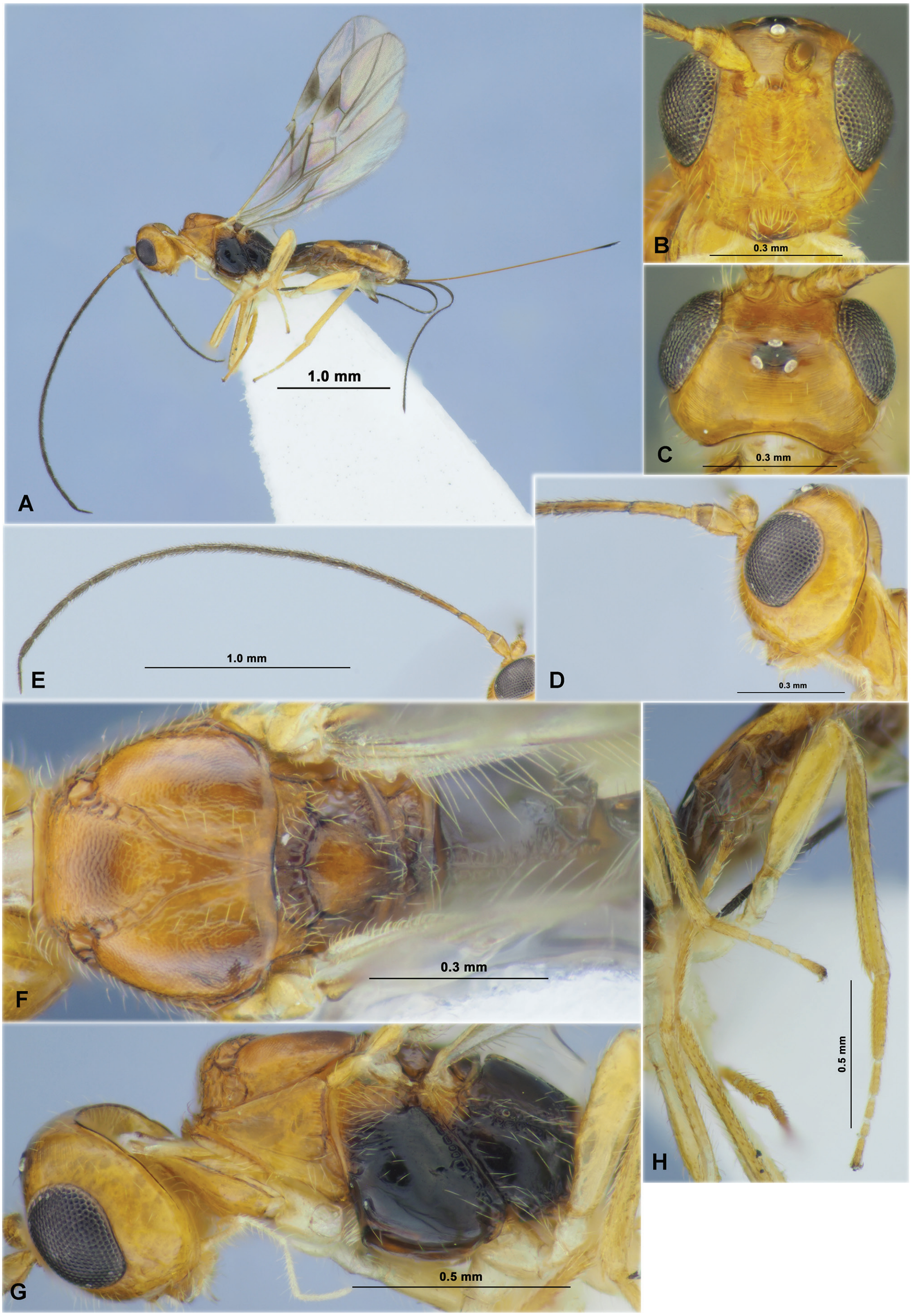

Figure 1. *Aivalykus kseniae* sp. nov. (female, holotype) **A** habitus, lateral view **B** head, front view **C** head, dorsal view **D** head, lateral view **E** antenna **F** mesosoma, dorsal view **G** head and mesosoma, lateral view **H** hind leg.

verse width 0.4–0.5× distance from edge of depression to eye, 0.3–0.4× width of face. Occipital carina reduced below, not fused with hypostomal carina.

Antenna. Antenna slender, almost filiform, 18–21-segmented, weakly longer than body. Scape 1.2× longer than its maximum width. First segment of flagellum not flattened, weakly curved, 3.8–4.0× longer than its apical width, 0.7–0.8× longer than second segment. Penultimate segment 4.0–4.5× longer than wide, 0.8–0.9× as long as first segment, as long as apical segment; the latter almost obtuse apically.

Mesosoma. Mesosoma 1.7–1.8× longer than high. Neck of prothorax short. Pronotal carina distinct. Mesoscutum highly and almost perpendicularly elevated above pronotum (lateral view), ~ 1.1× wider than its medial length (dorsal view). Notauli deep in anterior 1/2, shallow in posterior 1/2, anteriorly distinctly crenulate. Prescutellar depression (scutal sulcus) deep, with five complete or sometimes partly incomplete longitudinal carinae, smooth between carinae, 0.3× as long as weakly convex scutellum. Subalar depression shallow, wide, distinctly obliquely striate. Precoxal sulcus very shallow and narrow, finely longitudinally aciculate or smooth, connected with prepectal carina anteriorly, running along ~ 1/2 of lower part of mesopleuron. Metanotum almost without tooth.

Wings. Fore wing 3.0–3.3× longer than its maximum width. Radial vein (r) arising almost from middle of pterostigma. Radial (marginal) cell weakly shortened. Metacarp (1-R1) almost as long as pterostigma. First radial abscissa (r) perpendicular to pterostigma, 0.7–0.9× as long as maximum width of pterostigma, 0.5–0.6× as long as first radiomedial vein (2-SR). Second radial abscissa (3-SR+SR1) distinctly evenly curved, 6.6–7.3× longer than first abscissa (r), 3.8–3.9× longer than first radiomedial vein (2-SR). Discoidal (first discal) cell ~ 2.0× longer than wide. Recurrent vein (m-cu) weakly antefurcal, 4.0–6.0× longer than second abscissa of medial vein (2-SR+M), 0.6–0.7× as long as first radiomedial vein (2-SR). Brachial (first subdiscal) cell narrow, gently closing apically weakly before recurrent vein (m-cu). Distance from nervulus (cu-a) to basal vein (1-M) 0.5–1.0× nervulus (cu-a) length. In hind wing medial (basal) cell closed antero-distally. Recurrent vein (m-cu) absent, or sometimes present, but short and strongly desclerotised.

Legs. Hind femur 3.8–4.0× longer than wide. Hind tarsus 0.75–0.80× as long as hind tibia. Hind basitarsus thickened, thicker than following segments, 0.7–0.8× as long as second–fifth segments combined. Second segment 0.4× as long as basitarsus, 1.1–1.3× longer than fifth segments (without pretarsus).

Metasoma. Metasoma 0.9–1.0× as long as head and mesosoma combined. First tergite without spiracular tubercles, spiracles situated on basal 1/3 of tergite, distinctly and linearly widened from base to apex. Maximum width of first tergite 1.7–2.0× its minimum width, length 1.10–1.15× its apical width, 1.3–1.5× length of propodeum. Second tergite without sublateral oblique depressions. Suture between second and third tergites indistinct. Medial length of second and third tergites combined 1.1–1.2× basal width of second tergite, 0.8× their maximum width. Ovipositor sheath 0.8× as long as body, 1.4–1.6× longer than metasoma, 2.0–2.2× longer than mesosoma, 0.8–0.9× as long as fore wing.

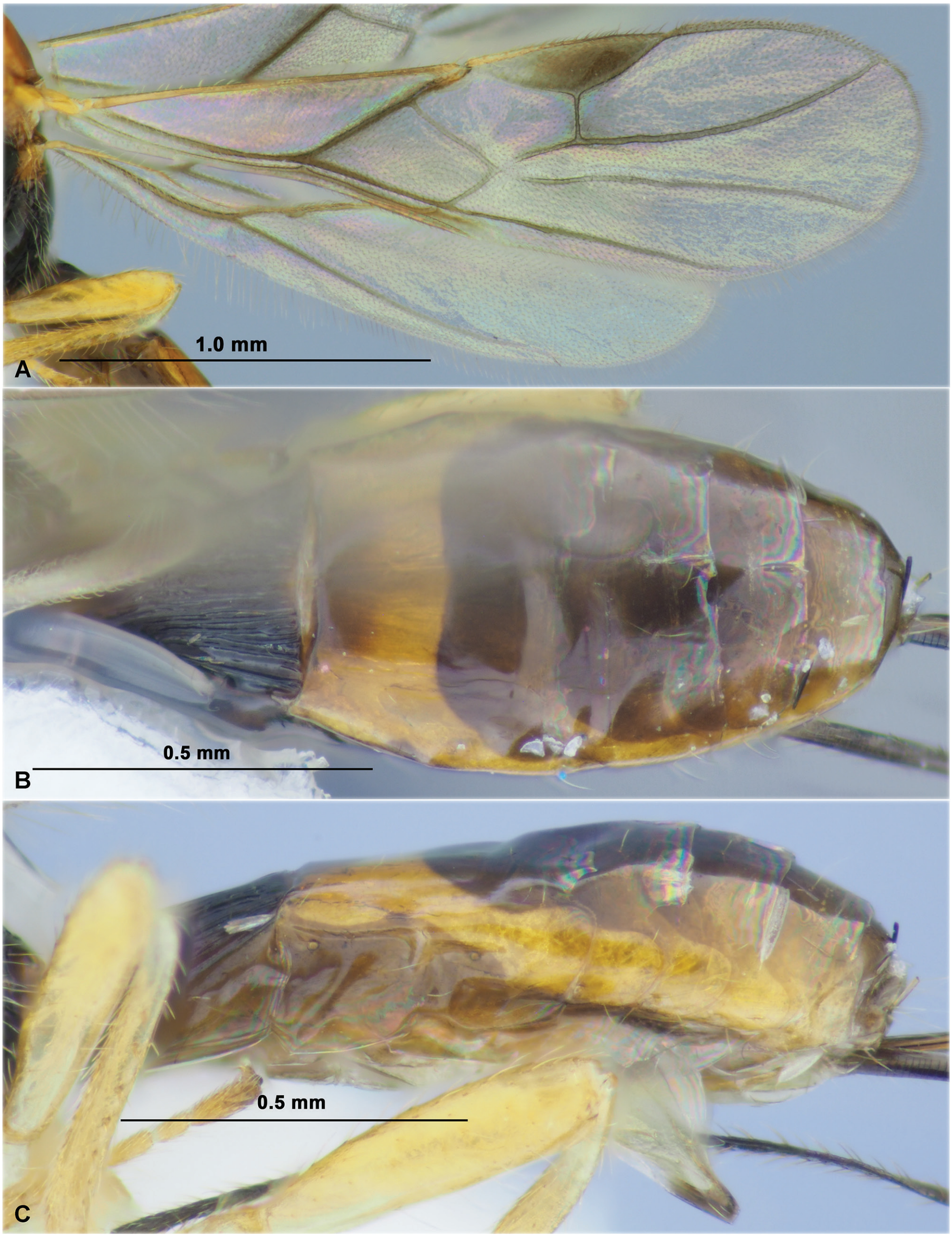

Figure 2. *Aivalykus kseniae* sp. nov. (female, holotype) **A** wings **B** metasoma, dorsal view **C** metasoma, lateral view.

Sculpture and pubescence. Vertex almost entirely aciculate; frons mainly smooth with fine aciculation posteriorly or widely and finely aciculate; temple smooth; face mainly smooth with sparse punctation, finely aciculate submedially on narrow stripes and below. Sides of pronotum mainly smooth but striate marginally. Mesoscutum distinctly and densely coriaceous, sometimes sculpture situated in irregular transverse dense striae anteriorly; with two middle and strongly convergent posteriorly longitudinal carina in posterior 1/2. Scutellum almost entirely smooth. but finely coriaceous laterally. Mesopleuron and metapleuron mainly smooth. Propodeum mainly smooth, with coarse and short rugulosity along median carinae in basal 2/3, with distinctly delineated by carinae, short and relatively wide smooth areola in posterior 1/3 of propodeum. Hind coxa and femur smooth. First metasomal tergite with distinct, complete, and closely situated dorsal carinae, entirely densely and distinctly striate. Remaining tergites completely smooth. Hind tibia on dorsal surface with rather sparse and semi-erect pale setae, length of these setae 0.3–0.5× maximum width of hind tibia.

Colour. Head and anterior 1/2 of mesosoma pale reddish brown to yellowish brown; posterior 1/2 of mesosoma and first metasomal tergite dark brown to black, remaining part of metasoma reddish brown with yellowish margins. Antenna dark brown to black (including subapical and apical segments), three basal segments yellowish brown. Palpi pale yellow. Legs brownish yellow or yellow. Ovipositor sheath black. Wings faintly infuscate; pterostigma brown, but pale yellow in its basal quarter.

Male. Unknown.

Etymology. Named after the daughter of the first author, Ksenia.

Distribution. Korean Peninsula.

Genus *Dendrosotinus* Telenga, 1941

Type species. *Dendrosoter ferrugineus* Marshall, 1888.

Notes. The genus *Dendrosotinus* Telenga, 1941 from the tribe Doryctini is recorded in the fauna of Korea for the first time.

Dendrosotinus (*Gildoria*) *gajwadongus* sp. nov.

https://zoobank.org/BA9A4A3F-5612-459E-8F90-EF755807AF90
Fig. 3

Type material. ***Holotype***: male, "S. Korea, Gyeongsangnam-do, Jinju-[shi], Gajwadong, V.1993, D.-S. Ku leg."(NIBR)

Comparative diagnosis. According to van Achterberg (2003), this species is similar to the briefly described Western Palaearctic *Dendrosotinus* (*Gildoria*) *planus* (Ratzeburg, 1848), but differs from the latter species by having the antenna 13-segmented (20-segmented in *D. planus*), brachial vein (CU1b) distinctly oblique to the mediocubital vein (2-CU1) (subperpendicular in *D. planus*), mesoscutum coarsely rugose-reticulate and without granulation (densely reticulate-granulate in *D. planus*), and second metasomal tergite longitudinally striate with reticulation (finely aciculate in *D. planus*).

Description. Male. Body length 1.3 mm; fore wing length 1.1 mm.

Head. Head width (dorsal view) 1.5× its median length, 1.2× width of mesoscutum. Head behind eyes (dorsal view) subparallel in anterior 1/2 and roundly narrowed in posterior 1/2. Transverse diameter of eye (dorsal view) 1.2× longer than temple.

Ridge on border of vertex and frons absent. Ocelli small, arranged in triangle with base 1.3× its sides. POL 1.5× Od, ~ 0.7× OOL. Eye bare, almost without emargination opposite antennal sockets, 1.1× as high as broad. Malar suture absent. Malar space 0.4× height of eye, 0.8× basal width of mandible. Face width 1.1× height of eye and 1.3× height of face and clypeus combined. Clypeus with distinct short lower flange. Clypeal suture distinct. Hypoclypeal depression subround, its width 0.6× distance from edge of depression to eye, 0.35× width of face. Occipital carina complete dorsally, obliterated ventrally at rather long distance and not fused with hypostomal carina.

Antenna. Antenna slender, filiform, 13-segmented, almost as long as body. Scape 1.6× longer than its maximum width, 1.4× longer than pedicel. First flagellar segment not widened, almost not curved, not convex and without sculpture on its outer side, weakly concave and smooth on inner side, ~ 5.0× longer than its maximum width, 0.8× as long as second segment. Penultimate segment 4.7× longer than wide, approximately as long as apical segment; the latter weakly acuminated.

Mesosoma. Mesosoma not depressed, its length 1.8× maximum height. Pronotum short, dorsally with weakly convex lobe, with distinct and high pronotal keel; side of pronotum with wide, shallow, and curved submedian furrow. Mesoscutum highly and convex-roundly elevated above pronotum (lateral view). Median lobe of mesoscutum distinctly protruding forwards. Notauli rather wide, deep anteriorly and shallow posteriorly, crenulate-rugulose. Prescutellar depression rather deep, relatively short, with four distinct carinae, finely rugulose between carinae, 0.3× as long as convex scutellum. Subalar depression shallow, wide, distinctly and widely rugose-reticulate. Precoxal sulcus distinct, relatively deep, straight, smooth, connected with prepectal carina anteriorly, running along anterior 1/2 of lower part of mesopleuron. Propodeum without lateral tubercles.

Wings. Fore wing 3.3× longer than its maximum width. Pterostigma 3.3× longer than wide. Radial vein (r) arising almost from middle of pterostigma. Radial (marginal) cell weakly shortened. Metacarp (1-R1) inside of radial (marginal) cell almost as long as pterostigma. Second radial abscissa (3-SR) 3.0× longer than first abscissa (r), 0.4× as long as weakly curved third abscissa (SR1), as long as first radiomedial vein (2-SR). Second radiomedial (submarginal) cell medium-sized, not narrowed distally, 2.6× longer than its maximum width, 1.7× longer than narrow brachial (subdiscal) cell. Recurrent vein (m-cu) distinctly postfurcal, 1.5× longer than second abscissa of medial vein (2-SR+M), 0.4× as long as first radiomedial vein (2-SR). Distance (1-CU1) between nervulus (cu-a) to basal vein (1-M) almost equal to nervulus (cu-a) length; nervulus (cu-a) straight and perpendicular to mediocubital vein (M+CU1). Parallel vein (CU1a) interstitial. Brachial (subdiscal) cell distally closed distinctly before recurrent vein (m-cu); apical vein of longitudinal anal vein (2A+3A) behind brachial vein absent. Hind wing with three hamuli, ~ 7.0× longer than wide. First abscissa of costal vein (C+SC+R) 0.6× as long as second abscissa (1-SC+R). First abscissa of mediocubital vein (M+CU) 0.6× as long as second abscissa (1-M). Recurrent vein (m-cu) mainly unsclerotised, oblique toward apex of wing, strongly antefurcal.

Legs. Fore tibia with fine spines arranged in almost single row. Hind coxa practically without basoventral tubercle. Hind femur without dorsal protuberance, ~ 3.0× longer than wide. Hind tarsus 0.9× as long as hind tibia. Basitarsus widened distally, with long ventral thorn on its inner corner, 0.45× as long as second–fifth segments combined. Second tarsal segment 0.4× as long as basitarsus, 0.5× as long as fifth segment (without pretarsus).

Metasoma. Metasoma almost as long as head and mesosoma combined. First tergite with small dorsope, with distinct spiracular tubercles in its basal 1/3; tergite distinctly and almost linearly widened from base to basal 1/3, then very weakly and sublinearly widened towards apex. Maximum width of first tergite 1.8× its minimum width; length of tergite 1.2× its apical width. Second suture rather distinct, shallow, weakly curved and without sublateral breaks. Second tergite 0.8× as long as its basal width, 1.2× longer than third tergite. Medial length of second and third tergites combined 1.4× basal width of second tergite, almost as long as their maximum width.

Sculpture and pubescence. Vertex and frons weakly and rather sparsely reticulate-coriaceous; face densely transversely striate laterally and smooth medially; temple smooth. Mesoscutum entirely distinctly and densely rugulose-reticulate, without additional granulation. Scutellum very finely and densely reticulate-granulate. Mesopleuron smooth in lower 1/2, reticulate-coriaceous in upper 1/2. Propodeum with areas delineated by distinct carinae; basolateral areas mainly reticulate-coriaceous but anteriorly partly smooth; areola long and narrow, with several transverse carinae, ~ 2.5× longer than maximum with, petiolate areas not delineated; basal carina short, 0.4× as long as anterior fork of areola. Hind coxae mainly smooth, but curvedly striate dorsally. Hind femur entirely smooth. First metasomal tergite entirely and sparsely curvedly striate, with distinct and dense reticulation between striae; second tergite entirely weakly longitudinally striate with reticulation. Remaining tergites smooth. Vertex widely glabrous medially, anteriorly, and laterally with sparse, short, and semi-erect white setae. Mesoscutum entirely with sparse, short, and white semi-erect setae. Metapleuron medially widely glabrous. Hind tibia dorsally with sparse, short, and semi-erect setae, its length 0.8–1.0× maximum width of hind tibia.

Colour. Head reddish brown, distinctly infuscate dorsally, brownish yellow ventrally. Mesosoma reddish brown, dark reddish brown on mesoscutum and scutellum, prosternum and propodeum brownish yellow. Metasoma brownish yellow in basal 1/2, reddish brown with dark transverse stripes on posterior margin of tergites in apical 1/2. Antenna brown, three basal segments yellow. Palpi pale yellow. Legs brownish yellow to yellow. Fore wing hyaline; pterostigma mainly brown, yellow basally.

Female. Unknown.

Etymology. Named after the type locality of the new species in South Korea, Gajwa-dong, Jinju City.

Distribution. Korean Peninsula.

Remarks. Despite the intensive study for the braconid fauna of the Korean Peninsula in the last period, only a single male of this species has been collected till now. However, the distinct diagnostic characters of this new species allow us to easily separate it from remaining described Asian species of *Dendrosotinus*.

A species of *Dendrosotinus* described in Chinese from Fujian Province (China), *D. wuyiensis* Shi, 2006 (Shi 2006), perhaps belongs to the genera *Ontsira* Cameron, 1900 or *Neurocrassus* Snoflak, 1945 according to the figures provided in the original description. However, only a study of the holotype of this species will allow to confirm its real taxonomic position.

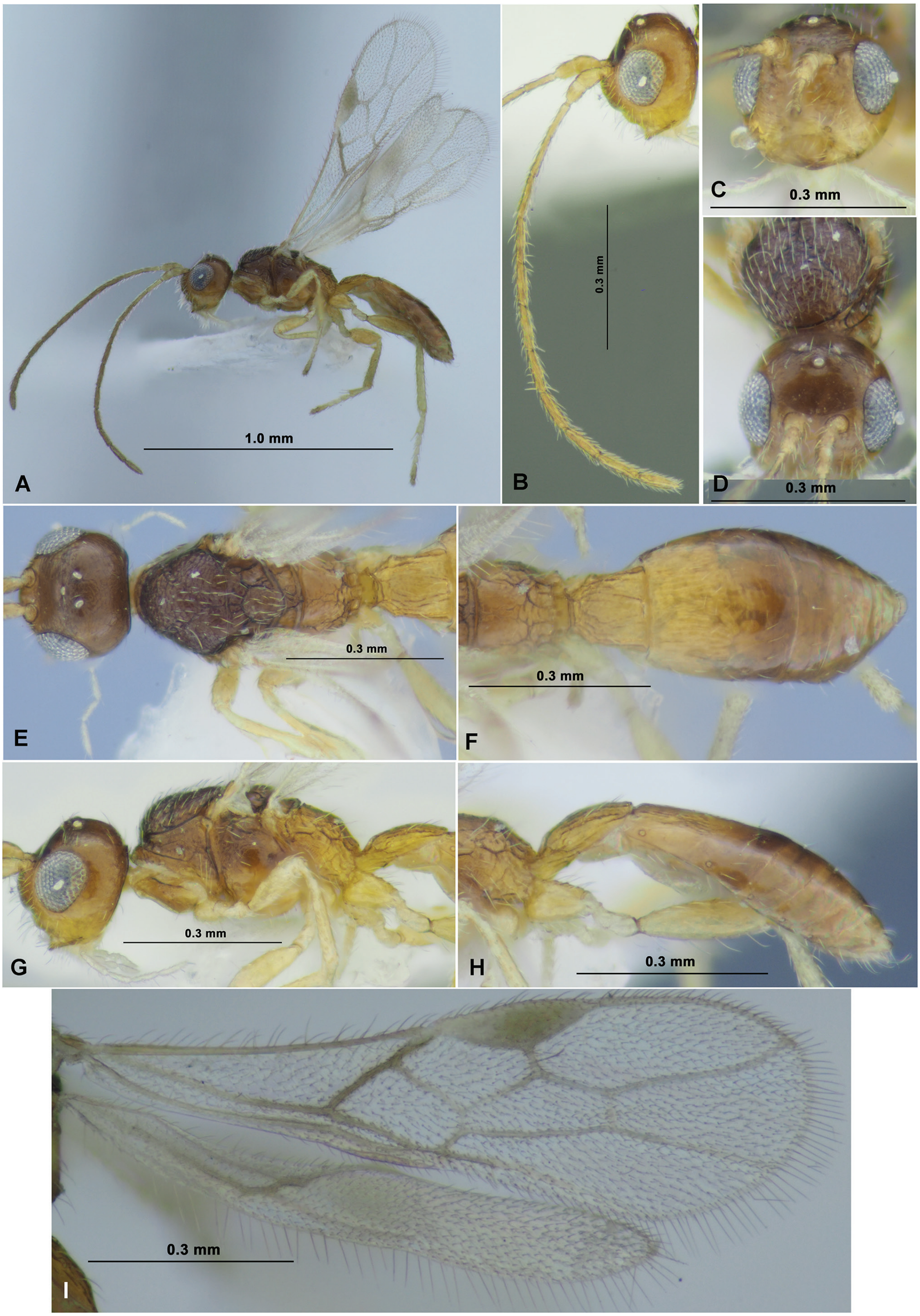

Figure 3. *Dendrosotinus* (*Gildoria*) *gajwadongus* sp. nov. (male, holotype) **A** habitus, lateral view **B** head and antenna, lateral view **C** head, front view **D** mesoscutum and head, dorso-anterior view **E** head, mesosoma and first metasomal tergite, dorsal view **F** propodeum and metasoma, dorsal view **G** head, mesosoma and first metasomal tergite, lateral view **H** propodeum and metasoma, lateral view **I** wings.

Key to the Asian species of the genus *Dendrosotinus*

1 Third antennal segment (especially of female) widened, more or less depressed and anteriorly sculptured. Recurrent vein (m-cu) of fore wing subinterstitial; brachial (subdiscal) cell moderately wide. (Subgenus *Dendrosotinus* s. str.). – Armenia, Azerbaijan, former Yugoslavia, France, Greece, Israel, Italy, Russia (North Caucasus), Saudi Arabia, Spain, Turkey, UAE.............. ***D.* (*D.*) *ferrugineus* (Marshall, 1888)**

– Third antennal segment slender, cylindrical, and anteriorly usually smooth. Recurrent vein (m-cu) of fore wing distinctly postfurcal; brachial (subdiscal) cell narrow (subgenus *Gildoria* Hedqvist, 1974)...**2**

2 Brachial (subdiscal) cell of fore wing closed distinctly before recurrent vein (m-cu)..**3**

– Brachial (subdiscal) cell of fore wing closed on or weakly before or behind of recurrent vein (m-cu) **5**

3 Antenna 13-segmented (Fig. 3B). Vertex very weakly coriaceous (Fig. 3D, E). Fore wing entirely hyaline (Fig. 3I). Mesoscutum coarsely rugose-reticulate and without granulation (Fig. 3D, E). – Basitarsus of hind tarsus with long ventral thorn on its inner corner (Fig. 3A). Body length 1.3 mm. – Korean Peninsula ....***D.* (*G.*) *gajwadongus* sp. nov.**

– Antenna 18–22-segmented. Vertex distinctly densely reticulate-areolate and with granulation. Fore wing faintly maculate, with rather distinctly infuscate transverse stripes. Mesoscutum transverse striate-rugose, and with additional granulation...... **4**

4 Transverse diameter of eye (dorsal view) 1.9–2.3× longer than temple. Malar space 0.4× maximum diameter of eye. Length of first tergite 1.1–1.2× its maximum posterior width. Second tergite without sublateral depression. Ovipositor sheath 0.5–0.6× as long as metasoma, 0.4–0.5× as long as fore wing. Body mainly pale reddish brown or reddish brown, darkened dorsally. Body length 2.2–2.8 mm. – Yemen................................***D.* (*G.*) *maculipennis* Belokobylskij, 2021**

– Transverse diameter of eye (dorsal view) 1.2–1.4× longer than temple. Malar space 0.6× maximum diameter of eye. Length of first tergite 1.3–1.4× its maximum posterior width. Second tergite with very shallow, subparallel, sublateral and almost straight depression in anterior 1/2. Ovipositor sheath 0.9–1.0× as long as metasoma, 0.7–0.8× as long as fore wing. Body mainly brownish yellow to partly yellow. Body length 2.0–2.5 mm. – UAE....... ***D.* (*G.*) *subelongatus* Belokobylskij, 2021**

5 Transverse diameter of eye 1.2–1.3× longer than temple (dorsal view). Parallel vein (CU1a) interstitial to mediocubital vein (2-CU1). First metasomal tergite as long as its apical width. Second metasomal tergite weakly rugulose-reticulate in medio-basal 1/2. Body length 3.3 mm. – Tajikistan.............***D. anthaxiae* Belokobylskij, 1983**

– Transverse diameter of eye 2.0–2.2× longer than temple (dorsal view). Parallel vein (CU1a) not interstitial to mediocubital vein (2-CU1), arising from anterior fourth of the vein (3-CU1) closing brachial (subdiscal) cell apically. First metasomal tergite 1.2–1.3× longer than apical width. Second metasomal tergite entirely striate with reticulation **6**

6 Vertex distinctly and densely transverse striate with fine reticulation between striae. Antenna 36-segmented. Hind femur 3.0× longer than wide. Third metasomal tergite sculptured baso-laterally. Ovipositor sheath 1.3× longer than metasoma. Body length 3.3 mm. – China (Taiwan)................ ***D. taiwanicus*** **Belokobylskij, 2010**

– Vertex weakly and densely granulate, without striation. Antenna 27-segmented. Hind femur 2.3× longer than wide. Third metasomal tergite entirely smooth. Ovipositor sheath 0.4× as long as metasoma. Body length 3.3 mm. – Vietnam... ***D. gratus*** **Belokobylskij, 1993**

Genus *Doryctes* Haliday, 1836

Type species. *Bracon obliteratus* Nees, 1834.

Subgenus *Plyctes* Fischer, 1981

Doryctes (*Plyctes*) *jinjuensis* sp. nov.

https://zoobank.org/70CA97A4-2D2D-4394-8529-91846C7BE301
Figs 4–6

Type material. ***Holotype*:** female, “S. Korea: Gyeongsangnam-do, Sancheong-gun, [Chahwang-myeon], 30 km NNW Jinju (Chinju), forest, bush, h = 800 m, 29.06.2002, S. Belokobylskij” (NIBR).

***Paratypes*.** 1 male, “Korea, Gyeongnam-do, Jinju-si [=shi], Gajwa-dong, 27. X.–3. XI.1987, Malaise trap. D-S Ku” (SMNE); 1 male, “Korea, Gyeongnam-do, Jinju-si [=shi], Gajwa-dong, 15.–21.VII.1989. Malaise trap (Black). D-S Ku” (ZISP); 1 male, “Korea, Gyeongbuk-do, Gyeongsan-si [=shi], Yeungnam University, 12.VIII.1987, J-Y Cha” (SMNE); 1 male, “Korea: KK [=GG], Suwon, Mt. Yeogi, MT (B1/B1), 8.IX.1997, June-Yeol Choi” (SMNE).

Comparative diagnosis. This new species is very similar to *Doryctes* (*Plyctes*) *diversus* (Szépligeti, 1910) and *D.* (*P.*) *malayensis* Fullaway, 1919; the differences between these species are given in the key below.

Description. Female. Body length 6.5 mm; fore wing length 5.0 mm.

***Head*.** Head width (dorsal view) 1.3× its median length, 1.15× maximum width of mesoscutum. Head behind eyes (dorsal view) weakly convex in anterior 1/2, roundly narrowed in posterior 1/2. Transverse diameter of eye 1.4× longer than temple (dorsal view). Ocelli medium-sized, arranged in triangle with base 1.2–1.3× its side. POL 1.3× OD, 0.6× OOL. Eye glabrous, with very weak emargination opposite of antennal socket, 1.15× as high as broad. Malar space 0.3× height of eye, 0.6× as long as basal width of mandible. Malar suture very shallow. Face width ~ 0.8× height of eye, 1.2× height of face and clypeus combined. Hypoclypeal cavity round, its diameter equal to distance from margin of cavity to border of eye, 0.5× as long as width of face. Occipital carina complete dorsally, obliterated below at rather long distance and not fused with hypostomal carina.

Antenna. Antenna slender, setiform, more than 43-segmented (apical segments missing). Scape 1.9× longer than its maximum width. First flagellar segment ~ 5.0× longer than its apical width, 1.05× longer than second segment. Subapical segment 4.7× longer than its maximum width.

Mesosoma. Length of mesosoma 2.1× longer than its height. Pronotum dorsally with weakly convex dorsal lobe (lateral view) and with distinct pronotal keel in anterior 1/3. Mesoscutum distinctly and curvedly elevated above pronotum. Median lobe of mesoscutum anteriorly distinctly convex and protruding forwards (dorsal view). Notauli anteriorly deep, wide and crenulate, posteriorly very shallow, narrow, and smooth, almost complete. Prescutellar depression rather deep, almost entirely distinctly rugose, with median carina, 0.4× as long as scutellum. Scutellum weakly convex, with weak lateral carinae. Subalar depression shallow, rather wide, weakly striate-rugose. Precoxal sulcus deep, long, smooth, without round cavity medially or posteriorly, running along anterior 2/3 of lower part of mesopleuron. Propodeum without lateral tubercles.

Wings. Fore wing 3.6× longer than its maximum width. Pterostigma 4.3× longer than maximum width. Radial vein (r) arising almost from middle of pterostigma. Second radial abscissa (3-SR) forming very obtuse angle with first radial abscissa (r) and twice longer than it, 0.4× as long as third radial abscissa (SR1), 1.8× longer than first radiomedial vein (3-SR). Second radiomedial (submarginal) cell relatively short and narrow, 3.0× longer than its maximum width, 1.2× longer than wide brachial (first subdiscal) cell. First medial abscissa (1-SR+M) distinctly sinuate. Recurrent vein (m-cu) distinctly antefurcal, 5.5× longer than second medial abscissa (2-SR+M), 1.3× longer than first radiomedial vein (3-SR). Distance (1-CU1) between nervulus (cu-a) and basal vein (1-M) 1.5× nervulus (cu-a) length. Parallel vein (CU1a) arising from posterior 1/3 of distal margin of brachial (first subdiscal) cell. Hind wing 5.0× longer than maximum width. First costal abscissa (C+SC+R) 0.6× as long as second abscissa (1-SC+R). First abscissa of mediocubital vein (M+CU) almost equal to second abscissa (1-M). Recurrent vein (m-cu) entirely straight, oblique, weakly antefurcal.

Legs. Hind coxa with low and wide dorsal protuberance, with distinct basoventral tubercle. Hind femur 3.0× longer than its maximum width. Hind tarsus almost as long as hind tibia. Hind basitarsus 0.8× as long as second–fifth segments combined; second segment of hind tarsus 0.4× as long as basitarsus, 1.3× longer than fifth segment (without pretarsus).

Metasoma. Metasoma 1.3× longer than mesosoma and head combined. First tergite without distinct spiracular tubercles, weakly and almost linearly widened from subbase to apex. Maximum width of first tergite 1.7× its minimum basal width; its length 1.2× maximum subapical width. Second tergite with fine, almost straight, and subparallel sublateral furrows; median length of second tergite 0.45× its basal width, 0.8× length of third tergite. Suture between second and third tergites present, shallow, wide, and weakly concave medially, with not deep sublateral bends. Third tergite without depression. Ovipositor sheath almost as long as metasoma, 1.5× longer than mesosoma and 0.65× as long as fore wing.

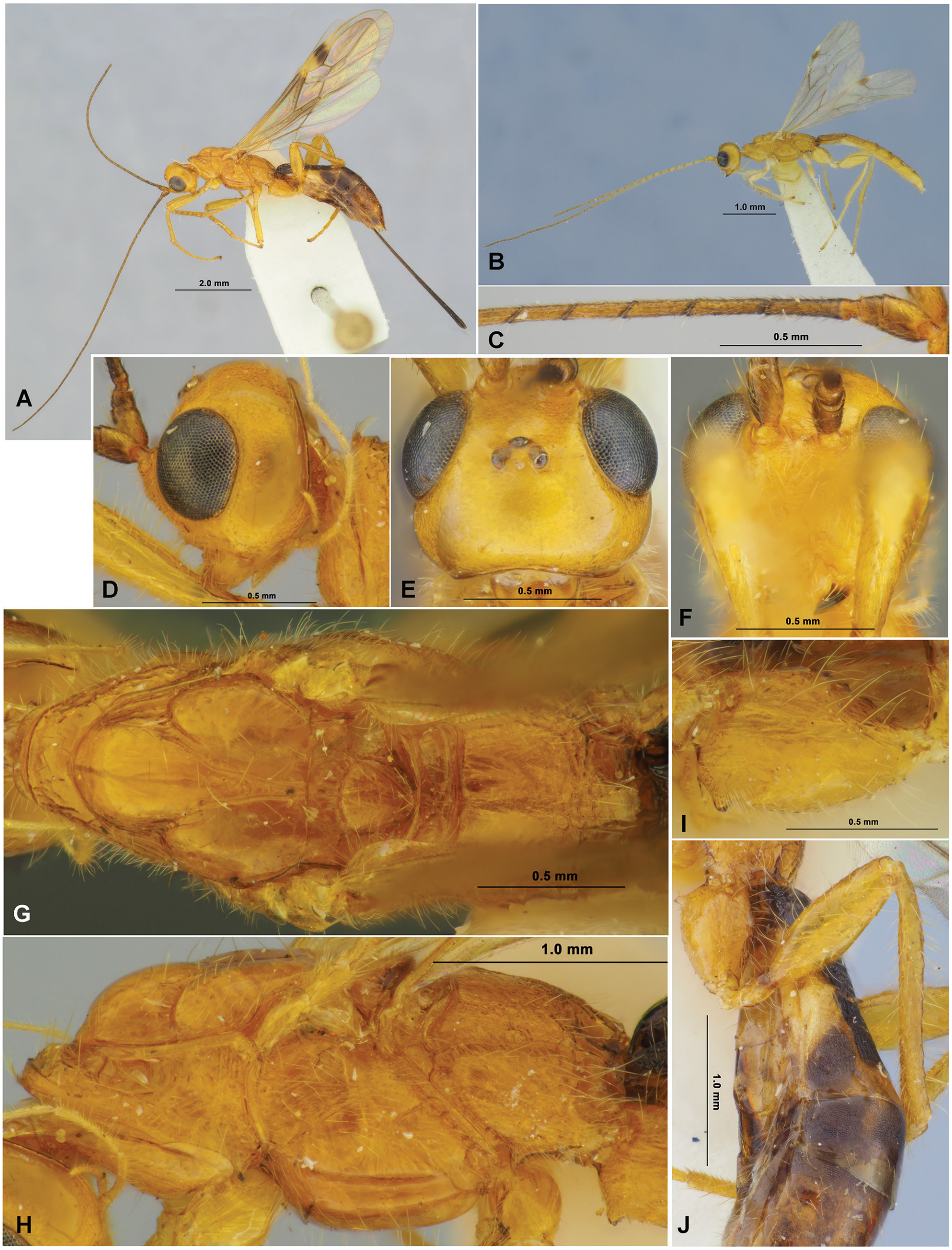

Figure 4. *Doryctes* (*Plyctes*) *jinjuensis* sp. nov. (female, holotype **A, C–J** male, paratype **B**) **A, B** habitus, lateral view **C** basal segments of antenna **D** head, lateral view **E** head, dorsal view **F** head, front view **G** mesosoma, dorsal view **H** mesosoma, lateral view **I** hind coxa, lateral view **J** hind leg.

Sculpture and pubescence. Vertex, frons, and temple smooth; face medially widely rugulose-striate, sparsely punctate to smooth laterally. Mesoscutum and scutellum smooth, with weak and short transverse striation between notauli in posterior 1/3 of

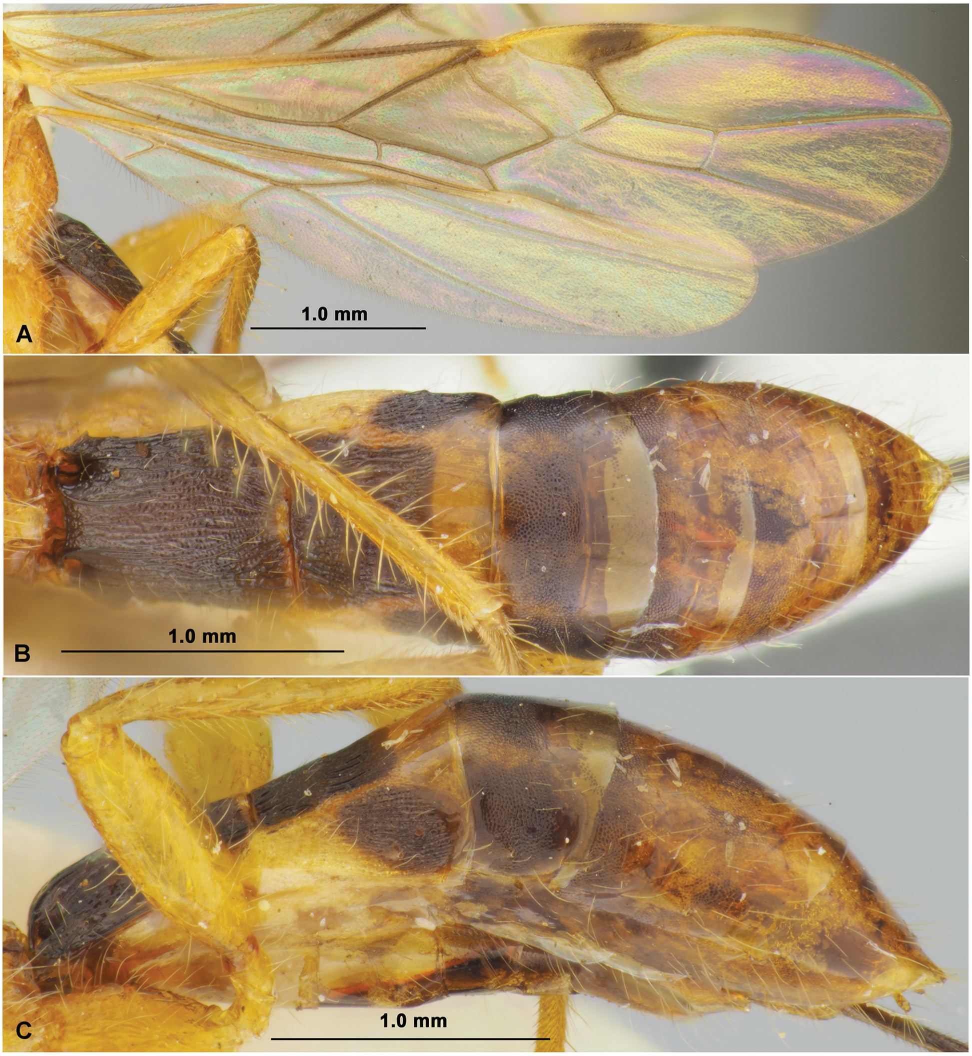

Figure 5. *Doryctes* (*Plyctes*) *jinjuensis* sp. nov. (female, holotype) **A** wings **B** metasoma, dorsal view **C** metasoma, lateral view.

mesoscutum. Mesopleuron mainly smooth. Propodeum with areas delineated by relatively weak carinae; basolateral areas long, smooth medially, reticulate-rugulose along carinae; areola rather long and narrow, densely rugose-reticulate with transverse striation, almost twice longer than its maximum width; petiolate area not delineated; basal carina relatively short, 0.3× as long as propodeum. Hind coxae mainly rugose-reticulate, weakly reticulate-coriaceous laterally; hind femur finely coriaceous to smooth. First and second metasomal tergites entirely and third in basal 1/2 densely striate with dense reticulation between striae; basal halves of second–seventh tergites very densely granulate-reticulate, with fine transverse striations posteriorly becoming weaker to posterior tergites; distal halves of third to seventh tergites smooth. Vertex widely gla-

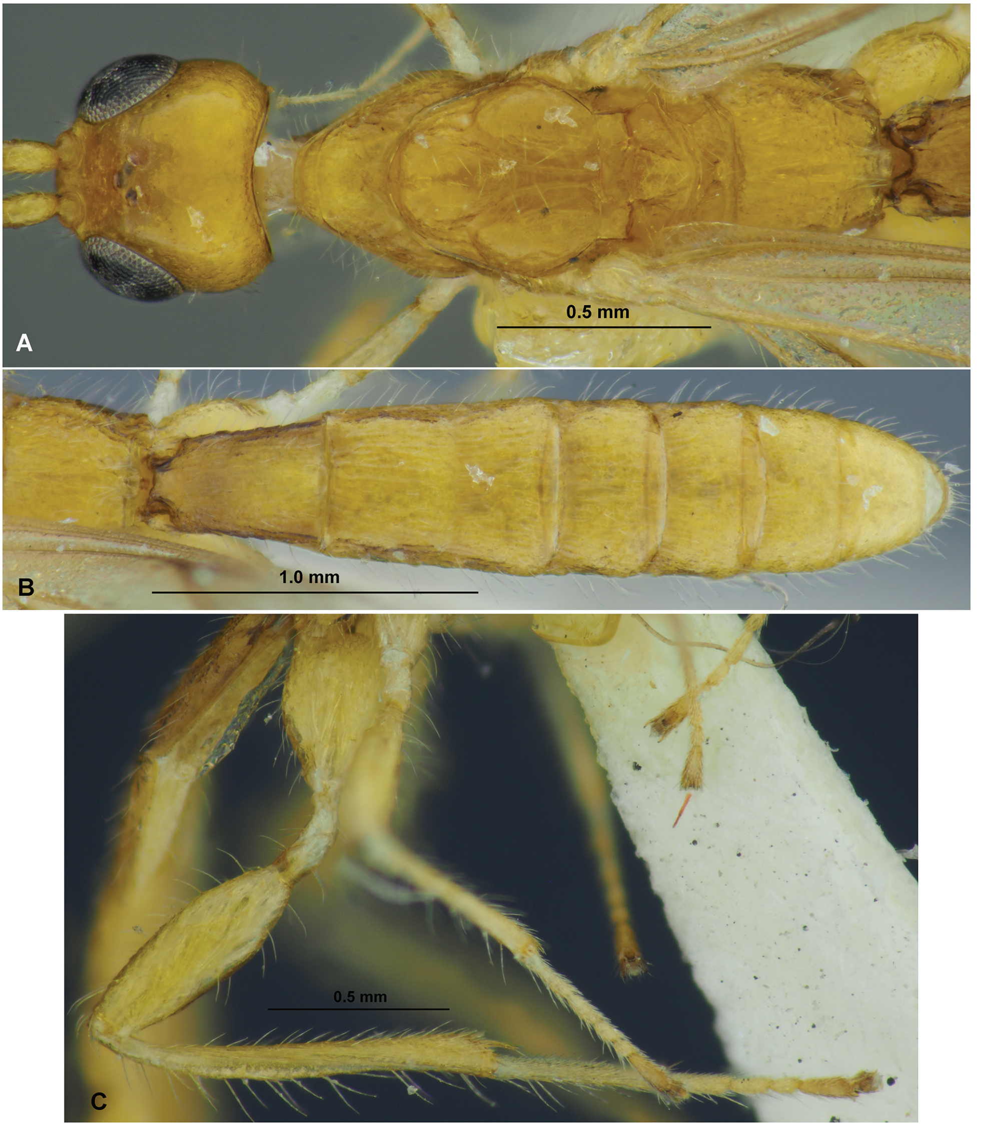

Figure 6. *Doryctes* (*Plyctes*) *jinjuensis* sp. nov. (male, paratype) **A** head and mesosoma, dorsal view **B** metasoma, dorsal view **C** hind leg, lateral view.

brous medially, posteriorly, and laterally with sparse, long, curved and almost erect yellow setae. Mesoscutum mainly glabrous, with rather sparse, long, curved and erect to semi-erect yellow setae along notauli and laterally. Metapleuron medially widely glabrous. Hind tibia dorsally with rather sparse, long, and erect yellow setae, its length 0.8–1.2× maximum width of hind tibia.

Colour. Head and mesosoma yellow to brownish yellow; metasoma dark reddish brown in basal 2/3 and reddish brown in apical 1/3, with lateral yellow spots on second tergite. Antenna dark brown, scape reddish brown dorsally. Palpi yellow. Legs mainly yellow, hind coxa brownish yellow, hind tibia yellow basally, similar colour as remainder parts of tibia. Wings very faintly infuscate. Pterostigma dark brown in medioposterior 1/3, yellow in basal 1/2 and apical fifth.

Male. Body length 4.2–5.3 mm; fore wing length 2.8–3.7 mm. POL 1.0–1.3× OD, 0.4–0.7× OOL. Rarely vertex anteriorly with very fine aciculation on short area. Antenna at least 35-segmented. Scape 1.4–1.5× longer than its maximum width. Penultimate segment 4.0× longer than wide; 0.8× as long as apical segment; the latter subacuminate apically. Mesosoma 2.2–2.4 (rarely almost 2.8) × longer than its height. Notauli posteriorly shallow but distinct; rarely area here with additional oblique striation. Prescutellar depression sometimes almost entirely smooth, usually weakly rugulose. Scutellum sometimes finely striate with striae curved posteriorly, but usually mainly smooth. Basolateral areas widely reticulate-rugulose, almost smooth only basally; areola indistinctly or distinctly delineated; basal carina ~ 0.4× as long as propodeum. Fore wing 3.9–4.3× longer than its maximum width. Pterostigma 4.0–4.3× longer than maximum width. Second radial abscissa (3-SR) 2.3–2.6× longer than first radial abscissa (r), 1.7–1.9× longer than first radiomedial vein (3-SR). Second radiomedial (submarginal) cell 2.7–3.3× longer than its maximum width, almost as long as brachial (first subdiscal) cell. Recurrent vein (m-cu) 2.5–3.3× longer than second medial abscissa (2-SR+M), almost as long as first radiomedial vein (3-SR). Hind wing 5.6–6.5× longer than maximum width. First abscissa of mediocubital vein (M+CU) 0.85–0.90× as long as second abscissa (1-M). Hind femur 3.2× longer than maximum width. Metasoma narrow, 1.1–1.2× longer than mesosoma and head combined. First tergite 1.5–1.6× longer than maximum subapical width; maximum width of first tergite 1.8–2.0× its minimum basal width. Second tergite with very fine and weakly divergent posteriorly sublateral furrows; median length of second tergite 0.8–1.0× its basal width, 1.1–1.3× length of third tergite. Basal 2/3–4/5 of third to sixth tergites densely longitudinally striate, densely granulate-reticulate between striae, their apical parts smooth. Colour. Body entirely or almost entirely yellow to brownish yellow, often first tergite distinctly infuscate at least laterally and basally. Antenna brown, yellow to brownish yellow in basal 1/3. Legs entirely yellow. Wings hyaline.

Etymology. Named after the type locality of the new species in South Korea, Jinju City, in the environment of which the holotype of the new species was collected.

Distribution. Korean Peninsula.

Key to the Asian species of the subgenus *Plyctes* Fischer, 1981

1 Brachial vein (CU1b) of fore wing subvertical to second abscissa of longitudinal anal vein (2-1A). Pterostigma always brown apically. Mesoscutum entirely with short, dense and semi-erect setae, without glabrous areas on lobes. Third tergite without wide subbasal transverse depression ....**Subgenus *Doryctes* s. str.**

– Brachial vein (CU1b) of fore wing distinctly slanted towards base of wing. Pterostigma pale brown or yellow apically. Mesoscutum with sparse, long, and semi-erect or erect setae along notauli and marginally, rather widely glabrous medially on all its lobes. Third tergite usually with wide crenulate subbasal transverse depression.........**2**

2 First abscissa of mediocubital vein (M+CU) of hind wing distinctly shorter than its second abscissa (1-M) .... **Subgenus *Neodoryctes* Szepligeti, 1914**

– First abscissa of mediocubital vein (M+CU) of hind wing equal to or longer than its second abscissa (1-M) (Subgenus Plyctes Fischer, 1981) **3**

3 First tergite short, its length 0.9–1.0× maximum width. Median length of second tergite ~ 0.3× its basal width. Ovipositor sheath shorter, 0.7–0.8× as long as metasoma and 0.30–0.45× as long as fore wing **4**

– First tergite long, its length 1.15–1.40× maximum width. Median length of second tergite 0.4–0.5× its basal width. Ovipositor sheath longer, 0.9–1.2× as long as metasoma and 0.6–0.9× as long as fore wing.. **6**

4 Face almost entirely smooth. Body length 5.8–6.4 mm. – China (Hainan) .... ***D.* (*P.*) *hainanensis* Belokobylskij, Tang, He & Chen, 2012**

– Face medially widely and distinctly subtransversely striate and often with fine rugulosity or punctation between striae... **5**

5 Mesoscutum almost entirely or mainly granulate-coriaceous. Radial vein (r) arising before middle of pterostigma. Hind femur 2.7–3.0× longer than its maximum width. Hind tibia weakly thickened. Propodeum with areas rather distinctly delineated by carinae. Sublateral bands of suture between second and third tergites less strongly expressed. Body length 2.2–4.5 mm. – Russia (Primorskiy kray), Korean Peninsula, Japan .... ***D.* (*P.*) *punctatus* Belokobylskij, 1984**

– Mesoscutum medially smooth, its lateral lobes very finely granulate-coriaceous. Radial vein (r) arising from middle of pterostigma. Hind femur 2.6× longer than its maximum width. Hind tibia distinctly thickened. Propodeum without areas delineated by carinae. Sublateral bands of suture between second and third tergites strongly expressed. Body length 5.5 mm. – Sri Lanka ....***D.* (*P.*) *solox* Enderlein, 1912**

6 Pterostigma entirely yellow. Temple longer, transverse diameter of eye 1.3× longer than temple (dorsal view). Hind tarsus 1.2× longer than hind tibia. Second segment of hind tarsus 1.6× longer than fifth segment (without pretarsus). First tergite long, its length 1.4× maximum width. – Setae on dorsal margin of hind tibia short, their length 0.8–1.0× maximum width of tibia. Body length 8.0 mm. – China (Yunnan)........................ ***D.* (*P.*) *flavistigma* Belokobylskij, Tang, He & Chen, 2012**

– Pterostigma medially widely brown, yellow basally and apically. Temple shorter, transverse diameter of eye 1.4–1.6× longer than temple (dorsal view). Hind tarsus almost as long as hind tibia. Second segment of hind tarsus 1.1–1.3× longer than fifth segment (without pretarsus). First tergite short, its length 1.15–1.30× maximum width **6**

6 Metasomal tergites behind third tergite entirely smooth. Body entirely yellow or brownish yellow. Hind femur entirely brownish yellow. Body length 9.8 mm. – India, Sierra Leone.. ***D.* (*P.*) *nigricornis* (Kriechbaumer, 1894) [*D.* (*P.*) *coxalis* (Turner, 1922)]**

– Metasomal tergites behind third tergite basally densely reticulate-coriaceous, usually on wide area. At least metasoma mainly reddish brown or dark brown. Hind femur often distinctly infuscate **7**

7 Setae on dorsal margin of hind tibia longer, their length 1.4–1.8× maximum width of tibia. Mesosoma pale reddish brown with dark spots in its posterior part. Hind tibia basally rather distinctly dark. Body length 4.4–9.2 mm. – Japan, China, India, Vietnam, Malaysia, Indonesia ....***D.* (*P.*) *malayensis* (Fullaway, 1919)**

– Setae on dorsal margin of hind tibia shorter, their length 0.8–1.2× maximum width of tibia. Mesosoma entirely yellow to brownish yellow or mostly reddish brown. Hind tibia basally yellow or brownish yellow **8**

8 Hind coxa with low and wide dorsal protuberance (Fig. 4I). Pterostigma of fore wing widely yellow in basal 1/3 (Fig. 5A). Recurrent vein (m-cu) of hind wing curved toward base of wing (Fig. 5A). Mesosoma entirely yellow to brownish yellow (Fig. 4A). Hind leg entirely yellow (Fig. 4J). Body length 4.2–6.5 mm. – Korean Peninsula .... ***D.* (*P.*) *jinjuensis* sp. nov.**

– Hind coxa without dorsal protuberance. Pterostigma of fore wing narrowly yellow in basal quarter only. Recurrent vein (m-cu) of hind wing curved toward apex of wing. Mesosoma anteriorly yellowish brown or reddish brown with dark spots, posteriorly distinctly infuscate on most part of propodeum and metapleuron. Hind leg mostly reddish brown to dark reddish brown. Body length 6.7–8.4 mm. – Indonesia .... ***D.* (*P.*) *diversus* (Szépligeti, 1910)**

Genus *Neoheterospilus* Belokobylskij, 2006

Type species. *Neoheterospilus koreanus* Belokobylskij, 2006.

Neoheterospilus (*Neoheterospilus*) *geochangus* sp. nov.

https://zoobank.org/E181E56A-5066-4867-894C-18ECDBE40F79
Figs 7, 8

Type material. ***Holotype*:** 1 female, Korean Peninsula, "Korea (GN), Geochang-gun, Geochang-eup, Science Museum Natural Enemy, VI.3–VI.27.2015 (Malaise Trap), Ku Deokseo" (NIBR).

Comparative diagnosis. This new species is similar to *Neoheterospilus* (*N.*) *subtropicalis* Belokobylskij, 2006 (Belokobylskij, 2006) from Japan, China, Korea and Vietnam, but differs from the latter species by having the 14-segmented slender antenna with first flagellar segment 6.5× longer than its apical width and 0.9× as long as second segment (thick and 16–17-segmented, with first flagellar segment 4.0–4.7× longer than its apical width and as long as second segment in *N. subtropicalis*), scape long, almost 2.0× longer than its maximum width (short, 1.3–1.5× in *N. subtropicalis*), precoxal sulcus running along almost the entire length of lower part of mesopleuron (only in anterior 1/2 in *N. subtropicalis*), basolateral areas of propodeum mainly rugulose-reticulate (almost entirely smooth in *N. subtropicalis*), areola of propodeum wide (narrow in *N. subtropicalis*), radial vein (r) of fore wing arising from middle of pterostigma (before middle in *N. subtropicalis*), second radiomedial vein (r-m) of the fore wing absent (present in *N. subtropicalis*), hind tibia distinctly thickened (rather slender in *N. subtropicalis*), basal area of second tergite not delineated by furrow (weakly delineated in *N. subtropicalis*), median length of second tergite (with apical area) 1.3× its basal width (almost equal in *N. subtropicalis*), ovipositor sheath not widened apically (distinctly widened in *N. subtropicalis*), and ovipositor sheath with sparse and long setae (with rather short and dense setae in *N. subtropicalis*).

N. geochangus sp. nov. is also similar to *Neoheterospilus* (*N.*) *curvicaudis* (Belokobylskij, 1994) from Vietnam, but it differs from the latter by the antenna 14-segmented and with the scape not compressed and long (20-segmented, with a weakly compressed and short scape in *N. curvicaudis*), penultimate segment of antenna 6.0× longer than wide and 1.1× longer than apical segment (4.0× longer than wide and 0.9× as long as the apical segment in *N. curvicaudis*), precoxal sulcus running along almost the entire length of the lower part of mesopleuron (along anterior 1/2 in *N. curvicaudis*), basolateral areas of propodeum mainly rugulose-reticulate (almost entirely smooth in *N. curvicaudis*), second radiomedial vein (r-m) of fore wing absent (present in *N. curvicaudis*), basal area of the second tergite absent (finely delineated by shallow furrow in *N. curvicaudis*), second suture of metasoma smooth (crenulate in *N. curvicaudis*), ovipositor sheath not widened apically (distinctly widened in *N. curvicaudis*), ovipositor sheath with sparse and long setae (with rather short and dense setae in *N. curvicaudis*), and pterostigma entirely pale brown (brown in *N. curvicaudis*).

Description. Female. Body length 1.7 mm; fore wing length 1.3 mm.

Head. Head width (dorsal view) 1.5× its median length. Occiput distinctly concave. Occipital carina mediodorsally straight, without medial break. Head behind eyes (dorsal view) distinctly and roundly narrowed. Transverse diameter of eye 1.5× longer than temple (dorsal view). POL 0.8× Od, 0.35× OOL. Eye 1.2× as high as broad. Malar space 0.35× eye height, 0.7× basal width of mandible. Face width 1.2× eye height and 1.5× height of face and clypeus combined. Hypoclypeal depression transverse and oval, its width 1.2× distance from edge of depression to eye, 0.5× width of face. Hypostomal flange narrow. Mandible medium size. Maxillary palpi almost as long as head height.

Antenna. Antenna slender, filiform, 14-segmented, weakly shorter than body. Scape relatively long, not compressed, straight apically, with sparse white setae on inner side; length of scape almost 2.0× its maximum width, 1.4× longer than enlarged pedicel. First flagellar segment 6.5× longer than its apical width, 0.9× as long as second segment. Penultimate segment 6.0× longer than wide, almost as long as first segment, 1.1× longer than apical segment; the latter acuminate apically.

Mesosoma. Mesosoma 1.9× longer than its height. Mesoscutum 0.7× as long as wide. Median lobe of mesoscutum almost straight anteriorly, with distinct subpointed lateral corners. Notauli distinct, rather deep, complete, and sparsely crenulate. Prescutellar depression with high median carina, smooth, 0.5× as long as weakly convex scutellum. Precoxal sulcus distinct, mainly crenulate, running along almost entire length of lower part of mesopleuron, but its posterior part visible as narrow stripe.

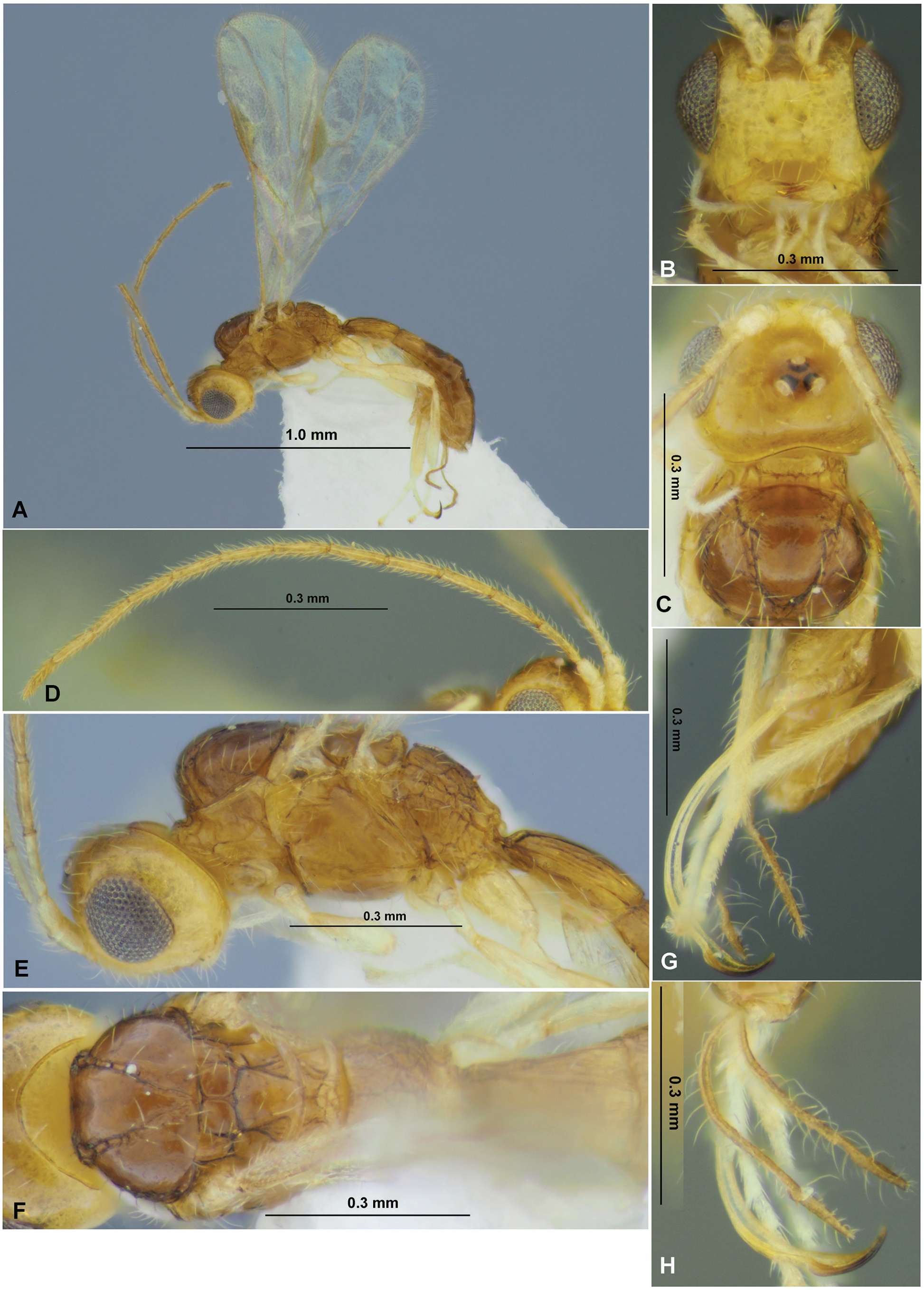

Figure 7. *Neoheterospilus geochangus* sp. nov. (female, holotype) **A** habitus, lateral view **B** head, front view **C** head and mesoscutum, dorsal view **D** antenna **E** head and mesosoma, lateral view **F** mesosoma, dorsal view **G** ovipositor and sheaths, lateral view **H** ovipositor and sheaths, dorsal view.

Wings. Fore wing almost 3.0× longer than wide. Metacarp 1.3× longer than wide pterostigma. Second radiomedial vein (r-m) probably absent. First radial abscissa 0.8× as long as width of pterostigma, ~ 0.15× as long as second abscissa (3-SR + SR1), 0.4× as long as trace of first radiomedial vein (2-SR). Second abscissa (3-SR + SR1) distinctly evenly curved. First abscissa of medial vein (1-SR+M) distinctly curved. Recurrent vein (m-cu) postfurcal to trace of first radiomedial vein (2-SR). Discoidal (discal) cell 1.8× longer than wide. Nervulus (cu-a) short and weakly postfurcal, distance (1-CU1) between basal vein (1-M) and nervulus (cu-a) almost equal to nervulus (cu-a) length. Hind wing 6.0× longer than wide. Second costal abscissa (1-SC+R) mainly absent. First abscissa of mediocubital vein (M+CU) almost as long as second abscissa (1-M). Recurrent vein (m-cu) interstitial, unsclerotised, perpendicular to mediocubital vein (1-M).

Legs. Hind femur 3.4× longer than wide. Hind tarsus 0.9× as long as hind tibia. Hind tibia distinctly thickened; hind tarsus thickened basally and narrowed distally. Hind basitarsus 0.4× as long as second–fifth segments combined. Second segment of hind tarsus 0.6× as long as basitarsus, almost as long as fifth segment (without pretarsus).

Metasoma. Metasoma 1.2× longer than head and mesosoma combined. First tergite with weak spiracular tubercles in basal 1/3, weakly and linearly widened toward apex, its length 1.5× apical width; apical width almost 2.0× basal width. Basal area of second tergite not delineated by transverse furrow; apical area wide and delineated anteriorly by deep and almost straight crenulate furrow, medial length of this area 0.5× length of remaining tergite. Median length of second tergite (with apical area) 1.3× its basal width, approximately twice length of third tergite. Ovipositor sheath slender and not widened apically but with small ventral process in its subapical part; ~ 0.5× as long as metasoma, 0.8× as long as mesosoma, 0.3× as long as fore wing. Ovipositor slender and upcurved, its apex as on figures (Fig. 7G, H), with distinct subbasal ventral excise, its thickened apical part medium length.

Sculpture and pubescence. Head entirely (including face) smooth. Mesoscutum mainly smooth, finely coriaceous anteriorly and along notauli at short areas, with weak convergent carinae in posterior 1/2. Scutellum and mesopleuron smooth at most part. Metapleuron entirely rugulose, finely sculptured anteriorly. Basolateral areas of propodeum short and wide, mainly rugulose-reticulate; remaining part of propodeum distinctly and rather densely rugose-reticulate and partly with transverse striation; areola more or less distinctly delineated by carinae, irregular shape, wide, approximately as long as wide; petiolate area delineated; basal carina situated in basal quarter. Hind coxa and femur smooth. First metasomal tergite distinctly, relatively sparsely and distally weakly curvedly longitudinally striate, with fine reticulation between striae, dorsal carinae distinct, complete, and convergent towards posterior margin. Second tergite distinctly and densely striate, but its apical area smooth. Remaining tergites smooth. Suture between second and third tergites smooth. Vertex almost entirely with sparse long and semi-erect white setae directed forwards. Mesoscutum mainly glabrous, with long, erect, and sparse white setae arranged narrowly along notauli and marginally. Mesopleuron glabrous in most part. Hind tibia with rather short, semi-erect and sparse white setae, their length 0.5–0.8× maximum width of tibia. Ovipositor sheath with sparse and long setae.

Figure 8. *Neoheterospilus geochangus* sp. nov. (female, holotype) **A** wings **B** propodeum and metasoma, dorsal view **C** metasoma and ovipositor, lateral view.

Colour. Head brownish yellow to yellow in lower 1/2. Mesosoma pale reddish brown, pale anteriorly. Metasoma reddish brown to yellowish brown in anterior 0.4 and reddish brown in posterior 0.6. Antennae pale brown, yellow basally. Palpi pale yellow. Legs yellow to pale yellow, coxae infuscate in basal halves. Ovipositor sheath brown. Fore wing hyaline. Pterostigma entirely pale brown.

Male. Unknown.

Etymology. Named after the type locality of the new species in South Korea, Geochang town.

Distribution. Korean Peninsula.

Genus *Spathius* Nees, 1819

Type species. *Cryptus clavatus* Panzer, 1809 (= *Ichneumon exarator* Linnaeus, 1758).

Spathius fumipennis sp. nov.

https://zoobank.org/5A13443D-3137-44DD-87C8-7861DA6BD55B
Figs 9, 10

Type material. ***Holotype*:** female, "Korea, Kyongsangbuk-do [Gyeongsangbuk-do], Chomch'on-up [Jeomchon-eup], Daesong Buljong [Daeseong Buljeong], 9.VI.1992, D.-S. Ku" (NIBR).

***Paratype*.** 1 female, "Korea, Chungnam-do, Cheongyang-gun, Jeongsan-myeon, Machi-ri, sweeping, 15.VI.1992, D-S Ku" (SMNE).

Comparative diagnosis. This new species belongs to the *S. fasciatus* Walker species group. *S. fuscipennis* sp. nov. is similar to Japanese *S. hikoensis* Belokobylskij, 1998 (Belokobylskij 1998), but differs from the latter species by having the occipital carina joined below with hypostomal carina (usually not joined and obliterated below in *S. hikoensis*); first flagellar segment 4.0× longer than its apical width (5.0–5.7× in *S. hikoensis*); the apical 1/2 of antenna completely dark and without pale subapical segments (with several pale subapical segments in *S. hikoensis*); the mesoscutum entirely weakly granulate-coriaceous (distinctly granulate in *S. hikoensis*); scutellum without lateral carinae (with distinct carinae in *S. hikoensis*); fore wing distinctly and evenly infuscate, pterostigma entirely brown (only faintly infuscate and pale in basal 1/3 in *S. hikoensis*); radial vein (r) arising distinctly behind middle of pterostigma, from its basal 2/3 (arising from basal 3/5 in *S. hikoensis*); hind femur weakly thicker, 4.1× longer than wide (slender, its length 4.3–4.8× longer than wide in *S. hikoensis*); setae on the dorsal surface of the hind tibia shorter, 0.7–1.0× as long as the maximum width of the tibia (long, 1.1–1.5× longer in *S. hikoensis*).

The new species is also similar to *S. clavator* Tang, Belokobylskij & Chen, 2015 (Tang et al. 2015) from China (Hainan), but differs from it by having the vertex almost entirely smooth (mainly rugulose-striate in *S. clavator*); malar space 0.6× eye height and almost equal to basal width of mandible (0.4× eye height and 0.7× basal width of mandible in *S. clavator*); occipital carina joined below with hypostomal carina (not joined and obliterated below in *S. clavator*); first flagellar segment 4.0× longer than its apical width (6.7× in *S. clavator*); mesoscutum entirely weakly granulate-coriaceous and without or with very short rugae (distinctly granulate and with long rugae in *S. clavator*); mesopleuron medially widely smooth, (entirely densely granulate with striation in *S. clavator*); hind femur slender, 4.1× longer than wide (thicker, its length 3.7× longer than wide in *S. clavator*); fore wing distinctly and evenly infuscate, pterostigma entirely brown (wing faintly infuscate, pterostigma pale in basal 1/3 in *S. clavator*); radial vein (r) of the fore wing arising distinctly behind the middle of the pterostigma, from its basal 2/3 (from middle in *S. clavator*); length of petiole 2.3× its apical width (2.7× in *S. clavator*); second tergite without separated laterotergites (with laterotergites separated in basal 1/2 in *S. clavator*).

Description. Female. Body length 4.7–4.8 mm; fore wing length 3.2–3.4 mm.

Head. Head width (dorsal view) 1.5× its median length, 1.2× width of mesoscutum. Head behind eyes (dorsal view) weakly convex in anterior 1/2 and roundly narrowed in posterior 1/2; transverse diameter of eye 1.2× length of temple. Ocelli medium-sized, arranged in triangle with base 1.1× its sides; POL 0.8× Od, 0.3× OOL. Eye glabrous, 1.2× as high as broad. Malar space 0.5–0.6× eye height and 1.0–1.3× basal width of mandible. Face width 1.3× eye height and 1.2–1.3× height of face and clypeus combined. Clypeal suture rather fine and complete. Clypeus weakly convex. Hypoclypeal depression transverse-oval, its width equal to distance from edge of depression to eye, 0.4–0.5× width of face. Occipital carina joined with hypostomal carina below upper base of mandible. Hypostomal flange wide and distinct. Vertex distinctly convex.

Antenna. Antenna weakly thickened, almost setiform, 29–30-segmented, almost as long as body. Scape 1.8–1.9× longer than its width. First flagellar segment 4.0–4.5× longer than its apical width, 1.2–1.3× longer than second segment. Penultimate segment 2.0–2.5× longer than its wide, 0.4× as long as first flagellar segment, 0.8–0.9× as long as apical segment; the latter weakly acuminated apically.

Mesosoma. Length of mesosoma 1.7× its height. Pronotal keel fine but distinct, its posterior branch medially widely fused with posterior margin of pronotum, anterior branch almost indistinct. Pronotum subanteriorly with rather distinct transverse carina. Pronotal lateral depression not delineated upper by carinae, wide, shallow, coarsely and rather densely curvedly crenulate. Mesoscutum highly and subvertically elevated above pronotum. Notauli complete, wide, rather deep anteriorly and more or less shallow posteriorly, densely, sparsely and distinctly crenulate with reticulation between rugae. Prescutellar depression rather deep, relatively long, with five almost complete carinae, finely rugulose or reticulate, 0.30–0.35× as long as scutellum. Scutellum weakly convex, without lateral carinae. Metanotum with short, wide and subpointed dorsal tooth. Subalar depression shallow, rather narrow, rugose-striate. Precoxal sulcus deep, wide, straight, oblique, distinctly crenulate, with fine reticulation, running along anterior 0.6 of lower length of mesopleuron, with shallow and relatively wide striate depression behind sulcus. Metapleural flange wide and short. Propodeum with distinct, short, and thick lateral tubercles.

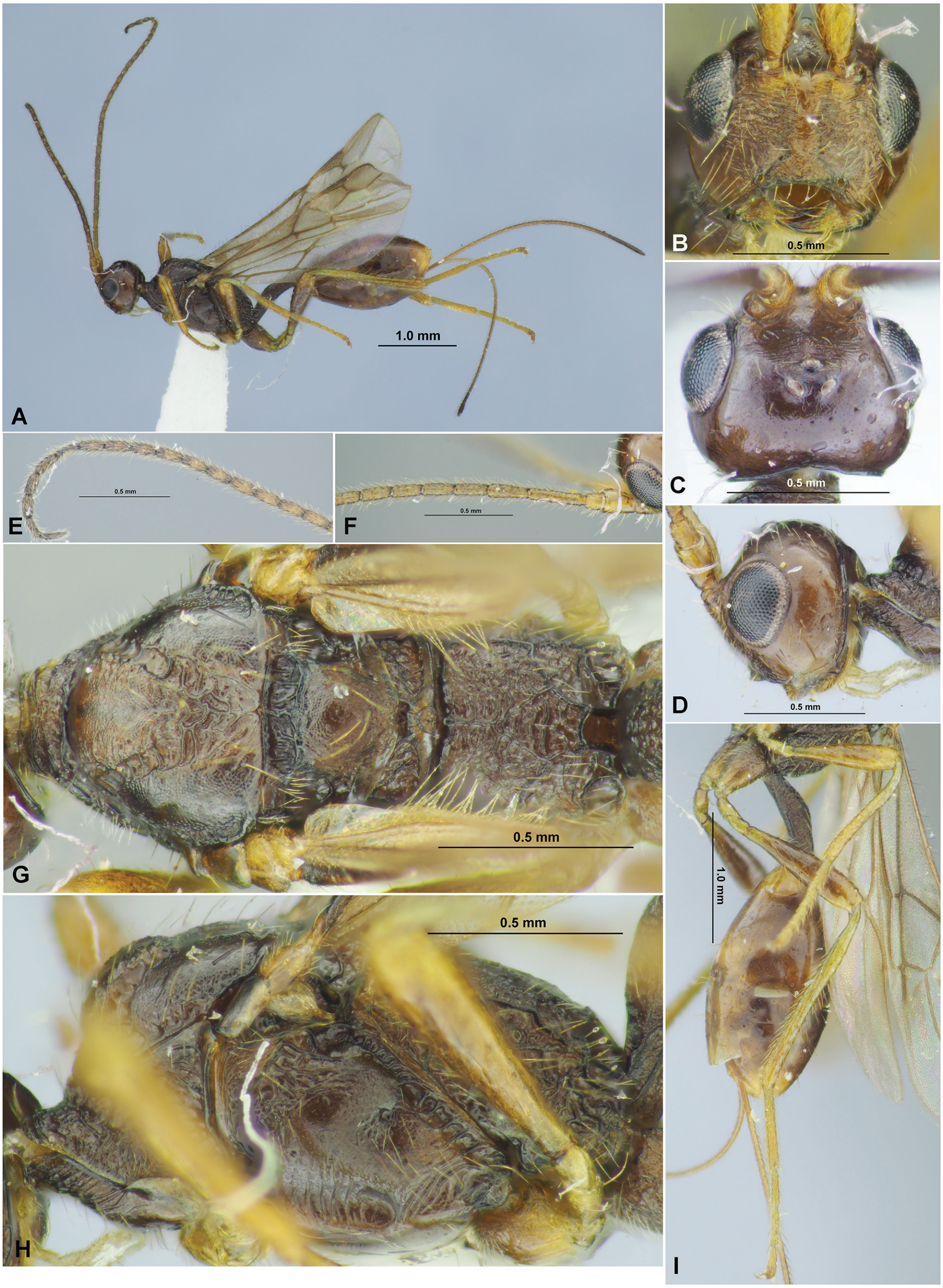

Figure 9. *Spathius fumipennis* sp. nov. (female, holotype) **A** habitus, lateral view **B** head, front view **C** head, dorsal view **D** head, lateral view **E** apical segments of antenna **F** basal segments of antenna **G** mesosoma, dorsal view **H** mesosoma, lateral view **I** hind leg.

Figure 10. *Spathius fumipennis* sp. nov. (female, holotype) **A** wings **B** metasoma, dorsal view **C** metasoma, lateral view **D** petiole, dorsal view **E** petiole, lateral view.

Wings. Fore wing 3.6–3.8× longer than wide. Pterostigma 4.2–5.0× longer than its maximum width. Radial vein (r) arising distinctly behind middle of pterostigma, inner distance of pterostigma from parastigma to radial vein (r) 1.7–1.8× its inner distance from radial vein to metacarp (1-R1). Radial (marginal) cell not shortened; metacarp (1-R1) 1.4× longer than pterostigma. First radial abscissa (r) 0.8–0.9× as long as maximum width of pterostigma. Second radial abscissa (3-SR) 2.8–3.0× longer than first abscissa and forming with it very obtuse angle, 0.4–0.5× as long as straight third abscissa (SR1), 0.9× as long as first radiomedial vein (2-SR). Second radiomedial (submarginal) cell not or only weakly narrowed distally, its length 2.7× maximum width, 1.3× length of brachial (subdiscal) cell. First medial abscissa (1-SR+M) straight or weakly sinuate. Recurrent vein (m-cu) weakly postfurcal, ~ 6.0× longer than second abscissa of medial vein (2-SR+M), 0.4× as long as first radiomedial vein (2-SR). Nervulus (cu-a) weakly postfurcal, distance (1-CU1) from nervulus (cu-a) to basal vein (1-M) 0.3–0.4× nervulus (cu-a) length. Parallel vein (CU1a) not interstitial, arising from anterior 0.3–0.4 of distal vein (3-CU1) of brachial (subdiscal) cell. Mediocubital vein (M+CU1) almost straight or weakly curved. Hind wing 4.5–5.0× longer than maximum width. First costal abscissa (C+SC+R) 0.6× as long as second abscissa (1-SC+R). First abscissa of mediocubital vein (M+CU) 0.70–0.75× as long as second abscissa (1-M). Recurrent vein (m-cu) not pigmented, transparent, rather long, weakly antefurcal, distinctly oblique towards base of wing.

Legs. Fore tibia with slender numerous and rather sparse spines arranged in single vertical line. Hind coxa 1.6× longer than its maximum width, with basoventral corner and small tooth. Hind femur claviform, 4.0–4.1× longer than wide. Hind tarsus 0.9–1.0× as long as hind tibia. Hind basitarsus 0.70–0.75× as long as second–fifth segments combined; second segment 0.45–0.50× as long as basitarsus, 1.1–1.3× longer than fifth segment (without pretarsus).

Metasoma. Petiole (lateral view) weakly and evenly curved ventrally, dorsally distinctly and regularly curved to its middle and almost straight in apical 1/2, thickened submedially; widened on spiracle level and weakly widened in apical 0.2–0.3 (dorsal view), with small spiracular tubercles in basal 1/3. Length of petiole 2.3–2.4× its apical width, almost 2.0× length of propodeum; apical width ~ 1.5× its width at level of spiracles. Second and following tergites without separate laterotergites. Second suture absent. Median length of second and third tergites combined 1.7–1.8× basal width of second tergite, 0.8× their maximum width. Ovipositor weakly curved down. Ovipositor sheath 1.3–1.4× longer than metasoma, 2.2–2.4× longer than mesosoma, 1.0–1.1× longer than fore wing.

Sculpture and pubescence. Vertex almost entirely smooth, only finely coriaceous near ocelli; frons almost entirely with distinct, dense, and curved transverse striae, with additional fine reticulation between striae. Face entirely or mainly (in upper 2/3) densely and coarsely striate, with rugulosity between striae below and laterally, finely reticulate-coriaceous to smooth in lower lateral 1/3. Temple entirely smooth. Mesoscutum entirely densely and weakly granulate-coriaceous, sometimes with short rugae near notauli and laterally, coarsely, and sparsely rugose in wide and short medioposterior area. Scutellum densely and finely to very finely coriaceous, with fine transverse aciculae anteriorly. Mesopleuron medially widely almost smooth, finely and densely rugulose-reticulate marginally. Propodeum with areas delineated by distinct carinae; basolateral areas entirely and densely granulate-rugulose; areola wide and rather long, transverse striae with rugulosity, almost as long as wide; petiolate area rather long and wide, distinctly separated from areola by curved carina; basal carina 0.7–1.0× as long as anterior fork of areola. Hind coxa dorsally partly densely transversely striate with dense rugosity in wide basal 1/2, laterally distinctly and densely rugulose-granulate. Hind femur mainly smooth, longitudinally striate dorsally. Petiole distinctly and sparsely striate, with dense to very dense rugulosity between striae, only densely rugose in basal 1/4. Second and following tergites entirely smooth. Vertex with sparse, short, and almost erect pale setae situated laterally and anteriorly, glabrous on wide medial part. Mesoscutum with sparse, long, and erect yellow setae laterally and along notauli, glabrous on wide medial parts of lobes. Mesopleuron widely glabrous. Setae of dorsal surface of hind tibia erect, rather dense, mainly long, their length 0.7–1.0× maximum width of tibia.

Colour. Body mainly dark reddish brown to almost black partly, metasoma posteriorly or already behind petiole and ventrally reddish brown. Antennae brown with dark brown apical quarter or mainly dark brown with two basal segments pale brown, without pale subapical segments. Palpi yellow or brownish yellow. Legs partly reddish brown or pale reddish brown, all trochanters and trochantelli, tibiae and tarsi yellow or yellowish brown, hind tibiae basally yellow on rather long distance. Ovipositor sheath mainly pale brown, almost black apically. Fore wing distinctly and evenly infuscate, faintly paler basally and apically. Pterostigma evenly brown or yellowish brown in basal third.

Male. Unknown.

Etymology. This species is named from the Latin *fumis* (= smoke) and *pennis* (= pen, "wing"), after its distinctly infuscate fore wing.

Distribution. Korean Peninsula.

New and rare species in the fauna of Korean Peninsula

**Dendrosoter middendorffii* (Ratzeburg, 1848)

Bracon (*Eurybolus*) *middendorffii* Ratzeburg, 1848: 32.
Dendrosoter middendorffii: Belokobylskij and Tobias 1986: 39; Belokobylskij 1996: 66; Belokobylskij and Maetô 2009: 93; Yu et al. 2016; Belokobylskij et al. 2019: 261.

Material examined. South Korea: 1 female, "S. Korea, Gyeongsangnam-do (GN), Geochang-gun, Namsang-myeon, Jeoncheok-ri, 35°37'23.1"N, 127°56'31.8"E, 11.06.2022, Tselikh, Lee, Belokobylskij", "Reared from the logs of *Pinus densiflora* infested by Curculionidae (Scolytinae) by 13.06.2022" (NIBR); 2 females, same locality and data (ZISP); 1 female, same locality and data, but emerged 29.VI.2022 (SMNE); 1 female, same locality and data, but emerged 2.VII.2022 (SMNE).

Distribution. *Korean Peninsula; Europe, Georgia, Armenia, Turkey, Israel, Iran, Russia (European part, Urals, south of Far East), Japan, India.

***Eodendrus eous* (Belokobylskij, 1988)**

Dendrosotinus eous Belokobylskij, 1988: 625.
Dendrosotinus (*Eodendrus*) *eous*: Belokobylskij 1998: 66.
Eodendrus eous: Belokobylskij et al. 2005: 2731; Belokobylskij and Maetô 2009: 153; Yu et al. 2016; Lee et al. 2020: 18.

Material examined. South Korea: 1 female, SW of Geochang-eup, forest on mountain, 35°40'15"N, 127°53'24"E – 35°40'19"N, 127°53'01"E, 20.06.2019, K. Samartsev (ZISP); 1 male, SW of Geochang-eup, forest on a mountain, 35°40'15"N, 127°53'24"E – 35°40'19"N, 127°53'01"E, 3.06.2019, K. Samartsev (ZISP); 1 female, "Korea (GB), Cheonbu3-gil, Buk-myeon, Ulleung-gun, VIII.15–VIII.31.2017 (Malaise trap), Ku Deokseo" (SMNE); 1 female, "Korea (GB), Hakpo-ri, Seo-myeon, Ulleung-gun, VIII.15–VIII.31.2017 (Malaise trap), Ku Deokseo" (SMNE); 1 female, "Korea: CN, Keumsan, Kunbuk, Sanan, Jajinbaengii, 19–24.V.1998, MT, Tripotin Pierre" (SMNE); 1 female, "Korea: GG, Suwon, Mt. Yeogi, Matsumura, 23.VI.1997, June-Yeol Choi" (SMNE).

Distribution. Korean Peninsula; Russia (south of the Far East), Japan.

****Guaygata mariae* (Belokobylskij, 1993)**

Neurocrassus mariae Belokobylskij, 1993: 163.
Guaygata mariae: Belokobylskij and Maetô 2006: 604; 2009: 160; Tang et al. 2013: 85; Yu et al. 2016.

Material examined. South Korea: 1 female, "Korea (GB), Cheonbu3-gil, Buk-myeon, Ulleung-gun, X.3–XI.14.2017 (Malaise trap), Ku Deokseo" (NIBR); 1 female, "Korea. Konbongsa, Kosong, Kangwon. 26.V.1993. Deok-Seo Ku" (SMNE).

Distribution. *Korean Peninsula; Russia (Primorskiy Territory), China (Jiangsu, Fujian); Japan (Honshu), Vietnam.

****Ipodoryctes signipennis* (Walker, 1860)**

Spathius signipennis Walker, 1860: 309.
Rhaconotus signipennis: Belokobylskij 2001: 134.
Ipodoryctes signipennis: Belokobylskij and Zaldívar-Riverón 2021: 44.

Material examined. South Korea: 1 female, "Korea [JN], Jeungdo-myeon, Daechori, Sinan-gun, 35°58'56"N, 126°9'23"E, 2020.VIII.31–IX.15, Coll. S.W. Choi & J.Y. Lee, The 5th National Ecosystem Survey" (NIBR).

Distribution. *Korean Peninsula; Russia (Far East), China, Japan, India, Sri Lanka, Vietnam, Indonesia.

****Leluthia* (*Leluthia*) *disrupta* (Belokobylskij, 1994)**

Pareucoryctes disruptus Belokobylskij, 1994: 23.
Leluthia (*Leluthia*) *disrupta*: Belokobylskij and Maetô 2009: 294; Li et al. 2015: 595; Yu et al. 2016.

Material examined. South Korea: 1 female, "Korea, Gangwon-do, Inje, Sangnam, Misan-ri, Wangseong-dong, Mt. Bangtaesan, 12.VIII.1986. Deok-Seo Ku" (NIBR).

Distribution. *Korean Peninsula; Russia (North Caucasus, south of Far East), Georgia.

***Leluthia* (*Leluthia*) *honshuensis* Belokobylskij & Maetô, 2006**

Leluthia (*Leluthia*) *honshuensis* Belokobylskij & Maetô, 2006: 607; 2009: 295; Yu et al. 2016; Kim et al. 2018: 135.

Material examined. South Korea: 1 female, "Korea, Gyeongnam-do, Hadong-gun, Bukcheon-myeon, Jikjeon-ri, Mt. Limyeong (Light trap), 28–29.VIII.2000, J-S Park" (SMNE).

Distribution. Korean Peninsula (Kim et al. 2018); Japan.

****Leluthia* (*Leluthia*) *nagoyae* Belokobylskij & Maetô, 2006**

Leluthia (*Leluthia*) *nagoyae* Belokobylskij & Maetô, 2006: 610; 2009: 299; Yu et al. 2016.

Material examined. South Korea: 1 male, "Korea (GN), Geochang-gun, Geochang-eup, Science Museum Natural Enemy, IX.4–XI.16.2020 (Malaise Trap), Ku Deokseo" (NIBR).

Distribution. *Korean Peninsula; Japan.

****Leluthia* (*Euhecabolodes*) *transcaucasica* (Tobias, 1976)**

Euhecabolodes transcaucasicus Tobias, 1976: 251.
Leluthia (*Euhecabolodes*) *transcaucasica*: Belokobylskij and Maetô 2009: 294; Li et al. 2015: 595; Yu et al. 2016.

Material examined. South Korea: 1 female, "Korea, Gyeonggi-do, Osan, Sucheong-dong, Gyeonggi-do, Forest Environment Research Institute (Light trap), 1.VI.1999, H-G Lee" (NIBR); 1 female, "Korea, Chungbuk-do, Danyang-gun, Danyang-eup, Cheongdong-ri, Cheondong valley, Mt. Sobaek, 14.VIII.1998. J-S Park" (SMNE).

Distribution. *Korean Peninsula; Czech Republic, Russia (Buryatia, south of the Far East), Georgia, Turkey, Iran, Kazakhstan, Mongolia.

Neoheterospilus (Neoheterospilus) subtropicalis* **Belokobylskij, 1996

Neoheterospilus (*Neoheterospilus*) *subtropicalis* Belokobylskij, 2006: 173; Belokobylskij and Maetô 2009: 316; Yu et al. 2016.

Material examined. South Korea: 1 female, "S. Korea: Gyeongsangnam-do, Goseong-gun, Hail-myeon, Suyang-ri, 34°58'08"N, 128°12'08.3"E, 18.VI.2022, Tselikh col." (NIBR).

Distribution. *Korean Peninsula; China, Japan, Vietnam.

Pareucorystes varinervis* **Tobias, 1961

Pareucorystes varinervis Tobias, 1961: 533; Yu et al. 2016; Belokobylskij 2019: 37.
Leluthia chinensis Li & van Achterberg, in Li et al. 2015: 595; Belokobylskij 2019: 37 (as synonym).

Material examined. South Korea: 1 female, "Gyeongnam-do, Namhae I., Mt. Geumsan, 2017.7.21–22 (LT), Deokseo Ku, Taeho Ahn, Hyerin Lee coll." (NIBR).

Distribution. *Korean Peninsula; Europe, Russia (European part, south of Far East), Azerbaijan, Kazakhstan, China.

Rhaconotinus (Rhaconotinus) tianmushanus* **(Belokobylskij & Chen, 2004)

Rhaconotus tianmushanus Belokobylskij & Chen, 2004: 349 (*Rhaconotus*); Yu et al. 2016.
Rhaconotinus (*Rhaconotinus*) *tianmushanus*: Belokobylskij and Zaldívar-Riverón 2021: 109.

Material examined. South Korea: 1 female, "S. Korea [GB], Changyeong-gun, Yueo-myeon, Daedae-ri, Uponeup, 3.VII.2015, Tselikh" (NIBR).

Distribution. *Korean Peninsula; China (Zhejiang).

Spathius deplanatus* **Chao, 1978

Spathius deplanatus Chao, 1978: 180; Belokobylskij 2003: 485; Chen and Shi 2004: 128; Belokobylskij and Maetô 2009: 558; Tang et al. 2015: 40; Yu et al. 2016.

Material examined. South Korea: 1 female, "Korea: KK, Suwon, Mt. Yeogi, MT (B1/B1), 23.IX.1998, June-Yeol Choi" (NIBR); 1 female, "Korea: KK, Suwon, Mt.

Yeogi, MT (Wh/Gr), 28.VII.1997, June-Yeol Choi" (SMNE);1 female, "Korea (GN), Geochang-gun, Science Museum Natural Enemy, XI.8–XI.23.2021 (Malaise Trap), Ku Deokseo, Lee Jaehyeon" (SMNE).

Distribution. *Korean Peninsula; China, Japan.

******Spathius honshuensis*** Belokobylskij, 1998**

Spathius honshuensis Belokobylskij, 1998: 83; 2003: 469; Belokobylskij and Maetô 2009: 599; Yu et al. 2016.

Material examined. South Korea: 1 male, "Korea: Seoul, Hongneung, National Institute of Forest Science, Light trap, 3.IX.1998, Kang Seung-Ho" (NIBR).

Distribution. *Korean Peninsula; Japan.

******Spathius longipetiolus*** Belokobylskij & Maetô, 2009**

Spathius longipetiolus Belokobylskij & Maetô, 2009: 631; Tang et al. 2015: 60; Yu et al. 2016.

Material examined. South Korea: 1 female, "Korea (GN), Geochang-gun, Science Museum Natural Enemy, VI.19–VII.19.2014 (Malaise Trap), Ku Deokseo" (NIBR); 1 female, same locality, but VIII.16–IX.4.2020 (SMNE); 2 females, "Korea (GN), Ungseokbong, Nae-ri, Sancheong-gun, VI.17.2017 (Sweeping), Ahn Taeho" (SMNE, ZISP); 1 female, "Korea (GB), Cheonbu3-gil, Buk-myeon, Ulleung-gun, VIII.16–VIII.30.2017 (Malaise trap), Ku Deokseo" (SMNE); 1 female, same label, but VIII.2–VIII.16.2017 (SMNE); 1 female, same label, but IX.10–IX.13.2017 (ZISP).

Distribution. *Korean Peninsula; China, Japan.

******Spathius pseudaspersus*** Belokobylskij, 2009**

Spathius pseudaspersus Belokobylskij, 2009: 455; Belokobylskij and Maetô 2009: 691; Tang et al. 2015: 91.

Material examined. South Korea: 2 females, "Korea (GN), Ungseokbong, Nae-ri, Sancheong-gun, VI.17.2017 (Sweeping), Ahn Taeho" (NIBR, SMNE); 1 female, "Korea (JN), Jangjoa-ri, Wando-eup, Wando-gun, IX.26–X.10.2020 (Malaise Trap), Ku Deokseo, Lee Jaehyeon" (SMNE); 1 female, "S. Korea [GB], Changyeong-gun, Irwol-myeon, Mt. Ilwol-san, 36°48'29"N, 129°05'25"E, 25.VII.2015, Tselikh" (ZISP).

Distribution. *Korean Peninsula; Russia (Far East), China (Jiangsu), Japan.

**Spathius sinicus* Chao, 1957

Spathius sinicus Chao, 1957: 3; 1977: 209; Chen and Shi 2004: 162; Tang et al. 2015: 106; Yu et al. 2016.

Spathius bellus Chao, 1957: 5; Chen and Shi 2004: 112; Tang et al. 2015: 106 (as synonym).

Spathius agrili Yang, in Yang et al. 2005: 638; Belokobylskij and Maetô 2009: 510; Tang et al. 2015: 106 (as synonym).

Material examined. South Korea: 1 female, "Korea: KK, Suwon, Mt. Yeogi, MT (B1/B1), 23.IX.1996, June-Yeol Choi" (NIBR); 1 female, same label, but 9.VI.1997 (SMNE); 1 female, "Korea: Kuonggi, Kwangju, Docheok, Sangrim, Mt. Taewha, 5.VIII.1998, Deok-Seo Ku (LT)" (SMNE); 1 female, "Gyeongbuk, Uiseong-gun, Gaeum-myeon, Hyunri-ri, Yongsan, Mt. Seonamsan, 9.V.1998. T-H Ahn (Sweeping)" (SMNE); 1 female, "Gyeongnam, Hadong-gun, Cheongam-myeon, Gunghangk-ri, Jusan, 1.VII.2002 (Sweeping), J-S Park" (SMNE); 1 female, "S. Korea: Gyeongsangnam-do, Sancheong-gun, 30 km NNW Jinju (Chinju), forest, bush, h = 800 m, 12.06.2002, S. Belokobylskij" (ZISP); 1 female, "South Korea, SW of Geochang-eup, forest on a mountain, 35°40'15"N, 127°53'24"E – 35°40'19"N, 127°53'01"E, 3.VI.2019, K. Samartsev (ZISP).

Distribution. *Korean Peninsula; China, Japan.

**Spathius tsukubaensis* Belokobylskij & Maetô, 2009

Spathius tsukubaensis Belokobylskij & Maetô, 2009: 730; Yu et al. 2016.

Material examined. South Korea: 1 female, "Korea, Gyeongbuk-do, Sangju-gun, Chupungryeong, VIII. 1989. D-S Ku" (NIBR); 1 female, "Korea: KK, Suwon, Mt. Yeogi, MT (B1/B1), 31.VII.1995, June-Yeol Choi" (SMNE); 1 female, "Korea (GB), Cheonbu3-gil, Buk-myeon, Ulleung-gun, VI.21–VII.5.2017 (Malaise trap), Ku Deokseo" (SMNE); 1 female, "Korea (JJ), Hala-Arboretum, Yeon-dong, Jeju-si, Jeju-do, VI.25–VII.09.2017, (Malaise Trap)" (SMNE).

Distribution. *Korean Peninsula; Japan.

Subfamily Rhyssalinae Foerster, 1863
Tribe Acrisidini Hellén, 1957

Genus *Acrisis* Foerster, 1863

Type species. *Acrisis gracilicornis* Foerster, 1863.

Acrisis brevicornis Hellén, 1957

Acrisis brevicornis Hellén, 1957 (female): 50; Tobias 1983: 165; Belokobylskij 1990: 36; 1998: 120; Yu et al. 2016.
Acrisis koponeni Tobias, 1983 (male): 163; Belokobylskij 1990: 36 (as synonym); 1998: 120; Yu et al. 2016.

Material examined. South Korea: 1 female, "Korea (GN), Geochang-gun, Science Museum Natural Enemy, VIII.23–IX.21.2014 (Malaise Trap), Ku Deokseo" (SMNE); 1 female, same label, but VIII.27–IX.21.2014 (SMNE); 1 female, same label, but VI.19–VII.19. 2014 (ZISP); 8 females, same label, but I. 1–VI.18.2015 (SMNE, ZISP); 2 females, same label, but VIII.8–IX.22.2015 (SMNE, ZISP); 1 female, same label, but IV.29–V.31.2017 (SMNE); 1 female, same label, but IX.4–IX.16.2020 (SMNE); 1 female, "Korea (GN), Geochang-gun, Science Museum Natural Enemy, VI.30–VII.14.2021 (Malaise Trap), Ku Deokseo, Lee Jaehyeon (SMNE); 1 female, same label, but IV.23–V.7.2022 (SMNE); 4 females, same label, but VI.4–VI.18.2022 (SMNE, ZISP); 2 females, "Korea (GN), Janggi-ri, Wicheon-myeon, Geochang-gun, IX.11–X.16.2015 (Malaise Trap), Ahn Taeho" (SMNE, ZISP); 1 male, same locality, but IV.1–V.17.2017; 1 female, "S. Korea [GB], Gumi-shi, Goa-eup, Goepyeong-ri, 944–91, 36°15'69"N, 128°37'75"E, 23.VI.2015, Tselikh" (ZISP); 1 female, "Korea (CB), Sanoe, Sinjeong, Boeun, 36°34'8.93"N, 127°48'35.52"E, 2020.VI.07–24, Coll. H.K. Lee & M.D. Yun, The 5th National Ecosystem Survey" (SMNE).

Distribution. Korean Peninsula; Spain, Hungary, Finland, Iran, Russia (north and north-west of the European part, south of Far East).

Genus *Proacrisis* Tobias, 1983

Type species. *Proacrisis rarus* Tobias, 1983.

**Proacrisis orientalis* Tobias, 1983

Proacrisis orientalis Tobias, 1983: 162 (female); Belokobylskij 1994: 74; 1998: 120; Yu et al. 2016.
Proacrisis striatus Tobias, 1983: 161 (male); Belokobylskij 1994: 74 (synonym); 1998: 120; Yu et al. 2016.

Material examined. South Korea: 1 female, "Korea [GW], Bangdon-ri, Girin-myeon, Inje-gun, VI.21–VII.29.2019 (Malaise Trap), HDS" (NIBR).

Distribution. *Korean Peninsula; Russia (Far East).

Tribe Histeromerini Fahringer, 1930

Genus *Histeromerus* Wesmael, 1838

Type species. *Histeromerus mystacinus* Wesmael, 1838.

******Histeromerus orientalis*** **Chou & Chou, 1991**

Histeromerus orientalis Chou & Chou, 1991: 473; van Achterberg 1992: 195; Maetô 1997: 440; Belokobylskij 1998: 110; Yu et al. 2016.

Material examined. South Korea: 1 female, "Korea [JJ], Eoseungsaengak, Haeando, Jeju-shi, Jejudo, V.15–V.28.2017, (Malaise Trap)" (NIBR).

Distribution. *Korean Peninsula; China (Taiwan), Japan (Ogasawara).

Discussion

The subfamily Doryctinae is rather well studied group of parasitoids in several East Asian countries. For example, on the basis of the last revision of the Japanese Doryctinae (Belokobylskij and Maetô 2009) totally 33 genera of this subfamily were recorded in the fauna of this Archipelago, including such rare for the Palaearctic region taxa as *Arhaconotus* Belokobylskij, 2001, *Asiaheterospilus* Belokobylskij & Konishi, 2001, *Cryptontsira* Belokobylskij, 2008, *Mimipodoryctes* Belokobylskij, 2001, *Nipponecphylus* Belokobylskij & Konishi, 2001, *Rhacontsira* Belokobylskij, 1998, *Ryukyuspathius* Belokobylskij, 2008, and *Spathiostenus* Belokobylskij, 1993. This subfamily is also abundant in China (32 genera) and rather similar to the Japanese fauna in its composition., which includes Palaearctic and Oriental elements. Already 26 doryctine genera were recorded in the fauna of Korean Peninsula, but this is clearly not complete information for the region. For example, at least some genera recorded already in Japan (*Caenophanes* Foerster, 1863, *Cryptontsira*, *Ecphylus* Foerster, 1863, *Mimipodoryctes*, *Parallorhogas* Marsh, 1993, and *Rhacontsira*) could be additionally found in the fauna of this peninsula. The less varied doryctine taxa are recorded in the Russian Far East, the northernmost Asian territory: only 20 genera were found here (Belokobylskij et al. 2019) and basically without any Oriental components in its composition.

The information about the discovery of the genera subfamily Rhyssalinae in the discussed region was usually much reduced. Such, only two rhyssaline genera (out of 11 worldwide known), *Lysitermoides* van Achterberg, 1995 and *Oncophanes* Foerster, 1863, were recorded in the fauna of Japan, and only single genus *Histeromerus* Wesmael, 1838 were found in China for now. On the other hand, already seven rhyssaline genera were recorded in the faunas of the Russian Far East and Korean Peninsula, but if in the first area the genera *Histeromerus* and *Tobiason* Belokobylskij, 2004 were not found till now, then on the latter territory the genera *Pseudobathystomus* Belokobylskij, 1986 and *Rhyssalus* Haliday, 1833 were not discovered yet; however both areas have five identical genera, namely *Acrisis* Foerster, 1863, *Proacrisis* Tobias, 1983, *Dolopsidea* Hincks, 1944, *Lysitermoides* van Achterberg, 1995, and *Oncophanes* Foerster, 1863.

Acknowledgements

The authors are grateful to Dr Ekaterina V. Tselikh, Dr Konstantin G. Samartsev, Mrs. Kyongim Kim, Ms. Hyojin Jung, Ms. Jaehyeon Lee, Dr Taeho Ahn, Dr Gimyon Kwon, and Dr Hyungeun Lee for collecting of braconid material and specimen preparation. We are also very thankful to Dr Konstantin G. Samartsev (St Petersburg, Russia), Dr Alejandro Zaldívar-Riverón (México City, México) and Prof. Cornelis van Achterberg (Leiden, the Netherlands) for their very useful corrections and suggestions for the first version of the manuscript. This work was funded in part by the State Research Project No 122031100272-3 for SAB, and was supported by a grant from the National Institute of Biological Resources (NIBR) and the 5th National Ecosystem Survey of the National Institute of Ecology (NIE), funded by the Ministry of Environment (MOE) of the Republic of Korea (NIBR201701203, NIBR201801201, NIBR202102204, NIBR202203201, and NIE-A-2020-01) for DSK.

References

Belokobylskij SA (1988) Three new species of the braconid wasps subfamily Doryctinae (Hymenoptera, Braconidae) from Primorskiy Territory. Zoologicheskij Zhurnal 67(4): 625–630. [In Russian]

Belokobylskij SA (1990) A contribution to the Braconidae fauna (Hymenoptera) of the Far East. Vestnik Zoologii 6: 32–39. [In Russian]

Belokobylskij SA (1993) East Asiatic species of the genus *Neurocrassus* (Hymenoptera: Braconidae). Zoosystematica Rossica 2(1): 161–172.

Belokobylskij SA (1994) A review of braconid wasps of subfamilies Doryctinae and Exothecinae (Hymenoptera, Braconidae) of the Far East, East Siberia and neighbouring territories. Trudy zapovednika "Daursky", Kiev 3: 5–77. [In Russian]

Belokobylskij SA (1996) A contribution to the knowledge of the Doryctinae of Taiwan (Hymenoptera: Braconidae). Zoosystematica Rossica 5(1): 153–191.

Belokobylskij SA (1998) Subfam. Doryctinae. In: Lehr PA (Ed.) Key to insects of the Russian Far East. Vol. 4. Neuropteroidea, Mecoptera, Hymenoptera. Pt 3. Dal'nauka, Vladivostok, 50–109. [In Russian]

Belokobylskij SA (2001) New species of the genera *Rhaconotus* Ruthe, *Ipodoryctes* Granger and *Arhaconotus* Blkb. from the Oriental Region (Hymenoptera: Braconidae, Doryctinae). Zoosystematica Rossica 10(1): 101–162.

Belokobylskij SA (2003) The species of the genus *Spathius* Nees, 1818 (Hymenoptera: Braconidae: Doryctinae) not included in the monograph by Nixon (1943). Annales Zoologici 53(3): 347–488.

Belokobylskij SA (2006) *Neoheterospilus* gen. n., a new genus of the tribe Heterospilini (Hymenoptera: Braconidae, Doryctinae) with highly modified ovipositor and a worldwide distribution. Insect Systematics & Evolution 37(2): 149–178. https://doi.org/10.1163/187631206788831119

Belokobylskij SA (2009) New species of the braconid wasps of the genus *Spathius* Nees (Hymenoptera, Braconidae, Doryctinae) from Japan and neighbouring territories. Entomologicheskoe Obozrenie 88(2): 438–465. [In Russian]

Belokobylskij SA (2019) Some taxonomical corrections and new faunistic records of the species from the family Braconidae (Hymenoptera) in the fauna of Russia. Proceedings of the Russian Entomological Society 90: 33–53. https://doi.org/10.47640/1605-7678_2019_90_33

Belokobylskij SA, Chen X (2002) Two new species of *Aivalykus* (Hymenoptera: Braconidae: Doryctinae) from China and Indonesia, with a key to species. European Journal of Entomology 99(1): 73–78. https://doi.org/10.14411/eje.2002.013

Belokobylskij SA, Chen X (2004) The species of the genus *Rhaconotus* Ruthe, 1854 (Hymenoptera: Braconidae: Doryctinae) from China with a key to species. Annales Zoologici 54(2): 319–359.

Belokobylskij SA, Ku DS (2021) Review of species of the genus *Heterospilus* Haliday, 1836 (Hymenoptera, Braconidae, Doryctinae) from the Korean Peninsula. ZooKeys 1079: 35–88. https://doi.org/10.3897/zookeys.1079.73701

Belokobylskij SA, Maetô K (2006) Review of the genera from the subfamily Doryctinae (Hymenoptera: Braconidae) new for Japan. Annales Zoologici 56(4): 675–752.

Belokobylskij SA, Maetô K (2009) Doryctinae (Hymenoptera, Braconidae) of Japan. Fauna mundi. Vol. 1. Warszawska Drukarnia Naukowa, Warszawa, 806 pp.

Belokobylskij SA, Tobias VI (1986) Subfam. Doryctinae. In: Medvedev GS (Ed.) Keys to insects of the USSR European part. Vol. 3. Hymenoptera. Pt. 4. Nauka, Leningrad, 21–72. [In Russian]

Belokobylskij SA, Zaldívar-Riverón A (2021) Reclassification of the doryctine tribe Rhaconotini (Hymenoptera, Braconidae). European Journal of Taxonomy. Monograph 741: 1–168. https://doi.org/10.5852/ejt.2021.741.1289

Belokobylskij SA, Chen X, Long KD (2005) Revision of the genus *Eodendrus* Belokobylskij (Hymenoptera: Braconidae, Doryctinae). Journal of Natural History 39(29): 2715–2743. https://doi.org/10.1080/00222930500114459

Belokobylskij SA, Tang P, Chen X (2013) The Chinese species of the genus *Ontsira* Cameron (Hymenoptera, Braconidae, Doryctinae). ZooKeys 345: 73–96. https://doi.org/10.3897/zookeys.345.5472

Belokobylskij SA, Samartsev KG, Il'inskaya AS [Eds] (2019) Annotated catalogue of the Hymenoptera of Russia. Volume II. Apocrita: Parasitica. Proceedings of the Zoological Institute Russian Academy of Sciences. Supplement 8. Zoological Institute RAS, St. Petersburg, 594 pp. https://doi.org/10.31610/trudyzin/2019.supl.8.5

Chao HF (1957) On south-eastern Chinese braconid-flies of the subfamily Spathiinae (Braconidae). Transactions of the Fujian Agricultural College 4: 1–18. [In Chinese]

Chao HF (1978) A study on Chinese Braconid wasps of the tribe Spathiini (Hymenoptera, Braconidae, Doryctinae). Acta Entomologica Sinica 21(2): 173–184. [In Chinese with English summary]

Chen JH, Shi QX (2004) Systematic studies on Doryctinae of China (Hymenoptera: Braconidae). Fujian Science and Technology Publishing House, Fujian, 274 pp. [In Chinese with English summary]

Chou LY, Chou K (1991) The Braconidae (Hymenoptera) of Taiwan. IV. Histeromerinae. Journal of Agricultural Research. China 40(4): 472–474.

Hellén W (1957) Zur Kenntnis der Braconidae: Cyclostomi Finnlands. Notulae Entomologicae 37(2): 33–52.

Kim MS, Kim CJ, Herard F, Williams DW, Kim IK, Hong KJ (2018) Discovery of *Leluthia honshuensis* Belokobylskij & Maeto (Hymenoptera: Braconidae) as a larval ectoparasitoid of the Asian longhorned beetle in South Korea. Journal of Asia-Pacific Biodiversity 11(1): 132–137. https://doi.org/10.1016/j.japb.2017.12.001

Ku DS, Belokobylskij SA, Cha JY (2001) Hymenoptera (Braconidae). Economic Insects of Korea 16. Insecta Koreana (Supplement 23): 1–283.

Lee HR, Belokobylskij SA, Ku DS, Byun BK (2020) Fifteen newly recorded species of the subfamily Doryctinae (Hymenoptera) in Korea. Animal Systematics, Evolution and Diversity 36(1): 17–24.

Li T, van Achterberg C, Xu ZC (2015) A new species of genus *Leluthia* Cameron (Hymenoptera: Braconidae) parasitizing *Agrilus* sp. (Coleoptera: Buprestidae) from China with a key to the East Palaearctic species. Zootaxa 4048(4): 594–600. https://doi.org/10.11646/zootaxa.4048.4.10

Maetô K (1997) New records of subfamilies and genera of Braconidae (Hymenoptera) from Japan. Japanese Journal of Entomology 65(2): 440–441.

Papp J (1984) Contributions to the braconid fauna of Hungary, V. Doryctinae. (Hymenoptera: Braconidae). Folia Entomologica Hungarica 45: 173–185.

Ratzeburg JTC (1848) Die Ichneumonen der Forstinsecten in forstlicher und entomologischer Beziehung. Zweiter Band. Nicolai'schen Buchhandlung, Berlin, 238 pp.

Shi QX (2006) A new record of the genus *Dendrosotinus* Telenga (Hymenoptera: Braconidae: Doryctinae) in China, with description of a new species. Entomological Journal of East China 15(1): 7–9. [In Chinese]

Tang P, Belokobylskij SA, He J, Chen X (2013) *Heterospilus* Haliday, 1836 (Hymenoptera: Braconidae, Doryctinae) from China with a key to species. Zootaxa 3683(3): 201–246. https://doi.org/10.11646/zootaxa.3683.3.1

Tang P, Belokobylskij SA, Chen XX (2015) *Spathius* Nees, 1818 (Hymenoptera: Braconidae: Doryctinae) from China with a key to species. Zootaxa. Monograph 3960(1): 1–132. https://doi.org/10.11646/zootaxa.3960.1.1

Tobias VI (1961) A new genus of the tribe Doryctini (Hymenoptera: Braconidae) and its taxonomic importance. Zoologicheskij Zhurnal 40(4): 529–535. [In Russian]

Tobias VI (1976) Braconids of Caucasus (Hymenoptera, Braconidae). Nauka, Leningrad, 286 pp. [In Russian]

Tobias VI (1983) On the recognition of the genus *Acrisis* Förster, 1862 and tribe Acrisidini Hellén, 1957 (Hymenoptera, Braconidae, Doryctinae). Trudy Vsesoyuznogo Entomologicheskogo Obshchestva 65: 155–168. [In Russian] van Achterberg C (1992) Revision of the genus *Histeromerus* Wesmael (Hymenoptera: Braconidae). Zoölogische Mededeelingen 66(9): 189–196.

van Achterberg C (1993) Illustrated key to the subfamilies of the Braconidae (Hymenoptera: Ichneumonoidea). Zoölogische Verhandelingen 283: 1–189.

van Achterberg C (2003) The West Palaearctic species of the genera *Gildoria* Hedqvist and *Platyspathius* Viereck, with keys to the species (Hymenoptera: Braconidae: Doryctinae). Zoölogische Mededeelingen 77(15): 267–290.

Walker F (1860) Characters of some apparently undescribed Ceylon insects. Annals & Magazine of Natural History 5(3): 304–311. https://doi.org/10.1080/00222936008697221

Yang ZQ, Strazanac JS, Marsh PM, van Achterberg C, Choi WY (2005) First recorded parasitoid from China of *Agrilus planipennis*: a new species of *Spathius* (Hymenoptera: Braconidae: Doryctinae). Annals of the Entomological Society of America 98(5): 636–642. https://doi.org/10.1603/0013-8746(2005)098[0636:FRPFCO]2.0.CO;2

Yu DS, van Achterberg C, Horstmann K (2016) Taxapad 2016. Ichneumonoidea 2015. Nepean, Ottawa, Ontario. [Database on flash-drive]

ZooKeys 1138: 89–141 (2023)
doi: 10.3897/zookeys.1138.90580
https://zookeys.pensoft.net

RESEARCH ARTICLE

A peer-reviewed open-access journal
ZooKeys
Launched to accelerate biodiversity research

Two new species of *Bryocamptus* (Copepoda, Harpacticoida, Canthocamptidae) from the Russian Arctic and comparison with *Bryocamptus minutus* (Claus, 1863)

Aleksandr Novikov[1], Dayana Sharafutdinova[1], Elena Chertoprud[2,3]

1 *Kazan Federal University, Kremlyovskaya St. 18, 420008 Kazan, Russia* **2** *Department of Hydrobiology, Biological Faculty, M.V. Lomonosov Moscow State University, Leninskie Gory, Moscow 119991, Russia* **3** *A.N. Severtsov Institute of Ecology and Evolution, Leninsky Prospect, 33, Moscow 119071, Russia*

Corresponding author: Aleksandr Novikov (aleksandr-novikov-2011@list.ru)

Academic editor: Danielle Defaye | Received 27 July 2022 | Accepted 7 December 2022 | Published 5 January 2023

https://zoobank.org/AD364502-AA60-4A3B-A7A8-CA3716D9B23F

Citation: Novikov A, Sharafutdinova D, Chertoprud E (2023) Two new species of *Bryocamptus* (Copepoda, Harpacticoida, Canthocamptidae) from the Russian Arctic and comparison with *Bryocamptus minutus* (Claus, 1863). ZooKeys 1138: 89–141. https://doi.org/10.3897/zookeys.1138.90580

Abstract

Two new species of *Bryocamptus* Chappuis, 1929 from the Russian Arctic from the *Bryocamptus minutus* species group are described: *Bryocamptus putoranus* **sp. nov.** and *Bryocamptus abramovae* **sp. nov.** A complete morphological comparison of the new species with the type species *Bryocamptus minutus* (Claus, 1863) was carried out. Significant interspecific differences were shown at the level of microcharacters, such as integumental sensillae and pores, ornamentation of segments of mouthparts and swimming legs, and pores on swimming legs. A significant correlation has also been shown in the shape of the caudal rami of the females and the antennules of the males, which is likely caused by an evolutionary sexual arms race. *Bryocamptus putoranus* **sp. nov.** and *B. minutus* have a similar structure of caudal rami, but completely different male antennules, which may indicate a convergent origin of modifications and highlights the importance of depicting male antennules in the species descriptions.

Keywords

Arctic invertebrates, biodiversity, intraspecific differences, sensillae and pores, sexual arms race

Introduction

Recent studies have shown a very low level of knowledge of the freshwater Harpacticoida fauna in the Russian Arctic. Previously, we discovered several new species from the genera *Moraria*, *Bryocamptus*, *Maraenobiotus*, *Canthocamptus* (Novikov and Sharafutdinova 2020; Novikov et al. 2021). In this paper, we consider three species of *Bryocamptus* from the *Bryocamptus* (*Bryocamptus*) *minutus* (Claus, 1863) species group with descriptions of two new species from the Arctic. This group was originally identified by K. Lang on the basis of a one-segmented mandibular palp (1948). Unfortunately, most descriptions of the freshwater Canthocamptidae of the last century were very often incomplete or quite poor. Often, figures and descriptions of mandibles were not given at all. Therefore, at this stage, it is impossible to clearly determine which species are included in this group, or to conduct a fully-fledged taxonomic analysis of the group, and even more so of the genus.

In modern taxonomy, in addition to molecular genetic analysis, an important component is the study of microcharacters that were generally not taken into account earlier. In recent years, more and more data were collected on the wide distribution of complexes of cryptic and pseudo-cryptic species of copepods (Lajus et al. 2015; Kochanova et al. 2021). Microcharacters make it possible to distinguish, more or less reliably, between such species (for example Hołyńska and Dahms 2004; Stoch and Bruno 2011; Karanovic and Krajicek 2012; Karanovic and Lee 2012). Such characters include ornamentation of limb segments, the structure of the somite integument, and in particular, sensillae and pores. In this work, we tried to present the most detailed description of three closely related species from different parts of the Palearctic. Despite the obvious and well-observed differences, we focus on small characters for the purpose of their possible future use.

Materials and methods

Material from the Lena River Delta (north-eastern Siberia) was collected during the "Lena-2019" expedition. Crustaceans from the Putorana Plateau were collected in August 2021 during an expedition by Moscow State University in the Natural Reserve Putoransky. In the first case a small plankton net (mesh size 80 μm) was used for collection. In the second case samples were taken with small plastic tubes (radius 1.2 cm). A description of the collection of materials in Estonia is given in the work of Fefilova (2010).

Samples were fixed in 4% formalin or 96% ethanol. Specimens were dissected under a stereomicroscope, with each element being placed in glycerol under a separate coverslip. Pieces of plasticine are used on the underside of the coverslip to prevent damage to the element. Next, series of photographs were taken using a USB camera, which were merged in the Helicon Focus 6 program. The drawings and photographs were taken with a microscope (LOMO Micmed 2, Russia). Rough drawings were obtained from printed photographs of elements, and the final drawings were prepared using the free program Inkscape 1.0.

All depicted limbs and other elements were examined from at least three individuals of each species: two females and one male, with the exception of the labrum and paragnaths, which were studied from only one individual. The numbering of pores and sensillae on somites is original and based on the structure of the integument of several freshwater species of Canthocamptidae. Roman numerals (for pores) or Arabic numerals (for sensillae) are used for numbering integumental elements. The designations for cephalothorax sensillae C, P, and L are used to simplify homology. Group P is the sensillae adjacent to the edge of the cephalothorax. Group C is the sensillae, which are located near the medial axis and the dorsal window. The notation L is used for all other sensillae.

Nomenclature and descriptive terminology follow Huys and Boxshall (1991), terminology of genital fields follows Moura and Pottek (1998), terminology of mandibular structure follows Mielke (1984), terminology and homology of maxillary structures follow Ferrari and Ivanenko (2008). The armature formulae of swimming legs are given according to Lang (1934). By the term "helle Stelle" we mean the inner cuticular disc at the base of the apical caudal setae (sensu Lang 1948).

For *B. abramovae* sp. nov. and *B. putoranus* sp. nov. only features that differ from *B. minutus* are described. All material was deposited in the Zoological Museum of Kazan Federal University (**KFU**).

Abbreviations used in the text

A1	antennule
A2	antenna
Ae	aesthetasc
Acr	acrothek
Ap	apophysis
P1–P6	legs 1–6
PS2–PS5	pedigerous somites 2–5
Exp1–Exp3	first–third segments of exopod
Enp1–Enp3	first–third segments of endopod

Taxonomic account

Subclass Copepoda H. Milne Edwards, 1840
Order Harpacticoida Sars, 1903
Family Canthocamptidae Sars, 1906
Genus *Bryocamptus* Chappuis, 1929

Subgenus *Bryocamptus* Chappuis, 1929

Remarks. Bryocamptus is a very large genus with ~ 135 species and subspecies in four subgenera: *B.* (*Arcticocamptus*) Chappuis, 1929, *B.* (*Bryocamptus)* Chappuis, 1928, *B.* (*Echinocamptus*) Chappuis, 1929 and *B.* (*Rheocamptus*) Borutzky, 1952.

Additionally, two subgenera were earlier designated as not valid *B.* (*Limocamptus*) Chappuis, 1929 and *B.* (*Pentacamptus*) Wiley, 1934.

In our opinion, this is one of the genera of the family most in need of revision. The first reason is that there are no clear diagnostic characters for the entire genus. Previously, this character was the two-segment exopod A2; however, this character is plesiomorphic for the entire family Canthocamptidae, so it may be an adequate solution to separate at least part of the subgenera into separate genera. The second reason is the blurred line between *B.* (*Bryocamptus*) and *B.* (*Rheocamptus*). Borutzky (1952) in the differences between these subgenera indicates the difference in segmentation of the endopods P1–P4, which again contrasts plesiomorphic and apomorphic characters. In our opinion, an essential part of the *B.* (*Rheocamptus*) species should in fact be transferred to the type subgenus.

Unfortunately, at the moment we do not have enough data and material to revise the subgenera, so in this work we adhere to the classification given by Dussart and Defaye (1990).

***Bryocamptus* (*Bryocamptus*) *minutus* (Claus, 1863)**

Subspecies. *B.* (*B.*) *minutus minutus* (Claus, 1863), *B.* (*B.*) *minutus schizodon* (Mrázek, 1893).

Nomen dubium. *B.* (*B.*) *minnesotensis* (Herrick, 1884).

Remarks. *Bryocamptus* (*B.*) *minutus* is a taxonomically rather complex species due to a rather long history of study and wide distribution. According to Article 45.6 of the International Code of Zoological Nomenclature, a number of forms of this species must be treated as separate subspecies (ICZN 1999). However, in the case of *B.* (*B.*) *minutus vejdovskyiformis* Thallwitz, 1916, this is probably a form that does not have subspecies status and is either an aberrant specimen(s) or simply variability (Thallwitz 1916). Simple dentiform and bifid spinules are also found in other related species, both within the same population and in one individual. This has been described in *B. hutchinsoni* Kiefer, 1929 (Wilson 1956), *B. vejdovskyi* (Mrázek, 1893) (Reed 1990) and also in *B. putoranus* sp. nov. (in this article).

A number of authors noted variability in the number of outer spines on the third exopodal segment of P4, which was the reason for Lang's description of the forms: *B. minutus* f. *typica* Lang, 1957 and *B. minutus* f. *bispinosa* Lang, 1957 (Lang 1957). We suggest that these forms do not have a taxonomic rank, since such variability is common for this group of species.

Another form of *B. minutus* f. *simplicidentata* (Willey, 1934) has been synonymized with *B. hutchinsoni* based on structure of caudal rami (Wilson 1956) but although figuring mistakenly and without literature support as valid in WORMS database (Walter and Boxshall 2021).

A rather interesting finding is described from the Iberian Peninsula as *B. minutus* (Caramujo and Boavida 2009). Based on the depicted limbs, it can be assumed that this is either *B. minutus schizodon* or a separate species. It differs from *B. minutus minutus* in the two-segmented endopod P2, short bifid spinules on the anal operculum, and slight displacement of the caudal setae to the ventral side of caudal rami. In general, these characters are already enough to distinguish a separate species.

Bryocamptus (*Bryocamptus*) *minutus minutus* (Claus, 1863)

Figs 1–9

B. (*B.*) *minutus vejdovskyiformis* Thallwitz, 1916: 238. syn. nov.

Material examined. Estonia • 2 ♀♀ dissected on three slides (BP 546/1-a, BP 546/1-b, BP 546/2); 1 ♂ on one slide (BP 546/3); 9 ♀♀ and 5 ♂♂ undissected preserved in 4% formalin (retained in the collection of the first author); Võrtsjärv Lake; 58.180888°N, 26.089441°E; 25 Sep. 2007; E. Fefilova leg; BP 546.

Supplementary description. Female. Body subcylindrical. Total body length from anterior margin of rostrum to posterior margin of caudal rami: 484 μm (n = 1). Cephalothorax (Fig. 1A, B; Appendix 1) wider than remaining somites, length 151 μm, largest width 124 μm. Naupliar eye not observed. Rostrum (Fig. 1C) small, fused with cephalothorax, with squared end, with one pair of sensillae. Posterior margin of cephalothorax and all pedigerous somites smooth.

Cephalothorax (Fig. 1A, B; Appendix 1) with dumbbell-shaped dorsal window, 10 pairs of pores, seven pairs of sensillae of central group (group C), 13 pairs of sensillae of marginal group (group P) and 20 pairs of ungrouped sensillae (in Table 4 and in Appendix 1 marked as L). Second pedigerous somite with lateral windows, dorsal unpaired pore, lateral pair of pores and eight pairs of sensillae. Third pedigerous somite with dorsal unpaired pore, lateral pair of pores and eight pairs of sensillae. Fourth pedigerous somite with dorsal unpaired pore, lateral pair of pores and eight pairs of sensillae. Fifth pedigerous somite with lateral pair of pores and four pairs of sensillae.

Abdomen (Fig. 2A–C) consisting of genital-double somite, two free abdominal somites and anal somite with caudal rami. All somites except anal somite on posterior margin serrated, on surface with spinular rows. Genital-double somite consists of last thoracic somite and first abdominal somite; longer than wide; anterior part with four pairs of sensillae, dorsal unpaired pore, lateral paired pores, ventro-lateral and lateral rows of spinules; posterior part with four pairs of sensillae, pairs of ventral and lateral pores and lateral rows of spinules.

P6 (Fig. 2C) fused with somite with one pinnate and one naked setae. Genital field (Fig. 2C) long, laterally with eight-pore sieves; copulatory pore displaced to posterior part of somite, copulatory duct chitinised with two additional tubes, extending proximally to pair of labyrinthic rounded ducts and one chitinised unpaired duct.

Second abdominal somite with three pairs of sensillae, pair of lateral pores; on posterior margin with lateral row of large spinules. Third abdominal somite with pair of lateral pores, on posterior margin with lateral row of large spinules and ventral row of small spinules. Anal somite with one pair of sensillae, ventral pair of large pores, lateral pair of pores, dorsal dots near base of caudal rami and lateral spinules. Anal operculum semilunar, with eight long bifid spinules.

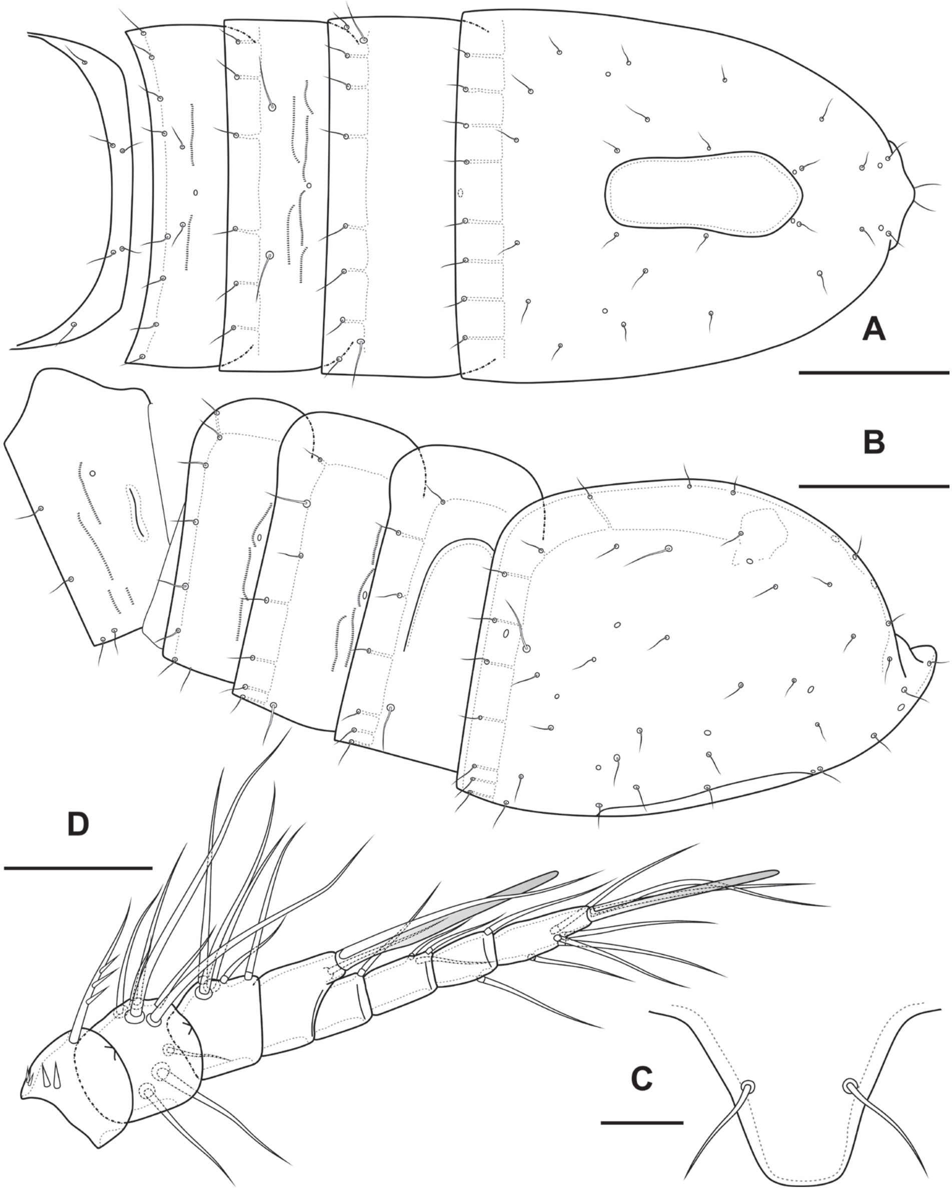

Figure 1. *Bryocamptus minutus*, female **A** cephalothorax and thoracic somites, dorsal **B** cephalothorax and thoracic somites, lateral **C** rostrum **D** antennule. Scale bars: 50 µm (**A, B**); 5 µm (**C**); 25 µm (**D**).

Caudal rami (Fig. 2A–E). Length/width ratio 1.6, with three ventral pores; with rows of spinules on ventral side at base of seta IV and rows spinules at base of setae II and III. Seta I small, located near seta II. Setae IV, V and VI displaced to ventral side of caudal ramus. Apical seta IV (Fig. 2D) unipinnate, with "helle Stelle" and massive dorsal bulb located distally "helle Stelle". Apical seta V long, bipinnate, with "helle Stelle". Seta VII triarticulated (Fig. 2B).

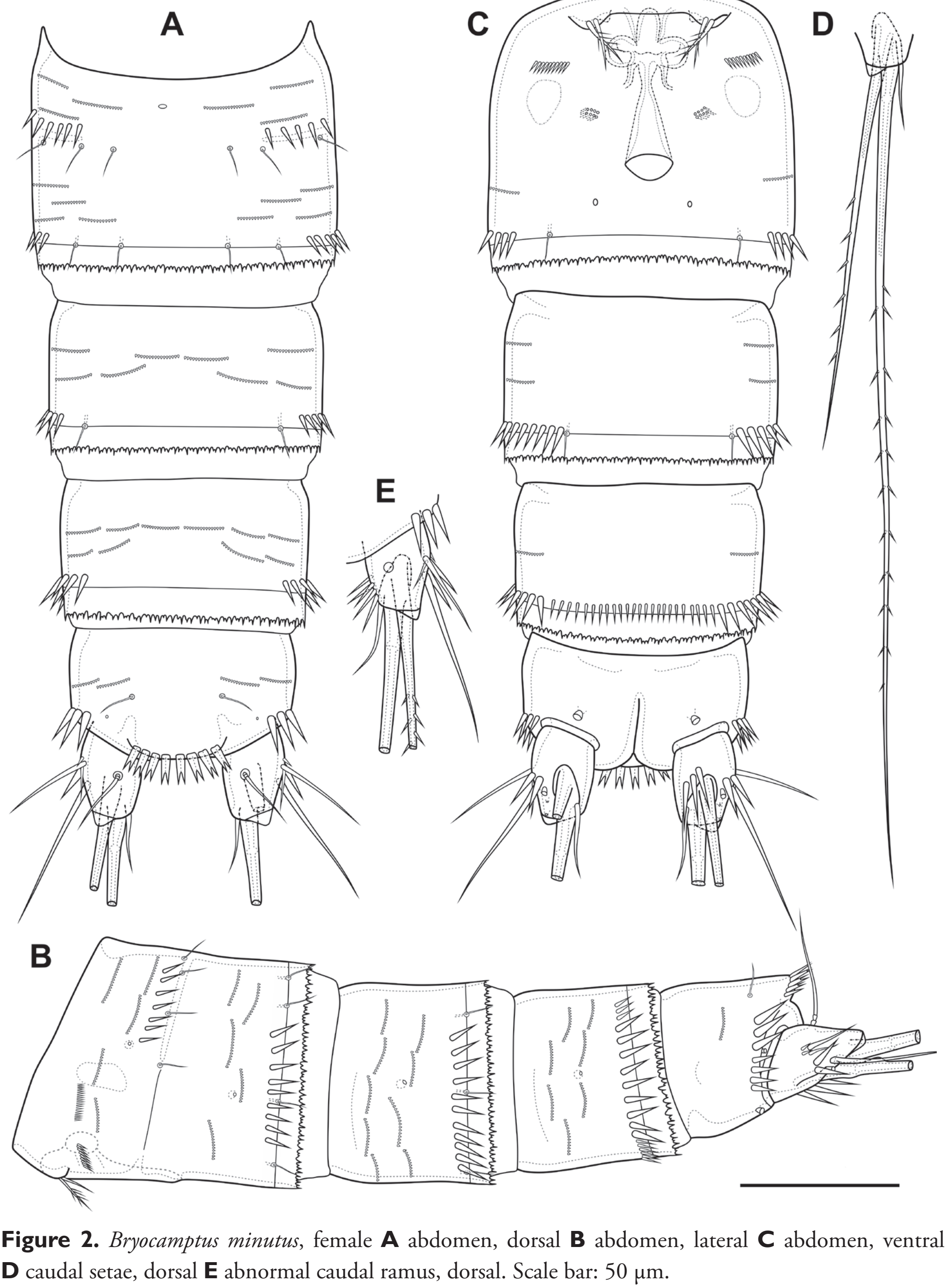

Figure 2. *Bryocamptus minutus*, female **A** abdomen, dorsal **B** abdomen, lateral **C** abdomen, ventral **D** caudal setae, dorsal **E** abnormal caudal ramus, dorsal. Scale bar: 50 μm.

Antennule (Fig. 1D) 8-segmented. Segment 1 short, with one pinnate seta and two rows of spinules. Other segments with bare setae. Segment 4 with fused basally seta and aesthetasc. Distal segment with acrothek consisting of aesthetasc and two setae fused basally. Armature formula: 1-[1],2-[9],3-[5],4-[1+(1+ae)],5-[1],6-[3],7-[2],8-[5+acr].

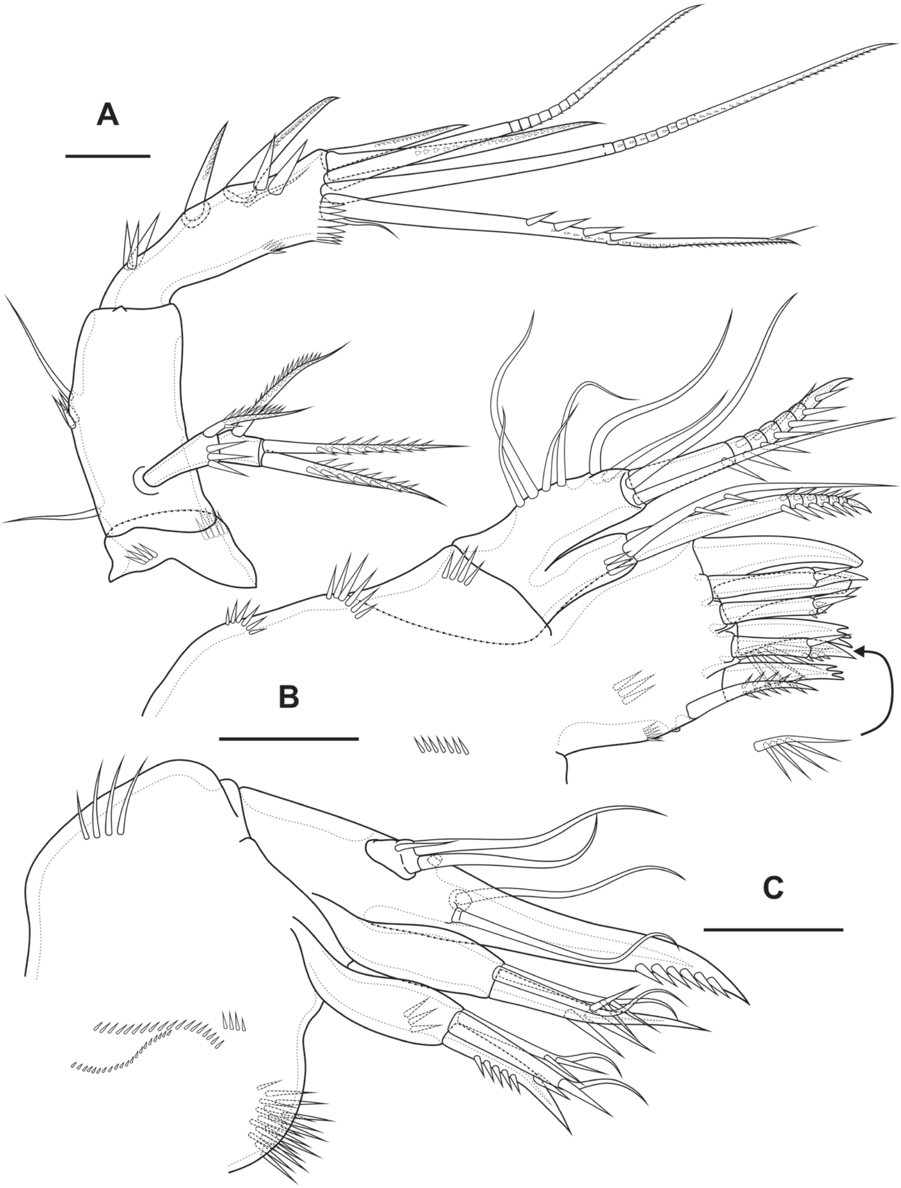

Figure 3. *Bryocamptus minutus*, female **A** antenna **B** maxillule **C** maxilla. Scale bars: 10 μm.

Antenna (Fig. 3A) with allobasis. Coxa with two rows of spinules. Allobasis with two naked setae and one spinular row at base of endopodal seta. Free endopodal segment with two lateral rows of big spinules, with two spinulose spines and slender seta; distally with two rows of spinules; apically with three geniculate setae, two long spines and one small accessory seta; outermost geniculate seta fused basally to small seta. Exopod two-segmented; first segment with one pinnate seta and row of spinules; second segment with three pinnate setae.

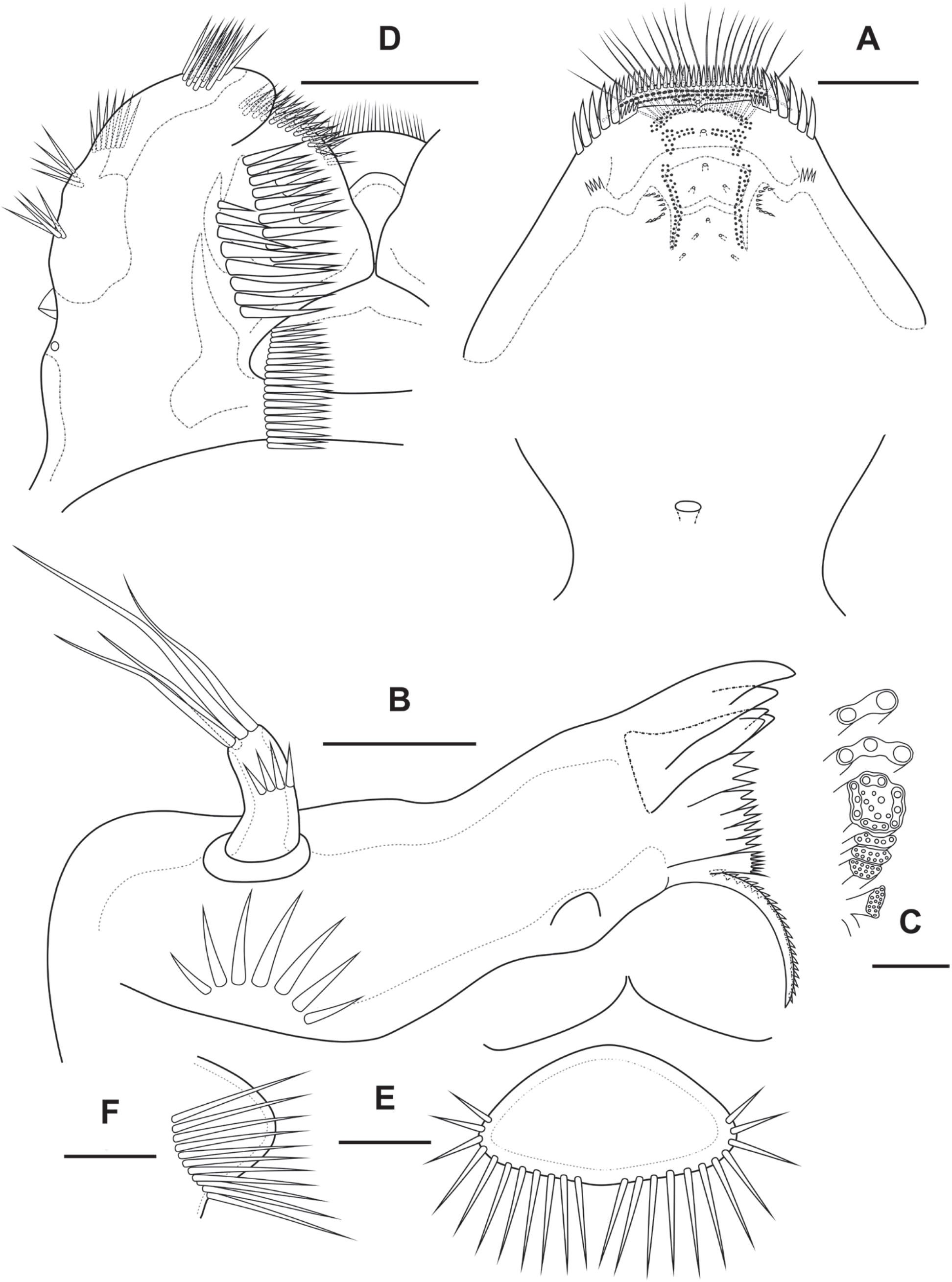

Figure 4. *Bryocamptus minutus*, female **A** labrum, posterior (black dots is bases of spinules) **B** mandible **C** scheme of teeth of mandibular gnathobase **D** paragnaths, anterior **E** cuticular process between maxillipeds and P1, ventral **F** cuticular process between maxillipeds and P1, lateral. Scale bars: 10 µm (**A, B, D**); 5 µm (**C, E, F**).

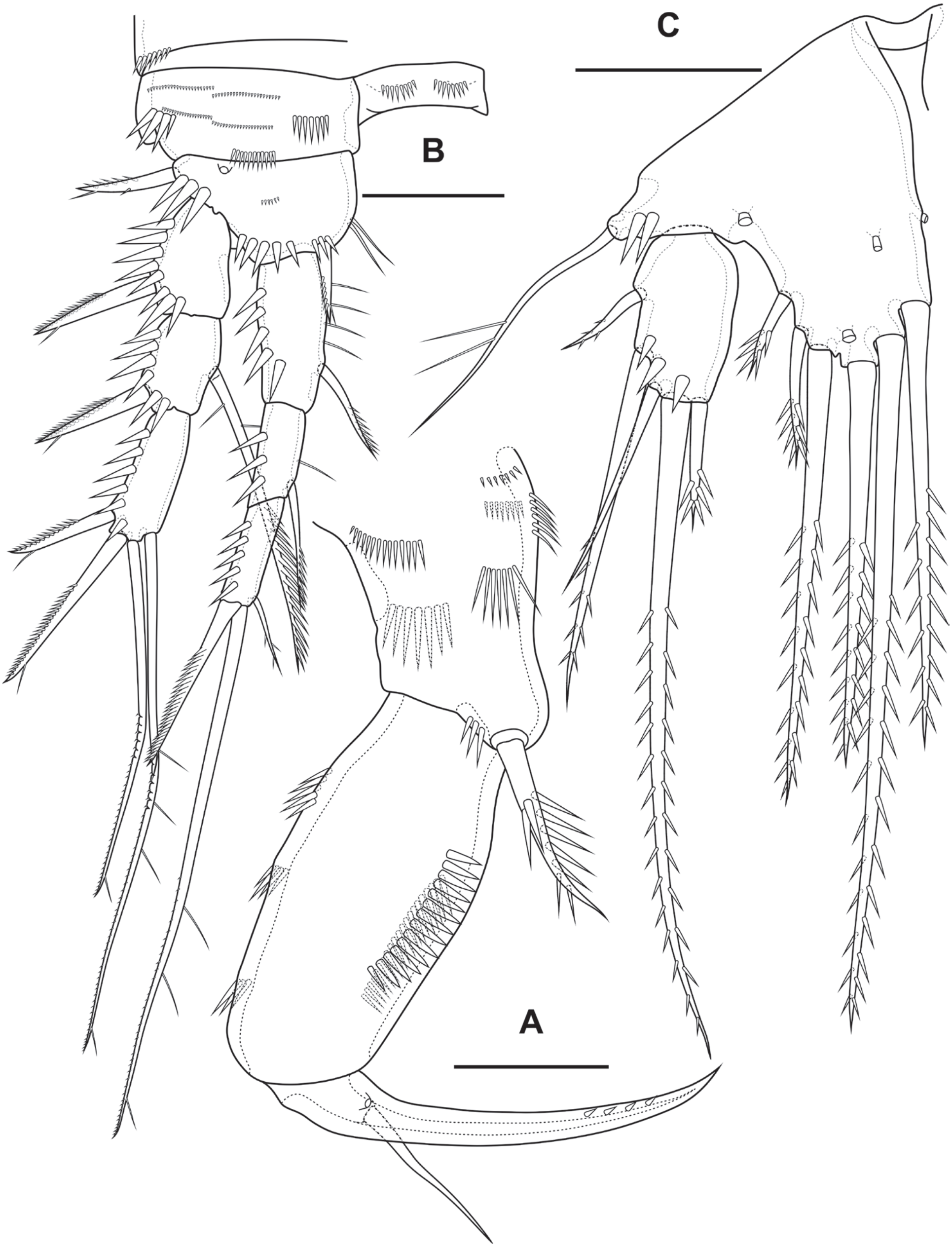

Figure 5. *Bryocamptus minutus*, female **A** maxilliped **B** P1, anterior **C** P5, anterior. Scale bars: 10 μm (**A**); 25 μm (**B, C**).

Labrum (Fig. 4A). On outer side with row of thin setules and large proximal pore. Distal margin with lateral rows of robust spinules, rows of fused spinules into comb and three rows of small spinules. On inner side medially with four unpaired pores, three pared pores, with lateral spinular row, semicircular spinular row and groups of thin setules.

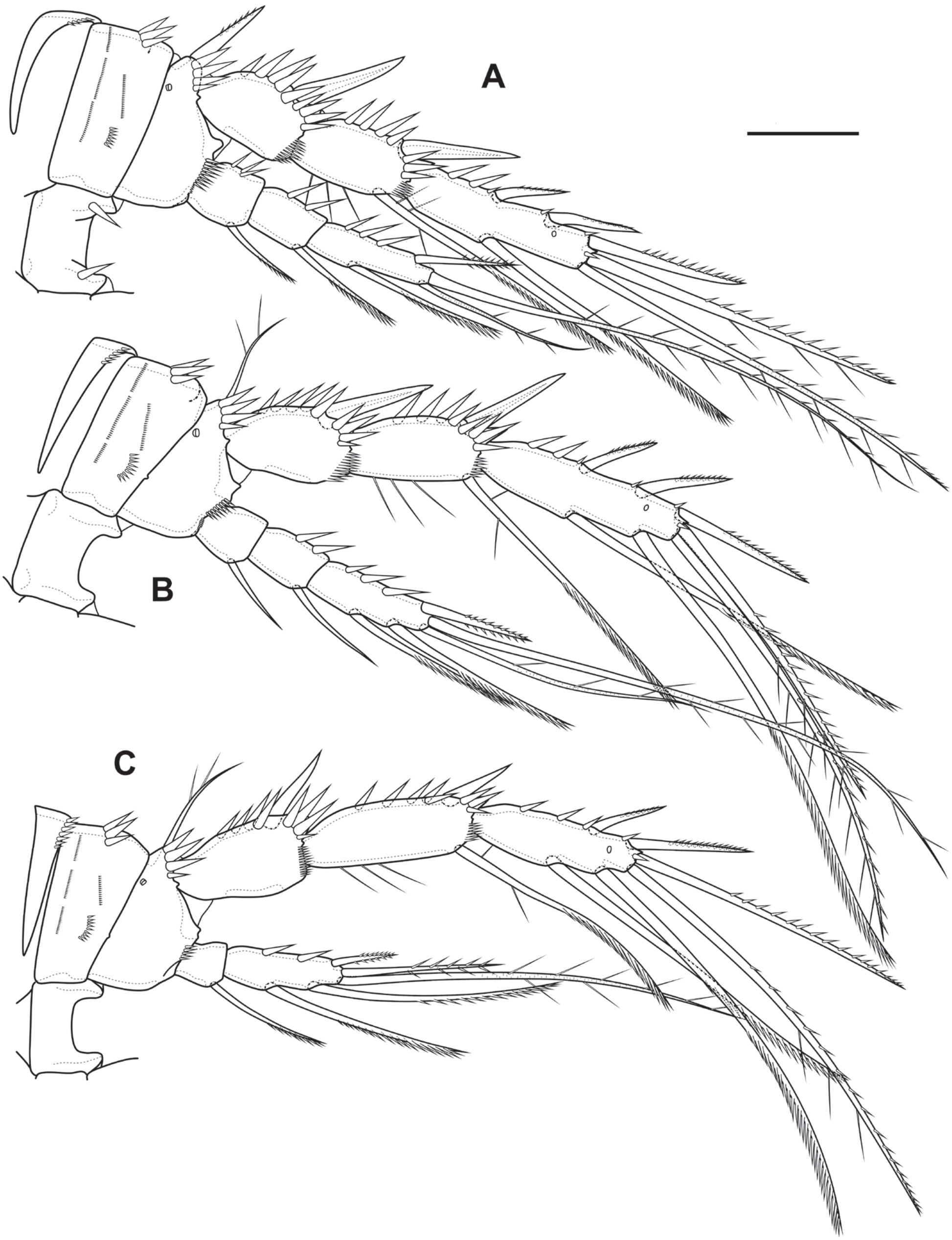

Figure 6. *Bryocamptus minutus*, female **A** P2, anterior **B** P3, anterior **C** P4, anterior. Scale bar: 25 µm.

Mandible (Fig. 4B, C). Coxa with spinules proximally. Gnathobase with pars incisiva, lacinia mobilis, complex dental battery and spinulose seta; pars incisiva two-pointed; lacinia mobilis three-pointed. Dental battery (Fig. 4C) consisting of five fused blocks of small short teeth, inner of which fused at base with seta. Pars molaris sharply edged. Palp one-segmented, with medial spinular row and four apical setae.

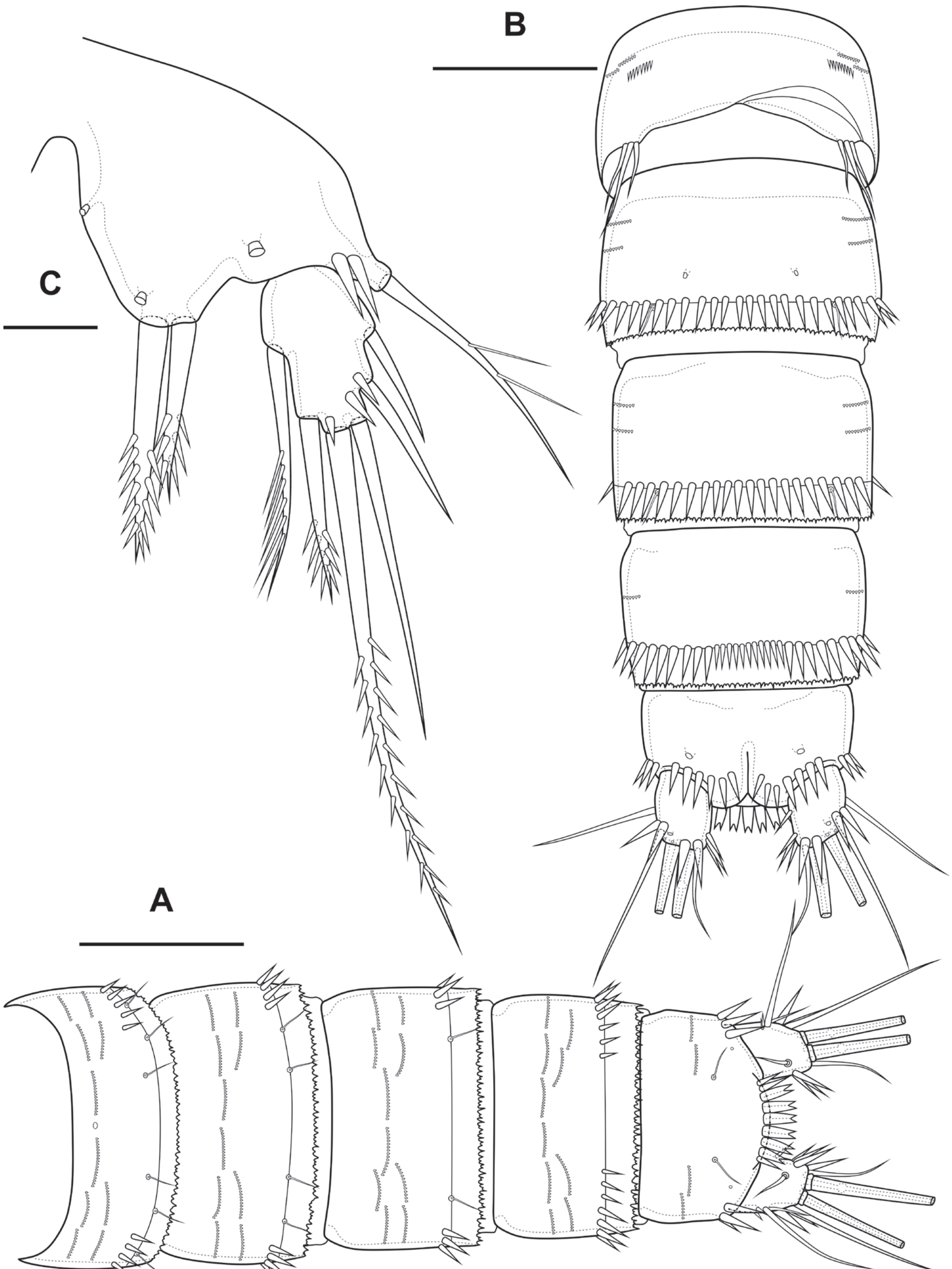

Figure 7. *Bryocamptus minutus*, male **A** abdomen, dorsal **B** abdomen, ventral **C** P5, anterior. Scale bars: 50 µm (**A, B**); 10 µm (**C**).

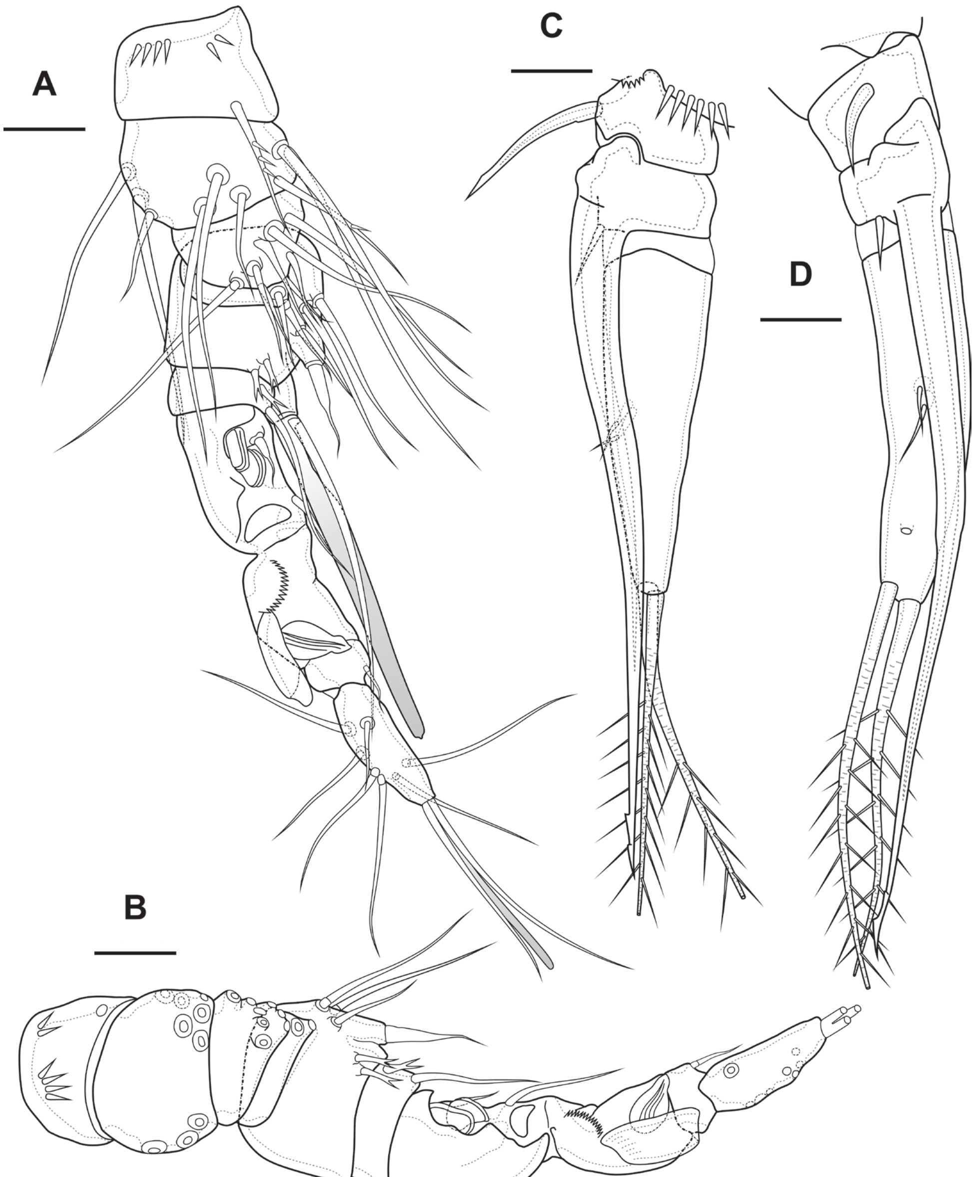

Figure 8. *Bryocamptus minutus*, male **A** antennule, anterior **B** antennule, dorsal **C** P3 endopod, anterior **D** P3 endopod, inner view. Scale bars: 10 µm.

Paragnaths (Fig. 4D) with paired lateral lobes and unpaired posterior rounded lobe. Lateral lobes wrapped in distal part forming “pocket”; proximally with lateral pore (probably); on outer side with four groups of long spinules; on inner side with three-four rows of spinules; on anterior side with three medial rows of strong spinules and proximal row of spinules.

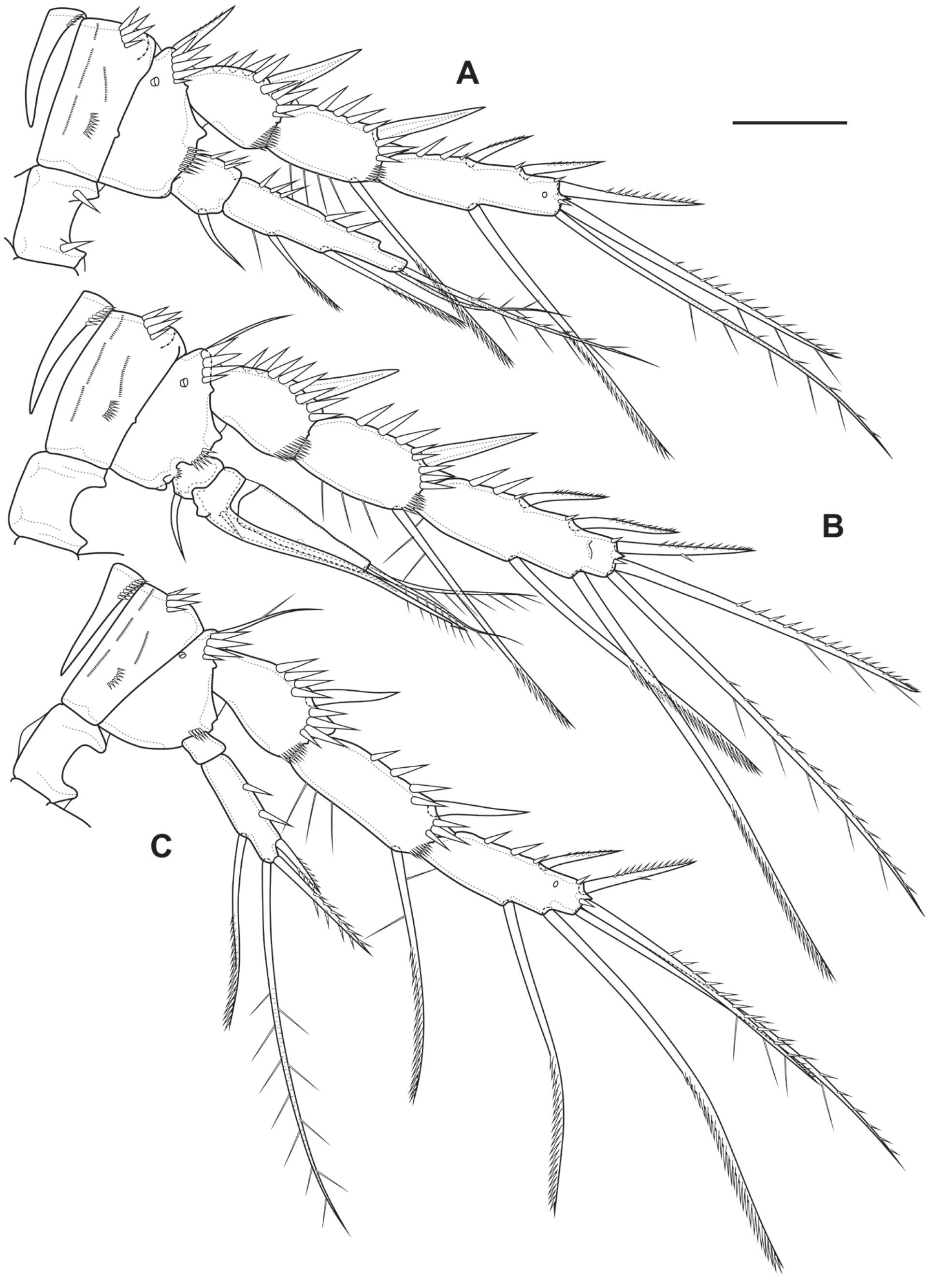

Figure 9. *Bryocamptus minutus*, male **A** P2, anterior **B** P3, anterior **C** P4, anterior. Scale bar: 25 µm.

Maxillule (Fig. 3B). Praecoxa with two rows of slender spinules on outer edge and one row of spinules on posterior side. Praecoxal arthrite medially with two rows of spinules and one proximal pore; distally with one simple strong spine, three strong spines with pectinate end, three biarticulate spines, one proximal bipinnate seta and one thin seta with long spinules. Coxa with row of spinules, coxal endite with one weakly pinnate and one spinulose geniculate setae. Basis with two subdistal setae and three distal setae, one of which spinulose and geniculate. Endopod and exopod incorporated into basis, each represented by two naked setae.

Maxilla (Fig. 3C). Basis with several rows of spinules on outer and inner edge as figured, with two endites. Proximal endite with spinular row, one spinulose spine and two pinnate setae, distal endite with one strong pinnate seta and two thin pinnate setae. Proximal endopodal segment with two setae, outer tube pore and massive distal claw. Distal endopodal segment with three naked setae, one of which proximal and small.

Maxilliped (Fig. 5A) subchelate. Syncoxa elongated with several rows of spinules as figured, distally with one pinnate seta. Basis with two rows of large spinules on anterior and posterior sides and three outer rows of small spinules. Endopod on posterior side with one seta, on anterior side with small protuberance, probably tube pore. Endopodal claw elongated, with row of small spinules.

Cuticular process between maxillipeds and P1 (Fig. 4E, F) in height approximately same as in length, with long spinules, ten spinules on each side. Spinules encircle from anterior-lateral margin to posterior margin.

P1 (Fig. 5B; Table 1) with three-segmented rami. Praecoxa with outer spinular row. Coxa rectangular, with seven spinular rows, four of which consisting of little spinules. Intercoxal sclerite wide, with one paired spinular rows. Basis with proximal pore, medial row of small spinules, rows of spinules at base of endopod and exopod, row of spinules at base of inner seta, inner row of spinules; with inner and outer strong spines. All endopodal and exopodal segments with outer spinules. First exopodal segment with one outer spinulose spine; second segment with inner pectinate seta and outer spinulose spine; third exopodal segment with two outer spinulose spines and two apical slender geniculate setae. Endopod longer than exopod. First endopodal segment reaching middle of second exopodal segment, with inner pectinate seta and inner spinular row; second endopodal segments with one inner pectinate seta, third segment with outer spinulose spine, apical long geniculate seta and inner small seta.

P2 (Fig. 6A; Table 1). Praecoxa with row of spinules. Coxa with one lateral row of large spinules and five rows of spinules on anterior side. Intercoxal sclerite with two large spinules. Basis with proximal pore, rows of spinules at base of endopod and exopod; with outer spine. All endopodal and exopodal segments with outer spinules. Exopod three-segmented; first exopodal segment with outer naked spine, apically with frill; second segment with outer naked spine, inner pectinate seta, inner slender spinules and apical frill; third segment with pore, three outer spinulose spines, two apical setae and one inner pectinate seta. Endopod three-segmented; first and second segments with inner seta; third segment with outer spinulose spine, two apical pinnate setae and one inner pectinate seta.

P3 (Fig. 6B; Table 1). Praecoxa with spinular row. Coxa with one lateral row of large spinules and five rows of spinules on anterior side. Intercoxal sclerite without spinules. Basis with outer seta, proximal pore, rows of spinules at base of endopod and exopod. Exopod three-segmented; first exopodal segment with outer naked spine, outer spinules, apically with frill; second segment with outer naked spine, outer spinules, inner pectinate seta, inner slender spinules and apical frill; third segment with pore, three outer spinulose spines, two apical setae and two inner pectinate setae. Endopod three-segmented; first and second segments with inner seta, second segment with outer spinules; third segment with outer spinules, outer spinulose spine, two apical pinnate setae and two inner pectinate setae.

P4 (Fig. 6C; Table 1). Praecoxa with spinular row. Coxa with one lateral row of large spinules and five rows of spinules on anterior side. Intercoxal sclerite without spinules. Basis with outer seta, proximal pore, rows of spinules at base of endopod and exopod. Exopod three-segmented; first exopodal segment with outer naked spine, outer spinules, apically with frill; second segment with outer naked spine, outer spinules, inner pectinate seta, inner slender spinules and apical frill; third segment with pore, two outer spinulose spines, two apical setae and two inner pectinate setae. Endopod two-segmented; first segment with inner seta, second segment with outer spinules, outer spinulose spine, two apical pinnate setae and two inner pectinate setae.

P5 (Fig. 5C) with separate right and left baseoendopods. Baseoendopod reaching ~ 1/2 of exopodal segment; with four pores, spinular row at base of outer seta; outer seta of basis pinnate, long. Endopodal lobe with four long bipinnate setae and two short bipinnate setae V and VI; with small process that may be pore between setae III and IV. Exopod with inner short pinnate seta, long apical pinnate seta, naked subapical seta and two pinnate outer setae.

Male. Sexual dimorphism expressed in the antennule, P2–P6, genital segmentation and ornamentation, shape of caudal rami. Cephalothorax and thoracic somites as in female. P6 (Fig. 7B) two asymmetric flaps fused to the somite, with three naked setae. Differences from female in abdomen structure as follows (Fig. 7A, B): first abdominal somite free; first to third abdominal somites with spinular row encircling somite ventrally and laterally; anal somite with ventral spinules; caudal rami with normal setae IV and V; anal operculum with nine bifid and simple spinules.

Antennule (Fig. 8A, B) 10-segmented, haplocer with geniculation between segments 7 and 8. Segment 5 with large aestetasc fused at base with long seta, with one strong caudate seta. Segment 7 with articular plate, with one filiform seta, one small caudate seta and with two modified laminar setae. Segment 8 with proximal dentate plate and two strong modified laminar setae. Segment 10 with acrothek consisting of slender aestetasc and two setae. Armature formula: 1-[1],2-[9],3-[8],4-[2],5-[6+(1+ae)],6-[2],7-[2+2 modified],8-[2 modified],9-[1],10-[7+acr].

P2 (Fig. 9A) as in female, except endopod. Endopod two-segmented. First segment with outer spinules and inner seta. Second segment with notch on distal outer margin, outer spinules, two apical pinnate slender setae and two inner pectinate setae.

Table 1. P1–P4 armature of examined specimens of *Bryocamptus minutus minutus*.

	Female endopod	Male endopod	Exopod
P1	1; 1; 1,1,1	1; 1; 1,1,1	0; 1; 0,2,2
P2	1; 1; 1,2,1	1; 2,2,0	0; 1; 1,2,3
P3	1; 1; 2,2,1	1; 1+ ap; 2,2,0	0; 1; 2,2,3
P4	1; 2,2,1	0; 1,2,1	0; 1; 2,2,2

P3 (Figs 8C, D, 9B): praecoxa, coxa, intercoxal sclerite as in female. Basis as in female, but with inner process. Exopod as in female, but third segment with broad slit-like pore. Endopod three-segmented. First endopodal segment with strong seta. Second endopodal segment with posterior seta and long apophysis with double tip. Third segment with two small inner setae, inner pore and two apical pinnate setae.

P4 (Fig. 9C): praecoxa, coxa, intercoxal sclerite, basis, exopod as in female. Endopod two-segmented; first segment short unarmed; second segment with outer spinules, spinulose spine, outer apical spiniform spinulose seta, inner apical bipinnate seta and inner pectinate seta.

P5 (Fig. 7C) right and left fused medially. Baseoendopod with three pairs of pores, outer spinular row and outer long pinnate seta; endopodal lobe with two strong spinulose apical spines. Exopod with spinules on anterior surface, three naked outer setae, long apical spinulose seta, one inner spinulose seta and one long inner pectinate seta with long setules.

Variability. We found variability in the structure of the caudal rami. Some females have an inner group of long spinules (Fig. 2E).

***Bryocamptus* (*Bryocamptus*) *abramovae* sp. nov.**

https://zoobank.org/D2258B3F-4D75-4D53-B4CA-259A0D2F20F0
Figs 10–18

Bryocamptus sp. 2 – Novikov et al. 2021: 271.
Bryocamptus sp. 1 – Novikov and Sharafutdinova 2022: 34.

Material. *Holotype*: Russia • ♀ dissected on two slides; Lena River Delta, Samoylov Island, Ruiba Lake; 72.373003°N, 126.489429°E; depth 1–1.5 m; 23 Aug. 2019; A. Novikov leg; BP 547/1-a, BP 547/1-b. ***Allotype*:** Russia •♂ dissected on one slide; collection data as for holotype; BP 547/2. ***Paratypes*:** 5 ♀ and 3 ♂ undissected, preserved in 4% formalin; collection data as for holotype; BP 547/4.

Additional material. Russia • 9 ♀♀ and 6 ♂♂ undissected; Lena River Delta, Jangylakh Sise Island, large nameless lake; 72.517921°N, 125.281147°E; 7 Aug. 2019; A. Novikov leg; retained in the collection of the first author.

Russia • 2 ♀♀ undissected; Lena River Delta, Baron Island, small thermokarst lake; 72.550939°N, 126.93597°E; 8 Aug. 2019; A. Novikov leg; retained in the collection of the first author.

Russia • 3 ♀♀ and 1 ♂ undissected; Lena River Delta, Kurungnah Sise Island, Krugloe Lake; 72.468859°N, 126.265658°E; 21 Aug. 2019; A. Novikov leg; retained in the collection of the first author

Russia • 4 ♀♀ and 2 ♂♂ undissected; Vrangel Island, large nameless lake; 70.954443°N, 179.567387°E; 26 Aug. 2021; A. Novichkova leg: retained in the collection of the first author.

Description. Female (based on holotype and paratypes). Body subcylindrical (Fig. 10A). Total body length from anterior margin of rostrum to posterior margin of caudal rami: 586 μm (n = 1). Cephalothorax (Fig. 10B, C; Appendix 1), wider as remaining somites, length 152 μm, largest width 113 μm. Naupliar eye red. Rostrum (Fig. 10D) small, fused with cephalothorax, with rounded end, with one pair of sensillae and pore located proximal to sensillae. Posterior margin of cephalothorax and all pedigerous somites smooth.

Cephalothorax (Fig. 10B, C; Appendix 1) with dumbbell-shaped dorsal window, seven pairs of pores, seven pairs of sensillae of central group (group C), eight pairs of sensillae of marginal group (group P) and 13 pairs of ungrouped sensillae (in Table 4 and in Appendix 1 marked as L). Second pedigerous somite with lateral windows, dorsal unpaired pore, lateral pair of pores and six pairs of sensillae. Third pedigerous somite with dorsal unpaired pore and six pairs of sensillae. Fourth pedigerous somite with dorsal unpaired pore and five pairs of sensillae. Fifth pedigerous somite with three pairs of sensillae.

Abdomen (Fig. 11A–C) consisting of genital-double somite, two free abdominal somites and anal somite with caudal rami. All somites except anal somite slightly wavy posterior margin, on surface with spinular rows. Genital-double somite consists of last thoracic somite and first abdominal somite; wider than long; anterior part with two pairs of sensillae, dorsal unpaired pore, ventro-lateral row of spinules; posterior part with three pairs of sensillae, pairs of ventral and lateral pores and lateral rows of spinules.

P6 (Fig. 11C) fused with somite with one pinnate and one naked setae. Genital field (Fig. 11C) short, laterally with eight-pore sieves; copulatory pore located medially, copulatory duct chitinised with two additional tubes, extending proximally to pair of labyrinthic rounded ducts and one chitinised unpaired duct.

Second and third abdominal somites as in *B. minutus*. Anal somite with one pair of sensillae, ventral pair of large pores, lateral pair of pores and lateral spinules. Anal operculum semilunar, with seven short bifid spinules.

Caudal rami (Fig. 11A–D). Length/width ratio 1.6, with three ventral pores; with rows of spinules on ventral and dorsal side at base of seta VI and rows spinules at base of setae II and III. Seta I small, located near seta II. Apical seta IV (Fig. 11D) bipinnate, without “helle Stelle”. Apical seta V long, bipinnate, with “helle Stelle”. Seta VI with wide base (Fig. 11C). Seta VII triarticulated (Fig. 11B).

Antennule (Fig. 12A) similar to that of *Bryocamptus minutus*. Differences expressed in more elongated segments, especially 3th and 4th segments; one of setae on segment 2 pinnate. Armature formula: 1-[1],2-[9],3-[5],4-[1+(1+ae)],5-[1],6-[3],7-[2],8-[5+acr].

Antenna (Fig. 12B) similar to that of *Bryocamptus minutus*. Allobasis and free endopodal segment slightly more elongated. Inner spinular row on coxa with extremely long spinules. Allobasis with proximal outer spinular row, basal seta pinnate.

Labrum (Fig. 12C) similar to that of *Bryocamptus minutus*, but without semicircular spinular row on inner side.

Mandible (Fig. 13A, B) similar to that of *Bryocamptus minutus*. The palp is shortened.

Paragnaths (Fig. 12D) similar to that of *Bryocamptus minutus*, with only three lateral groups of spinules and with a more well-defined pocket.

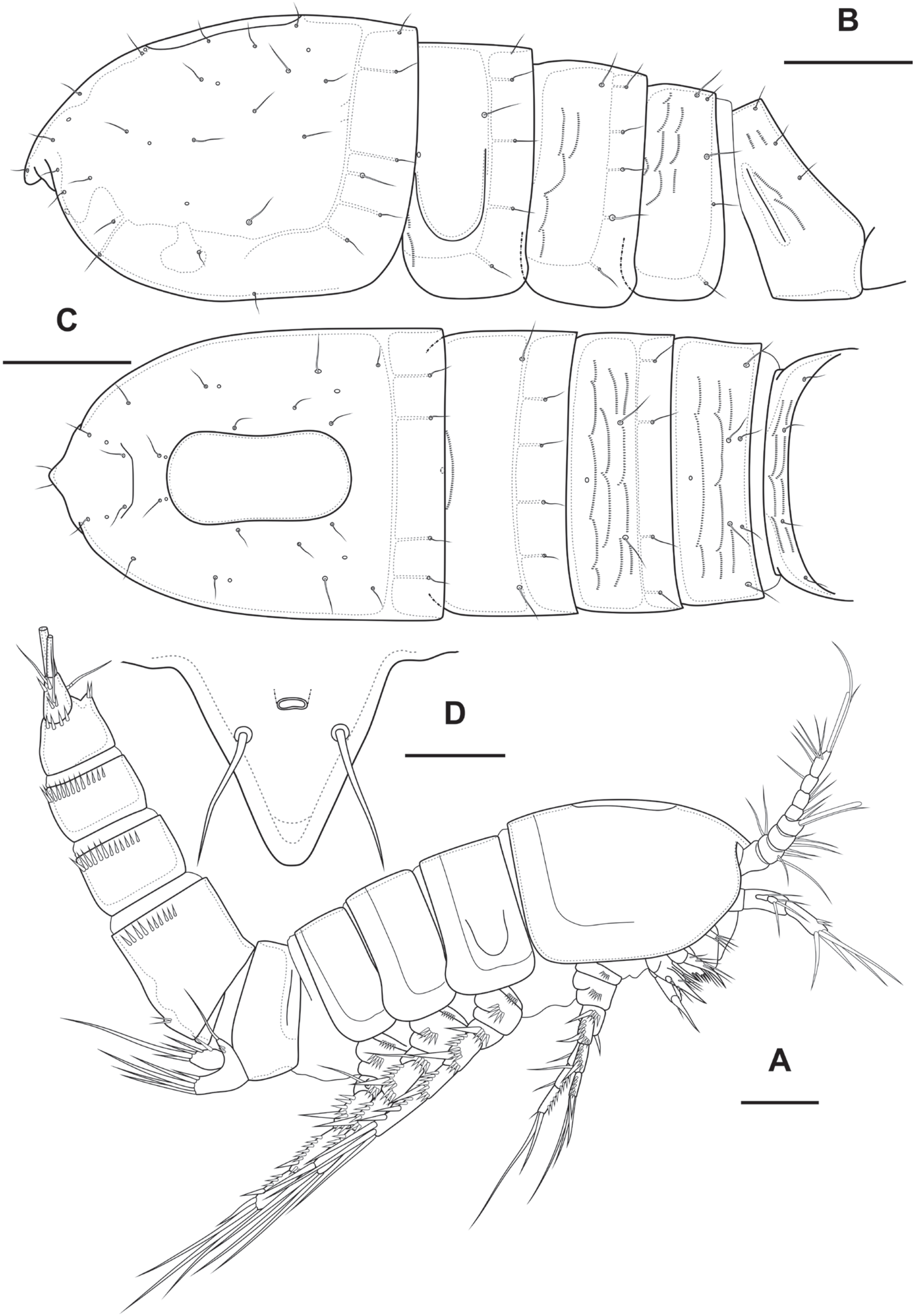

Figure 10. *Bryocamptus abramovae* sp. nov., female **A** habitus, lateral **B** cephalothorax and thoracic somites, dorsal **C** cephalothorax and thoracic somites, lateral **D** rostrum. Scale bars: 50 µm (**A–C**); 5 µm (**D**).

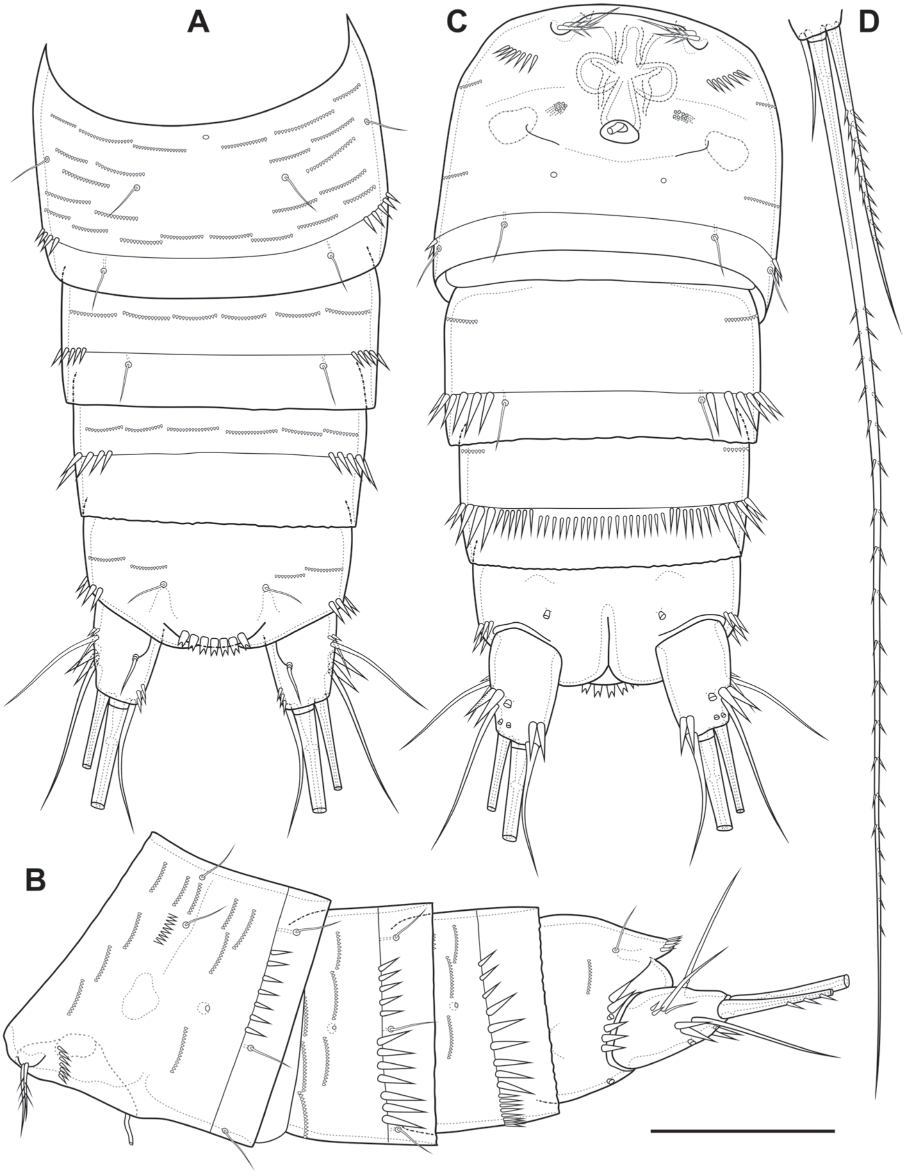

Figure 11. *Bryocamptus abramovae* sp. nov., female **A** abdomen, dorsal **B** abdomen, lateral **C** abdomen, ventral **D** caudal setae, dorsal. Scale bar: 50 μm.

Maxillule (Fig. 13C) similar to that of *Bryocamptus minutus*. Basis with two groups of spinules.

Maxilla (Fig. 13D) as in *Bryocamptus minutus*, only with slight differences in length and armature of setae.

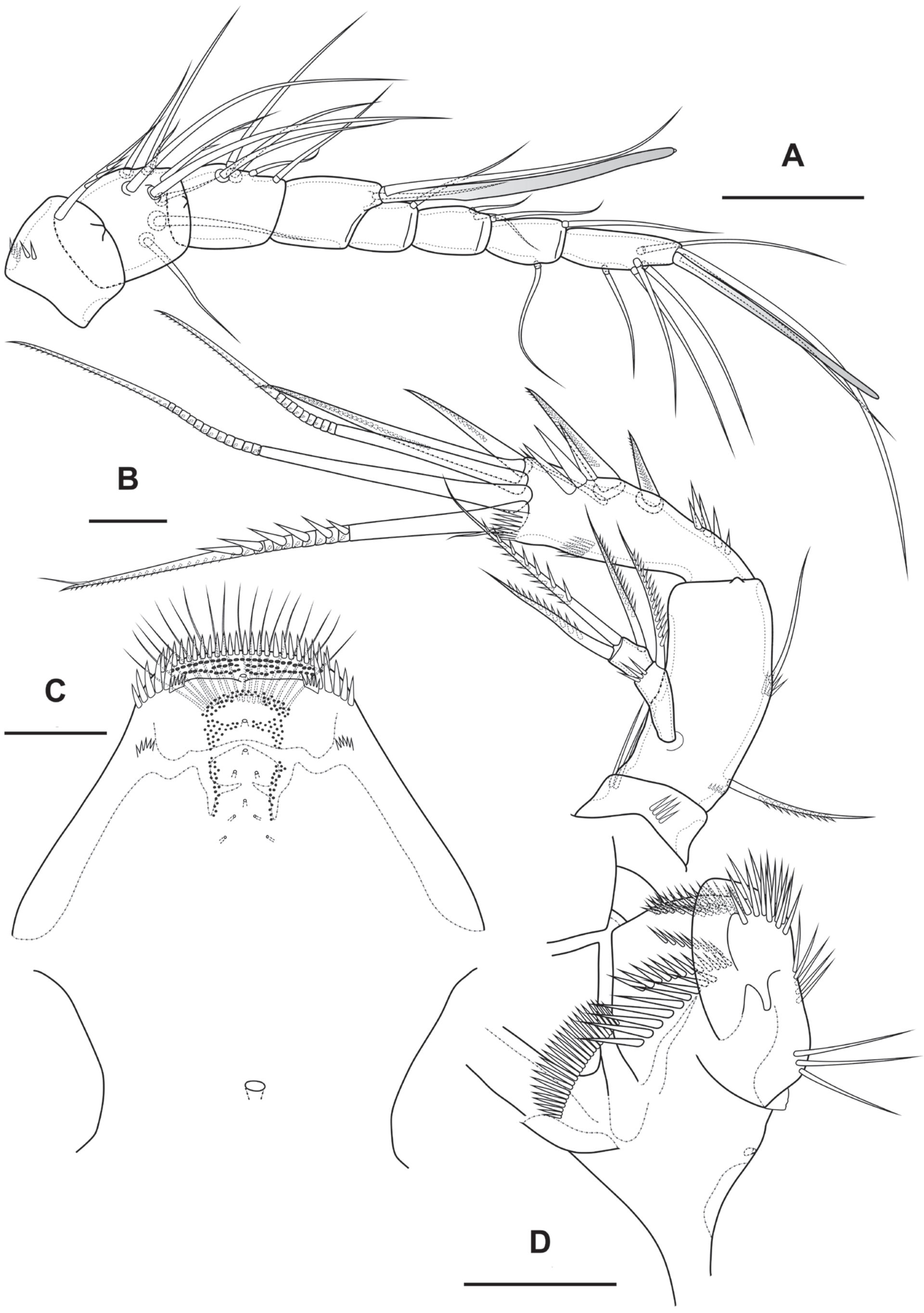

Figure 12. *Bryocamptus abramovae* sp. nov., female **A** antennule **B** antenna **C** labrum, posterior (black dots is bases of spinules) **D** paragnaths, anterior. Scale bars: 25 µm (**A**); 10 µm (**B–D**).

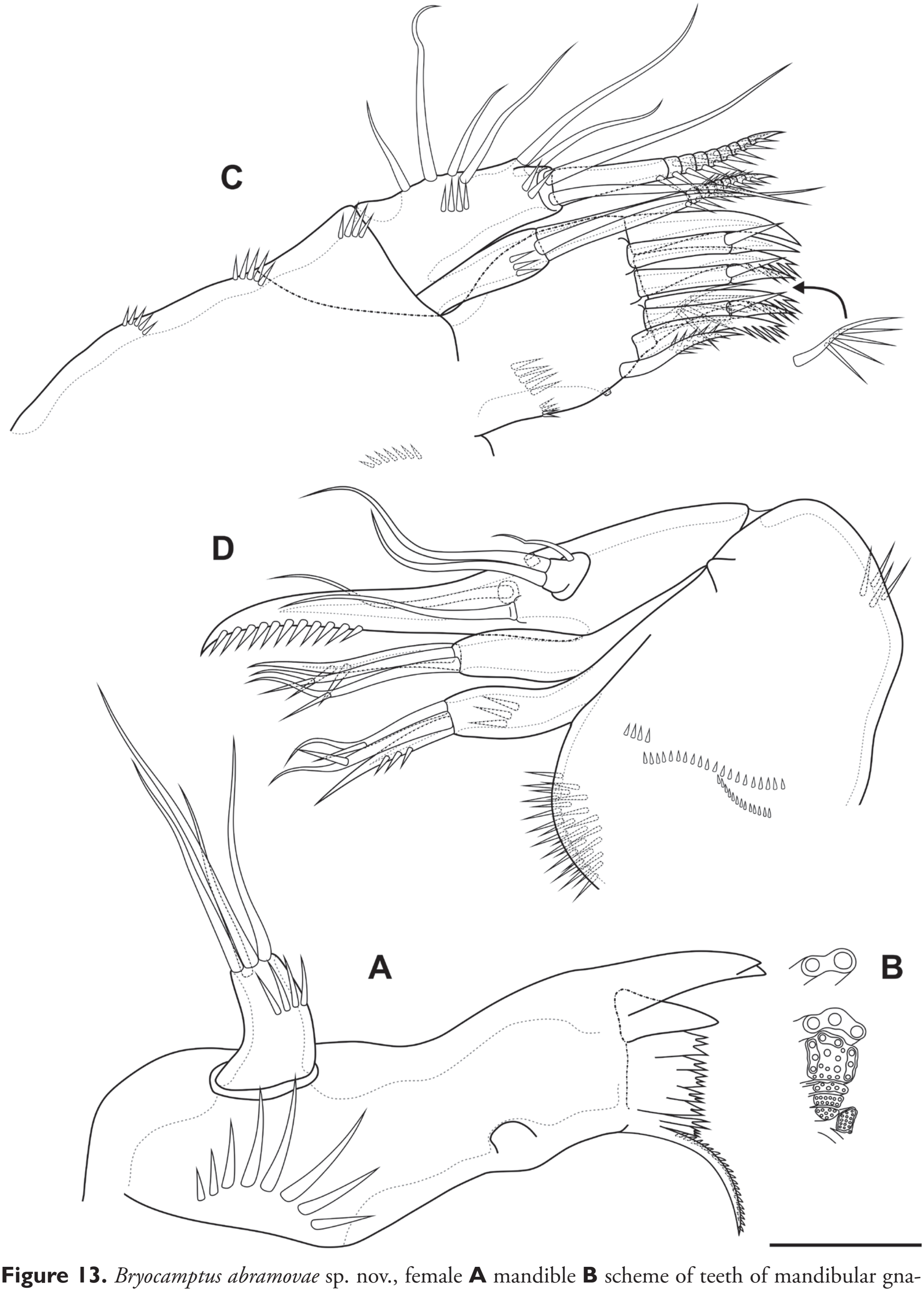

Figure 13. *Bryocamptus abramovae* sp. nov., female **A** mandible **B** scheme of teeth of mandibular gnathobase **C** maxillule **D** maxilla. Scale bar: 10 μm.

Maxilliped (Fig. 14A) similar to that of *Bryocamptus minutus*. Differences are only in shorter syncoxa and basis.

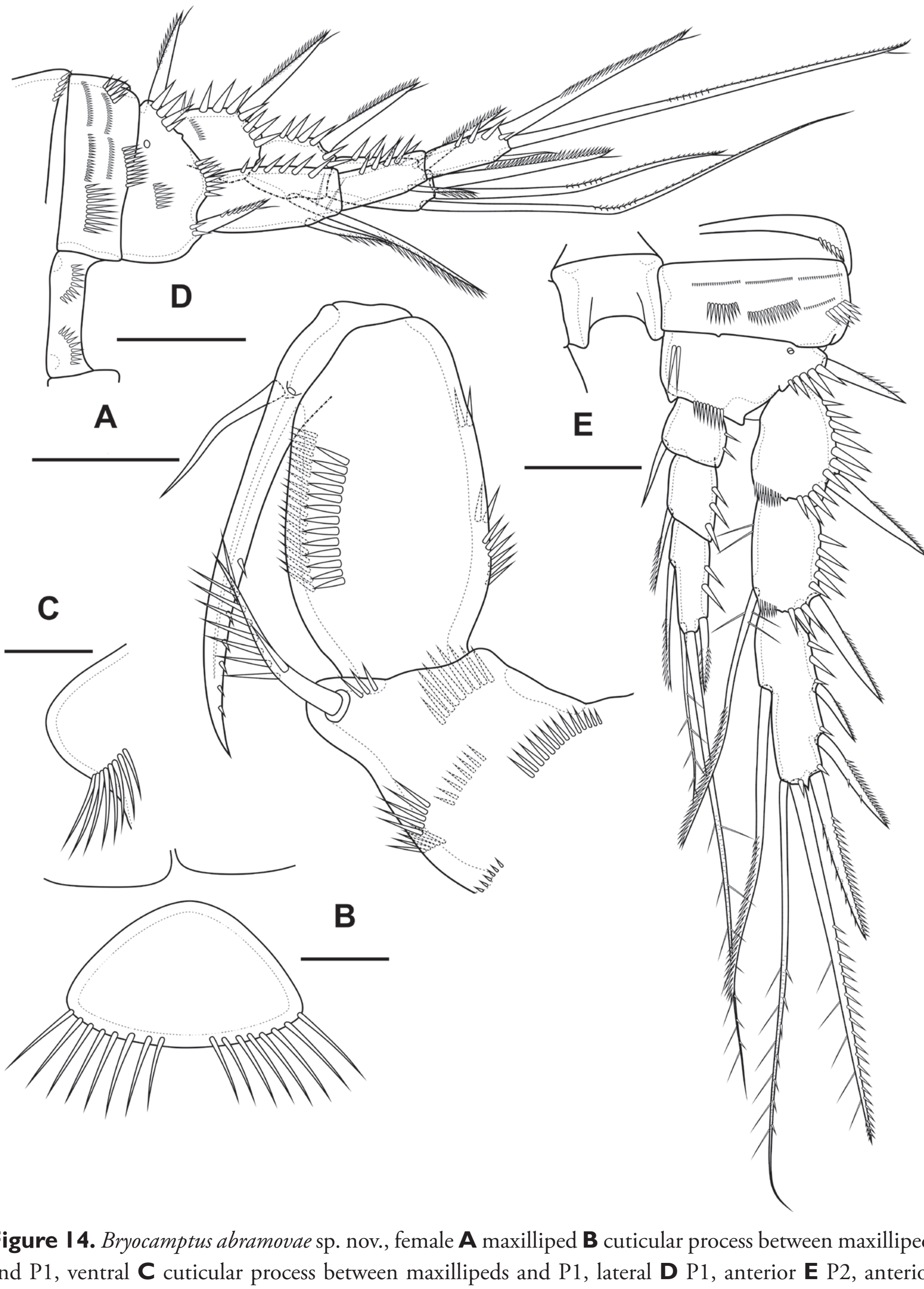

Figure 14. *Bryocamptus abramovae* sp. nov., female **A** maxilliped **B** cuticular process between maxillipeds and P1, ventral **C** cuticular process between maxillipeds and P1, lateral **D** P1, anterior **E** P2, anterior. Scale bars: 10 μm (**A**); 5 μm (**B, C**); 25 μm (**D, E**).

Cuticular process between maxillipeds and P1 (Fig. 14B, C) in height approximately same as in length, with long spinules, seven spinules on each side. Spinules on posterior margin.

P1 (Fig. 14D; Table 2) similar to that of *Bryocamptus minutus*. Basis without inner spinules. First exopodal segment with row of small spinules on anterior side. First endopodal segment reaching end of second exopodal segment. First and second endopodal segments with smooth inner side. Differences also noticeable in shorter exopodal and endopodal segments and larger spinules on coxa and basis.

P2 (Fig. 14E; Table 2). Praecoxa with row of spinules. Coxa with one lateral row of large spinules, two anterior rows of large spinules and four anterior rows of small spinules. Intercoxal sclerite naked. Basis with proximal pore, inner group of long spinules, rows of spinules at base of endopod and exopod; with outer spine. All endopodal and exopodal segments with outer spinules. Exopod three-segmented; first exopodal segment with outer spinulose spine, apically with frill; second segment with outer spinulose spine, inner pectinate seta, inner slender spinules and apical frill; third segment with three outer spinulose spines, two apical setae and one inner pectinate seta. Endopod three-segmented; first and second segments with inner seta; third segment with outer spinulose spine, two apical pinnate setae and one inner pectinate seta.

P3 (Fig. 15A; Table 2). Praecoxa with spinular row. Coxa with one lateral row of large spinules, two anterior rows of large spinules and four anterior rows of small spinules. Intercoxal sclerite without spinules. Basis with outer seta, proximal pore, inner group of long spinules and rows of spinules at base of endopod and exopod. Exopod three-segmented; first exopodal segment with outer spinulose spine, outer spinules, apically with frill; second segment with outer spinulose spine, outer spinules, inner pectinate seta, inner slender spinules and apical frill; third segment with three outer spinulose spines, two apical setae and two inner pectinate setae. Endopod three-segmented; first and second segments with inner seta, second segment with outer spinules; third segment with outer spinules, outer spinulose spine, two apical pinnate setae and two inner pectinate setae.

P4 (Fig. 15B; Table 2). Praecoxa with spinular row. Coxa with one lateral row of large spinules, two anterior rows of large spinules and four anterior rows of small spinules. Basis with outer seta, proximal pore, rows of spinules at base of endopod and exopod. Exopod three-segmented; first exopodal segment with outer spinulose spine, outer spinules, apically with frill; second segment with outer spinulose spine, outer spinules, inner pectinate seta, inner slender spinules and apical frill; third segment with two outer spinulose spines, two apical setae and two inner pectinate setae. Endopod two-segmented; first segment with inner pectinate seta, second segment with outer spinules, outer spinulose spine, apical spiniform spinulose seta, apical pinnate seta and two inner pectinate setae.

P5 (Fig. 15C) with separate right and left baseoendopods. Baseoendopod reaching ~ 2/3 of exopodal segment; with four pores, spinular row at base of outer seta; outer seta of basis pinnate, long. Endopodal lobe with four long bipinnate setae and one short bipinnate seta V; with small process that may be pore between setae III and IV. Exopod inner thin pinnate seta, long apical pinnate seta, naked subapical seta and two pinnate outer setae.

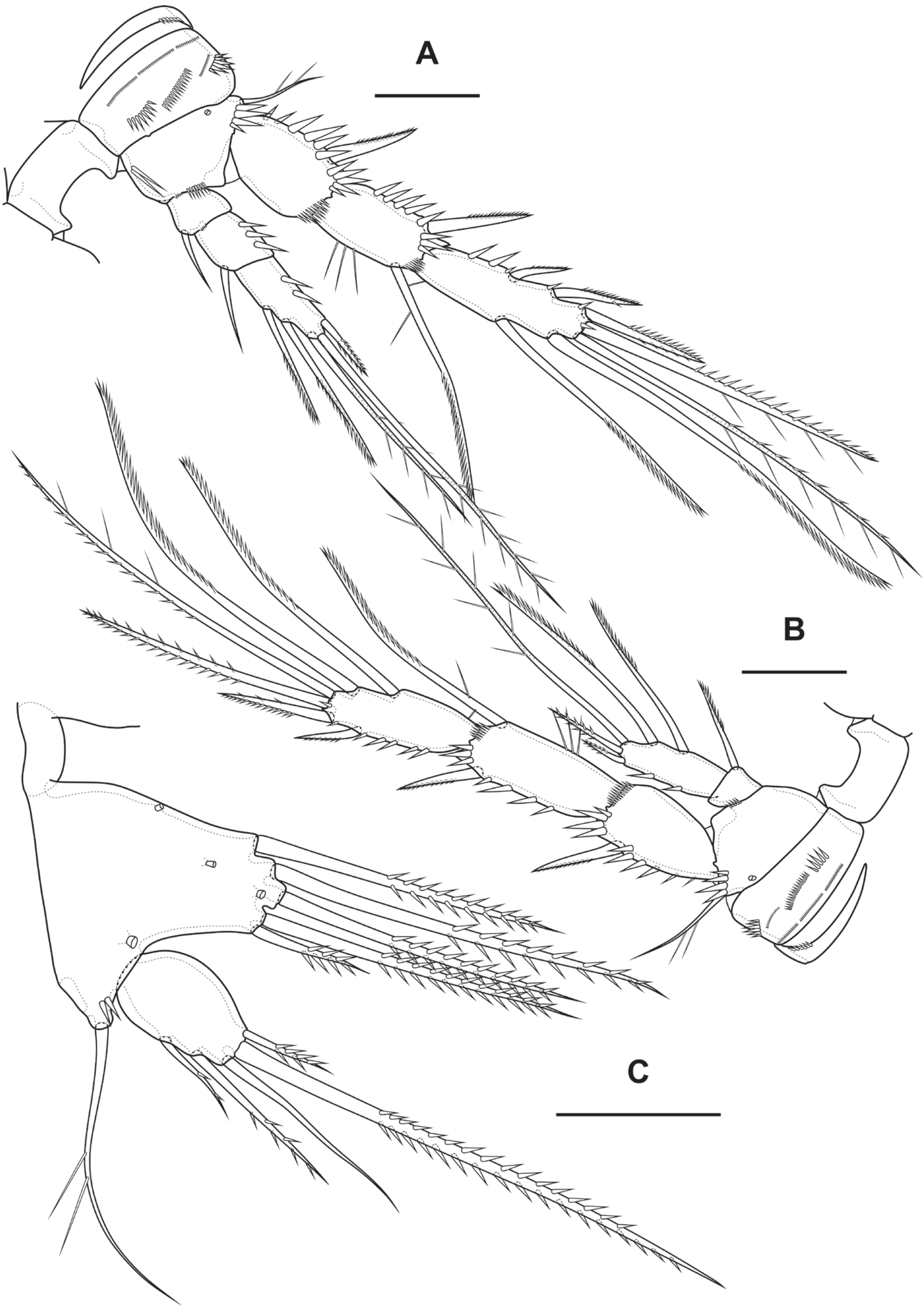

Figure 15. *Bryocamptus abramovae* sp. nov., female **A** P3, anterior **B** P4, anterior **C** P5, anterior. Scale bars: 25 μm.

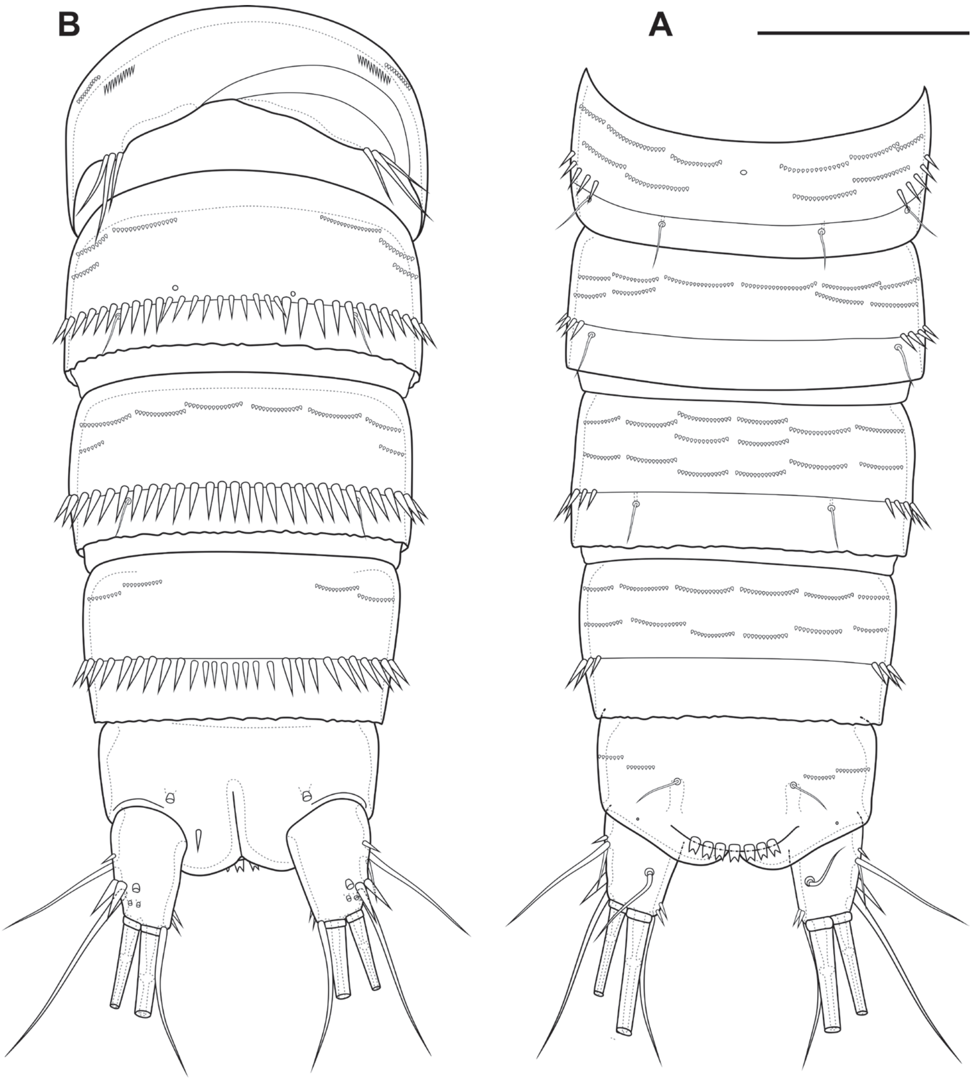

Figure 16. *Bryocamptus abramovae* sp. nov., male **A** abdomen, dorsal **B** abdomen, ventral. Scale bar: 50 µm.

Male. Sexual dimorphism expressed in the antennule, P2–P6, genital segmentation and ornamentation, shape of caudal rami. Cephalothorax and thoracic somites as in female. P6 (Fig. 16B) two asymmetric flaps fused to the somite, with three naked setae. Differences from female in abdomen structure as follows (Fig. 16A, B): first abdominal somite free; first to third abdominal somites with spinular row encircling somite ventrally and laterally; anal somite with ventral spinule and without lateral spinules; caudal rami without ventral spinules; seta IV with “helle Stelle”.

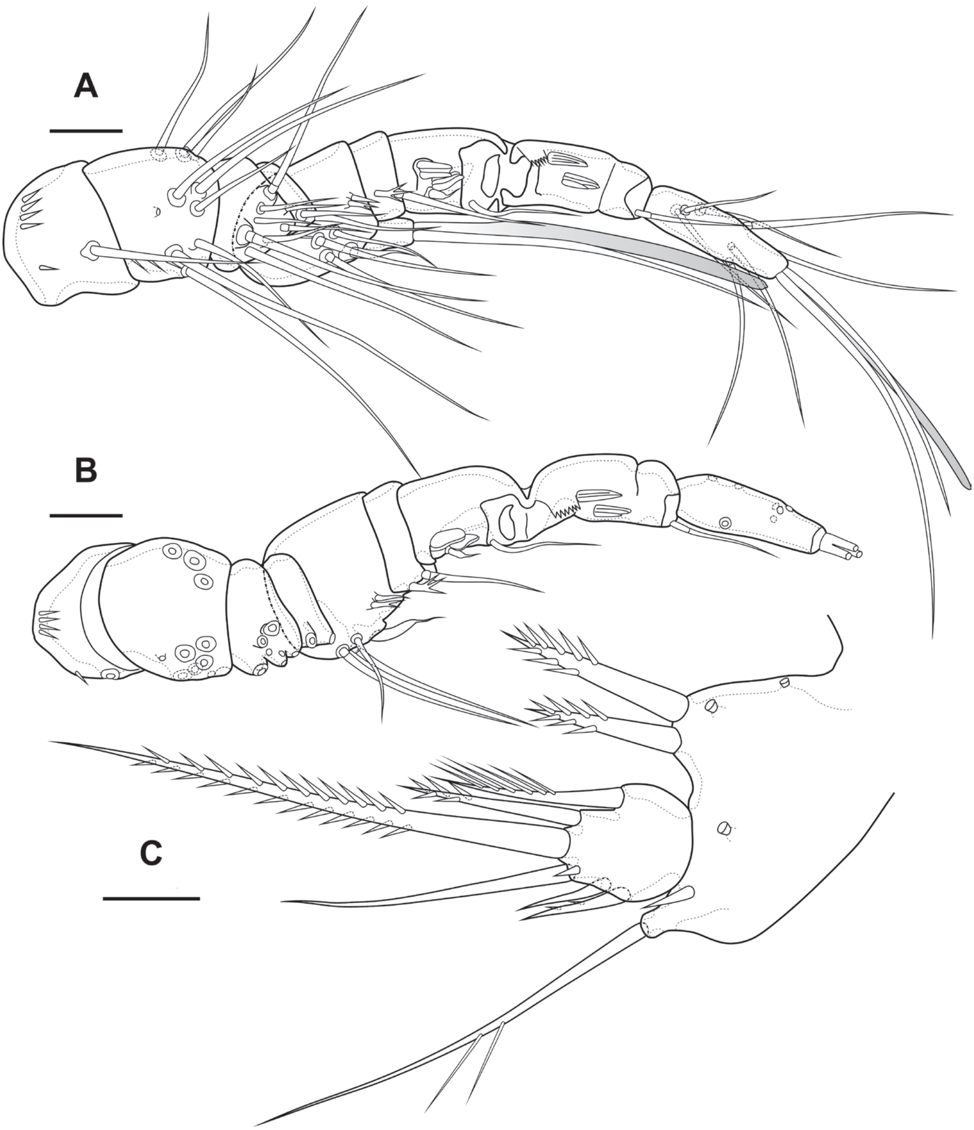

Figure 17. *Bryocamptus abramovae* sp. nov., male **A** antennule, anterior **B** antennule, dorsal **C** P5, anterior. Scale bars: 10 μm.

Table 2. P1 – P4 armature of *Bryocamptus abramovae* sp. nov.

	Female endopod	Male endopod	Exopod
P1	1; 1; 1,1,1	1; 1; 1,1,1	0; 1; 0,2,2
P2	1; 1; 1,2,1	1; 2,2,0	0; 1; 1,2,2-3
P3	1; 1; 2,2,1	1; 1+ ap; 2,2,0	0; 1; 2,2,2-3
P4	1; 2,2,1	0; 0,2,1	0; 1; 2,2,2-3

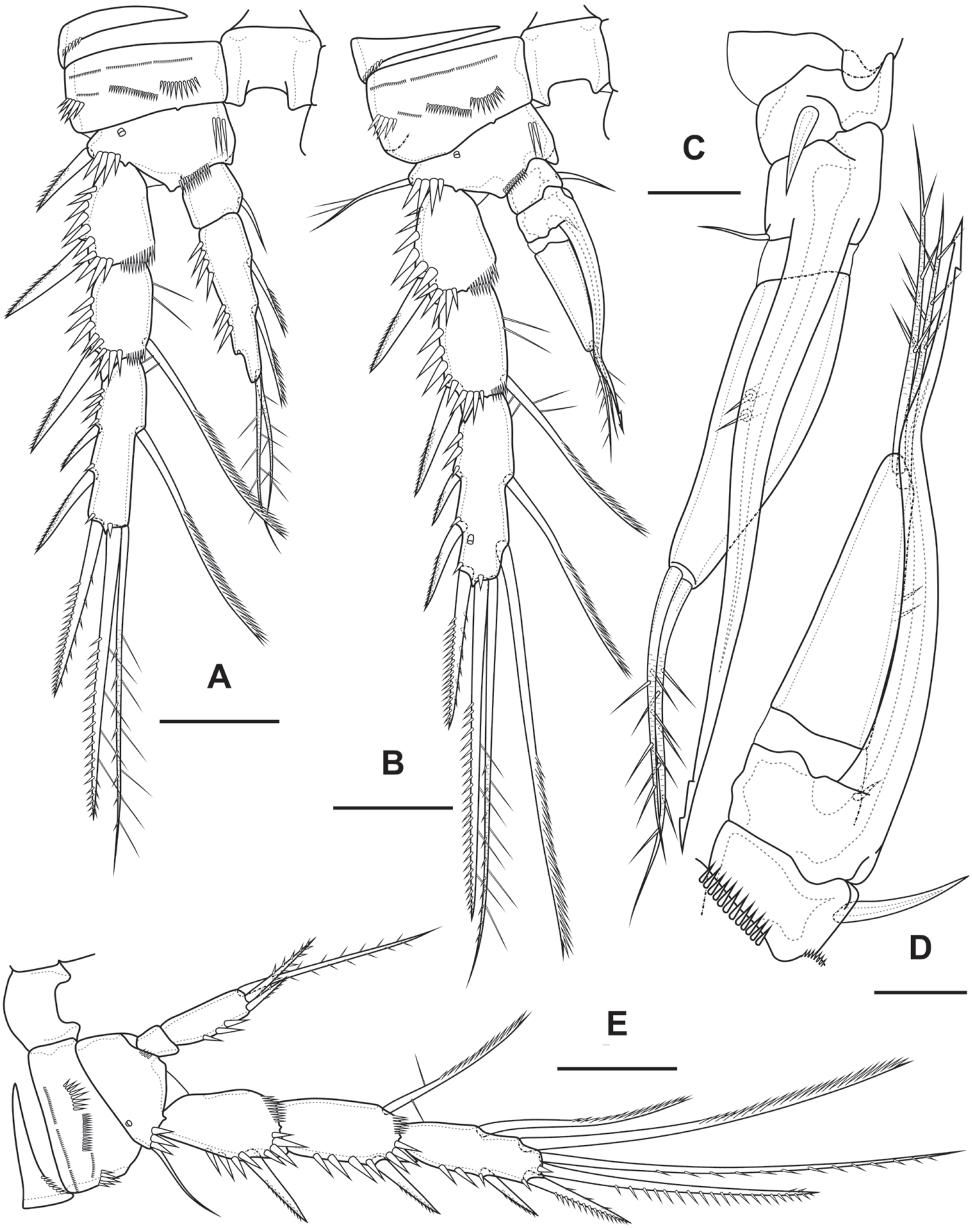

Figure 18. *Bryocamptus abramovae* sp. nov., male **A** P2, anterior **B** P3, anterior **C** P3 endopod, anterior **D** P3 endopod, inner view **E** P4, anterior. Scale bars: 25 μm (**A, B, E**); 10 μm (**C, D**).

Antennule (Fig. 17A, B) 10-segmented, haplocer with geniculation between segments 7 and 8. Segments 1, 3, 4, 5, 6, 9, and 10 almost like in *B. minutus*, but more elongated. Segment 2 with small pore on anterior side. Segment 7 with articular plate, with one filiform seta, one small caudate seta and with two modified laminar setae.

Segment 8 with proximal short dentate plate and two modified laminar setae. Armature formula: 1-[1],2-[9],3-[8],4-[2],5-[6+(1+ae)],6-[2],7-[2+2 modified],8-[2 modified],9-[1],10-[7+acr].

P2 (Fig. 18A) as in female, except endopod. Endopod two-segmented. First segment with inner seta. Second segment with notch on distal outer margin, outer spinules, two apical pinnate slender setae and two inner pectinate setae.

P3 (Fig. 18B–D): praecoxa, coxa, intercoxal sclerite as in female. Basis as in female, but with larger inner process. Exopod as in female, but third segment with pore. Endopod three-segmented. First endopodal segment with strong seta. Second endopodal segment with posterior thin seta and long apophysis with double tip. Third segment with two small inner setae and two apical pinnate setae.

P4 (Fig. 18E): praecoxa, coxa, intercoxal sclerite, basis, exopod as in female. Endopod two-segmented; first segment short, unarmed; second segment with outer spinules, spinulose spine, outer apical spiniform spinulose seta and inner apical bipinnate seta.

P5 (Fig. 17C) right and left fused medially. Baseoendopod with three pairs of pores, outer spinule and outer long pinnate seta; endopodal lobe with two strong spinulose apical spines. Exopod with spinule on anterior surface, two equal length outer setae, naked outer subapical seta, long apical spinulose seta, one inner spinulose seta and one long inner pectinate seta with long setules.

Variability. Individuals with two outer spines on the third exopodal segments of P2–P4 were found.

Etymology. This species is named after Ekaterina Abramova, teacher and mentor of the first author.

Remarks. The species is well distinguished from other species of the *B. minutus* group by the presence of only five setae on the endopodal lobe of females P5 and by simple caudal rami with unmodified setae.

***Bryocamptus* (*Bryocamptus*) *putoranus* sp. nov.**
https://zoobank.org/0591F5CD-A09C-4D37-AC8B-DC1CC93E8B3B
Figs 19–27

Material. ***Holotype*:** Russia • ♀ dissected on two slides; Russia, Putorana Plateau, large nameless lake in the upper flow of the Neral River; 68.901987°N, 94.170533°E; depth 0.5–1 m; 4 Aug. 2021; E. Chertoprud leg; BP 548/1-a, BP 548/1-b. ***Allotype*:** Russia •♂ dissected on one slide; collection data as for holotype; BP 548/2. ***Paratypes*:** Russia • ♀ dissected on two slides (BP 548/3-a, BP 548/3-b) and ♂ dissected on one slide (BP 548/4); Putorana Plateau, large nameless lake; 68.898348°N, 94.174442°E; depth 0.5–1 m; 4 Aug. 2021; E. Chertoprud leg.

Description. Female (based on holotype and paratype). Body subcylindrical (Fig. 19A). Total body length from anterior margin of rostrum to posterior margin of caudal rami: 527 µm (n = 1). Cephalothorax (Fig. 19B, C; Appendix 1), wider than remaining somites, length 144 µm, largest width 112 µm. Naupliar eye not observed.

Rostrum (Fig. 21A) small, fused with cephalothorax, with rounded end, with one pair of sensillae and pore located distal to sensillae. Posterior margin of cephalothorax and all pedigerous somites smooth.

Cephalothorax (Fig. 19B, C; Appendix 1) with dumbbell-shaped dorsal window, seven pairs of pores, seven pairs of sensillae of central group (group C), 13 pairs of sensillae of marginal group (group P) and 21 pairs of ungrouped sensillae (marked as L in Table 4 and in Appendix 1). Second pedigerous somite with lateral windows, dorsal unpaired pore, lateral pair of pores and eight pairs of sensillae. Third pedigerous somite with dorsal unpaired pore, lateral pair of pores and nine pairs of sensillae. Fourth pedigerous somite with dorsal unpaired pore, lateral pair of pores and eight pairs of sensillae. Fifth pedigerous somite with lateral pair of pores and four pairs of sensillae.

Abdomen (Fig. 20A–C) consisting of genital-double somite, two free abdominal somites and anal somite with caudal rami. All somites except anal somite with wavy posterior margin, on surface with spinular rows. Genital-double somite consists of last thoracic somite and first abdominal somite; wider than long; anterior part with four pairs of sensillae, dorsal unpaired pore, lateral paired pores, ventro-lateral and lateral rows of spinules; posterior part with four pairs of sensillae, pairs of ventral and lateral pores and lateral rows of spinules.

P6 (Fig. 20C) fused with somite with two pinnate setae. Genital field (Fig. 20C) long, laterally with eight-pore sieves; copulatory pore displaced to posterior part of somite, copulatory duct chitinised with two additional tubes, extending proximally to pair of labyrinthic rounded ducts and one chitinised unpaired duct.

Second, third abdominal and anal somites as in *B. minutus*. Anal operculum semilunar, with seven long simple spinules. Caudal rami (Fig. 20A–D). Length/width ratio 1.5, with three ventral pores; with rows of spinules on ventral and dorsal side at base of seta IV and rows spinules at base of setae II and III. Seta I small, located near seta II. Setae IV, V and VI displaced to ventral side of caudal ramus. Apical seta IV (Fig. 20D) bipinnate, with massive bulbous base and "helle Stelle". Apical seta V long, bipinnate, with "helle Stelle". Seta VII triarticulated (Fig. 20B).

Antennule (Fig. 20B) similar to that of *Bryocamptus minutus*. Differences expressed in more elongated segments, especially 3rd and 4th segments; one of setae on segment 2 pinnate. Armature formula: 1-[1],2-[9],3-[5],4-[1+(1+ae)],5-[1],6-[3],7-[2],8-[5+acr].

Antenna (Fig. 21B) similar to that of *Bryocamptus minutus*. Allobasis and free endopodal segment slightly shorter. Allobasis with proximal outer spinular row, basal seta pinnate; without spinular row at base of endopodal seta.

Labrum (Fig. 22A) similar to that of *Bryocamptus minutus*, but without semicircular spinular row on inner side.

Mandible (Fig. 21D, E). Coxa and gnathobase as in *Bryocamptus minutus*. The palp elongated, with three apical setae.

Paragnaths (Fig. 22B) similar to that of *Bryocamptus minutus*, with only two groups of spinules on anterior side and without proximal spinular row.

Maxillule (Fig. 22C) similar to that of *Bryocamptus minutus*. Coxal endite without spinules; basis with group of spinules.

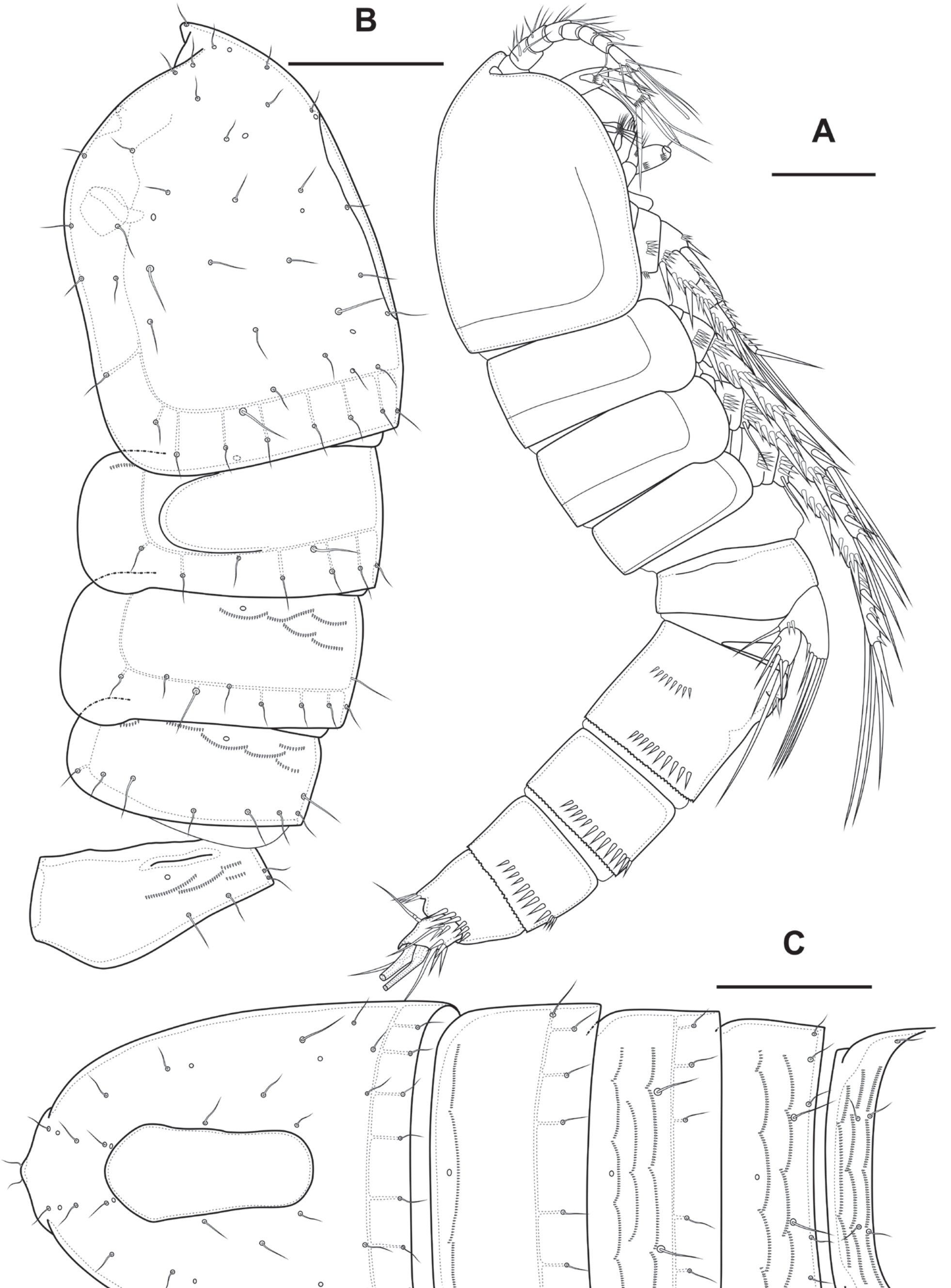

Figure 19. *Bryocamptus putoranus* sp. nov., female **A** habitus, lateral **B** cephalothorax and thoracic somites, lateral **C** cephalothorax and thoracic somites, dorsal. Scale bars: 50 µm.

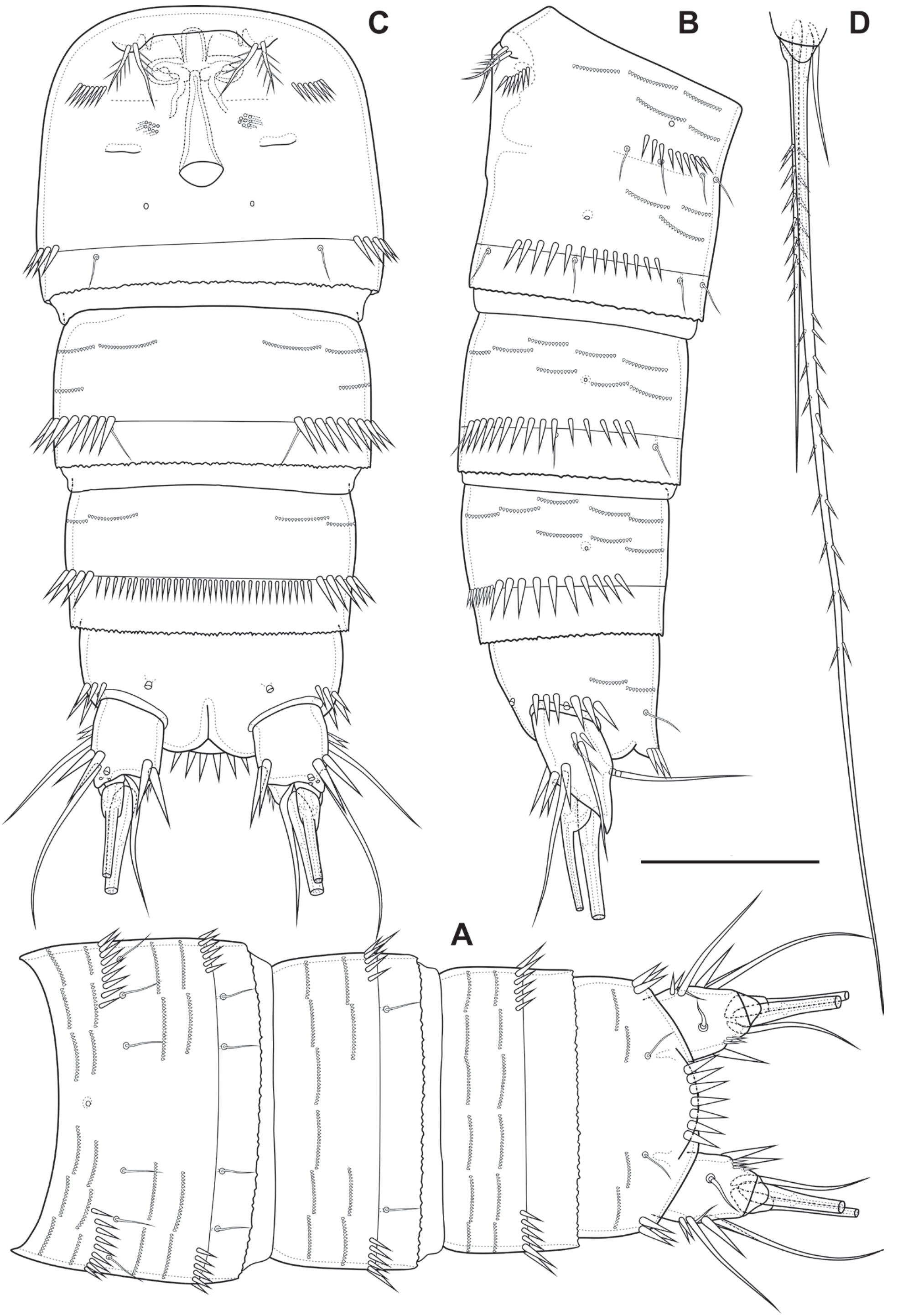

Figure 20. *Bryocamptus putoranus* sp. nov., female **A** abdomen, dorsal **B** abdomen, lateral **C** abdomen, ventral **D** caudal setae, dorsal. Scale bar: 50 μm.

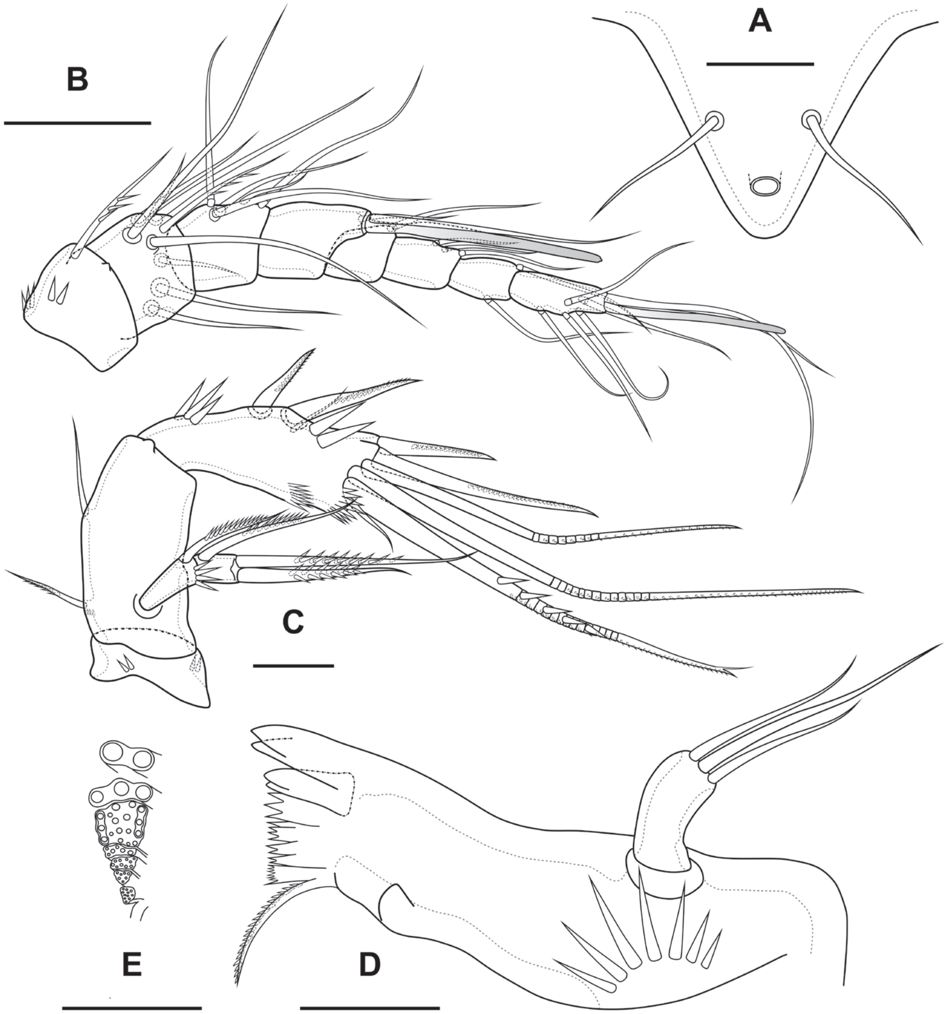

Figure 21. *Bryocamptus putoranus* sp. nov., female **A** rostrum **B** antennule **C** antenna **D** mandible **E** scheme of teeth of mandibular gnathobase. Scale bars: 5 µm (**A**); 10 µm (**B–E**).

Maxilla (Fig. 22D) as in *Bryocamptus minutus*, only with slight differences in length and armature of setae.

Maxilliped (Fig. 23A) similar to that of *Bryocamptus minutus*. Differences are only in shorter syncoxa and basis.

Cuticular process between maxillipeds and P1 (Fig. 23B, C) extremely high, with long spinules, five spinules on each side. Spinules on posterior margin.

P1 (Fig. 23D) almost like in *Bryocamptus minutus*. Basis with two inner groups of long spinules. First exopodal segment with inner spinules. First endopodal segment reaching end of second exopodal segment. Second endopodal segments with smooth inner side. Differences also noticeable in shorter exopodal and endopodal segments.

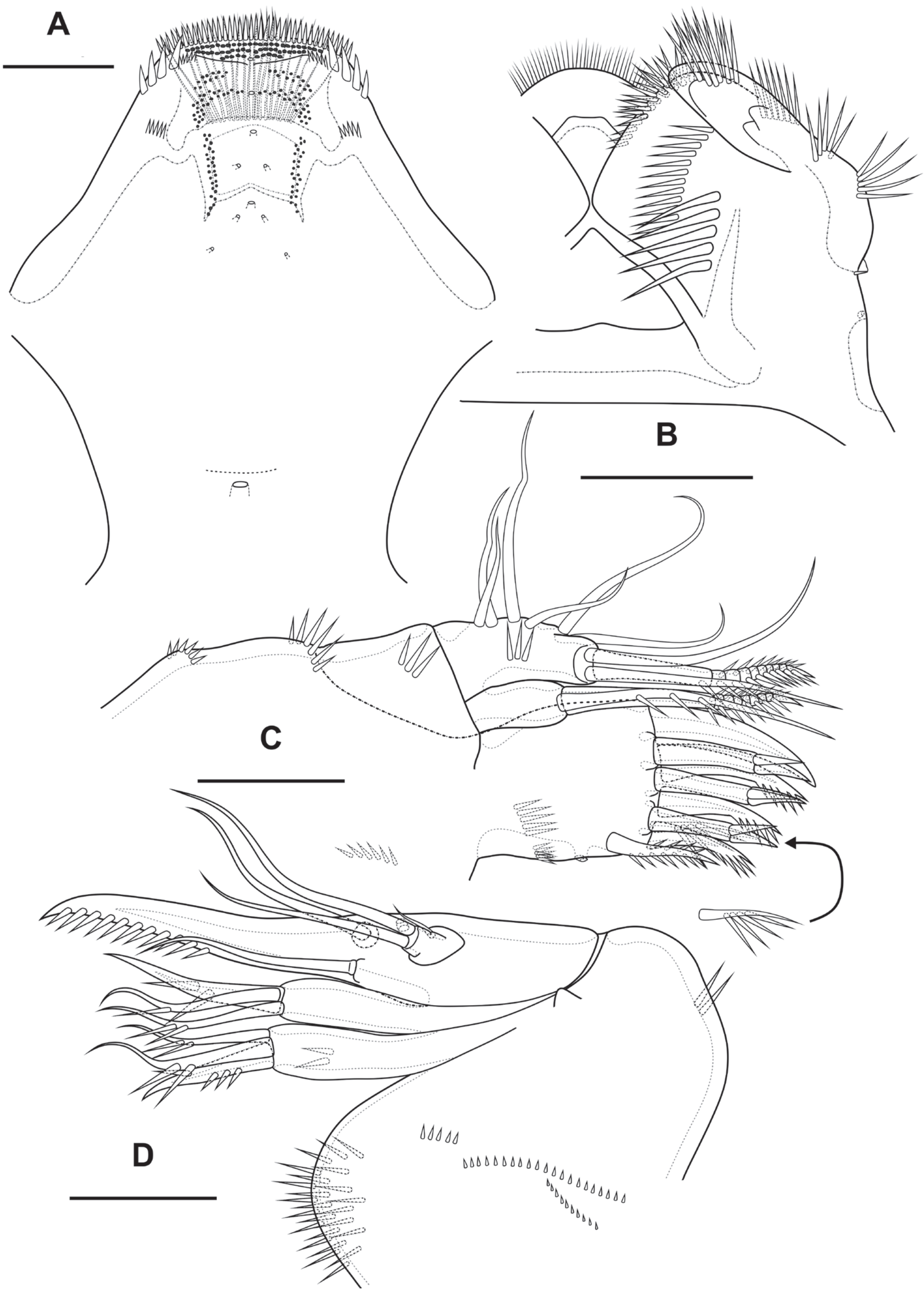

Figure 22. *Bryocamptus putoranus* sp. nov., female **A** labrum, posterior (black dots is bases of spinules) **B** paragnaths, anterior **C** maxillule **D** maxilla. Scale bars: 10 μm.

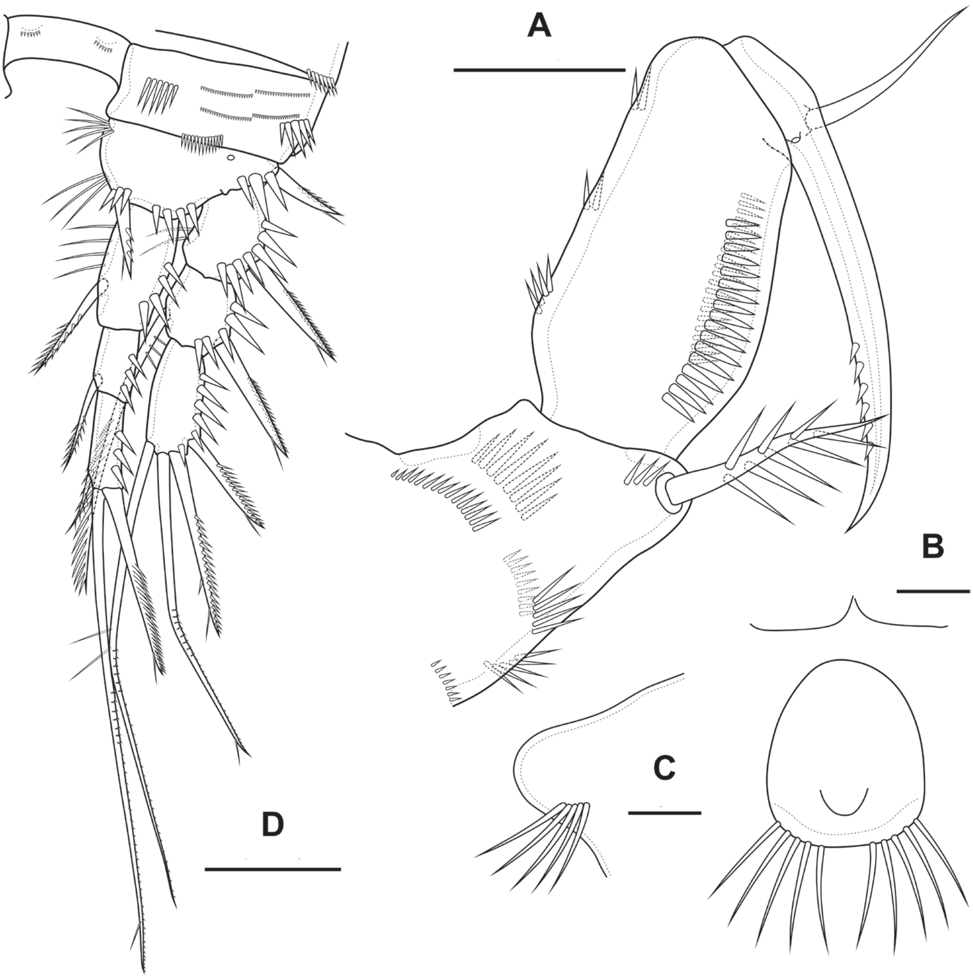

Figure 23. *Bryocamptus putoranus* sp. nov., female **A** maxilliped **B** cuticular process between maxillipeds and P1, ventral **C** cuticular process between maxillipeds and P1, lateral **D** P1. Scale bars: 10 µm (**A**); 5 µm (**B, C**); 25 µm (**D**).

P2 (Fig. 24A; Table 3). Praecoxa with row of spinules. Coxa with one lateral row of large spinules, two anterior rows of large spinules and four anterior rows of small spinules. Intercoxal sclerite naked. Basis with proximal pore, rows of spinules at base of endopod and exopod; with outer spine. All endopodal and exopodal segments with outer spinules. Exopod three-segmented; first exopodal segment with outer spinulose spine, apically with frill; second segment with outer spinulose spine, inner pectinate seta, inner slender spinules and apical frill; third segment with three outer spinulose spines, two apical setae and one inner pectinate seta. Endopod two-segmented; first segment with inner seta; second segment with distinct border between ancestral segments, outer spinulose spine, two apical pinnate setae and two inner pectinate setae.

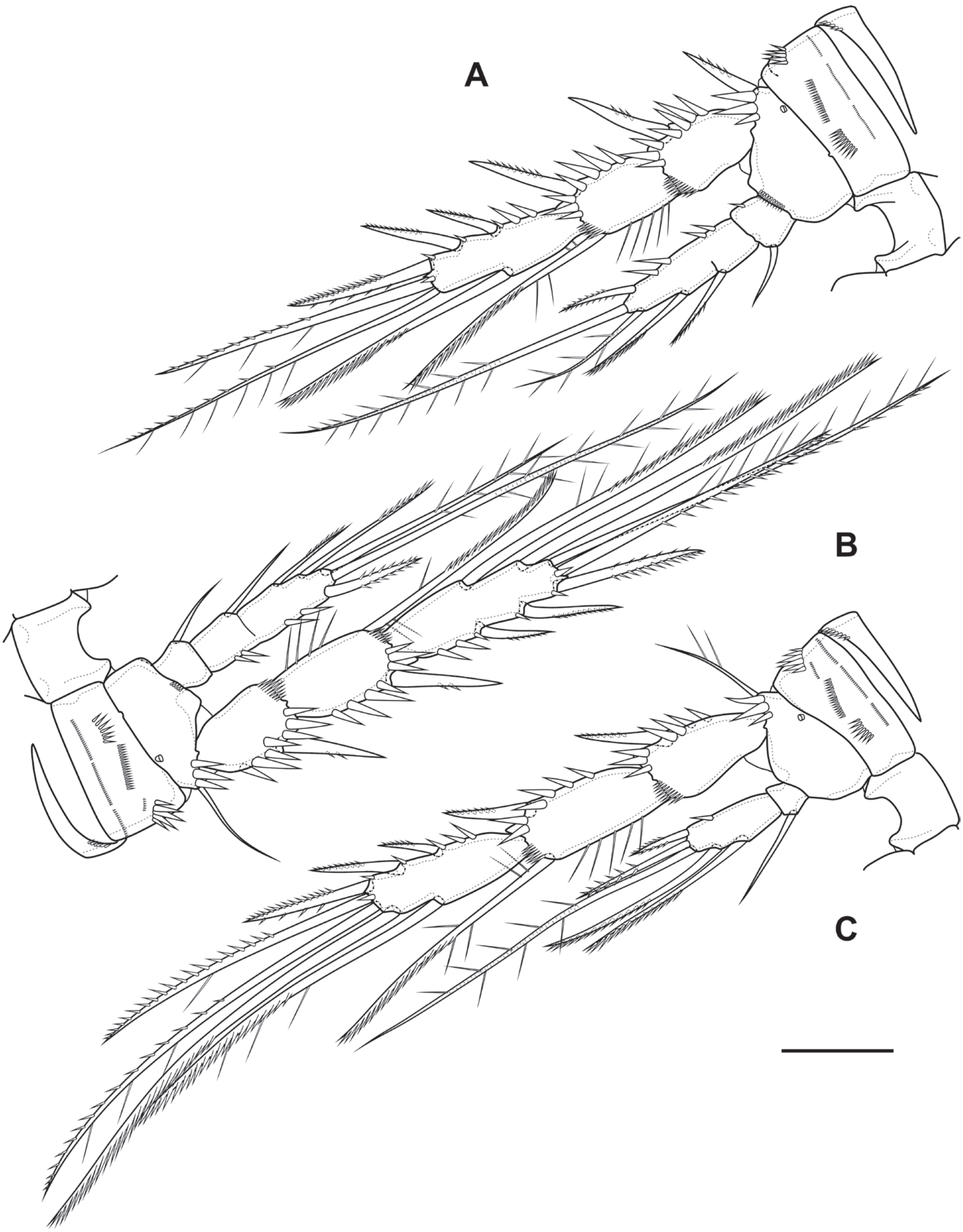

Figure 24. *Bryocamptus putoranus* sp. nov., female **A** P2, anterior **B** P3, anterior **C** P4, anterior. Scale bar: 25 µm.

P3 (Fig. 24B; Table 3). Praecoxa with spinular row. Coxa with one lateral row of large spinules, two anterior rows of large spinules and four anterior rows of small spinules. Intercoxal sclerite without spinules. Basis with outer seta, proximal pore, and rows of spinules at base of endopod and exopod. Exopod three-segmented; first exopodal segment with outer spinulose spine, outer spinules, apically with frill; second segment with outer spinulose spine, outer spinules, inner pectinate seta, inner slender spinules and apical frill; third segment with three outer spinulose spines, two apical setae and two inner pectinate setae. Endopod two-segmented; first segment with inner seta; second segment with distinct border between ancestral segments, outer spinules, outer spinulose spine, two apical pinnate setae and three inner setae.

P4 (Fig. 24C; Table 3). Praecoxa with spinular row. Coxa with one lateral row of large spinules, two anterior rows of large spinules and four anterior rows of small spinules. Basis with outer seta, proximal pore, rows of spinules at base of exopod. Exopod three-segmented; first exopodal segment with outer spinulose spine, outer spinules, apically with frill; second segment with outer spinulose spine, outer spinules, inner pectinate seta, inner slender spinules and apical frill; third segment with three outer spinulose spines, two apical setae and two inner pectinate setae. Endopod two-segmented; first segment with inner seta, second segment with outer spinule, outer spinulose spine, apical spiniform spinulose seta, apical pinnate seta and two inner pectinate setae.

P5 (Fig. 25A) with separate right and left baseoendopods. Baseoendopod reaching ~ 1/2 of exopodal segment; with four pores, spinule at base of outer seta; outer seta of basis pinnate, long. Endopodal lobe with four long bipinnate setae and two short bipinnate setae V and VI; with small process that may be pore between setae III and IV. Exopod with inner spinule, inner strong pinnate seta, long apical pinnate seta, naked subapical seta and two pinnate outer setae.

Male. Sexual dimorphism expressed in the antennule, P2–P6, genital segmentation and ornamentation, shape of caudal rami. Cephalothorax and thoracic somites as in female. P6 (Fig. 26B) two asymmetric flaps fused to the somite, with one naked and one pinnate setae. Differences from female in abdomen structure as follows (Fig. 26A, B): first abdominal somite free; first to third abdominal somites with spinular row encircling somite ventrally and laterally; anal somite with ventral spinules; caudal rami with normal setae IV and V; anal operculum with eight simple spinules.

Antennule (Fig. 25C, D) 10-segmented, haplocer with geniculation between segments 7 and 8. Segments 1, 3, 4, 5, 6, 9, and 10 similar to those of *B. minutus*, but differ in length. Segment 2 with small pore on anterior side. Segment 7 with articular plate, with one filiform seta, one small caudate seta and with two large modified laminar setae. Segment 8 with proximal long dentate plate and three modified laminar setae. Armature formula: 1-[1],2-[9],3-[8],4-[2],5-[6+(1+ae)],6-[2],7-[2+2 modified],8-[3 modified],9-[1],10-[7+acr].

Table 3. P1 – P4 armature of *Bryocamptus putoranus* sp. nov.

	Female endopod	Male endopod	Exopod
P1	1; 1; 1,1,1	1; 1; 1,1,1	0; 1; 0,2,2
P2	1; 2,2,1	1; 2,2,0	0; 1; 1,2,2-3
P3	1; 3,2,1	1; 1+ ap; 2?,2,0	0; 1; 2,2,3
P4	1; 2,2,1	0; 0,2,1	0; 1; 2,2,2-3

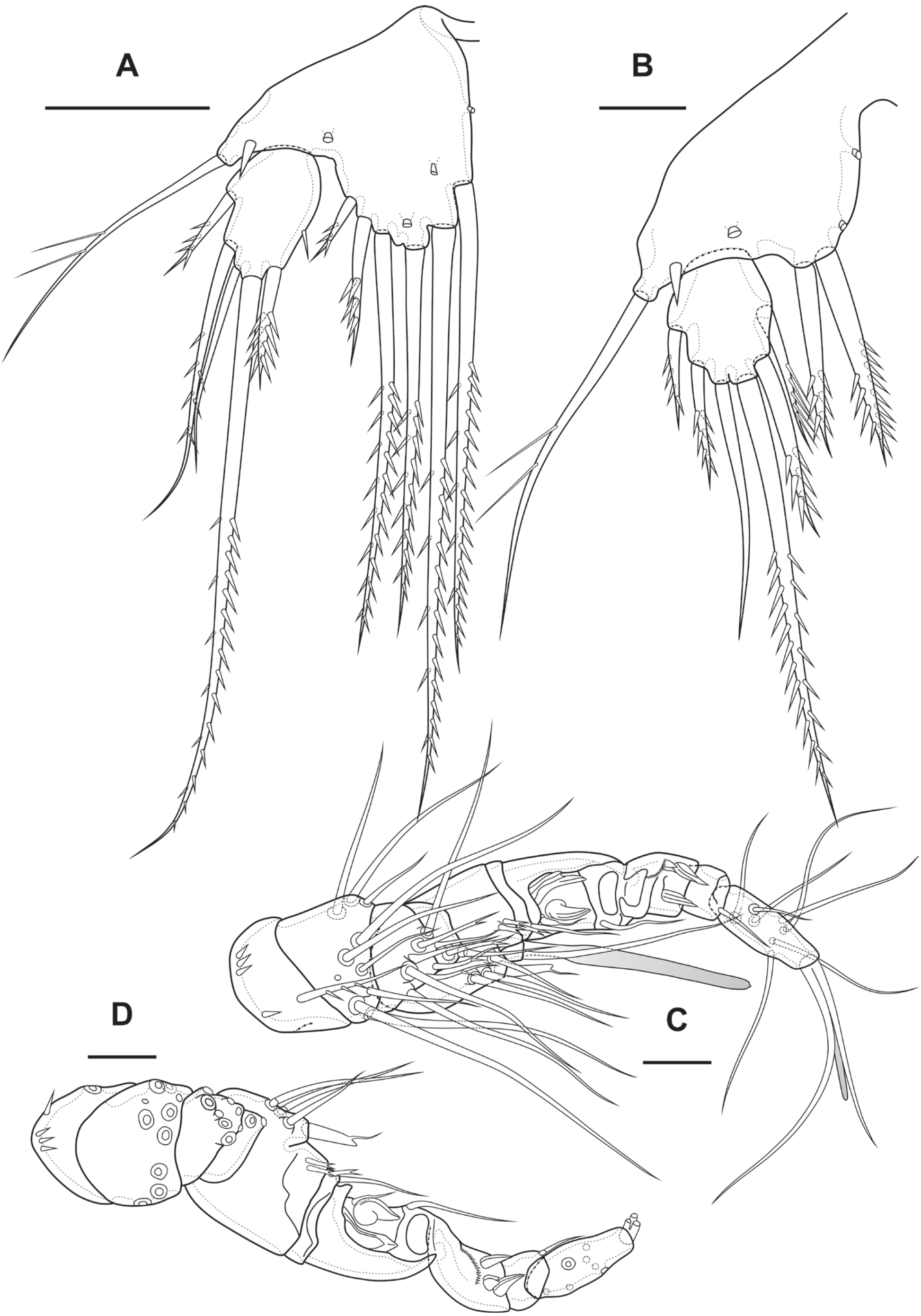

Figure 25. *Bryocamptus putoranus* sp. nov., female **A** P5, anterior; male **B** P5, anterior **C** antennule, anterior **D** antennule, dorsal. Scale bars: 25 µm (**A**); 10 µm (**B–D**).

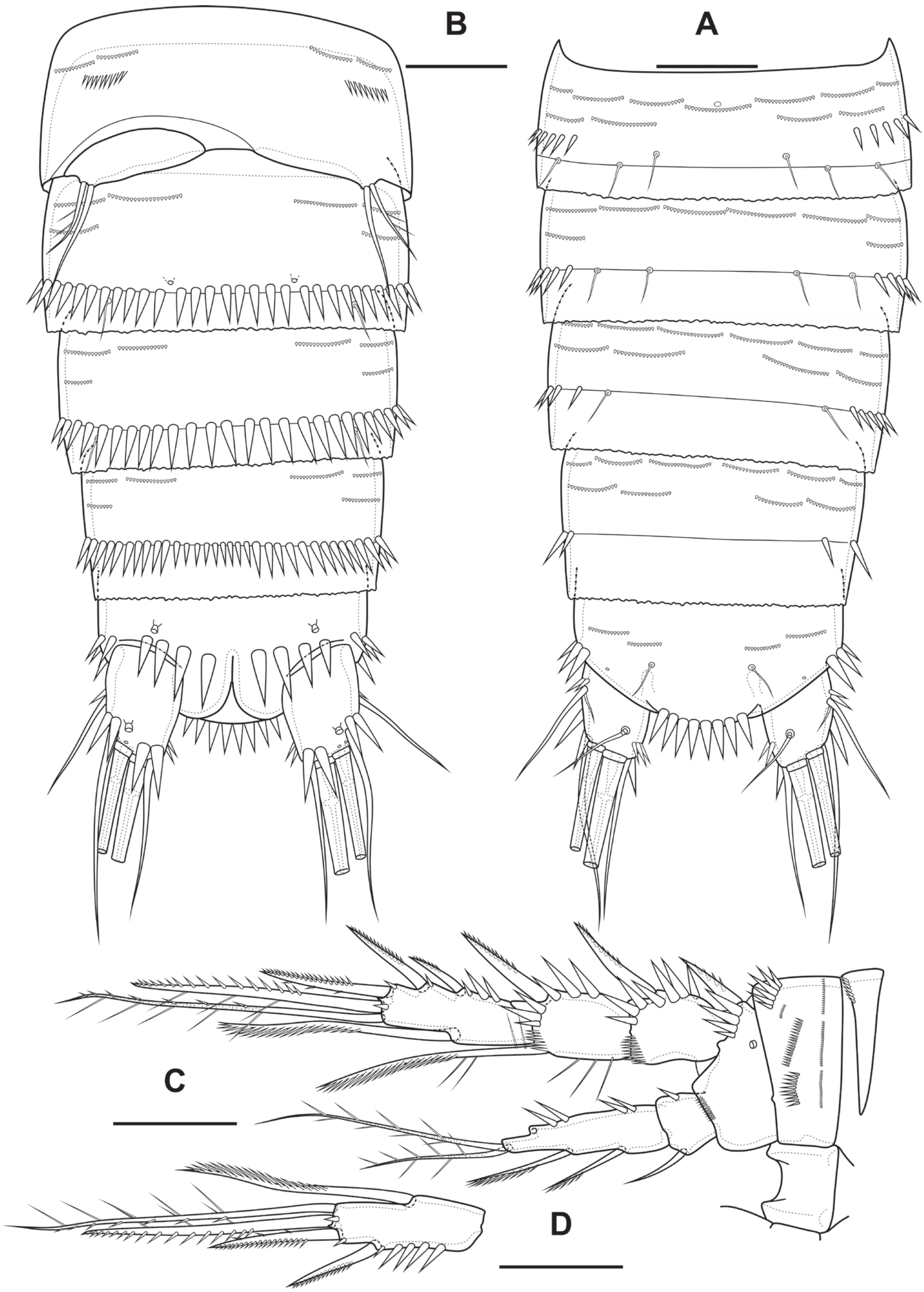

Figure 26. *Bryocamptus putoranus* sp. nov., male **A** abdomen, dorsal **B** abdomen, ventral **C** P2, anterior **D** P2 Exp3, variance Scale bars: 25 µm.

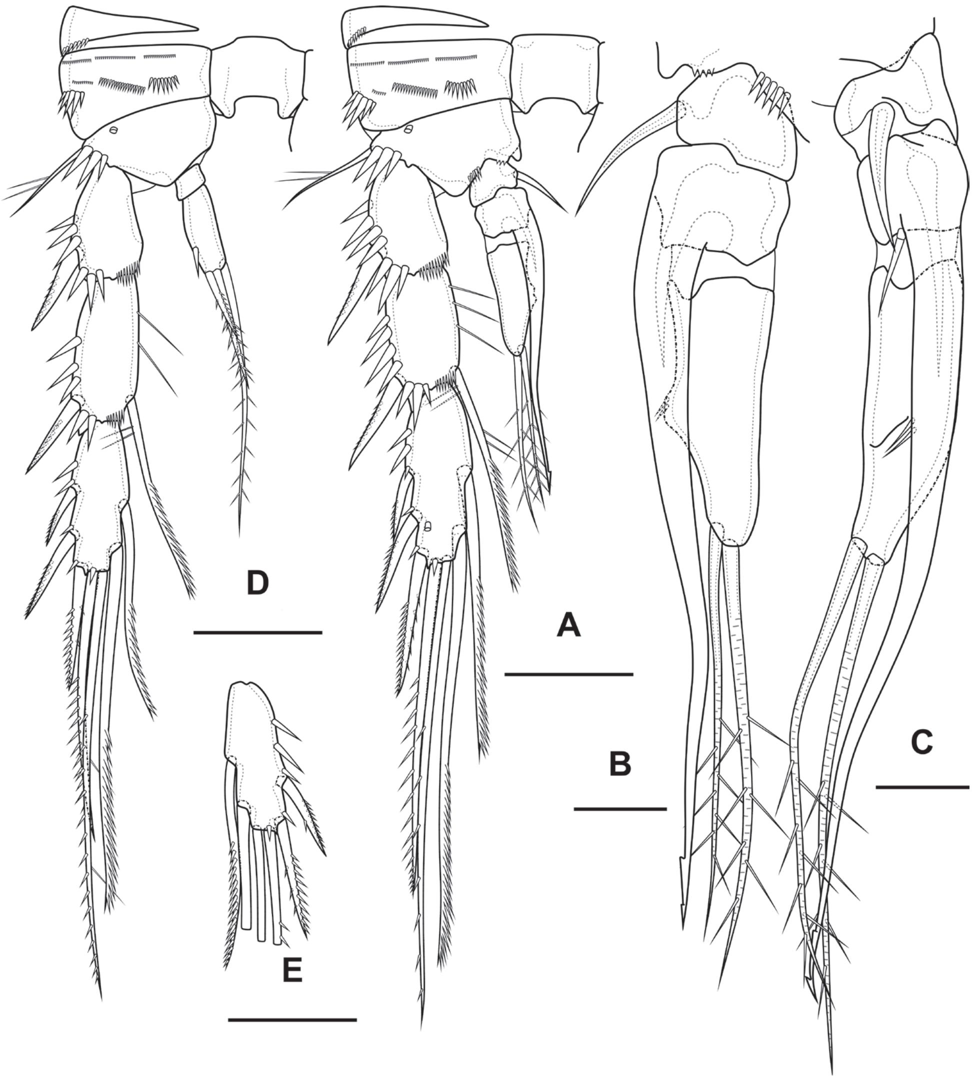

Figure 27. *Bryocamptus putoranus* sp. nov., male **A** P3, anterior **B** P3 endopod, anterior **C** P3 endopod, inner view **D** P4, anterior **E** P4 Exp3, variance. Scale bars: 25 μm (**A, D, E**); 10 μm (**B, C**).

P2 (Fig. 26C, D) as in female, except endopod. Endopod two-segmented. First segment with outer spinule and inner seta. Second segment with notch on distal outer margin, outer spinules, two apical pinnate slender setae and two inner pectinate setae.

P3 (Fig. 27A–C): praecoxa, coxa, intercoxal sclerite as in female. Basis as in female, but with inner process. Exopod as in female, but third segment with pore. Endopod three-segmented. First endopodal segment with strong seta. Second endopodal segment with posterior seta and long apophysis with double tip. Third segment with probably two small inner setae and two apical pinnate setae.

P4 (Fig. 27D, E): praecoxa, coxa, intercoxal sclerite, basis, exopod as in female. Endopod two-segmented; first segment short, unarmed; second segment with outer spinule, spinulose spine, outer apical spiniform spinulose seta and inner apical bipinnate seta.

P5 (Fig. 27B) right and left fused medially. Baseoendopod with three pairs of pores, outer spinule and outer long pinnate seta; endopodal lobe with two strong spinulose apical spines. Exopod with two outer spinulose setae, naked outer subapical seta, long apical spinulose seta, one inner spinulose seta and one inner pectinate seta with long setulles.

Variability. Individuals with two outer spines on the third exopodal segment of P2 and P4 were found (Figs 26D, 27E). One female was also found with both simple and bifid spinules on the anal operculum.

Etymology. The species is named so because it was found on the Putorana Plateau.

Remarks. The species as a whole is similar to *B. hutchinsoni*, including the structure of caudal rami; however, it differs well in two-segmented endopods P2 and P3. Another find of *B. hutchinsoni* (Carter 1944) differs markedly in the structure of its caudal rami and is not similar to *B. putoranus* sp. nov.

Discussion

Bryocamptus minutus species group

We agree with Lang (1948) that the *B. minutus* group can reliably differ from other *Bryocamptus* s. str. species precisely in the structure of the mandibular palp. In addition, it is also necessary to consider the structure of the caudal rami and the anal somite. Species of this group always have a small number (5–15) of large spinules on the anal operculum, and often these spinules are bifid, as if two spinules are fused together. Bifid spinules can also be a characteristic feature of some species (*B. minutus*, *B. aberrans* Apostolov & Pesce, 1991, *B. abramovae* sp. nov.) (Apostolov and Pesce 1991), and are also often found in species with simple spinules as a result of intraspecific variability (*B. hutchinsoni*, *B. putoranus* sp. nov., *B. vejdovskyi miniformis* Kiefer, 1934) (Kiefer 1934). The anal somite of females of this species lacks ventral spinular rows.

Table 4. Table of differences in the composition of pores and sensillae on cephalothorax and thoracic somites (designations in Appendix 1).

Somite	**Cephalothorax**																
Species	I	VI	XI	XIV	P 1	P 3	P 10	P 13	P 17	L 6	L 9	L 16	L 18	L 19	L 29	L 35	L 36
B. minutus	-	+	+	+	+	+	+	+	+	+	+	+	+	-	+	+	+
B. abramovae	+	-	-	-	-	-	-	-	-	-	-	-	-	-	-	-	-
B. putoranus	+	-	-	-	+	+	+	+	+	+	+	+	+	+	+	+	+

Somite	**PS2**			**PS3**				**PS4**				**PS5**
Species	3	8	II	2	7	10	II	4	8	9	II	1
B. minutus	+	+	+	+	+	-	+	+	+	+	+	+
B. abramovae	-	-	-	-	-	-	-	-	-	-	-	-
B. putoranus	+	+	+	+	+	+	+	+	+	+	+	+

At the same time, the use of armature and segmentation of swimming legs is rather doubtful. In species of this group, there is often variability in the number of spines on the distal exopodal segments P2–P4, especially P4 (*B. minutus*, *B. putoranus* sp. nov., *B. abramovae* sp. nov.). The three-segmented endopods of the swimming legs are also partially or completely fused in some species (*B. putoranus* sp. nov., *B. aberrans*) (Apostolov and Pesce 1991).

Based on the structure of the mandibular palp, the shape of P5, the armature of the abdominal somites, the shape of the caudal rami and the armature of the anal operculum, we believe that the *B. minutus* group should include the following species: *B. abramovae* sp. nov., *B. aberrans*, *B. hutchinsoni*, *B. minutus*, *B. pilosus* Flössner, 1989, *B. putoranus* sp. nov., *B. vejdovskyi*. Some species with incomplete descriptions can also most likely be attributed to this group: *B. intercalaris* Shen & Tai, 1973, *B. nenggaoensis* Young, 2010. In particular, descriptions and figures of mandibles are not given for these species; however, according to other characters, they could belong to the group (Shen and Tai 1973, Young 2010). For the species *B. bogoriensis* Kiefer, 1933, *B. borutzkyi* Petkovski, 1969 and *B. washingtonensis* Wilson, 1958, the descriptions are incomplete, so it is difficult to assign them to any group.

Another very similar species is *B.* (*B.*) *campaneri* (Reid, 1994) from Brazil, described only on the female. It resembles representatives of the group in the structure of caudal rami with reduced seta IV and anal somite of female without ventral group of spinules. However, this species has a two-segmented mandibular palp with a seta on the proximal segment (Reid 1994). It is likely that with the discovery and study of males of this species, it will also need to be included in the *B. minutus* species group with an expansion of the group characters.

Bryocamptus minutus species group appears to have a Holarctic distribution. In general, among freshwater Harpacticoida, this distribution is characteristic of many genera and groups of species, such as *Canthocamptus* Westwood, 1836 (Novikov and Sharafutdinova 2022), *Pesceus* Özdikmen, 2008, *Attheyella* (*Neomrazekiella*) Özdikmen & Pesce, 2006 (Borutzky 1952). The only species outside the Holarctic is *B. nenggaoensis* described from Taiwan (Young 2010). Difficulties arise when considering species with a wide range. Thus, the taxonomic status of many North American forms of species described in the Palearctic, in particular *B. vejdovskyi* and *B. minutus*, is unknown. Wilson mentions this as a problem with *B. minutus-hutchinsoni-vejdovskyi* and points out that there are probably significantly more species. (1956). A step towards solving this problem was the description of *B. pilosus*, related to *B. vejdovskyi* (Flössner 1989), but it is still far from being solved. It is likely that *B. vejdovskyi miniformis* with bifid spinules (Kiefer 1934) is also a separate Nearctic species. Some species from Europe also are described in a large number of varieties and forms (Thallwitz 1916; Lang 1957). Many taxonomists considered these forms and subspecies only intraspecific variability (Lang 1948; Borutzky 1952); however, it may well turn out that they will also be separate species.

Unfortunately, even now, descriptions of freshwater species of Copepoda are very incomplete and rather approximate. Even such significant structures as the antennules of females often are drawn with an incomplete number of setae. Antennules of males are often either not drawn or drawn very superficially. The problem of poor-quality descriptions was discussed by Hamond (1987); when compared with the best descriptions of that time, he wrote: “Subsequent students of freshwater copepods should emulate these authors as far as is technically possible. If they cannot produce drawings as good as theirs they should stay away from the formidably exacting demands of modern taxonomic practice” (Hamond 1987).

We hope that this work can be used in the future to unravel such a complex genus as *Bryocamptus*, and that the authors of original descriptions will not neglect even small, but taxonomically important, details.

Analysis of differences between studied species

The conclusions of this chapter are made on the basis of representatives of one population of each species. These characters are fairly stable within the studied populations; however, we cannot say how stable they are over a larger geographical area.

There are very large differences in the ornamentation of the limbs, which is undoubtedly homologous and can be used in taxonomy. However, this should be done with caution, until it is fully understood to what extent these characters are subject to intraspecific variability. Although for other groups of copepods, some elements of micro-ornament have been shown to be very effective in distinguishing closely related species. For example, in the taxonomy of Cyclopidae, ornamentation of antenna allobasis (Fiers and Van de Velde 1984), maxilla basis (Hołyńska et al. 2021), coxa of P4 (Van de Velde 1984) are used widely. Another difficult feature is that during the preparation of specimens or during the life of these crustaceans, some of the spines, especially long ones, can break off, and some wear out, so it is necessary to study at least a few individuals of each species.

There can be two mechanisms for the reduction of groups of spinules. The first is a decrease in the number of spinules until their complete disappearance. This is typical condition for one of the groups of spinules on the first segment of the female antennule, in the studied *Bryocamptus* it is one-two spinules, and for example in *Maraenobiotus* they are already completely absent (Novikov and Sharafutdinova 2020). The second mechanism is a strong decrease in these spines, also up to complete disappearance. Here, the best example is the ornamentation of the coxae of P2–P4. Several rows of small spinules are clearly visible in primitive Canthocamptidae, as *Canthocamptus* or *Attheyella* (Novikov and Sharafutdinova 2022), may be almost invisible in *B. minutus* group, and completely absent, for example, on the coxa of P4 of *B.* (*Rheocamptus*) *pygmaeus* (Sars, 1863) (Novikov and Fefilova 2021).

The ornamentation of the cephalothorax and thoracic somites showed significant differences between the three species studied, shown in Table 4.

The demonstrated interspecific variability opens up great scope for the separation of complex groups of species. However, the high variability in the structure of the integument complex (composition of sensillae and pores on somites) between closely related species impairs its applicability in phylogenetic reconstructions. *Bryocamptus abramovae* sp. nov. has a greatly reduced number of these elements, despite the absence of other major differences from the other two species. *Bryocamptus putoranus* sp. nov. and *B. minutus* have an almost identical composition of sensillae and pores on somites. It is also possible for some taxa of copepods that pores (but not sensillae) on somites may appear *de novo* within some lineages, for example, in the family Artotrogidae Brady, 1880 (Siphonostomatoida), species of which have a huge number of large pores on somites (McKinnon 1988).

The rostrum also has significant interspecific variability. The studied species differ in the presence/absence of the pore, its position, and the shape of the distal margin.

Antennules of females have predominantly morphometric differences in the shape of the segments and the length of the setae. Also, one of the setae on the second segment in *B. abramovae* sp. nov. and *B. putoranus* sp. nov. is armed with spinules, in contrast to *B. minutus*.

The antenna also differs significantly in the shape of the segments. The most variable part is the allobasis. Depending on the species, the presence/absence of groups of spinules at the bases of the setae, as well as the armature of the proximal seta of the allobasis, varies. The labrum is almost the same in the studied species, except for a semicircular row of spines on the posterior surface of *B. minutus*.

Mandibles have long been considered one of the most important elements in harpacticoid taxonomy (Lang 1948). In the studied species, differences were found in the number of apical setae on the mandibular palp and in the presence of a group of spinules on the palp, which are absent only in *B. putoranus* sp. nov. Interestingly enough, the studied species have an absolutely identical structure of gnathobases down to the number of small spinules of dental batteries, which probably indicates an identical type of diet. Here it is important to take into account that the gnatobases are quite strongly obliterated over time, which was found in some individuals of *B. minutus*. Therefore, to study them, relatively recently molted individuals are needed. Paragnaths in the studied species differ in shape and number of outer and anterior rows of spinules.

Three groups of spinules are subject to interspecific variability on maxillules, one of which is on the coxal endite, and the other two are on the basis. As with mandibles, some setae of the arthrite are also subject to wear. Therefore, characteristic strong setae with a pectinate end cannot be found in a number of individuals of the same species (Fig. 3B). It should also be noted that in our previous works we have always missed one of the setae of arthrite, which bears very long spinules. Re-examination of the material showed that this seta is present in all species previously described by us: *Maraenobiotus supermario* Novikov & Sharafutdinova, 2020, *Mesopsyllus glacialis* Novikov & Sharafutdinova, 2021, *Heteropsyllus spiridonovi* Novikov & Sharafutdinova, 2021 and *Heteropsyllus spongiophilus* Novikov & Sharafutdinova, 2021.

Maxilla and maxilliped turned out to be identical in ornamentation, differing only in different shape of segments, length of setae, and, to some extent, armament of setae. The processes between the maxillipeds and P1 differ in shape, height, and number of spinules. Thus, *B. minutus* has the largest number of spines that extend onto the anterior side of the process. *Bryocamptus putoranus* is notable for its unusually high process.

P1 is quite different in the studied species. In addition to differences in the shape and length of the segments, the species also differ in the presence/absence of two inner and one frontal groups of spinules on the basis. The inner surface of the exopod and endopod is also armed to varying degrees in different species.

P2–P4 of females, in addition to segmentation, the shape of the segments, and the number of outer spines on the third segment of the P4 exopod, also differ in microcharacters. Intercoxal sclerite of P2 of *B. minutus* has two large spinules. Coxae P2–P4 of *B. abramovae* sp. nov. and *B. putoranus* sp. nov. have an additional group of large spinules. The P2–P3 basis of *B. abramovae* sp. nov. has an inner group of long spinules and a relatively large inner process. The basis of P4 of *B. putoranus* sp. nov. lacks a row of spinules near the base of the endopod. The outer spines of P2–P3 Exp1-Exp2 of *B. minutus* are naked, unlike the other two species. P2–P4 Exp3 of *B. minutus* have a pore. P2 and P4 of males have approximately the same differences as in females. Only the P4 Enp2 of *B. minutus* is distinguished by the presence of four setae, instead of three in *B. abramovae* sp. nov. and *B. putoranus* sp. nov.

The structure of the P3 endopod, on closer examination, can be one of the most important taxonomic characters distinguishing closely related species. In particular, for the genus *Lourinia* Wilson, 1924, closely related to Canthocamptidae, a very strong interspecific variability in the P3 apophysis was described recently; it can vary in length and curvature, as well as in the shape of the tip (Karaytuğ et al. 2021). The three studied species also have significant differences in the structure of the endopod. They differ considerably in elongation, *B. putoranus* sp. nov. and *B. abramovae* sp. nov. have relatively shortened segments. *Bryocamptus putoranus* sp. nov., in addition to this, has a large outgrowth on the third segment, while in the other two species the inner edge of the segment is even. *Bryocamptus minutus* has a pore on the third segment. The shape and length of the apophysis also varies considerably. The absolute length of the apophysis in lateral view and the ratio to the length of the third endopodal segment, respectively: *B. minutus* 77 μm and 2.02; *B. abramovae* sp. nov. 56 μm and 1.80; *B. putoranus* sp. nov. 70 μm and 2.59.

P5 of females of the studied species also differ significantly. First of all, the shape of the endopodal lobe and exopod and the length of the setae. *Bryocamptus abramovae* sp. nov. lacks the inner seta of the endopodal lobe. The exopod of *B. minutus* bears several spinules on the anterior surface. P5 of males are very similar and differ in the shape of the exopods and the armature of the exopodal setae.

P6 of females almost do not differ. However, the P6 of males of *B. putoranus* sp. nov. bears only two setae instead of three. The genital field of females of different species differs primarily in proportions. Abdominal somites of *B. abramovae* sp. nov. has a reduced number of sensillae, as is the case with thoracic somites. The armature of the anal operculum also varies: in *B. minutus* with long bifid spinules, in *B. abramovae* sp. nov. with short bifid spinules, and in *B. putoranus* sp. nov. with long simple spinules.

Relationships between caudal rami of females and antennules of males

One of the most interesting details found is the very close relationship between the shape of the caudal rami and the shape of the male antennules. During mating, the antennules of males of some harpacticoids, in particular most canthocamptids, are used to grasp the caudal setae of females (Wolf 1905). To this end, many segments of the male antennule are strongly modified. A joint is formed between segments 7 and 8, and the segments themselves in Canthocamptidae bear modified laminar setae, probably necessary to increase the efficiency of capturing the female. The large segment 5 probably serves more as a location for the large muscles brought directly to the joint. The least modified antennules among Canthocamptidae can be found in the genus *Canthocamptus*, where all laminar setae have a standard appearance, and the shape of the caudal rami of females does not undergo any modification (Novikov and Sharafutdinova 2022).

Of the studied species, females of *B. abramovae* sp. nov. have the least modified caudal rami. This finds a close relationship with male antennules, which have simple segments 7 and 8, as well as unmodified laminar setae on these segments. Females of B. *putoranus* sp. nov. have caudal setae displaced to the ventral side. This is reflected in a slightly altered shape of segments 7 and 8 of the male antennule, as well as in a noticeable increase in laminar setae on segment 7. *Bryocamptus minutus* has the most interesting structure of these parts. Females have strongly displaced apical setae, while male on segment 8 has two strongly enlarged laminar setae, one of which forms a kind of elongated plate, which is probably necessary for close grasping of displaced apical setae from below.

The similar shape of the caudal rami of *B. minutus* and *B. putoranus* sp. nov. could suggest that this character is a synapomorphy of these species. However, the mechanisms that allow males to copulate more effectively with a female are completely different. In *B. minutus*, development reaches laminar setae on segment 8, while in *B. putoranus* sp. nov., on segment 7. Probably, the mating efficiency strongly depends on the coevolution of these two parts; different mechanisms for increasing this efficiency most likely indicate the convergent acquisition of displaced apical caudal setae. This also emphasizes the importance of the detailed illustration of male antennules in species descriptions.

However, the question arises, why should females acquire caudal branches that are difficult to grasp? This is an example of an evolutionary sexual arms race between the sexes of the same species, also noted for members of *Maraenobiotus* (Brancelj and Karanovic 2015). The reasons for such evolutionary mechanisms are not yet fully understood. A fairly well-studied example is the sexual arms race in water striders (Arnqvist and Rowe 2002a; Perry et al. 2017). Male water striders can keep females for quite a long time, impairing their survival (impairs the efficiency of foraging and defense against predators) (Rowe et al. 1994). For prolonged mating, males have modified genitals and abdomen (Arnqvist and Rowe 2002b).

As with water striders, it is probably beneficial for the *Bryocamptus* male to keep the female as long as possible to protect the female from fertilization by other males. At the same time, this is not beneficial for the female, since it most likely has a negative effect on protection from predators and the efficiency of foraging. Accordingly, females acquire such caudal rami that males cannot hold them for a long time. And males acquire modified antennules in parallel.

The incompatible shape of the caudal branches of the females and the antennules of the males serve as a mechanism for reproductive isolation (premating isolation). This is one of the microevolutionary processes leading to rapid allopatric and sympatric speciation, for example, in the extremely diverse Baikalian *Moraria* (*Baikalomoraria*) Borutzky, 1931 (Borutzky 1952). Therefore, the different shape of the caudal rami and their setae within the same species most likely indicates the presence of already divergent species, which has already been described for *Maraenobiotus* (Brancelj and Karanovic 2015). But it is probably much more common, for example, forms with different caudal rami are described in *Attheyella* (*Attheyella*) *tahoensis* Bang, Baguley & Moon, 2015 (Bang et al. 2015), and in different species of *Kikuchicamptus* Novikov & Sharafutdinova, 2022 (Chang and Ishida 2001).

Acknowledgements

We would like to thank Ekaterina Abramova (Lena Delta Reserve) and Waldemar Schneider for their assistance in collecting samples in the Lena River Delta. We also thank the management and staff of AWI Potsdam, IPGG SB RAS and Lena Delta Reserve for the opportunity to take part in expeditions to the Lena River Delta. We are grateful to the staff of the Putoransky Scientific Reserve and united directorate of Taymyr Reserves, especially to the deputy for scientific work Mikhail Bondar for help in organizing expeditionary works. We thank Elena Fefilova for providing *B. minutus*. Also we thank our colleagues from Wrangel Island Nature Reserve and Anna A. Novichkova for providing material from the island, collected in the framework of the research collaboration project between the Reserve and Biological faculty of Lomonosov Moscow State University. Thanks to Russell Shiel for editing English. The work was supported by the Russian Foundation for Basic Research (project no. 20-04-00145).

References

Apostolov AM, Pesce GL (1991) Copepodes Harpacticoides cavernicoles de Bulgarie. 4. *Bryocamptus* (*Bryocamptus*) *aberrans* n. sp., un nouveaux Harpacticoide stygobie du nord-ouest de Bulgarie (Crustacea: Copepoda). Rivista di Idrobiologia 30: 297–301.

Arnqvist G, Rowe L (2002a) Antagonistic coevolution between the sexes in a group of insects. Nature 415(6873): 787–789. https://doi.org/10.1038/415787a

Arnqvist G, Rowe L (2002b) Correlated evolution of male and female morphologies in water striders. Evolution 56: 936–947. https://doi.org/10.1111/j.0014-3820.2002.tb01406.x

Bang HW, Baguley JG, Moon H (2015) First record of harpacticoid copepods from Lake Tahoe, United States: Two new species of *Attheyella* (Harpacticoida, Canthocamptidae). ZooKeys 479: 1–24. https://doi.org/10.3897/zookeys.479.8673

Borutzky EV (1952) Harpacticoida presnykh vod [Harpacticoida of fresh waters]. Fauna SSSR, Rakoobraznye [Fauna of the USSR, Crustacea] 3: 1–424. https://doi.org/10.5962/bhl.title.46313

Brancelj A, Karanovic T (2015) A new subterranean *Maraenobiotus* (Crustacea: Copepoda) from Slovenia challenges the concept of polymorphic and widely distributed harpacticoids. Journal of Natural History 49(45–48): 2905–2928. https://doi.org/10.1080/00222933.2015.1022620

Caramujo M-J, Boavida M-J (2009) The practical identification of harpacticoids (Copepoda, Harpacticoida) in inland waters of Central Portugal for applied studies. Crustaceana 82(4): 385–409. https://doi.org/10.1163/156854009X404761

Carter ME (1944) Harpacticoid copepods of the region of Mountain Lake, Virginia (with description of *Moraria virginiana* n. sp.). Journal of the Elisha Mitchell Scientific Society 60: 158–166.

Chang C-Y, Ishida T (2001) Two New Species of *Canthocamptus mirabilis* Group (Copepoda, Harpacticoida, Canthocamptidae) from South Korea. Proceedings of the Biological Society of Washington 114: 114–2.

Dussart B, Defaye D (1990) Répertoire mondial des Crustacés Copépodes des eaux intérieures: III. Harpacticoïdes. E. J. Brill, Leiden, 384 pp.

Fefilova E (2010) On the Estonian fauna of Harpacticoida (Crustacea, Copepoda). Estonian Journal of Ecology 59(4): 281. https://doi.org/10.3176/eco.2010.4.03

Ferrari FD, Ivanenko VN (2008) The identity of protopodal segments and the ramus of maxilla 2 of copepods (Copepoda). Crustaceana 81(7): 823–835. https://doi.org/10.1163/156854008784771702

Fiers F, Van de Velde I (1984) Morphology of the antenna and its importance in the systematics of the Cyclopidae. Crustaceana (Supplement 7): 182–199.

Flössner D (1989) *Bryocamptus pilosus* n. sp. (Copepoda: Harpacticoida) from North America. Hydrobiologia 179: 129–134. https://doi.org/10.1007/BF00007600

Hamond R (1987) Non-marine harpacticoid copepods of Australia. I. Canthocampptidae of the genus *Canthocamptus* Westwood s. lat. and *Fibulacamptus*, gen. nov., and including the description of a related new species of *Canthocamptus* from New Caledonia. Invertebrate Systematics 1(8): 1023–1247. https://doi.org/10.1071/IT9871023

Hołyńska M, Dahms H-U (2004) New diagnostic microcharacters of the cephalothoracic appendages in *Cyclops* OF Müller, 1776 (Crustacea, Copepoda, Cyclopoida). Zoosystema 26: 175–198.

Hołyńska M, Sługocki Ł, Ghaouaci S, Amarouayache M (2021) Taxonomic status of Macaronesian *Eucyclops agiloides azorensis* (Arthropoda: Crustacea: Copepoda) revisited – morphology suggests a Palearctic origin. European Journal of Taxonomy 750: 1–28. https://doi.org/10.5852/ejt.2021.750.1357

Huys R, Boxshall GA (1991) Copepod evolution. The Ray Society, London, 468 pp.
ICZN [International code of zoological nomenclature] (1999) International code of zoological nomenclature. International Trust for Zoological Nomenclature.
Karanovic T, Krajicek M (2012) When anthropogenic translocation meets cryptic speciation globalized bouillon originates; molecular variability of the cosmopolitan freshwater cyclopoid *Macrocyclops albidus* (Crustacea: Copepoda). Annales de Limnologie-International Journal of Limnology 48(1): 63–80. https://doi.org/10.1051/limn/2011061
Karanovic T, Lee W (2012) A new species of *Parastenocaris* from Korea, with a redescription of the closely related *P. biwae* from Japan (Copepoda: Harpacticoida: Parastenocarididae). Journal of Species Research 1(1): 4–34. https://doi.org/10.12651/JSR.2012.1.1.004
Karaytuğ S, Sak S, Alper A, Sönmez S (2021) Resolving the *Lourinia armata* (Claus, 1866) complex with remarks on the monophyletic status of Louriniidae, Monard 1927 (Copepoda: Harpacticoida). Zootaxa 5051(1): 346–386. https://doi.org/10.11646/zootaxa.5051.1.15
Kiefer F (1934) Neue Ruderfusskrebse aus Nordamerika. Zoologischer Anzeiger 108: 206–207.
Kochanova E, Nair A, Sukhikh N, Väinölä R, Husby A (2021) Patterns of cryptic diversity and phylogeography in four freshwater copepod crustaceans in European lakes. Diversity 13(9): 448. https://doi.org/10.3390/d13090448
Lajus D, Sukhikh N, Alekseev V (2015) Cryptic or pseudocryptic: Can morphological methods inform copepod taxonomy? An analysis of publications and a case study of the *Eurytemora affinis* species complex. Ecology and Evolution 5(12): 2374–2385. https://doi.org/10.1002/ece3.1521
Lang K (1934) Marine Harpacticiden von der Campbell-Insel und einigen anderen südlichen Inseln. Acta Universitatis Lundensis. New Series 2: 1–56.
Lang K (1948) Monographie der Harpacticiden I + II. Nordiska Bokhandeln, Lund, 1683 pp.
Lang K (1957) Harpacticoiden aus der asiatischen Türkei. Arkiv för Zoologi 11: 45–51.
McKinnon AD (1988) Five artotrogid copepods (Siphonostomatoida) from southern Australia. Invertebrate Systematics 2(8): 973–993. https://doi.org/10.1071/IT9880973
Mielke W (1984) Some remarks on the mandible of the Harpacticoida (Copepoda). Crustaceana 46(3): 257–260. https://doi.org/10.1163/156854084X00162
Moura G, Pottek M (1998) *Selenopsyllus*, a new genus of Cylindropsyllinae (Copepoda, Harpacticoida) from Atlantic and Antarctic deep waters. Senckenbergiana Maritima 28(4–6): 185–209. https://doi.org/10.1007/BF03043149
Novikov AA, Fefilova EB (2021) Morphology of the cephalothorax integument of *Bryocamptus pygmaeus* (Copepoda: Harpacticoida: Canthocamptidae), based on a new research method. Zoosystematica Rossica 30(2): 320–330. https://doi.org/10.31610/zsr/2021.30.2.320
Novikov A, Sharafutdinova D (2020) A new species of *Maraenobiotus* (Copepoda, Harpacticoida) from Lena River Delta (North-Eastern Siberia). Zootaxa 4852(2). https://doi.org/10.11646/zootaxa.4852.2.3
Novikov A, Sharafutdinova DN (2022) Revision of the genus *Canthocamptus* (Copepoda: Harpacticoida) with a description of a new species from the Lena River Delta (North-eastern Siberia). European Journal of Taxonomy 826: 33–63. https://doi.org/10.5852/ejt.2022.826.1833

Novikov AA, Abramova EN, Sabirov RM (2021) Fauna of freshwater Harpacticoida (Copepoda) in the Lena River Delta. Zoologichesky zhurnal 100: 264–274. https://doi.org/10.31857/S0044513421010049

Perry JC, Garroway CJ, Rowe L (2017) The role of ecology, neutral processes and antagonistic coevolution in an apparent sexual arms race. Ecology Letters 20(9): 1107–1117. https://doi.org/10.1111/ele.12806

Reed EB (1990) *Tachidius incisipes* Klie and other harpacticoids from northwestern Canada (Crustacea: Copepoda). Proceedings of the Biological Society of Washington 103: 341–349.

Reid JW (1994) Two new species of copepods (Copepoda: Harpacticoida: Canthocamptidae) of particular biogeographical interest from central Brazil. Nauplius 1: 13–38.

Rowe L, Arnqvist G, Sih A, Krupa JJ (1994) Sexual conflict and the evolutionary ecology of mating patterns: Water striders as a model system. Trends in Ecology & Evolution 9: 289–293. https://doi.org/10.1016/0169-5347(94)90032-9

Shen CJ, Tai AY (1973) Preliminary analysis of the characteristics of the harpacticoid copepod fauna of China and description of some new species. Acta Zoologica Sinica 19: 365–384.

Stoch F, Bruno M-C (2011) *Acanthocyclops magistridussarti* sp. nov., from ground waters of peninsular Italy, with comments on the intraspecific variability of the antennary basis ornamentation (Copepoda, Cyclopoida, Cyclopidae). In: Studies on Freshwater Copepoda: a Volume in Honour of Bernard Dussart. Brill, 489–506. https://doi.org/10.1163/9789004188280_022

Thallwitz J (1916) Über Dimorphismus des Männchen bei einem Süßwasserharpacticiden. Zoologischer Anzeiger 46: 238.

Van de Velde I (1984) Revision of the African species of the genus *Mesocyclops* Sars, 1914 (Copepoda: Cyclopidae). Hydrobiologia 109(1): 3–66. https://doi.org/10.1007/BF00006297

Walter TC, Boxshall GA (2021) The World of Copepods - *Bryocamptus* (*Bryocamptus*) *minutus simplicidentata* (Willey, 1934). https://www.marinespecies.org/copepoda/aphia.php?p=taxdetails&id=606654 [March 21, 2022]

Wilson MS (1956) North American harpacticoid Copepods: 1. Comments on the known freshwater species of the Canthocamptidae. 2. *Cantohocamptus oregonensis*, n. sp. from Oregon and California. Transactions of the American Microscopical Society 75(3): 290–307. https://doi.org/10.2307/3223958

Wolf E (1905) Die Fortpflanzungsverhältnisse unserer einheimischen Copepoden. G. Fischer.

Young S-S (2010) Four new species of freshwater harpacticoid copepods (Canthocamptidae: Copepoda) from Mountain lakes of Taiwan. Taiwan journal of Biodiversity 12: 327–340.

Appendix 1

Numbering of integumental sensillae and pores of cephalothorax and thoracic somites of the studied species.

The numbering of pores and sensillae on somites is original and based on the structure of the integument of several freshwater species of Canthocamptidae. Roman numerals (for pores) or Arabic numerals (for sensillae) are used for numbering integumental elements. The designations for cephalothorax sensillae C, P, and L are used to simplify homology. Group P is the sensillae adjacent to the edge of the cephalothorax. Group C is the sensillae, which are located near the medial axis and the dorsal window. The notation L is used for all other sensillae.

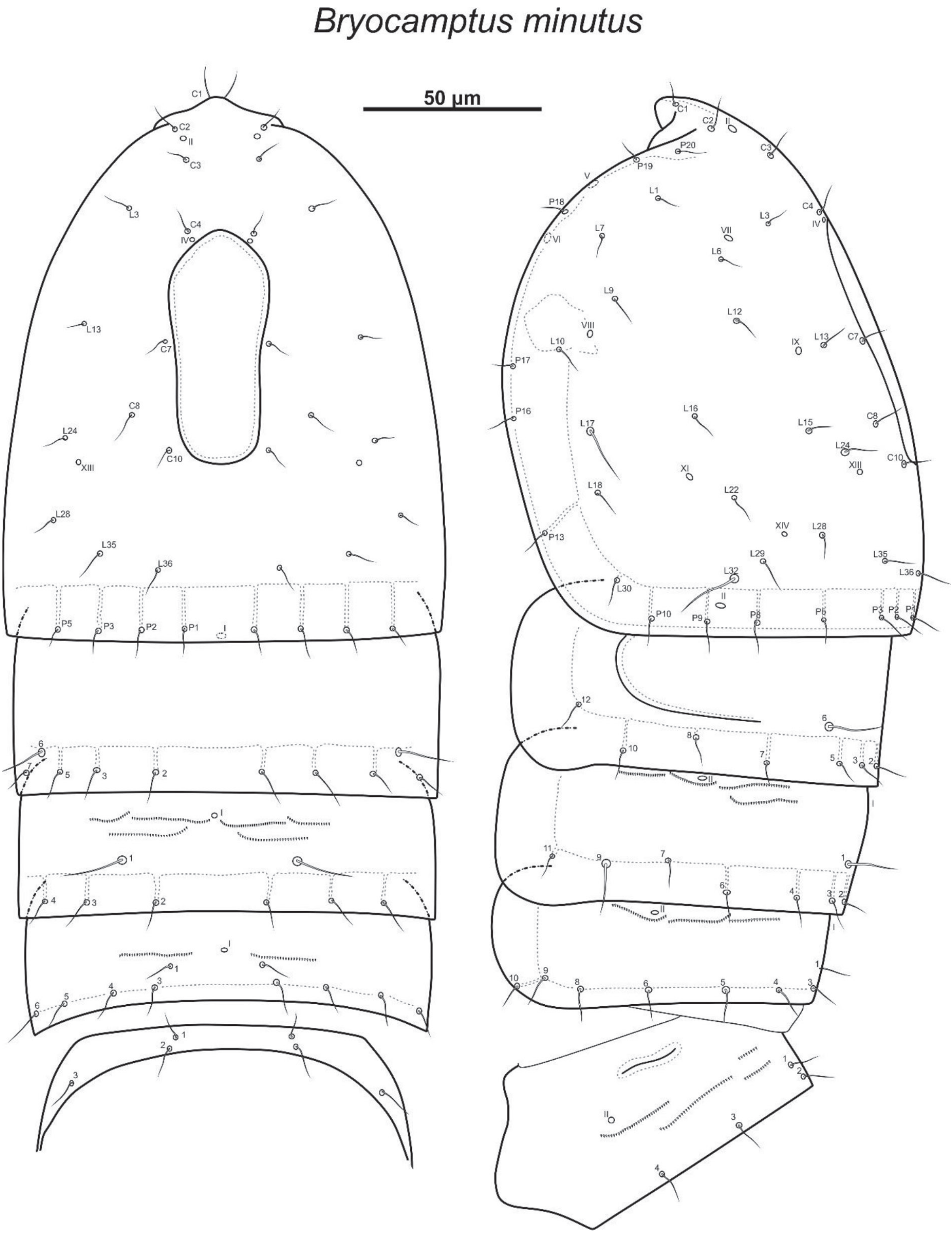

Figure A1. *Bryocamptus minutus.*

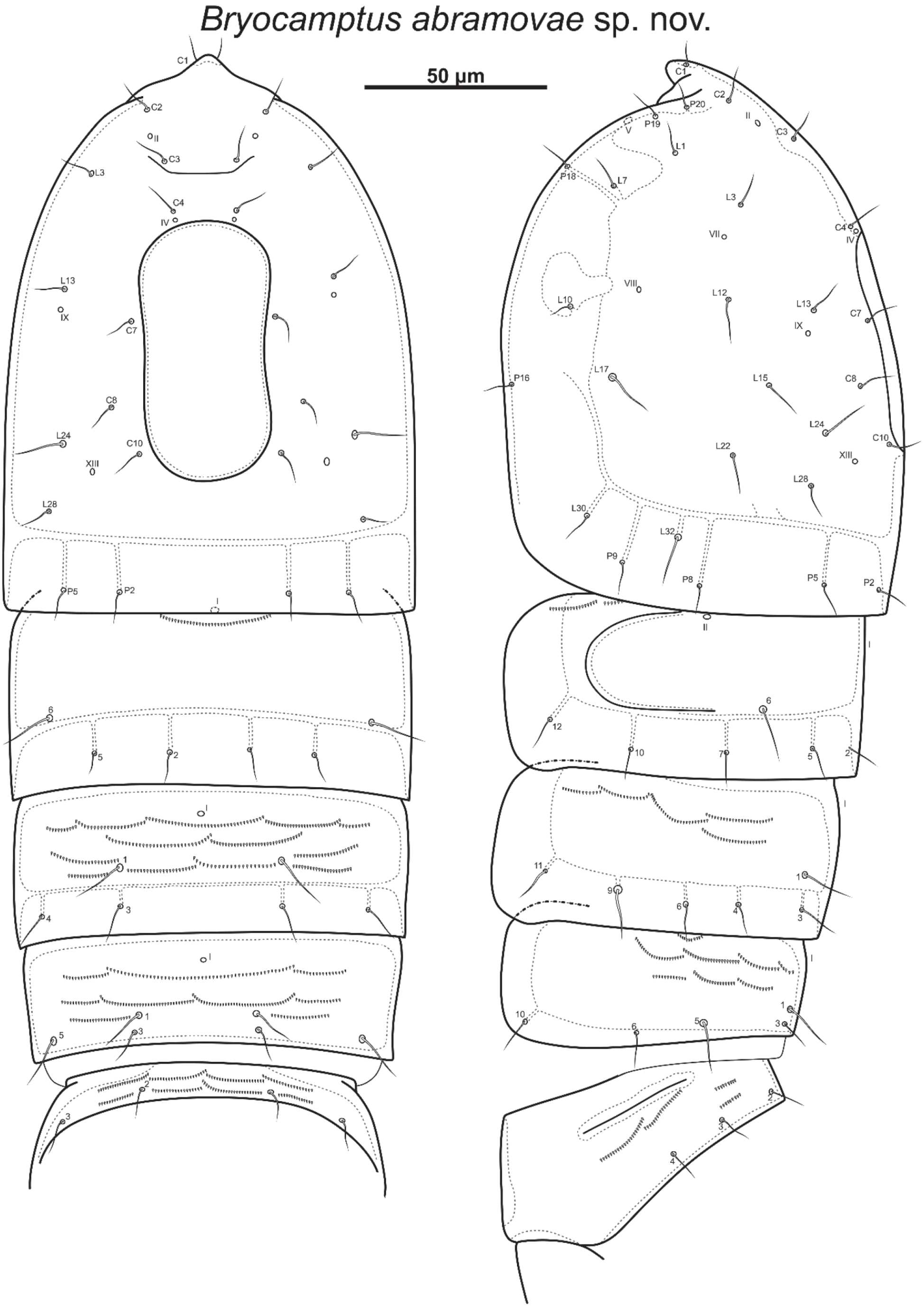

Figure A2. *Bryocamptus abramovae* sp. nov.

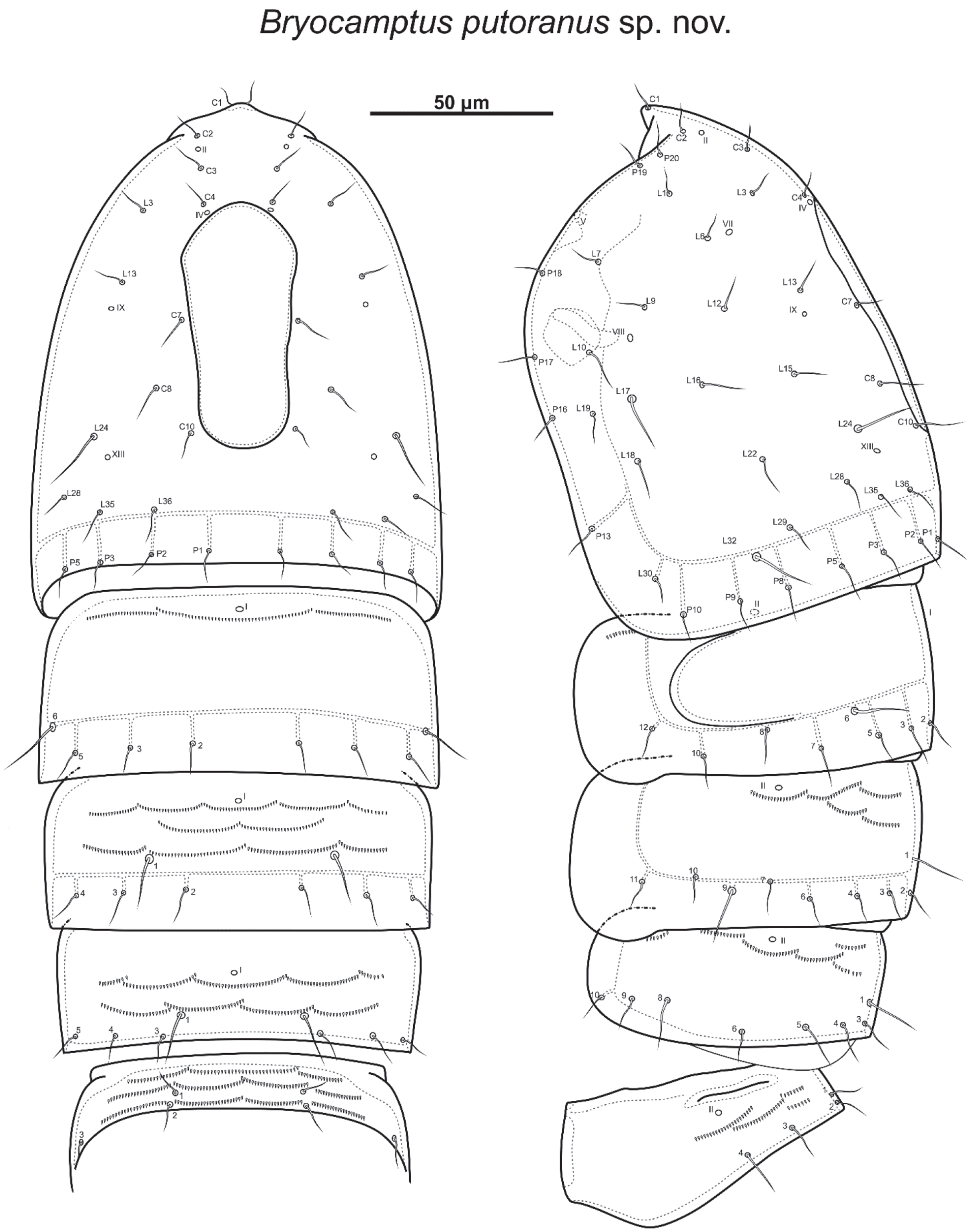

Figure A3. *Bryocamptus putoranus* sp. nov.

ZooKeys 1138: 143–160 (2023)
doi: 10.3897/zookeys.1138.96424
https://zookeys.pensoft.net

RESEARCH ARTICLE

A peer-reviewed open-access journal
ZooKeys
Launched to accelerate biodiversity research

Two new species of the genus *Symphylella* (Symphyla, Scolopendrellidae) from China and the significance of the frons chaetotaxy

Ya-Li Jin[1], Yun Bu[1]

1 *Natural History Research Center, Shanghai Natural History Museum, Shanghai Science & Technology Museum, Shanghai, 200041, China*

Corresponding author: Yun Bu (buy@sstm.org.cn)

Academic editor: Bruce A. Snyder | Received 17 October 2022 | Accepted 12 December 2022 | Published 5 January 2023

https://zoobank.org/B3E1F9F6-368F-476F-9A03-E2C35736BBFD

Citation: Jin Y-L, Bu Y (2023) Two new species of the genus *Symphylella* (Symphyla, Scolopendrellidae) from China and the significance of the frons chaetotaxy. ZooKeys 1138: 143–160. https://doi.org/10.3897/zookeys.1138.96424

Abstract
Symphylella macrochaeta **sp. nov.** and *Symphylella longispina* **sp. nov.** from China are described and illustrated. *Symphylella macrochaeta* **sp. nov.** is characterized by 10 extremely long macrosetae arranged as 4/4/2 on the frons, tergites with broad triangular processes, and 4+4 setae on the first tergite. *Symphylella longispina* **sp. nov.** is characterized by a thick and prominent labrum, distinctly long proximal spines on the mandible, eight macrosetae arranged as 4/2/2 on frons, 3+3 setae on first tergite, and narrow triangular processes on the tergites. Detailed comparisons of the new species with similar species are presented. In addition, the frons chaetotaxy of *Symphylella* is illustrated and discussed for the first time and proposed as a significant diagnostic character for the taxonomic study of the genus.

Keywords
Chaetotaxy, frons, mandible, Myriapoda, taxonomy

Introduction

Symphylans are minute soil arthropods present in various habitats, and some species are important crop pests (Chau 2015; Jin and Bu 2022). However, the diversity of symphylans in China is poorly known, with only eight species recorded until now (Bu and Jin 2018; Jin and Bu 2018, 2019, 2020; Jin et al. 2019). *Symphylella* Silvestri, 1902 is a diverse group of symphylans with 51 species described worldwide (Bu and Jin 2018; Jin et al. 2019; Jin and Bu 2020), but only four have been recorded in China: *S. macropora* Jin & Bu, 2019 and *S. zhongi* Jin & Bu, 2019 from Tibet (Jin et al. 2019), and *S. communa* Jin & Bu, 2020 and *S. minuta* Jin & Bu, 2020 from East China (Jin and Bu 2020). During the last five years, the symphylan fauna from Xinjiang, Zhejiang and Shanghai was investigated and two new species of *Symphylella* were identified. They are described in the present paper. The frons chaetotaxy of the six Chinese species of *Symphylella* is compared in detail.

Materials and methods

Specimens were obtained by extraction of soil and litter samples from broad-leaf and bamboo forests using Berlese-Tullgren funnels. Specimens were preserved in 80% ethanol. They were mounted on slides using Hoyer's solution and dried in an oven at 50 °C. Observations were performed under a phase contrast microscope (Leica DM 2500). Photographs were taken with a digital camera (Leica DMC 4500) mounted on the microscope. Line drawings were made using a drawing tube. All specimens are deposited in the collections of Shanghai Natural History Museum (**SNHM**), Shanghai, China.

Results

Taxonomy

Family Scolopendrellidae Bagnall, 1913

Genus *Symphylella* Silvestri, 1902

Type species. *Symphylella isabellae* (Grassi, 1886), described from Italy.

***Symphylella macrochaeta* Jin & Bu, sp. nov.**
https://zoobank.org/EDC04E98-38F3-43BD-A6F0-927F77D4A12C
Figs 1–3, Tables 1–3

Diagnosis. *Symphylella macrochaeta* sp. nov. is characterized by 10 extremely long macrosetae arranged as 4/4/2 on the frons, 4+4 setae on the first tergite and broad triangular processes on tergites.

Material examined. ***Holotype*:** female (slide no. ZJ-ZS-SY2020029) (SNHM), China, Zhejiang Province, Zhoushan City, Changgang Mountain Forest Park, extracted from soil samples of broad-leaf forest, alt. 250 m, 30°2'N, 121°7'E, 17-XI-2020, coll. Y. L. Jin et al.

***Paratypes*:** 10 females (slides no. ZJ-ZS-SY2020006, ZJ-ZS-SY2020008, ZJ-ZS-SY2020014–ZJ-ZS-SY2020016, ZJ-ZS-SY2020024–ZJ-ZS-SY2020028) (SNHM), same data as holotype. 2 females (slides no. SH-JZGY-SY2017032, SH-JZGY-

SY2017034), China, Shanghai, Jiuzi Park, extracted from soil and litter samples of bamboo forest, alt. 14 m, 31°15'N, 121°28'E, 25-V-2017, coll. Y. L. Jin.

***Non-type specimens*:** 18 juveniles with 7–10 pairs of legs, same data as holotype; 5 juveniles with 9 or 10 pairs of legs, China, Shanghai, Jiuzi Park, extracted from soil and litter samples of bamboo forest, alt. 14 m, 31°15'N, 121°28'E, 25-V-2017, coll. Y. L. Jin; 1 juvenile with 10 pairs of legs, China, Shanghai, Tianma Mountain,

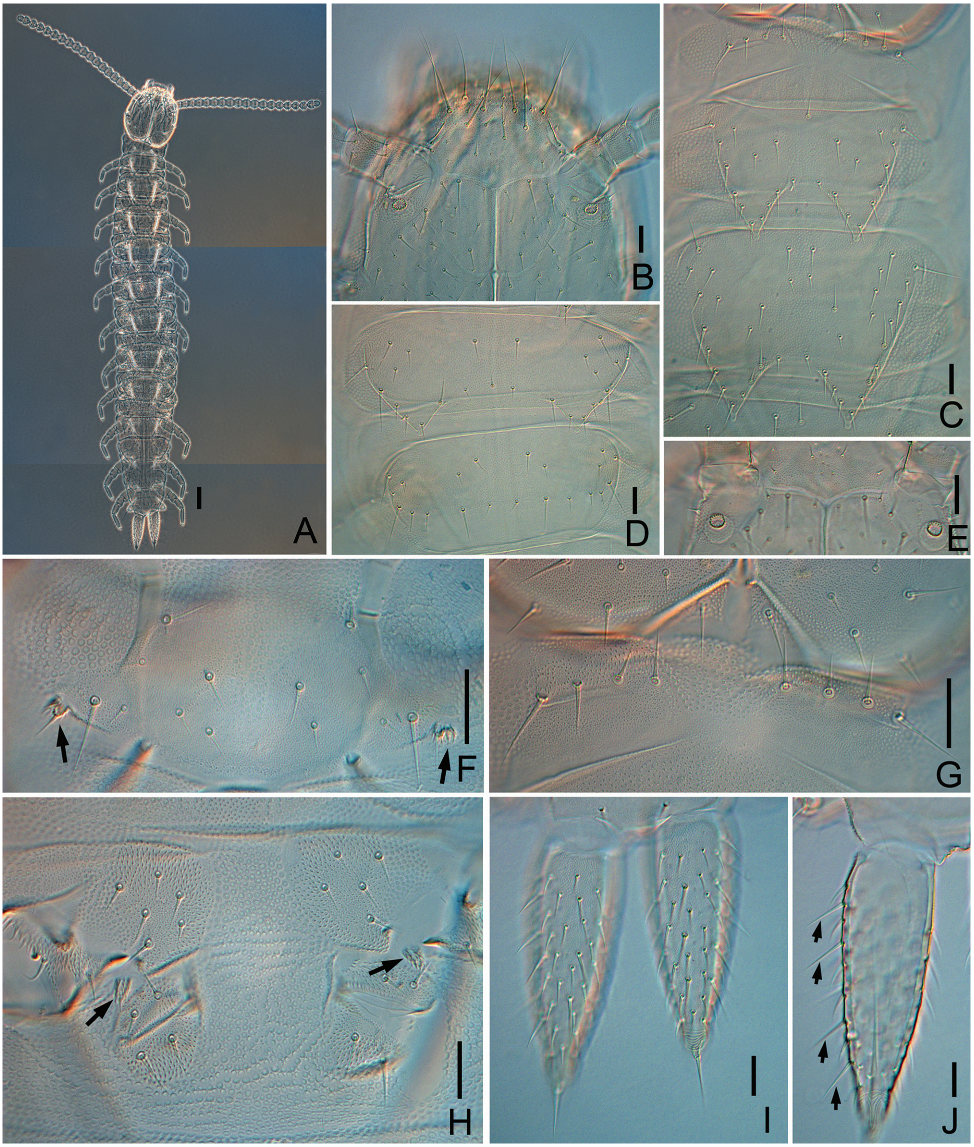

Figure 1. *Symphylella macrochaeta* sp. nov. **A** habitus, dorsal view **B** head, anterior part, dorsal view **C** tergites 1–3 **D** tergites 13–14 **E** Tömösváry organ **F** first pair of legs (arrows indicate reduced legs) **G** tergite 1 **H** styli and coxal sacs on base of leg 3 (arrows indicate styli). **I** cerci, dorsal view **J** left cercus, ventral view (arrows indicate long and erect outer setae). Scale bars: 100 µm (**A**); 20 µm (**B–J**).

extracted from soil samples of bamboo forest, alt. 98 m, 31°5'N, 121°9'E, 10-V-2017, coll. Y. Bu.

Description. Adult body 2.1 mm long in average (1.9–2.2 mm, *n* = 11), holotype 2.1 mm (Fig. 1A).

Head length 250–280 μm, width 223–265 μm, with widest part on equal level of points of articulation of mandibles. Central rod distinct in both anterior (65–70 μm) and posterior (75–85 μm) parts, with an obvious middle node-like interruption. Head dorsally covered with setae of different lengths (Fig. 1B). Frons with 5+5 lateral setae, 10 extremely long macrosetae (58–73 μm) arranged as 4/4/2 (counted from anterior row to posterior row) and 4–5.6 times as long as antero-central seta (a0) (Fig. 3H), and 20–21 short to medium-length setae (8–16 μm) (Figs 1B, 3H). Cuticle on anterolateral part of head with coarse granules (Fig. 1B).

Tömösváry organ globular, diameter 15–20 μm, about half of greatest diameter of third antennomere (35–40 μm), opening round (9–12 μm), inner margins of opening covered with regular vertical striae (Fig. 1E).

Mouthparts. Mandible composed by pars incisivus (*pi*) and pars molaris (*pm*), with movable appendage lacinia mobilis (*lm*) inserted between them. Pars incisivus with 4 distinct thick teeth, pars molaris with 4 smaller teeth and 2 proximal spines,

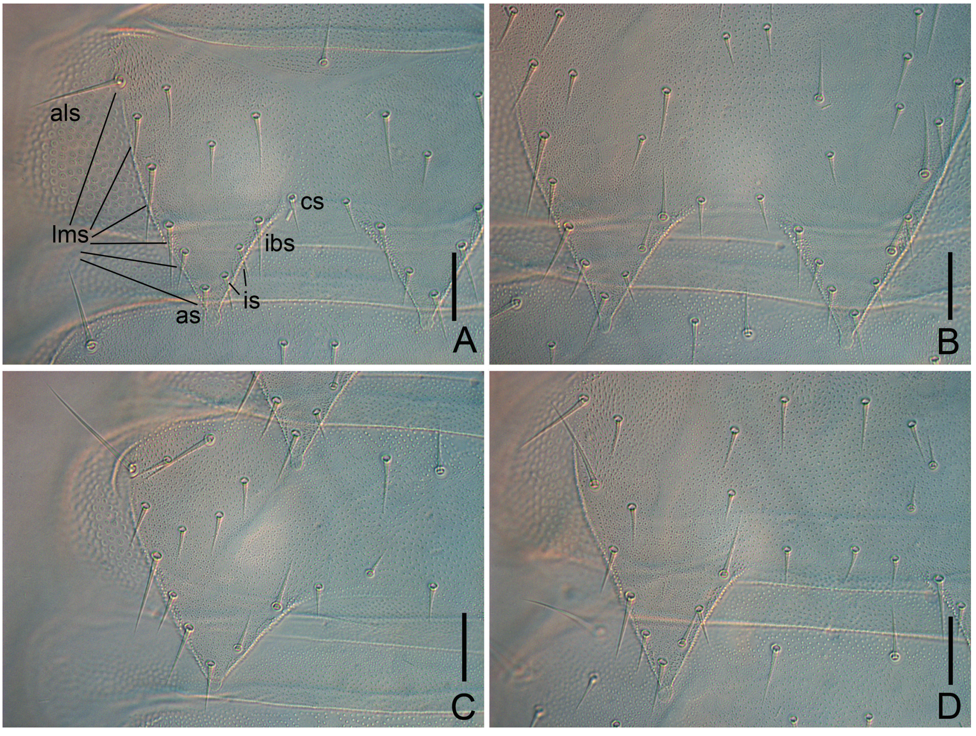

Figure 2. *Symphylella macrochaeta* sp. nov. **A** tergite 2 (*als* – anterolateral seta, *lms* – lateromarginl setae, *as* – apical seta, *is* – inserted seta, *ibs* – inner basal seta, *cs* – central seta) **B** tergite 3 **C** tergite 4, left side **D** tergite 5, left side. Scale bars: 20 μm.

and lacinia mobilis with only 1 blunt process observed from lateral view (Fig. 3A). First maxilla has 2 lobes, inner lobe with 6 hook-shaped teeth and pubescent apically, palp pointed (Fig. 3B). Anterior part of second maxilla with many small protuberances, each carrying 1 seta, distal setae thicker and spiniform; posterior part with sparse setae. Cuticle of second maxilla covered with dense pubescence.

Antennae with 16–20 antennomeres (18 in holotype), about 0.2 of body length. First antennomere cylindrical, length about 0.5–0.8 of greatest diameter (width 33–40 μm, length 18–25 μm), with 6 or 7 setae in 1 whorl, longest inner seta 16–18 μm (Fig. 3C). Second antennomere wider (35–38 μm) than long (27–33 μm), with 8 setae evenly inserted around antennal wall with interior setae (15 μm) slightly longer than exterior ones (11 μm) (Fig. 3C). Chaetotaxy of third antennomere similar to preceding ones. Setae on proximal antennomeres longer and on distal antennomeres shorter. Proximal antennomeres with only primary whorl of setae (Fig. 3C). Secondary whorl appearing ventrally on antennomeres 6–8. Four kinds of sensory organs observed on antenna: rudimentary spined sensory organs (*rso*) on dorsal side of most antennomeres (Fig. 3C, D); spined sensory organs (*so*) with more surrounding spines and larger than *rso*, only present on apical antennomere (Fig. 3D, E); cavity-shaped organs (*co*) on antennomeres 6 and 7 next to subapical one (Fig. 3D); bladder-shaped organs (*bo*) on antennomeres 9–11 next to subapical one increasing in number on subdistal antennomeres to 15 in maximum (Fig. 3D, E). Apical antennomere subspherical, with its length as long as width (28–30 μm), with 5 spined sensory organs consisting of 3 or 4 curved spines around a central pillar and 12–16 setae located distally (Fig. 3D, E). All antennomeres covered with short pubescence. Chaetotaxy and sensory organs on antennae of holotype are given in Table 1.

Table 1. Numbers of setae and sensory organs on antennae of *Symphylella macrochaeta* sp. nov. (holotype).

Antennomere	Primary whorl setae	Secondary whorl setae	Rudimentary spined sensory organs	Cavity-shaped organs on dorsal side	Bladder-shaped organs
1	6		1		
2	8		1		
3	8		1		
4	9		1		
5	9		1		
6	11		1	1	
7	11	2	1	1	
8	11	2	0	1	
9	10	3	0	1	
10	11	3	1	1	1
11	11	4	1	1	1
12	11	5	1	1	1
13	11	6	1	1	2
14	11	6	0	1	3
15	10	7	0	1	3
16	10	6		3	5
17	10	6		3	8

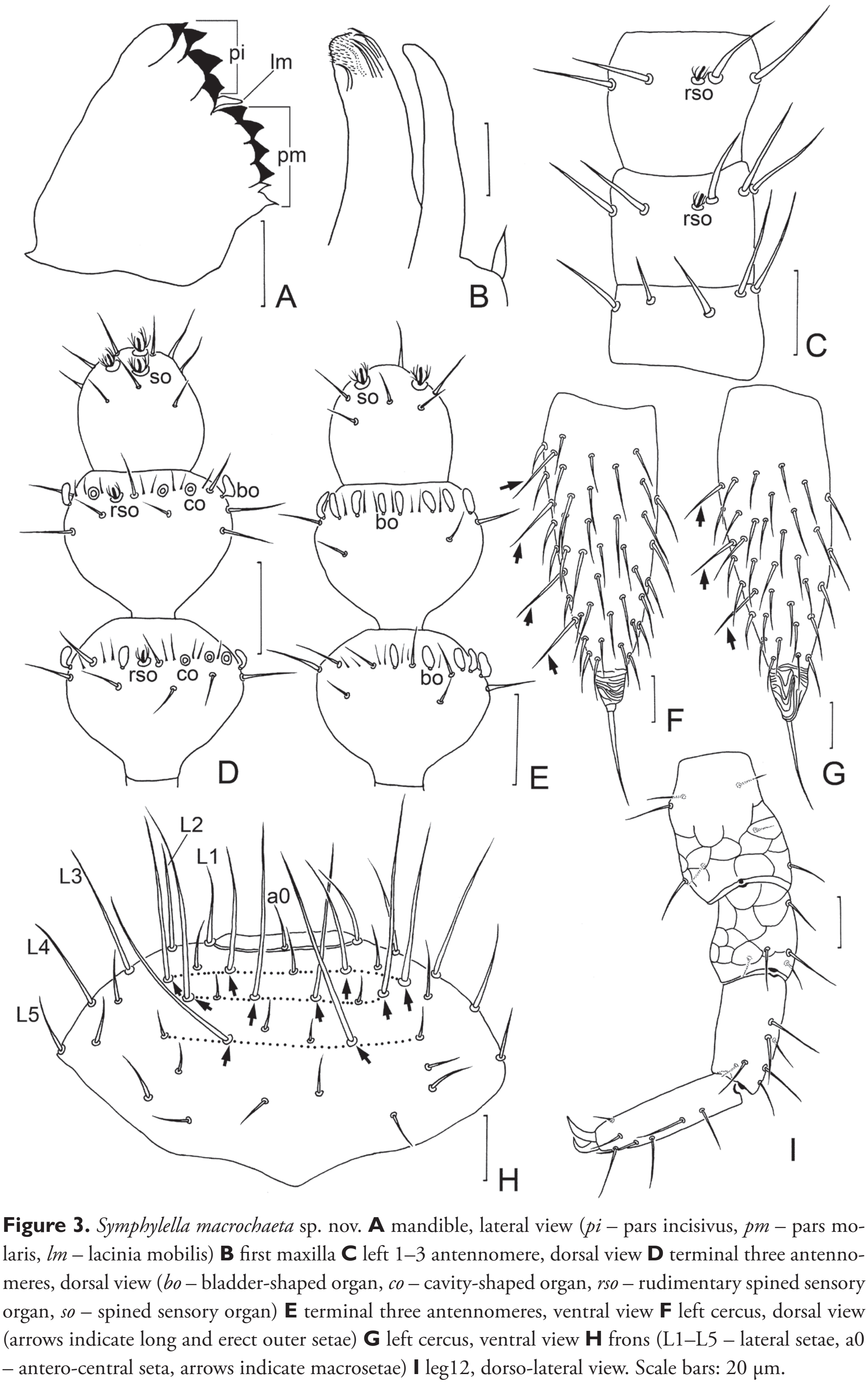

Figure 3. *Symphylella macrochaeta* sp. nov. **A** mandible, lateral view (*pi* – pars incisivus, *pm* – pars molaris, *lm* – lacinia mobilis) **B** first maxilla **C** left 1–3 antennomere, dorsal view **D** terminal three antennomeres, dorsal view (*bo* – bladder-shaped organ, *co* – cavity-shaped organ, *rso* – rudimentary spined sensory organ, *so* – spined sensory organ) **E** terminal three antennomeres, ventral view **F** left cercus, dorsal view (arrows indicate long and erect outer setae) **G** left cercus, ventral view **H** frons (L1–L5 – lateral setae, a0 – antero-central seta, arrows indicate macrosetae) **I** leg12, dorso-lateral view. Scale bars: 20 µm.

Trunk with 17 tergites. Tergites 2–13, and 15 each with 1 pair of triangular processes. Length from base to tip of processes somewhat shorter than or same as its basal width; basal distance between processes longer than their length from base to tip except on tergites 2 and 3 (Table 3). All processes with roundish swollen ends (Figs 1C, 2A–D). Definition of chaetotaxy on tergite as follow: anterolateral setae (*als*) located on anterolateral angle of each tergite; apical seta (*as*) most close to process apex; lateromarginl setae (*lms*) located on lateral margin of process and including *als* and *as*; inner basal setae (*ibs*) located on inner base of process; inserted setae (*is*) present between *ibs* and *as*; central setae (*cs*) present between base of processes; other setae including all setae except above nominated ones (Fig. 2A). Anterolateral setae of tergites 2, 3, 5, 6, 8, 9 11 and 12 slightly shorter than length of process of same tergite, that of tergites 4, 7, 10, 13 and 15 subequal or slightly longer than length of process of same tergite. Processes with 1 or 2 inserted setae. All tergites pubescent (Fig. 2A–D).

Tergites. Tergite 1 reduced, with 4+4 setae of different length (Fig. 1G). Tergite 2 complete, with 2 broad triangular posterior processes, 6 or 7 lateromarginal setae, 1 or 2 inserted setae, 1 or 2 central setae (Table 2), with anterolateral setae 0.8–0.9 time as long as length of process, length of processes 0.8–1.0 time as long as broad, basal distance between processes 0.6–0.9 time as long as their length (Figs 1C, 2A). Tergite 3 complete, broader and longer than preceding one, with ratios of 0.7–0.9, 0.8–1.0, and 0.6–0.9 respectively, 8–10 lateromarginal setae, 1 or 2 inserted setae, 1–3 central setae (Figs 1C, 2B). Tergite 4 broader than tergite 3, with ratios 1–1.3, 0.6–0.7, and 1.3–2.5 respectively, 5–7 lateromarginal setae (Fig. 2C). Chaetotaxy of tergites 5–7, 8–10, and 11–13 similar as tergites 2–4 (Fig. 2D). Pattern of alternating tergite lengths of 2 short-tergites followed by long-tergite only disrupted at caudal end (Table 3). Tergites 14 and 16 without processes and with 17–26 and 12–17 setae respectively (Fig. 1D). Tergite 17 with 27–38 setae. Chaetotaxy and measurements of tergites are given in Tables 2 and 3.

Table 2. Chaetotaxy of tergites of *Symphylella macrochaeta* sp. nov. (holotype in brackets).

Tergite	Lateromarginal setae	Inserted setae	Central setae	Other setae
1		4+4		
2	6–7 (6)	1–2 (2)	1–2 (2)	6–10 (6)
3	8–10 (8)	1–2 (2)	1–3 (2)	14–25 (14)
4	5–7 (6)	1–2 (1)	3–5 (3)	10–15 (11)
5	5–7 (6)	1–2 (2)	2–4 (3)	7–13 (12)
6	8–10 (9)	1–2 (2)	2–4 (4)	17–28 (20)
7	5–7 (6)	1–2 (2)	4–6 (4)	10–14 (11)
8	5–7 (6)	1–3 (2)	3–5 (4)	10–14 (10)
9	8–10 (9)	1–3 (1)	3–5 (3)	20–27 (22)
10	5–6 (6)	1–2 (1)	4–6 (4)	9–14 (11)
11	5–8 (6)	1–2 (1)	3–5 (4)	7–14 (9)
12	7–10 (8)	1–2 (2)	3–5 (3)	15–24 (15)
13	4–7 (5)	0–2 (1)	2–5 (3)	8–14 (8)
14				17–26 (21)
15	6–9 (7)	0/2 (0)	2–4 (3)	14–19 (14)
16				12–17 (14)
17				27–38 (29)

Table 3. Measurements of tergites and processes of *Symphylella macrochaeta* sp. nov. (mean ± se, *n* = 11, in μm) (holotype in brackets).

Tergite	Length	Width	Length of processes	Basal width of processes	Basal distance between processes
1	24 ± 7 (23)	141 ± 13 (138)			
2	48 ± 5 (45)	144 ± 7 (150)	37 ± 3 (33)	41 ± 3 (43)	28 ± 4 (32)
3	102 ± 14 (100)	186 ± 25 (180)	41 ± 4 (42)	45 ± 3 (47)	33 ± 3 (37)
4	57 ±7 (55)	194 ± 17 (205)	33 ± 3 (35)	49 ± 5 (52)	60 ± 8 (65)
5	71 ± 12 (65)	183 ± 10 (190)	41± 5 (45)	43 ± 4 (45)	62 ± 7 (67)
6	121 ± 9 (125)	223 ± 38 (235)	47± 5 (47)	48 ± 4 (47)	62 ± 6 (67)
7	70 ± 9 (65)	229 ± 18 (242)	36 ± 5 (40)	48 ± 6 (50)	85 ± 10 (95)
8	74 ± 5 (82)	204 ± 13 (205)	45 ± 4 (50)	45 ± 3 (50)	77 ± 10 (85)
9	114 ± 26 (120)	253 ± 21 (250)	46 ± 4 (50)	46 ± 4 (50)	72 ± 6 (75)
10	76 ± 14 (82)	235 ± 23 (250)	34 ± 3 (37)	48 ± 4 (50)	92 ± 16 (100)
11	73 ± 7 (70)	207 ± 13 (210)	41 ± 4 (45)	43 ± 3 (42)	78 ± 9 (85)
12	115 ± 7 (115)	255 ± 12 (260)	41 ± 4 (45)	47 ± 7 (50)	74 ± 9 (77)
13	68 ± 10 (60)	233 ± 24 (245)	28 ± 5 (32)	48 ± 6 (55)	89 ± 12 (90)
14	68 ± 10 (60)	205 ± 20 (210)			
15	93 ± 9 (90)	226 ± 21 (247)	28 ± 3 (32)	45 ± 5 (52)	67 ±8 (75)
16	72 ± 6 (80)	185 ± 25 (200)			
17	110 ± 8 (125)	172 ± 21 (175)			

Legs. First pair of legs reduced to 2 small hairy cupules, each with 1 long seta (9–10 μm) (Fig. 1F). Basal areas of legs 2–12 each with 3–8 setae (Fig. 1H). Leg 12 0.8–0.9 time as long as length of head (Fig. 3I), trochanter 1.1–1.2 times as long as wide (50–75 μm, 41–67 μm), with 7 setae; femur almost as long as wide (35–40 μm, 30–40 μm), with 5 setae and dorsal protruding longest setae (18–25 μm) about 0.6 time of greatest diameter of podomere; tibia nearly1.6–1.9 times longer than wide (45–55 μm, 25–30 μm), with 5 dorsal setae: 3 straight and protruding, 2 slightly curved and depressed, longest setae 0.7–1.0 of greatest diameter of tibia, 2 ventral setae distinctly shorter than dorsal ones; tarsus cylindrical, about 3–4.3 times as long as wide (58–75 μm, 16–19 μm) with 6 dorsal setae: 3 or 4 straight and protruding, others curved and depressed, longest setae (15–22 μm) same with greatest width of podomere, 1 ventral seta close to claw distinctly shorter than dorsal ones. Claws curved, anterior one somewhat broader than posterior one, posterior one more curved than former. Trochanter and femur with cuticular thickenings in pattern of large scales laterally (Fig. 3I). All legs covered with dense pubescence except areas with cuticular thickenings.

Coxal sacs present at bases of legs 3–9, fully developed, each with 4 or 5 setae on surface (Fig. 1H). Corresponding area of leg 2, 10, 11, and 12 replaced by 2–4 setae respectively.

Styli present at base of legs 3–12, slender (length 6–9 μm, width 4–6 μm), basal part with dense straight hairs; distal quarter hairless and with blunt apex (3–5 μm) (Fig. 1H).

Sense calicles located on 2 ventral protuberances of last tergite, posterior to base of leg 12, with smooth margin around pit. Sensory seta inserted in cup center, extremely long (110–140 μm).

Cerci about 0.5–0.6 of head length, 2.5–3 times as long as its greatest width (125–170 µm, 50–63 µm), densely covered with 75–90 subequal setae (Figs 1I–J, 3F–G). Two types of setae inserted on cercus: 7 and 8 long and erect setae located in outer side, and others slightly curved and depressed. Longest outer seta (25–30 µm) 0.4–0.6 of greatest width of cerci (Figs 1J, 3F–G), terminal area short (25–30 µm), circled by 9 layers of curved ridges. Terminal setae (25–32 µm) almost as long as terminal area (Figs 1I, 3F–G).

Etymology. From the Greek words "macro" meaning "large" and "chaeta" meaning "seta". The species name "macrochaeta" is feminine and refers to extremely long setae on the frons.

Distribution. China (Shanghai, Zhejiang).

Remarks. *Symphylella macrochaeta* sp. nov. has 10 extremely long macrosetae on the frons, which can distinguish it from all other congeners. It is similar to *S. communa* from East China and *S. asiatica* Scheller, 1971 from India and Sri Lanka in the shapes of the central rod, tergites, and leg 12, but the new species differs in the chaetotaxy of the first tergite (4+4 setae in *S. macrochaeta* sp. nov. and *S. communa* vs 3+3 setae in *S. asiatica*) and in the shape of stylus (slender in *S. macrochaeta* sp. nov. vs subconical in *S. communa* and conical in *S. asiatica*). The new species can also be compared to *S. macropora* from Tibet in the shape of tergites and processes, but it can be easily separated by the shape and the size of the opening of the Tömösváry organ (moderate and round in *S. macrochaeta* sp. nov. vs large and elongate in *S. macropora*).

Symphylella longispina Jin & Bu, sp. nov.

https://zoobank.org/C577A20B-B66D-43DE-8D99-339661E7374E
Figs 4–5, Tables 4–6

Diagnosis. *Symphylella longispina* sp. nov. is characterized by apparently thickened labrum, distinctly long proximal spines on the pars molaris of the mandible, eight macrosetae arranged as 4/2/2 on the frons, 3+3 setae on the first tergite and narrow triangular processes on tergites.

Material examined. ***Holotype*:** female (slide no. XJ-SY20160003) (SNHM), China, Xinjiang, Bole City, Hariturege National Forest Park, extracted from soil samples from the forest of *Populus euphratica*, alt. 1125 m, 40°08'N, 81°46'E, 31-VIII-2016, coll. C. W. Huang.

***Paratypes*:** 5 females (slides no. XJ-SY20160001, XJ-SY20160002, XJ-SY20160004, XJ-SY20160005, XJ-SY20160006) (SNHM), same data as holotype.

Description. Adult body 2.4 mm long in average (1.8–2.6 mm, n = 6), holotype 2.4 mm (Fig. 4A).

Head length 210–225 µm, width 190–225 µm, with widest part on equal level of points of articulation of mandibles. Central rod well developed but thin, divided into 2 portions by node-like sub-median interruption, with anterior 48–50 µm and posterior 60–70 µm. (Fig. 4B). Dorsal side of head moderately covered with setae of different lengths. Frons with 5+5 lateral setae, 8 macrosetae (23–28 µm) arranged as

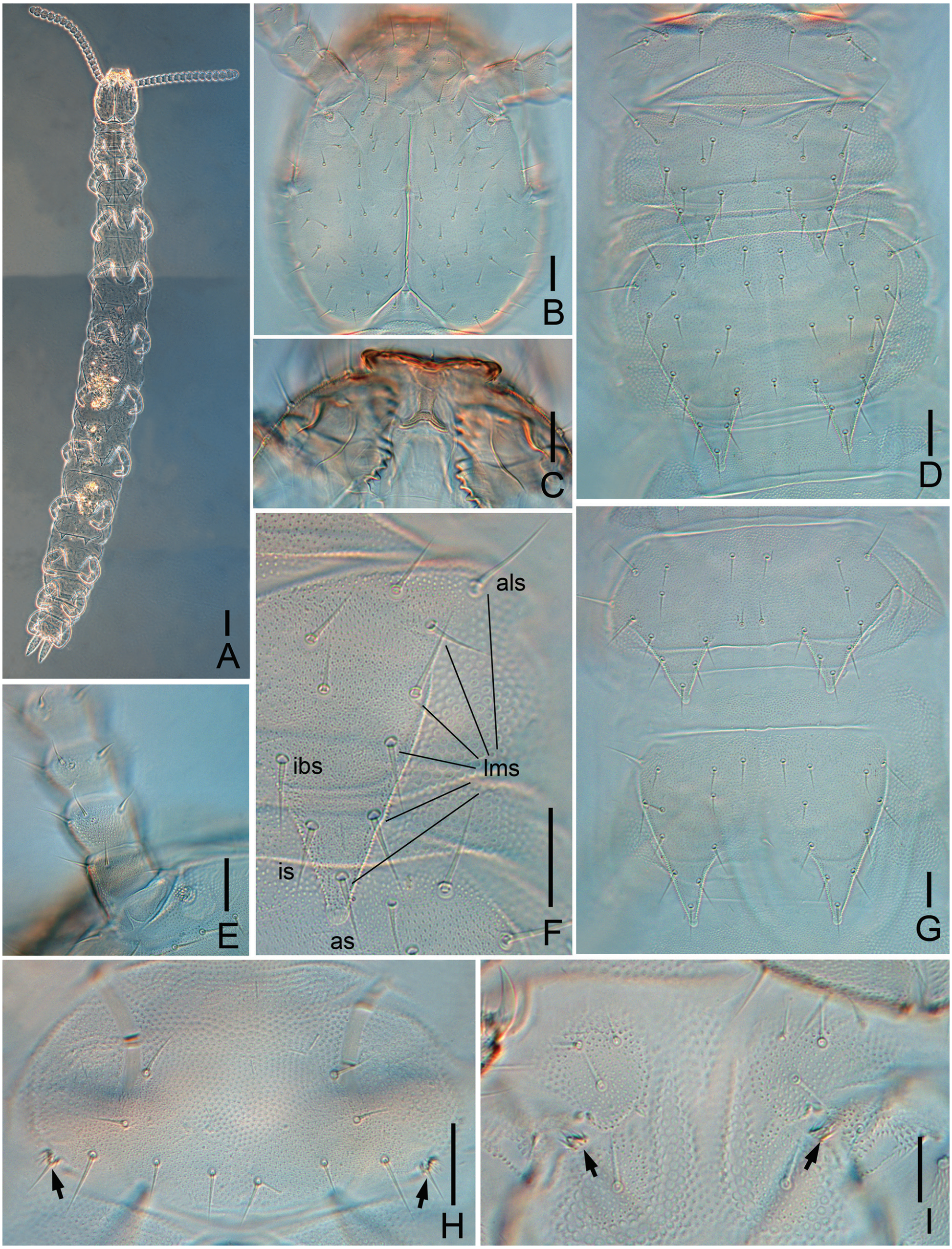

Figure 4. *Symphylella longispina* sp. nov. **A** habitus, dorsal view **B** head, dorsal view **C** labrum and mandible **D** tergites 1–3 **E** Tömösváry organ and antennomeres 1–4 **F** tergite 2, right side (*als* – anterolateral seta, *lms* – lateromarginl setae, *as* – apical seta, *is* – inserted seta, *ibs* – inner basal seta) **G** tergites 4–5 **H** first pair of legs (arrows indicate the reduced legs) **I** styli and coxal sacs on base of leg 12 (arrows indicate styli). Scale bars: 100 μm (**A**); 20 μm (**B–I**).

Table 4. Numbers of setae and sensory organs on antennae of *Symphylella longispina* sp. nov. (holotype).

Antennomere	Primary whorl setae	Secondary whorl setae	Rudimentary spined sensory organs	Cavity-shaped organs on dorsal side	Bladder-shaped organs
1	6				
2	8		1		
3	8		1		
4	9		1		
5	10		1		
6	10		1		
7	10		1	1	
8	10		0	1	
9	10		0	1	
10	10	1	0	1	
11	10	1	1	1	
12	11	3	1	1	1
13	11	4	0	1	3
14	11	4	0	1	5
15	11	5		2	9
16	11	4		3	13
17	10	5		2	13

4/2/2 and 2.8–3.7 times as long as antero-central seta (a0) (Fig. 5H), and 16 moderate setae (14–17 µm) (Figs 4B, 5H). Cuticle on anterolateral part of head with coarse granules (Fig. 4B).

Tömösváry organ globular, diameter 12–16 µm, shorter than half of greatest diameter of third antennomere (33–35 µm), opening small and round (4–6 µm), with distinct vertical inner striae (Fig. 4B, E).

Mouthparts. Labrum apparently thickened and protruding (Figs 4C, 5H). Mandible similar to *S. macrochaeta* sp. nov., but pars molaris with extremely long proximal spines (Figs 4C, 5A). First maxilla has 2 lobes, inner lobe with 6 hook-shaped teeth and pubescent apically, palp pointed and slightly incurved (Fig. 5B). Anterior part of second maxilla with many small protuberances, each carrying 1 seta, distal setae thick; posterior part with sparse setae. Cuticle of second maxilla covered with dense pubescence.

Antennae with 16–20 antennomeres (holotype with 18), about 0.2 of body length. First antennomere cylindrical, almost same as wide as long (width 24–28 µm, length 25–28 µm), with 5–7 setae in 1 whorl, longest inner seta 14–15 µm (Figs 4E, 5C). Second antennomere wider (29–33 µm) than long (24–25 µm), with 8 setae evenly inserted around antennal wall with interior setae (15 µm) slightly longer than exterior ones (11 µm) (Figs 4E, 5C). Chaetotaxy of third antennomere similar to preceding ones. Setae on proximal antennomeres longer and on distal antennomeres shorter. Proximal antennomeres with only primary whorl of setae, in middle and subapical antennomeres with several minute setae in secondary whorl. Four kinds of sensory organs observed on antenna: rudimentary spined sensory organs on dorsal side of most antennomeres

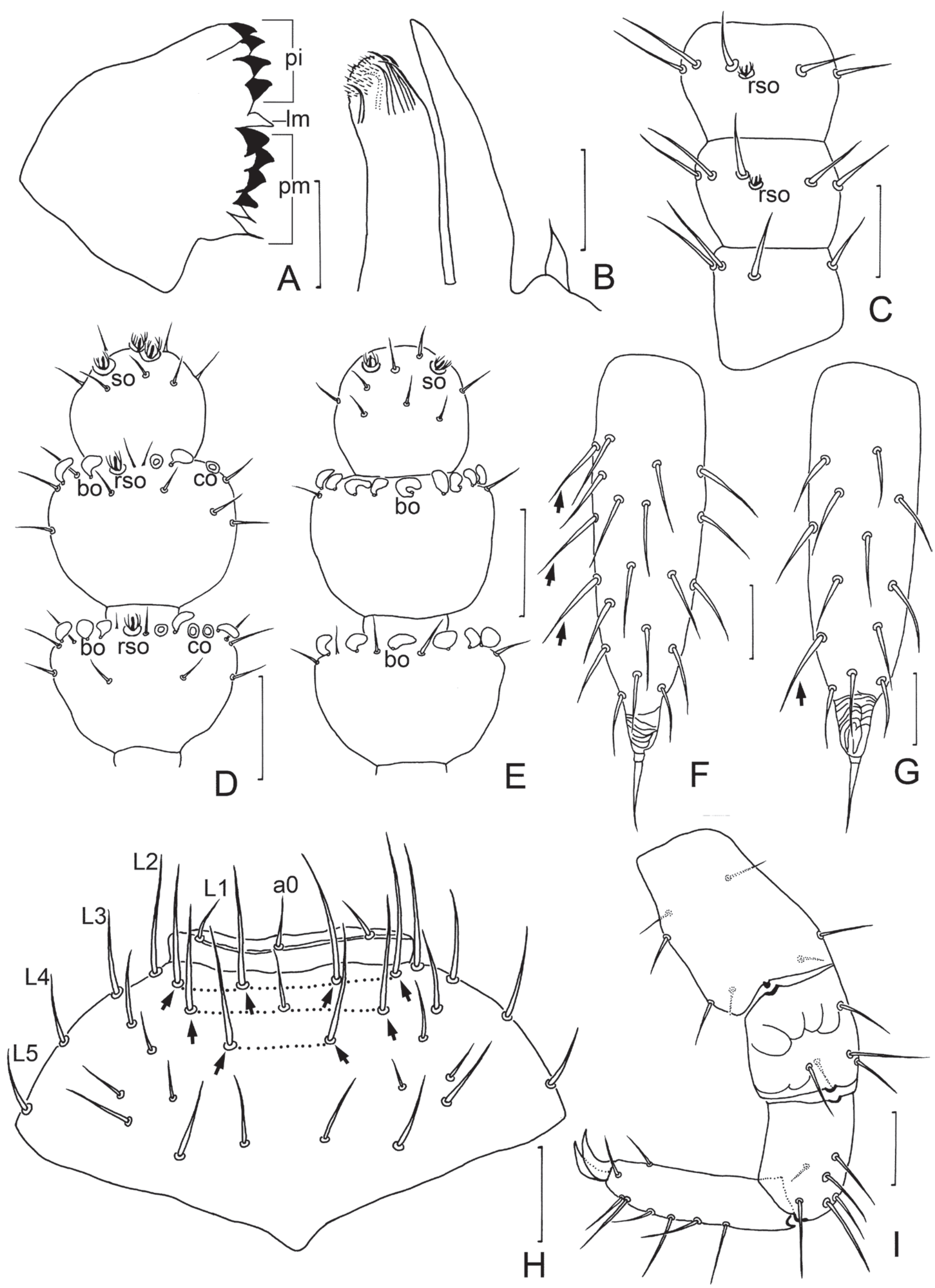

Figure 5. *Symphylella longispina* sp. nov. **A** mandible, lateral view (*pi* – pars incisivus, *pm* – pars molaris, *lm* – lacinia mobilis) **B** first maxilla **C** left 1–3 antennomeres, dorsal view **D** terminal three antennomeres, dorsal view (*bo* – bladder-shaped organ, *co* – cavity-shaped organ, *rso* – rudimentary spined sensory organ, *so* – spined sensory organ) **E** terminal three antennomeres, ventral view **F** left cercus, dorsal view (arrows indicate long and erect outer setae) **G** left cercus, ventral view **H** frons (L1–L5 – lateral setae, a0 – antero-central seta, arrows indicate macrosetae) **I** leg 12, dorso-lateral view. Scale bars: 20 µm.

except first antennomere (Fig. 5C, D); spined sensory organs only present on terminal antennomere (Fig. 5D, E); cavity-shaped organs on antennomeres 10 and 11 next to apical one, increasing in number to 4 in maximum (Fig. 5D); bladder-shaped organs irregular, round, oval or curved, present on antennomeres 5 and 6 next to apical one increasing in number on subdistal antennomeres to 13 in maximum (Fig. 5D, E). Apical antennomere subspherical, somewhat wider than long (width 25–28 μm, length 15–20 μm), five spined sensory organs consisting of 3 or 4 curved spines around a central pillar and 13–17 setae on distal half (Fig. 5D, E). All antennomeres covered with short pubescence. Chaetotaxy and sensory organs of antennae of holotype are given in Table 4.

Trunk with 17 tergites. Tergites 2–13 and 15 each with 1 pair of triangular processes. Length from base to tip of processes slightly longer than its basal width except for tergites 4, 7, 10 and 13, in which processes almost as broad as long; basal distance between processes of tergites distinctly longer than their length from base to tip (Table 5). All processes with distinct rounded end-swellings (Fig. 4D, F, G). Anterolateral setae of tergites 2, 3, 4, 6, 7, 9 and 10 distinctly longer than other lateromarginal setae, that of tergites 5, 8, 11–13 and 15 subequal or slightly shorter than longest ones of other lateromarginal (Fig. 4D, F, G). Anterolateral setae of tergites shorter than or subequal to process of same tergite. Processes with 1 inserted seta (*is*) (Fig. 4F). All tergites pubescent (Fig. 4F).

Tergites. Tergite 1 reduced, with 3+3 subequal setae (Fig. 4D). Tergite 2 complete, with 2 triangular posterior processes, 5 or 6 lateromarginal setae, 1 inserted seta, 1 central seta (Table 5), anterolateral setae 0.7–0.8 of length of process, processes 1.1–1.2 times as long as broad, basal distance between processes 1–1.2 times as long as their length (Fig. 4D, F). Tergite 3 complete, broader and longer than preceding one with ratios of 0.7–0.9, 1.1–1.3, and 1.1–1.3 respectively, 7 or 8 lateromarginal setae (Fig. 4D). Tergite 4 broader than tergite 3, with ratios 1–1.2, 0.9–1, and 1.3–1.9 respectively, 5 lateromarginal setae (Fig. 4G). Chaetotaxy of tergites 5–7, 8–10, and 11–13 similar as tergites 2–4. Pattern of alternating tergite lengths of 2 short tergites followed by 1 long tergite only disrupted at caudal end (Table 6). Tergites 14 and 16 without processes and with 15–18 and 10–14 setae respectively. Tergite 17 with 10–14 setae. Chaetotaxy and measurements of tergites are given in Tables 5 and 6.

Legs. First pair of legs reduced to 2 small hairy cupules, each with 1 long seta (9–11 μm) (Fig. 4H). Basal areas of legs 2–12 each with 3–5 setae. Leg 12 about 0.6–0.8 of head length (Fig. 5I), trochanter 1.3–1.6 times longer than wide (45–50 μm, 32–36 μm), with 6 or 7 subequal setae in total; femur almost as long as wide (25–33 μm, 25–30 μm), with 5 setae, longest dorsal seta 17–20 μm in length, pubescent dorsally, laterally with cuticular thickenings in pattern of scales; tibia nearly 1.3–1.9 times longer than wide (28–40 μm, 21–23 μm), with 6 or 7 setae, longest dorsal one 14–18 μm; tarsus subcylindrical, 3–3.5 times as long as wide (45–48 μm, 13–16 μm) with 6 dorsal setae: 4 straight and protruding, 2 slightly curved and depressed, longest setae (14–17 μm) about same length of greatest width of podomere, 2 ventral setae close to claw and distinctly shorter than dorsal ones. Claws curved, anterior one broader than posterior one. All legs covered with dense pubescence except areas with cuticular thickenings.

Table 5. Chaetotaxy of tergites of *Symphylella longispina* sp. nov. (holotype in brackets).

Tergite	Lateromarginal setae	Inserted seta	Central setae	Other setae
1		3+3		
2	5–6 (6)	1 (1)	1 (1)	5–7 (6)
3	7–8 (7)	1 (1)	1 (1)	16–19 (16)
4	5 (5)	1 (1)	1–2 (2)	8–8 (8)
5	5 (5)	1 (1)	1–2 (1)	7–10 (8)
6	7–8 (7)	1 (1)	2–3 (2)	15–20 (20)
7	5 (5)	1 (1)	2–3 (2)	8–10 (8)
8	5 (5)	1 (1)	2 (2)	0–11 (9)
9	7–8 (7)	1 (1)	2–3 (3)	16–20 (18)
10	5 (5)	1 (1)	2–3 (3)	8–10 (8)
11	5–6 (5)	1 (1)	2–3 (2)	6–10 (9)
12	6–7 (7)	0/1 (1)	2–3 (3)	15–20 (17)
13	4–5 (5)	0/1 (1)	1–2 (2)	7–8 (7)
14				15–18 (16)
15	4–7 (5)	0/1 (1)	1–2 (2)	8–14 (14)
16				10–14 (14)
17				10–14 (14)

Table 6. Measurements of tergites and processes of *Symphylella longispina* sp. nov. (mean ± se, *n* = 6, in μm) (holotype in brackets).

Tergite	Length	Width	Length of processes	Basal width of processes	Basal distance between processes
1	27 ± 3 (25)	126 ± 2 (125)			
2	45 ± 6 (50)	123 ± 10 (130)	32 ± 2 (34)	28 ± 2 (30)	33 ± 3 (33)
3	97 ± 16 (90)	151 ± 8 (155)	34 ± 2 (37)	28 ± 2 (32)	39 ± 2 (40)
4	60 ± 8 (62)	162 ± 9 (170)	31 ± 2 (29)	34 ± 1 (33)	47 ± 6 (50)
5	60 ± 12 (75)	138 ± 5 (140)	35 ± 4 (39)	28 ± 3 (30)	52 ± 5 (50)
6	115 ± 12 (125)	181 ± 17 (192)	39 ± 3 (41)	31 ± 4 (33)	60 ± 4 (63)
7	72 ± 12 (85)	191 ± 10 (202)	38 ± 4 (36)	39 ± 6 (35)	65 ± 7 (75)
8	71 ± 12 (80)	160 ± 9 (170)	35 ± 3 (38)	27 ± 3 (29)	65 ± 5 (70)
9	124 ± 10 (138)	199 ± 6 (205)	37 ± 3 (41)	30 ± 3 (34)	68 ± 7 (75)
10	74 ± 12 (90)	196 ± 17 (207)	36 ± 3 (37)	36 ± 6 (36)	74 ± 5 (80)
11	72 ± 9 (80)	171 ± 5 (175)	35 ± 1 (34)	29 ± 3 (25)	70 ± 6 (78)
12	121 ± 18 (125)	201 ± 14 (217)	37 ± 4 (38)	30 ± 6 (32)	66 ± 7 (70)
13	71 ± 6 (75)	184 ± 16 (207)	29 ± 3 (27)	36 ± 12 (30)	66 ± 9 (72)
14	68 ± 10 (75)	164 ± 8 (175)			
15	99 ± 10 (100)	180 ± 13 (200)	27 ± 2 (30)	26 ± 3 (26)	55 ± 8 (65)
16	71 ± 7 (75)	148 ± 16 (162)			
17	92 ± 9 (92)	131 ± 9 (135)			

Coxal sacs present at bases of legs 3–9, fully developed, each with 4 setae on surface. Corresponding area of leg 2, 10, 11 and 12 replaced by 1–3 setae (Fig. 4I).

Styli present at base of legs 3–12, subconical (length 5 μm, width 3 μm), basal part with straight hairs; distal quarter hairless and with blunt apex (3 μm) (Fig. 4I).

Sense calicles with smooth margin around pit. Sensory seta inserted in cup center, extremely long (115–120 μm).

Cerci about half length of head, 3.3–3.8 times as long as its greatest width (108–115 μm, 30–34 μm), sparsely covered with 33–39 subequal setae (Fig. 5F, G). Two types of setae inserted on cercus: 4 or 5 long and erect setae located in outer side, and others slightly curved and depressed. Longest outer seta (20 μm) 0.6–0.7 of greatest width of cerci, terminal area short (16–18 μm), circled by 6–8 layers of curved ridges. Terminal setae (15–16 μm) slightly shorter than terminal area (Fig. 5F, G).

Etymology. The species name is derived from the Latin words "*longus*" and "*spina*" meaning "long spine". It is feminine and refers to the extremely long proximal spines on the pars molaris of the mandible.

Distribution. Known only from the type locality.

Remarks. *Symphylella longispina* sp. nov. has a thickened and prominent labrum and irregular bladder-shaped organs on antennae, which separate it from all other congeners. It is most similar to *S. asiatica* Scheller, 1971 from India and Sri Lanka in the shape and chaetotaxy of the tergites, but the new species differs in the distal part of the processes (distinctly swollen in *S. longispina* sp. nov. vs small and slender in *S. asiatica*), in the shape and chaetotaxy of cerci (subcylindrical and with sparse setae in *S. longispina* sp. nov. vs conical and with dense setae in *S. asiatica*), and in the shape of the palp of the first maxilla (slightly curved in *S. longispina* sp. nov. vs straight in *S. asiatica*). The new species is also similar to *S. brincki* Scheller, 1971 from Sri Lanka in the chaetotaxy of the tergites, but they can be easily separated by the central rod (with a middle node-like interruption in *S. longispina* sp. nov. vs with a narrow transverse interruption in *S. brincki*), by the end of the processes (with round end-swellings in *S. longispina* sp. nov. vs spatulate end-swellings in *S. brincki*), and by the shape and chaetotaxy of cerci (3.3–3.8 times as long as wide and with sparse setae in *S. longispina* sp. nov. vs 2.3 times as long as wide and with dense setae in *S. brincki*).

Discussion

Symphylella is one of the most common and diverse group of symphylans with a wide global distribution (Szucsich and Scheller 2011; Bu and Jin 2018). The central rod on the head, the Tömösváry organ, the processes of tergites, the stylus, and the cercus are commonly used as diagnostic characters for species of this genus and, thus, were previously described and illustrated in detail (Scheller 1971; Szucsich and Scheller 2011). However, in recent years, we have found that some of characters, such as the first maxilla, the mandible, and the head chaetotaxy, are differ among species and good for species diagnosis (Jin and Bu 2018, 2019, 2020; Jin et al. 2019), but they were often overlooked by former specialists.

The mandible structure of Symphyla was carefully studied and compared with other arthropods by former colleagues (Richter et al. 2002; Edgecombe et al. 2003). According to their excellent scanning electron photomicrographs, the mandibular gnathal edge of *Hanseniella* (Scutigerellidae) is composed of the pars incisivus (pi) and pars molaris (pm), with lacinia mobilis inserted between. We have observed the similar

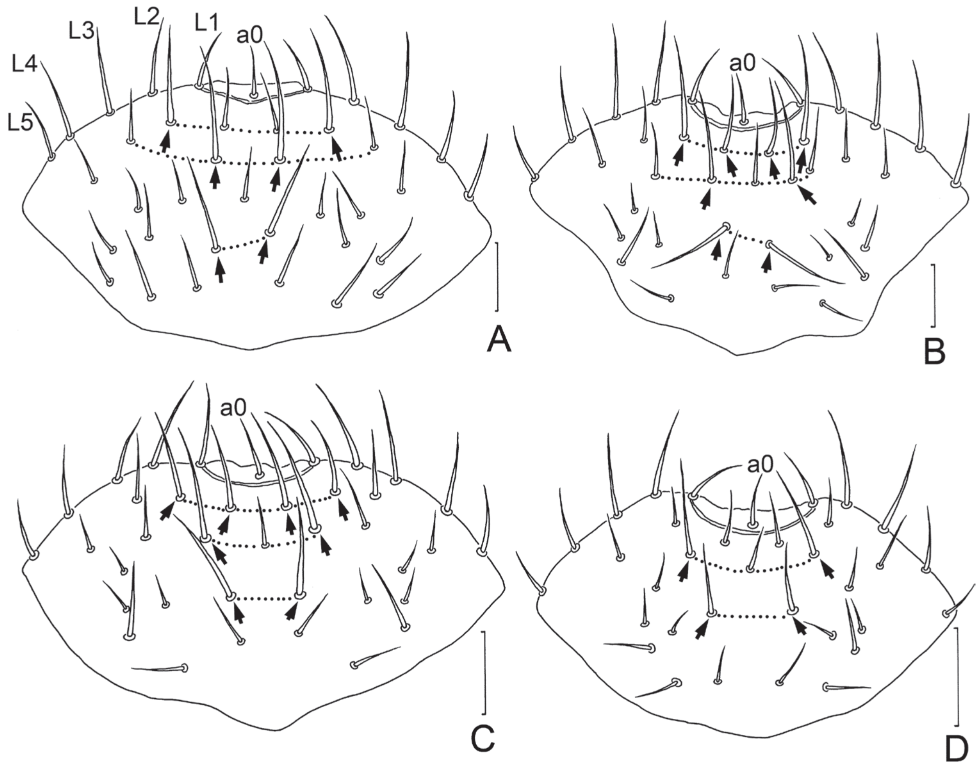

Figure 6. Frons of *Symphylella* spp. from China. **A** *S. macropora* **B** *S. zhongi* **C** *S. communa* **D** *S. minuta*. Scale bars: 20 μm. (L1–L5 – lateral setae, a0 – antero-central seta, arrows indicate macrosetae).

Table 7. Comparison of chaetotaxy on frons of *Symphylella* spp. from China.

Characters	*S. macrochaeta* sp. nov.	*S. longispina* sp. nov.	*S. macropora*	*S. zhongi*	*S. communa*	*S. minuta*
Number of macrosetae (M)	10	8	6	8	8	4
Formula of M-setae	4/4/2	4/2/2	2/2/2	4/2/2	4/2/2	0/2/2
length of M-setae (μm)	58–73	21–28	25–37	22–37	20–30	12–20
length of a0 setae (μm)	12–15	7–8	12	12–15	10–16	7–11
M/a0	4–5.6	2.8–3.7	2–3	1.5–2.7	1.6–2.7	1.4–2.4

parts in the species of *Symphylella* (Scolopendrellidae) using light microscopy, but the shape and composition of each part are different to that of *Hanseniella*. The structure of mandible is varied among species of *Symphylella*, which can be diagnostic character of species. To obtain a better perspective overall of mandible structures in Symphyla, the study of more species using SEM method is needed.

In our study of *Symphylella* specimens from Zhejiang and Shanghai, we observed that the extremely long setae on the frons of *S. macrochaeta* sp. nov. differ from other Chinese congeners (Fig. 3H). Thus, we checked the other four species recorded in

China and compared their frons chaetotaxy (Fig. 6A–D). As a result, we confirmed that the frons chaetotaxy is a useful diagnostic character in the taxonomy of *Symphylella* (Table 7).

According to our observations, the frons of *Symphylella* spp. often has well-differentiated macrosetae located on the 2/3 anterior part and 5+5 setae on the lateral margin. The quantity, length, arrangement, and ratio to antero-central seta of the macrosetae vary among species but vary little among conspecific individuals (Table 7). A broader study to reexamine the type materials of all other described species of *Symphylella* is needed to supplement the missing data.

Acknowledgements

We sincerely thank Dr Jing-Yang Li, Mrs Si-Qi Yang and Mr Cheng-Wang Huang for their generous help in the collection. We appreciate Dr Nerivania Nunes Godeiro for the linguistic corrections to the manuscript. Special thanks are given to Dr Derek Hennen (USA) and an anonymous reviewer for their valuable comments in review of the manuscript. This research was supported by the National Natural Science Foundation of China (no. 32170471) and the Research Foundation of Shanghai Science and Technology Museum.

References

Bu Y, Jin YL (2018) Progress on the systematic study of Symphyla. Chinese Bulletin of Life Sciences 30(5): 500–509. https://doi.org/10.13376/j.cbls/2018060 [In Chinese with English summary]

Chau NN (2015) Garden centipede *Scutigerella immaculata* Newport, 1845, an arthropod pest for the vegetable in Da Lat, Vietnam. Tap Chi Sinh Hoc 37(4): 411–417. https://doi.org/10.15625/0866-7160/v37n4.7398

Edgecombe GD, Richter S, Wilson GDF (2003) The mandibular gnathal edges: Homologous structures throughout Mandibulata? African Invertebrates 44(1): 115–135.

Jin YL, Bu Y (2018) First record of *Scolopendrellopsis* from China with the description of a new species (Myriapoda, Symphyla). ZooKeys 789: 103–113. https://doi.org/10.3897/zookeys.789.27356

Jin YL, Bu Y (2019) Occurrence of *Millotellina* (Myriapoda, Symphyla) in China with the description of two new species. Zootaxa 4691(3): 215–224. https://doi.org/10.11646/zootaxa.4691.3.2

Jin YL, Bu Y (2020) Two new species of the genus *Symphylella* (Symphyla, Scolopendrellidae) from East China. ZooKeys 1003: 1–18. https://doi.org/10.3897/zookeys.1003.60210

Jin YL, Bu Y (2022) Research progresses in the damage of symphylan pests to crops and their control. Plant Protection 48(5): 30–37. https://10.16688/j.zwbh.2021445 [In Chinese with English summary]

Jin YL, Bu Y, Jiang Y (2019) Two new species of the genus *Symphylella* (Symphyla, Scolopendrellidae) from Tibet, China. ZooKeys 845: 99–117. https://doi.org/10.3897/zookeys.845.33566

Richter S, Edgecombe GD, Wilson GDF (2002) The *lacinia mobilis* and similar structures – a valuable character in arthropod phylogenetics? Zoologischer Anzeiger 241(4): 339–361. https://doi.org/10.1078/0044-5231-00083

Scheller U (1971) Symphyla from Ceylon and Peninsular India. Entomologica Scandinavica (Supplement 1): 98–187.

Szucsich N, Scheller U (2011) Symphyla. In: Minelli A (Ed.) Treatise of Zoology—Anatomy, Taxonomy, Biology: The Myriapoda, (Vol. 1). Brill, Leiden, 445–466. https://doi.org/10.1163/9789004188266_021

ZooKeys 1138: 161–173 (2023)
doi: 10.3897/zookeys.1138.90338
https://zookeys.pensoft.net

RESEARCH ARTICLE

A peer-reviewed open-access journal
ZooKeys
Launched to accelerate biodiversity research

The subfamily Dermestinae (Coleoptera, Dermestidae) from Saudi Arabia

Jiří Háva[1], Mahmoud S. Abdel-Dayem[2,3], Hathal M. Aldhafer[2]

1 *Private Entomological Laboratory and Collection, Rýznerova 37/37, CZ-252 62 Únětice u Prahy, Prague-West, Czech Republic* **2** *King Saud University Museum of Arthropods (KSMA), Plant Protection Department, College of Food and Agricultural Sciences, King Saud University, P.O. Box 2460 Riyadh 11451, Saudi Arabia* **3** *Entomology Department, Faculty of Science, Cairo University, Giza, 12613, Egypt*

Corresponding author: Mahmoud S. Abdel-Dayem (mseleem@ksu.edu.sa)

Academic editor: Thomas Philips | Received 26 July 2022 | Accepted 18 December 2022 | Published 5 January 2023

https://zoobank.org/E4C18E91-8B1E-4656-BC09-8D147E87082F

Citation: Háva J, Abdel-Dayem MS, Aldhafer HM (2023) The subfamily Dermestinae (Coleoptera, Dermestidae) from Saudi Arabia. ZooKeys 1138: 161–173. https://doi.org/10.3897/zookeys.1138.90338

Abstract
In this study, the fauna of Saudi Arabian Dermestinae (Coleoptera, Dermestidae) is summarised. Six *Dermestes* species and single species from two Marioutini genera, *Mariouta and Rhopalosilpha*, are reported. *Dermestes* (*Dermestinus*) *undulatus* Brahm, 1790 and *Dermestes* (*Dermestes*) *haemorrhoidalis* Küster, 1852 are newly recorded from Saudi Arabia. A list of Dermestinae species from the Arabian Peninsula is provided with their distributions.

Keywords
Beetles, Dermestini, distribution, fauna, Marioutini, new records

Introduction

Dermestinae is a subfamily of Dermestidae with a worldwide distribution, but concentrated in the Holarctic and Afrotropical areas. According to Háva (2015, 2022), there are approximately 95 species assigned to only five genera under two tribes: Dermestini with three genera, *Derbyana* Lawrence & Ślipiński, *Dermalius* Háva, and *Dermestes* Linnaeus, 1758, and Marioutini with two genera, *Mariouta* Pic and *Rhopalosilpha*

Arrow; additionally there is the fossil tribe Paradermestini with one genus, *Paradermestes* Deng, Ślipiński, Ren & Pang (Háva 2015, 2022). The genus *Dermestes* is the largest genus in Dermestinae and recently included 89 species and subspecies worldwide (Háva 2015, 2022). Members of the subfamily are generally recognised by their elongate body structure, lack of ocelli, and males with small tufts of erect setae on the abdominal ventrites (females are without tufts). Larvae are zoonecrophagous.

The first data concerning Dermestinae of Saudi Arabia date back to the second half of the 20th century. In the early 1960s, the Egyptian entomologist F. Shalaby (1961) was perhaps the first who catalogued data on *Dermestes maculatus* DeGeer, 1774. The work of the Polish entomologist M. Mroczkowski (1979) was the first important faunistic study on the Saudi Arabian Dermestidae fauna. His work was based on the collection made by W. Büttiker who intensively explored many areas of Saudi Arabia, and he recorded three *Dermestes* species. Mroczkowski and Ślipiński (1997) published their review and keys to world genera and species of the tribe Marioutini and reported *Mariouta stangei* Reitter, 1910 and *Rhopalosilpha wasmanni* Arrow, 1929 from Saudi Arabia.

From the beginning of the 21st century and during the last two decades, the forensic importance of dermestid beetles attracted the attention of many workers from Saudi Arabia (e.g., Abouzied 2014; Alajmi et al. 2016; Al-Shareef and Al-Mazyad 2017; Al-Shareef and Zaki 2017; Mashaly 2017; Shaalan et al. 2017; Mashaly et al. 2018, 2019; Al-Dakhil and Alharbi 2020; Al-Qahtni et al. 2020). However, the faunistic data on Dermestinae were published as part of general surveys of insects or beetles (Abdel-Dayem et al. 2017, 2020; Elgharbawy 2018). The systematic, faunistic, and distribution of Dermestinae in Saudi Arabia are still not well known, and few works have been published. This paper aims to summarise the known Saudi Arabian Dermestinae and update distribution data.

Materials and methods

The data on the distribution of the species in the subfamily Dermestinae (Coleoptera, Dermestidae) in Saudi Arabia is based on three main sources. The first are the historical works of Shalaby (1961), Mroczkowski (1979), Mroczkowski and Ślipiński (1997), and additionally the recent publication of Abouzied (2014), Abdel-Dayem et al. (2017, 2020), Al-Shareef and Zaki (2017), Mashaly (2017), Elgharbawy (2018), Mashaly et al. (2019), Al-Dakhil and Alharbi (2020), and Al-Qahtni et al. (2020). The second source are specimens preserved in the insect collections of the King Saud University Museum of Arthropods (**KSMA**) in Riyadh, Saudi Arabia, the Florida State Collection and Arthropods (**FSCA**), and the collection of the first author. The third source is an extended field survey conducted by the second and third authors, which is still ongoing. The collected specimens were deposited in the collections of KSMA, unless otherwise indicated (JHAC: Jiří Háva). The nomenclature follows Motyka et al. (2022). A note entry summarises published and current data on the species distribution within

Saudi Arabia. The general range and the world distribution data were derived from the catalogues of Háva (2015, 2022).

For each material lot examined, the following label data are provided as follows: Country name (in capital letters) at the beginning. Then each record starts with a bullet point (•) followed by the number of examined specimens followed by sex (if determined) or "ex" (if the specimen sex could not be recognised because the abdomen was lost, damaged, or other reasons); Saudi Province followed by a comma (,), governorate, locality; geographical coordinates; elevation (m), collection date; collector(s) name followed by "leg."; method of collection (bait trap (**BT**), handpicking (**HP**), light trap (**LT**), malaise trap (**MT**), pitfall trap (**PT**), sweeping net (**SW**)), the identifier name followed by "det.", and the depository collection acronym. The material examined was arranged in alphabetical order with respect to the Saudi province, governorate, and locality name. Data were then arranged in chronological order according to the month of collection. Records with the same locality data, except for slight differences (such as date of collection, altitude, collector/s), were reported together with the second label, given "same collection data as for preceding" and followed by a semicolon (;) and the different data.

The following acronyms of type depositories are used in the text:

JHAC Jiří Háva, Private Entomological Laboratory & Collection, Únětice u Prahy, Prague-West, Czech Republic;
FSCA Florida State Collection and Arthropods, Gainesville, USA;
KSMA King Saud University Museum of Arthropods, Plant Protection Department, College of Food and Agriculture Sciences, King Saud University, Riyadh, Saudi Arabia.

Results

Family Dermestidae Latreille, 1804
Subfamily Dermestinae Latreille, 1804
Tribe Dermestini Latreille, 1804
Genus *Dermestes* Linnaeus, 1758
Subgenus *Dermestes* s. str.

***Dermestes* (*Dermestes*) *ater* DeGeer, 1774**
Fig. 1A, B

Material examined. Saudi Arabia • 1 ♂; Eastern Province, An Nuayriah, Al Sarar; 27°25'45.5"N, 48°27'0.0"E; 60 m a.s.l.; 2 Mar. 2011; H. Al Dhafer; H. Setyaningrum & A. Al Ansi leg.; collected from carcasses on the road;, J. Háva det.; KSMA • 1 ♀; Makkah Province, Jeddah, "Ras Halibah" [Ras Hatibah];, 7 May. 1982; W. Büttiker leg.;JHAC • 4 ex; Riyadh Province, Dirab, Al-Dhab Farm; 5 Oct. 1986; collected from chicken farm waste, J. Háva det.; KSMA; • 1 ex; Riyadh, Al-Wahah Farm; 12 Oct. 1989; J. Háva det.; KSMA.

Note. This species was previously recorded in Eastern Province at Al Hofuf (Mroczkowski 1979); Dammam (Mroczkowski 1979), Dhahran (Mroczkowski 1979), and Riyadh Province at Riyadh (Mroczkowski 1979). The listed specimens were collected from low elevation areas (<600 m) in central, eastern, and southwestern Saudi Arabia (Fig. 4A).

Distribution. Cosmopolitan (Háva 2007, 2015, 2022).

***Dermestes* (*Dermestes*) *haemorrhoidalis* Küster, 1852**

Fig. 1C, D

Material examined. Saudi Arabia • Riyadh Province, 1 ♀; Al Zulfi, Rawdhat Al Sablh; 26°22.429'N, 44°58.241'E; 670 m a.s.l.; 26 Aug. 2015; H. Al Dhafer, M. Abdel-Deyem, A. El Torkey, A. El Gharbawy, & A. Solimanleg leg.; LT; J. Háva det.; KSMA.

Note. The female specimen was collected at a low elevation (670 m) in a sandy area in central Saudi Arabia (Fig. 4A). This represents a new record for Saudi Arabia.

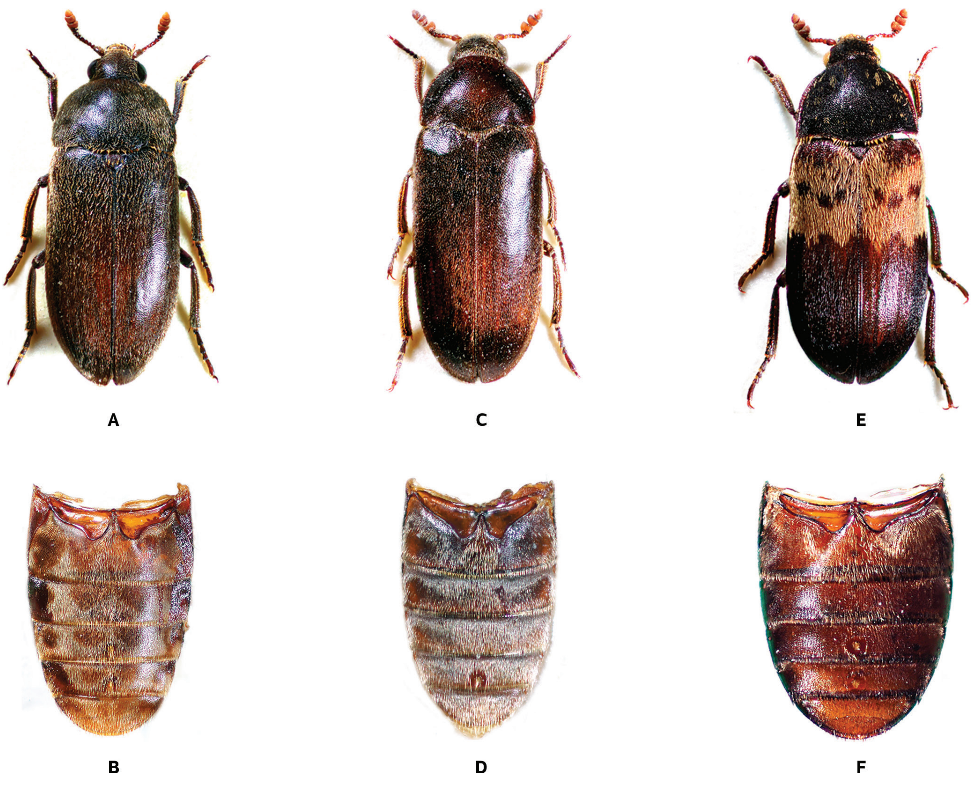

Figure 1. Dorsal habitus and abdominal ventrites (photos by A. Herrmann) of *Dermestes* species **A, B** *D. ater* DeGeer, 1774 **C, D** *D. haemorrhoidalis* Küster, 1852 **E, F** *D. lardarius* Linnaeus, 1758.

Distribution. Nearly cosmopolitan (Háva 2015, 2022), where it is widely distributed in Europe; North Africa; Africa: Burundi, Congo, Madagascar, South Africa, Tanzania, Zambia; Asia: China (Liaoning), Iran, Japan, Mongolia, Oman, Russia, South Korea, Vietnam; Australia: New Zealand (introduced); North America: USA; South America: Argentina, Bolivia, Brazil, Peru, Uruguay.

Dermestes (*Dermestes*) *lardarius* Linnaeus, 1758

Fig. 1E, F

Material examined. Saudi Arabia • 1 ♀; Makkah Province, Jeddah, "Ras Halibah" [Ras Hatibah]; 7 May. 1982; W. Büttiker leg.; JHAC.

Note. Dermestes lardarius was previously reported from Saudi Arabia without a specific locality (Hagstrum and Subramanyam 2009). The only known female representing this species in Saudi Arabia was collected from the coastal area in Jeddah (Makkah Province) (Fig. 4D).

Distribution. Cosmopolitan (Háva 2011, 2015, 2022).

Subgenus *Dermestinus* Zhantiev, 1967

Dermestes (*Dermestinus*) *frischii* Kugellan, 1792

Fig. 2A–C

Material examined. Saudi Arabia • 2 ♂; Baha Province, Al Mandaq, Amadan; 20°12'11"N, 41°13'43"E; 14 Oct. 2010; H.Aldhafer & H.Fadl leg.; M.S. Abdel-Dayem det.; KSMA • 1 ex; Asir Province, Bareq, Thloth Al Mandhar, Wadi Baqrah; 18°47.476'N, 41°56.310'E; 331 m a.s.l.; 20 Apr. 2011; H. Fadl & H. Setyaningrum leg.; LT;M.S. Abdel-Dayem det.; KSMA • 1 ♀; Eastern Province, Al Jubail, Ras al Ghar; 26°15'34"N, 49°52'01"E; 16 Apr. 2010; H. Al Dhafer leg.; HP; J. Háva det.; KSMA • 3 ♂, 4 ♀; Eastern Province, An Nuayriyah, Al Sarar; 27°25'45.5"N, 48°27'00"E; 60 m a.s.l.;, 2 Mar. 2011; H. Al Dhafer, H. Setyaningrum & A. Al Ansi leg.; collected from Carcases; M.S. Abdel-Dayem det.; KSMA • 1 ex; same collection data as for preceding; J. Háva det.; KSMA • 5 ex; Eastern Province, Dammam, near shore; 26°21'3.744"N, 50°13'41.462"E; 3 m a.s.l.; 15 Oct. 2018; A. Alqurashi leg.; PT beside rabbit carcass, M.S. Abdel-Dayem det.; KSMA. • 1 ♂; Makkah Province, Jeddah, Shoiba; 20°51'N, 39°24'E; 1 m a.s.l.; 19 Oct. 1982; W. Büttiker leg.; JHAC • 2 ♂, 1 ♀; Makkah Province, Taif, Al Wesam District; 21°12'17"N, 40°20'43"E; 11 Oct. 2010; H. Al Dhafer, B. Kondratieff, H. Fadl & A. El Gharbawy leg.; M.S. Abdel-Dayem det.; KSMA • 1 ♂, 1 ♀; Riyadh Province, Ad Diriah, Ad Diriah Desert; 6 May. 2010; H. Al Dhafer, A. El Gharbawy & A. El Torkey leg.; MT; M.S. Abdel-Dayem det.; KSMA • 1 ♂, 4 ♀; same collection data as for preceding; Al Amariyah, Animal Production Dept. Farm KSU; 31 Mar. 2008;, LT;M.S. Abdel-Dayem det.; KSMA • 2 ♂, 3 ♀; same collection data as for preceding; Aljabilah, Prince Bander Farm; 26 Apr. 2008; M. Otybi leg.; LT; M.S. Abdel-Dayem det.; KSMA • 1 ♂; same collection data as for preceding; 3 May. 2008; M. Otybi leg.; LT; M.S. Abdel-Dayem det.; KSMA • 1 ♂; same collection data as for preceding; 31 May. 2008; M. Otybi leg.; LT; M.S. Abdel-Dayem det.; KSMA • 1 ♀; same collection data as for preceding; Al Obaiteh, 50 km W. Riyadh, Obikan Farm; 7 May. 2007; M. Otybi leg.; LT; J. Háva det.; KSMA • 1 ♀; same collection data as for preceding; Thonyan Al Thonyan Farm; 28 Jul. 2007; H. Al Ayedh & H. Al Dhafer leg.; LT; M.S. Abdel-Dayem det.; KSMA • 3 ♂, 4 ♀; same collection data as for preceding; Education Farm KSU; 1 Apr. 2008; J. Háva det.; KSMA • 7 ♀; same collection data as for preceding; 2 Apr. 2008; M.S. Abdel-Dayem det.; KSMA • 4 ♂, 6 ♀; same collection data as for preceding; 3 Apr. 2008; M.S. Abdel-Dayem det.; KSMA • 14 ex; same collection data as for preceding; 5 Apr. 2008, M.S. Abdel-Dayem det.; KSMA • 7 ♂, 8 ♀; same collection data as for preceding; 7 Apr. 2008; M.S. Abdel-Dayem det.; KSMA • 2 ♂, 6 ♀; same collection data as for preceding; 9 Apr. 2008; M.S. Abdel-Dayem det.; KSMA • 1 ♂, 11 ♀; same collection data as for preceding 11 Apr. 2008; M.S. Abdel-Dayem det.; KSMA • 1 ♀; same collection data as for preceding; 20 Apr. 2011; H. Setyaningrum leg.; J. Háva det.; KSMA • 1 ♂; Riyadh Province, Alkharj, Al-Shahwan Farm; 24 Mar. 2010; A. Al-Hasbel leg.; SW; J. Háva det.; KSMA • 1 ♀; Riyadh Province, Huraymala, Wadi Huraymala; 770 m a.s.l.; 24 Nov. 1988; C.W. Mills leg.; J. Háva det.; FSCA • 1 ♀; Riyadh Province, Mozahmiya, Al Khararah; 24°24'21"N, 46°14'40"E; 17 Apr. 2012; H. Al Dhafer, H. Fadl, A. El Torkey, M. Abdel-Dayem & A. Al Ansi leg.; LT; M.S. Abdel-Dayem det.; KSMA • 1 ♂, 1 ♀; Riyadh Province, Rumah, Rawdhat khorim; 29 Apr. 2011; Y. Aldryhim leg.; LT; M.S. Abdel-Dayem det.; KSMA • 1 ex; same collection data as for preceding; 25°25.943'N, 47°13.863'E; 572 m a.s.l.; 6 Mar. 2012; PT; M.S. Abdel-Dayem det.; KSMA • 1 ex; same collection data as for preceding; 27 May. 2012; LT; M.S. Abdel-Dayem det.; KSMA.

Note. Mroczkowski (1979) documented this species in Jeddah. Recently it was collected at Jeddah from rabbit carcasses (Al-Shareef and Al-Mazyad 2017) and human remains (Al-Shareef and Zaki 2017), and at Riyadh from camel, dog, and goat carcasses (Mashaly et al. 2019) and human corpses (Alajmi et al. 2016). This species has also been collected from sheep carcasses in Riyadh, Jazan, and Arar (Mashaly et al. 2018). The listed specimens were collected at different elevations (7–1920 m) in the central, east, and lowlands and mountainous areas of southwest Saudi Arabia (Fig. 4B).

Distribution. Cosmopolitan (Háva 2007, 2015, 2022).

***Dermestes* (*Dermestinus*) *maculatus* DeGeer, 1774**

Fig. 2D–F

Material examined. Saudi Arabia • 2 ♀; Baha Province, Al Mandaq, Amadan; 20°12'11"N, 41°13'43"E; 14 Oct. 2010; H. Al Dhafer, B. Kondratieff, H. Fadl & A. El Gharbawy leg.; J. Háva det.; KSMA • 4 ♀; same collection data as for preceding; 14 Oct. 2010; H.Aldhafer & H.Fadl leg.; J. Háva det.; KSMA • 12 ex; Baha Province, Al Baha, Al-Baher Mountain; 15 Mar. 2010; J. Háva det.; KSMA • 1 ♀; Asir Provence, Khamis Mushayt; 2050 m a.s.l.; 9 Jan. 1998; J. Háva det.;, JHAC • 1 ex; Makkah Province; Taif; 21°12'17"N, 40°20'43"E; 11 Oct. 2010; H. Al Dhafer, B. Kondratieff, H. Fadl & A. El Gharbawy leg.; M.S. Abdel-Dayem det.; KSMA • 6 ex; Eastern Province; Dammam, near shore; 26°21'3.744"N, 50°13'41.462"E; 3 m a.s.l.; 15 Oct.

2018, A. Alqurashi leg.; PT beside rabbit carcass; M.S. Abdel-Dayem det.; KSMA • 1 ♀; Riyadh Province, Ad Diriyah, Al Amariyah, Animal Production Dept. Farm KSU; 23 Mar. 2011; H. Setyaningrum leg.; BT; M.S. Abdel-Dayem det.; KSMA • 1 ex; Riyadh Province, Riyadh; Oct.1989; M.S. Abdel-Dayem det.; KSMA • 4 ex; Riyadh Province, Ad Diriyah, Al Amariyah; 28 Jan. 2008; D. Boy Valenza leg., M.S. Abdel-Dayem det.; KSMA • 2 ex; same collection data as for preceding; Albeer Farm; 29 Oct. 2008; A. Al-Ahmari leg.; SW; M.S. Abdel-Dayem det.; KSMA • 1 ex, same collection data as for preceding; 8 Dec. 2010; SW; M.S. Abdel-Dayem det.; KSMA • 2 ♀; Riyadh Province, Ad Diriyah, Education Farm KSU; 1 Apr. 2008; J. Háva det.; KSMA • 1 ex; same collection data as for preceding; 31 Mar. 2008; M.S. Abdel-Dayem det.; KSMA • 1 ex; same collection data as for preceding; 2 Apr. 2008; M.S. Abdel-Dayem det.; KSMA • 1 ex; same collection data as for preceding; 3 Apr. 2008; M.S. Abdel-Dayem det.; KSMA • 3 ex; same collection data as for preceding; 5 Apr. 2008; M.S. Abdel-Dayem det.; KSMA • 1 ex; same collection data as for preceding; 7 Apr. 2008; M.S. Abdel-Dayem det.; KSMA • 3 ex; same collection data as for preceding; 9 Apr. 2008; M.S. Abdel-Dayem det.; KSMA • 2 ex; same collection data as for preceding; 11 Apr. 2008; M.S. Abdel-Dayem det.; KSMA • 1 ex; same collection data as for preceding; 3 Nov. 2009; H. Setyaningrum leg.; M.S. Abdel-Dayem det.; KSMA • 6 ex; Riyadh Province, Riyadh, Al-Wahah Farm; 15 May. 2021; M.S. Abdel-Dayem det.; KSMA • 1 ex; Riyadh Province, Shaqra; 21 May. 1978; HP from mill waste; J. Háva det.; KSMA.

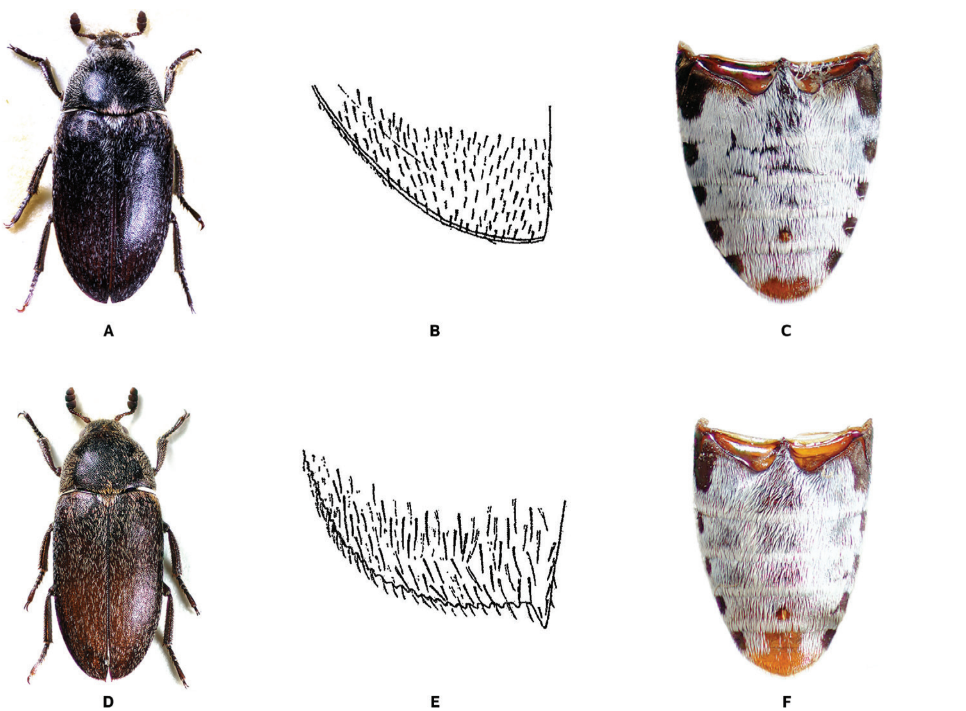

Figure 2. Dorsal habitus, apical part of elytron and abdominal ventrites (photographs by A. Herrmann) of *Dermestes* species. **A–C** *D. frischii* Kugellan, 1792 **D–F** *Dermestes maculatus* DeGeer, 1774.

Note. Dermestes maculatus is the most common species within the subfamily Dermestinae in Saudi Arabia. It was previously collected from rabbit carcasses at Baha (Abouzied 2014), Al-Ahsa (Shaalan et al. 2017), t Madinah (Al-Dakhil and Alharbi 2020), Jeddah (Al-Shareef and Al-Mazyad 2017), and Riyadh (Mashaly 2017). It has been collected from sheep carcasses in Jizan and Northern Border (Mashaly et al. 2018). Al-Qahtni et al. (2020) have reported the species from dead human bodies in Riyadh. Also, it was collected by other methods from Makkah Province, Jeddah (Shalaby 1961; Mroczkowski 1979) and Riyadh Province, Dierab (Elgharbawy 2018). The species was collected in both low- and highlands (10–2330 m) in the following provinces: Asir, Baha, Eastern Province, Madinah, Makkah, and Riyadh (Fig. 4C).

Distribution. Cosmopolitan (Háva 2011, 2015, 2022).

***Dermestes* (*Dermestinus*) *undulatus* Brahm, 1790**

Fig. 3A, B

Material examined. Saudi Arabia • 1 ♀; Asir Province, Khamis Mushayt; 2050 m a.s.l.; 9 Jan.1998;, J. Háva det.; JHAC.

Note. The only specimen known (a female) was collected from the highlands in southwestern Saudi Arabia (Fig. 4A). This is a new record for Saudi Arabia.

Distribution. Holarctic species (Háva 2015, 2022).

Tribe Marioutini Jacobson, 1913
Genus *Mariouta* Pic, 1898

***Mariouta stangei* Reitter, 1910**

Fig. 3C

Record. Saudi Arabia • Eastern Province, Al-Ahsa, Salwah, 248 km S (Rub al Khali) (Mroczkowski and Ślipiński 1997).

Note. This species is only known from a single specimen preserved in the NHMB collection. This specimen was collected by W. Büttiker in May 1985 at a location in the Empty Quarter (Rub al Khali), 248 km south of the town of Salwa in southeastern Saudi Arabia, located near the border with Qatar (Fig. 4D).

Distribution. This taxon is known from the Sultanate of Oman, Pakistan, Saudi Arabia, Sudan, and Turkmenistan (Háva 2015, 2022).

Genus *Rhopalosilpha* Arrow, 1929

***Rhopalosilpha wasmanni* Arrow, 1929**

Fig. 3D

Record. Saudi Arabia • Eastern Province, Hofuf (Mroczkowski and Ślipiński 1997).

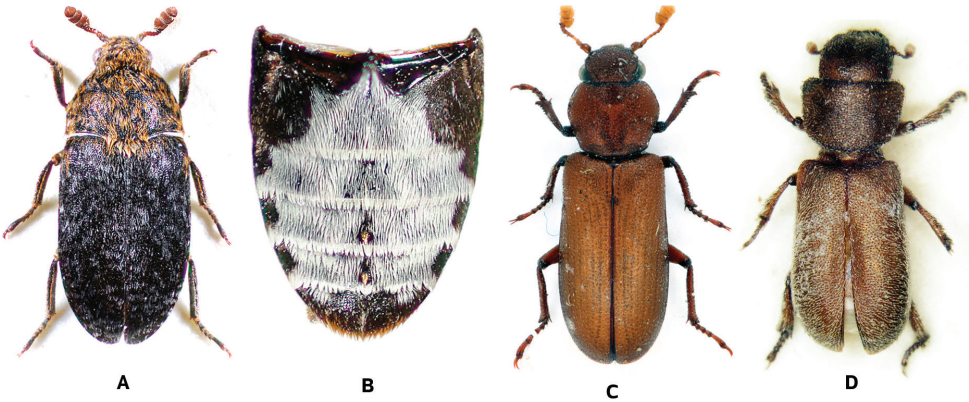

Figure 3. A, B *Dermestes undulatus* Brahm, 1790 (photographs by A. Herrmann) **A** dorsal habitus **B** Abdominal ventrites **C** *Mariouta stangei* Reitter, 1910 (photographs by K. Matsumoto) **D** *Rhopalosilpha wasmanni* Arrow, 1929 (photographs by J. Háva).

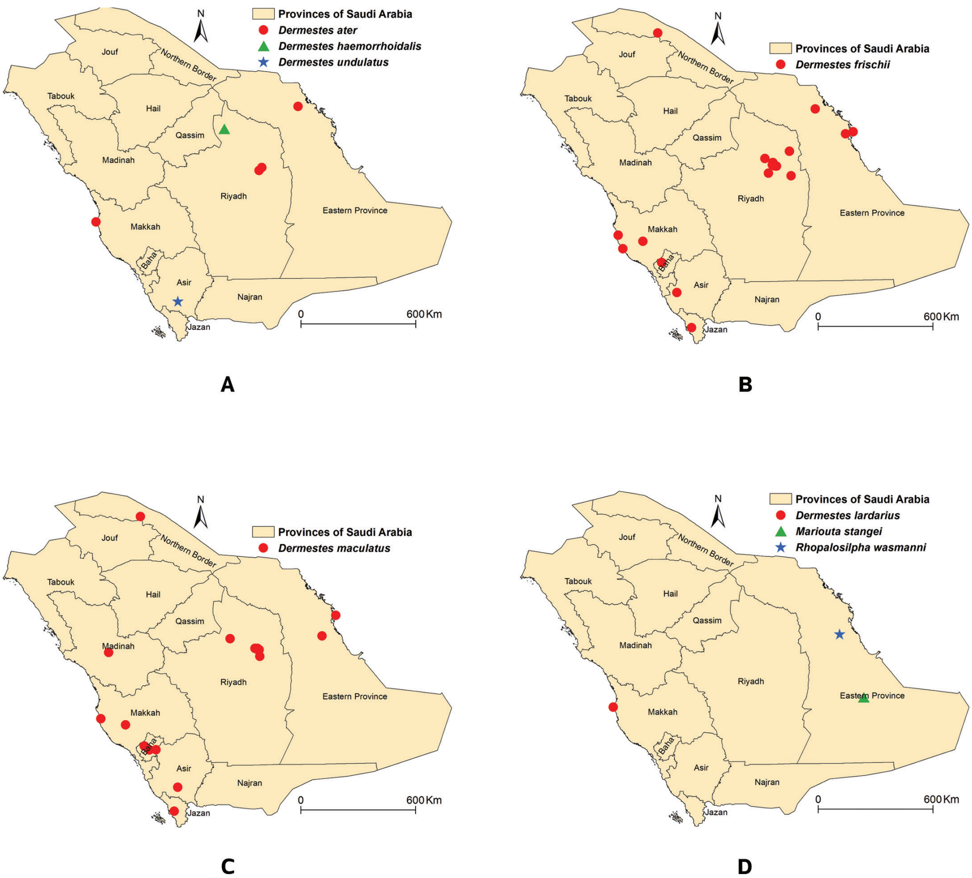

Figure 4. Distribution map of the Dermestinae species in Saudi Arabia **A** *Dermestes ater*, *D. haemorrhoidalis*, and *D. undulatus* **B** *D. frischii* **C** *D. maculatus* **D** *D. lardarius*, *Mariouta stangei*, and *Rhopalosilpha wasmanni*.

Note. Rhopalosilpha wasmanni is only known from a single specimen in the NHMB collection. It was collected from Hofuf in eastern Saudi Arabia by W. Büttiker (Mroczkowski and Ślipiński 1997) (Fig. 4D).

Distribution. This very rare species is known only from Iran, Jordan, and Saudi Arabia (Háva 2015, 2022).

Discussion

The first forensic case being solved using insects was during the 13th century in China, while the first systematic studies of forensic entomology took place in Germany during the 19th century (Benecke 2001). Despite the earlier published data documenting the Saudi fauna of Dermestinae (Shalaby 1961; Mroczkowski 1979), forensic entomology in this country began only during the last two decades. Accordingly, several studies were conducted during this period in four areas: at the centre of the country (Alajmi et al. 2016; Mashaly 2017; Mashaly et al. 2018, 2019; Al-Qahtni et al. 2020), in the east (Shaalan et al. 2017), in the west (Al-Shareef and Al-Mazyad 2017; Al-Shareef and Zaki 2017; Al-Dakhil and Alharbi 2020), and in the southwest (Abouzied 2014). Taxonomic and faunal studies are needed to support this growing interest in forensic entomology in Saudi Arabia.

During the late stage of decay of animal remains, *Dermestes* species are one of the predominant taxa among forensic insects (Magni et al. 2015). *Dermestes frischii* and *D. maculatus* have been the most frequently documented dermestid beetles in forensic studies in Saudi Arabia (Alajmi et al. 2016; Mashaly et al. 2018). The current study listed eight species in three genera (*Dermestes*, *Mariouta*, and *Rhopalosilpha*) in two tribes (Dermestini and Marioutini) belonging to the subfamily Dermestinae. *Dermestes haemorrhoidalis* and *D. undulatus* are recorded for the first time from Saudi Arabia. Based on the world distribution range, the Saudi Dermestinae fauna is dominated by the widespread cosmopolitan or nearly cosmopolitan species, which includes all members of the tribe Dermestini (e.g., *Dermestes ater*, *D. haemorrhoidalis*, *D. lardarius*, *D. frischii*, *D. maculatus*, *D. undulatus*; Háva 2015, 2022) (Table 1), while the members of tribe Marioutini, *Mariouta stangei* and *Rhopalosilpha wasmanni* have a narrower distribution range and appear to have Saharo-Sindian elements (Háva 2015, 2022).

The analysis of data based on the examination of museum specimens and literature records revealed that *D. frischii* and *D. maculatus* are the most abundant and distributed over a fairly wide range in Saudi Arabia. These findings are consistent with what has been documented in several other studies (Shalaby 1961; Mroczkowski 1979; Abouzied 2014; Alajmi et al. 2016; Shaalan et al. 2017; Elgharbawy 2018; Al-Dakhil and Al-Harbi 2020). However, the remaining Dermestinae are rare or very rare species, either documented from a few specimens (e.g., *D. ater*) or a single specimen (e.g., *D. haemorrhoidalis*, *D. lardarius*, *D. undulatus*, *M. stangei*, and *R. wasmanni*). This may be due to different feeding behaviours or a rarity of these species in the Saudi fauna. Although *D. ater*, *D. haemorrhoidalis*, *D. lardarius*, and *D. undulatus* have been reported from human cadavers (Charabidze et al. 2014; Kadej et al. 2020), none of the forensic

Table 1. List of *Dermestes* species from the Arabian Peninsula. Notes: recorded (*) or not recorded (–).

	Kuwait	Saudi Arabia		Yemen		Oman	United Arab Emirates	Qatar
		Farasan Archipelago	Saudi Arabia mainland	Yemen mainland	Socotra Island			
Dermestes (*Dermestinus*) *maculatus* DeGeer, 1774	*	–	*	*	*	*	*	*
Dermestes (*Dermestinus*) *frischii* Kugellan, 1792	*	–	*	*	*	*	*	*
Dermestes (*Dermestinus*) *undulatus* Brahm, 1790	–	–	*	–	–	–	–	–
Dermestes (*Dermestes*) *ater* DeGeer, 1774	–	–	*	*	–	*	*	*
Dermestes (*Dermestes*) *haemorrhoidalis* Küster, 1852	–	–	*	–	–	–	–	–
Dermestes (*Dermestes*) *lardarius* Linnaeus, 1758	–	–	*	*	–	–	*	–

entomological studies in Saudi Arabia reported any of them. As for *Mariouta stangei* and *Rhopalosilpha wasmanni*, no information is available that documents their feeding habits.

Despite more than 60 years since the first faunistic study (Shalaby 1961), we may still have an imprecise idea about the actual species number and faunal composition of Dermestinae in Saudi Arabia. In conclusion, the few numbers of faunistic studies on the Dermestinae in Saudi Arabia and the registration of two new records in the current study indicate that there are more species that have yet to be discovered.

Acknowledgements

We are grateful to Dr Iftekhar Rasool, Plant Protection Department, College of Food and Agriculture Sciences, King Saud University, Saudi Arabia, for processing and arranging specimens for dispatch. The authors extend their appreciation to the Deputyship for Research & Innovation, Ministry of Education in Saudi Arabia for funding this research work through the project no. IFKSURG-2-000.

References

Abdel-Dayem MS, Fad HH, El-Torkey AM, Elgharbawy AA, Aldryhim YN, Kondratieff BC, Al Ansi AN, Aldhafer HM (2017) The beetle fauna (Insecta, Coleoptera) of the Rawdhat Khorim National Park, Central Saudi Arabia. ZooKeys 653: 1–78. https://doi.org/10.3897/zookeys.653.10252

Abdel-Dayem MS, Abu El-Ghiet UM, Elsheikh TM, Elgharbawy AA, Al-Fifi ZIA, Aldhafer HM (2020) The first survey of the Beatles (Coleoptera) of the Farasan Archipelago of the southern Red Sea, Kingdom of Saudi Arabia. ZooKeys 959: 17–86. https://doi.org/10.3897/zookeys.959.51224

Abouzied EM (2014) Insect colonization and succession on rabbit carcasses in Southwestern Mountains of the Kingdom of Saudi Arabia. Journal of Medical Entomology 51(6): 1168–1174. https://doi.org/10.1603/ME13181

Al-Dakhil AA, Alharbi SA (2020) A preliminary investigation of the entomofauna composition of forensically important necrophagous insects in Al-Madinah Al Munawwarah region, Kingdom of Saudi Arabia. Journal of Taibah University for Science 14(1): 1127–1133. https://doi.org/10.1080/16583655.2020.1805176

Alajmi RA, AlGhufaili H, Farrukh A, Aljohani H, Mashaly AM (2016) First report of necrophagous insects on human corpses in Riyadh, Saudi Arabia. Journal of Medical Entomology 53(6): 1276–1282. https://doi.org/10.1093/jme/tjw113

Al-Qahtni AH, Al-Khalifa MS, Mashaly AM (2020) Two human cases associated with forensic insects in Riyadh, Saudi Arabia. Saudi Journal of Biological Sciences 27(3): 881–886. https://doi.org/10.1016/j.sjbs.2019.12.027

Al-Shareef LAH, Al-Mazyad MMF (2017) Beetles (Insecta, Coleoptera) associated with rabbit carcasses in three habitats in Jeddah, Kingdom of Saudi Arabia. Australian Journal of Basic and Applied Sciences 11(2): 139–145.

Al-Shareef LAH, Zaki MK (2017) Arthropods associated with human remains and determination of postmortem interval in Jeddah, Kingdom of Saudi Arabia. The Journal of American Science 13(3): 106–114. https://doi.org/10.7537/marsjas130317.11

Benecke M (2001) A brief history of forensic entomology. Forensic Science International 120(1–2): 2–14. https://doi.org/10.1016/S0379-0738(01)00409-1

Charabidze D, Colard T, Vincent B, Pasquerault T, Hedouin V (2014) Involvement of larder beetles (Coleoptera: Dermestidae) on human cadavers: a review of 81 forensic cases. International Journal of Legal Medicine 128(6): 1021–1030. https://doi.org/10.1007/s00414-013-0945-1

Elgharbawy AA (2018) Survey and population studies of Insects at Dierab Area, South Riyadh, Saudi Arabia. Al Azhar Bulletin of Science 29(1): 47–54. https://doi.org/10.21608/absb.2018.33763

Hagstrum DW, Subramanyam B (2009) Stored-product Insect Resource. American Association of Cereal Chemists International, St. Paul, 509 pp.

Háva J (2007) New species and new records of Dermestidae (Insecta: Coleoptera) from the Arabian Peninsula including Socotra Island. Fauna of Arabia 23: 309–317.

Háva J (2011) Contribution to the Dermestidae (Coleoptera) from the Arabian Peninsula—1. Latvijas Entomologs 50: 5–8.

Háva J (2015) World Catalogue of Insects. (Vol. 13). Dermestidae (Coleoptera). Brill, Leiden/Boston, [xxvi +] 419 pp. https://doi.org/10.1163/9789004286610

Háva J (2022) Dermestidae World (Coleoptera) [Version 2018, updated January 2022]. https://doi.org/10.24394/NatSom.2022.38.19 [Accessed on: 2022-12-19]

Kadej M, Szleszkowski Ł, Thannhäuser A, Jurek T (2020) A mummified human corpse and associated insects of forensic importance in indoor conditions. International Journal of Legal Medicine 34(5): 1963–1971. https://doi.org/10.1007/s00414-020-02373-2

Magni PA, Voss SC, Testi R, Borrini M, Dadour IR (2015) A biological and procedural review of forensically significant *Dermestes* species (Coleoptera: Dermestidae). Journal of Medical Entomology 52(5): 755–769. https://doi.org/10.1093/jme/tjv106

Mashaly AM (2017) Carrion beetles succession in three different habitats in Riyadh, Saudi Arabia. Saudi Journal of Biological Sciences 24(2): 430–435. https://doi.org/10.1016/j.sjbs.2016.02.015

Mashaly AM, Al-Ajmi RA, Al-Johani HA (2018) Molecular identification of the carrion beetles (Coleoptera) in selected regions of Saudi Arabia. Journal of Medical Entomology 55(6):1423–1430. https://doi.org/10.1093/jme/tjy116

Mashaly AM, Al-Ajmi RA, Rady A, Al-Musawi Z, Farrukh A (2019) Species richness of scavenger insects on different carcass types. Tropical Biomedicine 36(3): 630–639.

Motyka M, Kusy D, Háva J, Jahodářová E, Bílkova R, Vogler AP, Bocak L (2022) Mitogenomic data elucidate the phylogeny and evolution of life strategies of Dermestidae (Coleoptera). Systematic Entomology 47(1): 82–93. https://doi.org/10.1111/syen.12520

Mroczkowski M (1979) Insects of Saudi Arabia. (Coleoptera, Dermestidae). Part 1, faunistic data. Fauna of Saudi Arabia 1: 212–214.

Mroczkowski M, Ślipiński SA (1997) Notes on the Marioutinae (Coleoptera: Dermestidae) with a review of the described species. Annales Zoologici 47: 11–16.

Shaalan EA, El-Moaty ZA, Abdelsalam S, Anderson GS (2017) A preliminary study of insect succession in Al-Ahsaa Oasis, in the Eastern region of the Kingdom of Saudi Arabia. Journal of Forensic Sciences 62(1): 239–243. https://doi.org/10.1111/1556-4029.13252

Shalaby F (1961) A preliminary survey of the insect fauna of Saudi Arabia. Bulletin de la Société Entomologique d'Egypte 45: 211–228.

ZooKeys 1138: 175–182 (2023)
doi: 10.3897/zookeys.1138.82224
https://zookeys.pensoft.net

RESEARCH ARTICLE

A peer-reviewed open-access journal
ZooKeys
Launched to accelerate biodiversity research

Parathlasia gen. nov. (Hemiptera, Cicadellidae, Ledrinae, Ledrini), a new leafhopper genus from Guizhou, China

Yu-Jian Li[1], Li-Na Jiang[1], Zi-Zhong Li[2], Ji-Chun Xing[2]

1 *School of Life Sciences, Qufu Normal University, Qufu, Shandong Province 273165, Qufu, China* **2** *Institute of Entomology, Guizhou University, Guiyang, Guizhou Province 550025, Guiyang, China*

Corresponding author: Yu-Jian Li (yujian528@163.com)

Academic editor: J. Adilson Pinedo-Escatel | Received 14 February 2022 | Accepted 15 December 2022 | Published 6 January 2023

https://zoobank.org/F71611BC-D19F-4975-82B9-0C6545B918C2

Citation: Li Y-J, Jiang L-N, Li Z-Z, Xing J-C (2023) *Parathlasia* gen. nov. (Hemiptera, Cicadellidae, Ledrinae, Ledrini), a new leafhopper genus from Guizhou, China. ZooKeys 1138: 175–182. https://doi.org/10.3897/zookeys.1138.82224

Abstract

Parathlasia **gen. nov.**, a new leafhopper genus and species of Ledrini, *P. guizhouensis* **sp. nov.**, from Guizhou, China are described. Morphological differences between the new genus to other related Chinese genera are discussed. A key to distinguish *Parathlasia* from other similar genera is given.

Keywords

Auchenorrhyncha, Homoptera, key, *Midoria*, morphology, new genus, new species, taxonomy, *Thlasia*, *Yelahanka*

Introduction

The leafhopper subfamily Ledrinae is a rather special group with many prominent and unique features (Jones and Deitz 2009). It is a large group distributed worldwide with a preference for the tropics and subtropics, usually feeding on trees and shrubs. Of the four (Dietrich 2005) or five (Jones and Deitz 2009) recognized tribes the largest, Ledrini, comprises leafhoppers with a dorsum coarsely pitted or knobbed, lamellate or foliaceous anterolaterally with the head spatulate and face generally concave (Fig. 1A, B), forewings punctate with extra apical veins (Fig. 1D) or venation reticulate in the apical two-thirds. China is one of the main distribution areas of Ledrinae in the world (Li and Li 2008), with more than 160 species belonging to 23 genera. While sorting and identifying ongoing samples of ledrine leafhoppers from China, we found a new genus (with one new species) similar in appearance to *Thlasia* Germar but sharing similarities also with other Chinese genera, which are extensively described and illustrated below.

Material and methods

Terminology used in this study is mainly based on Dietrich (2005) and Jones and Deitz (2009). Dry specimens were used for preparing descriptions and illustrations. External morphology was observed under a stereoscopic microscope. Body length was measured with an ocular micrometer, in millimeters, from the apex of head to the apex of the forewing at rest. Genital segments were examined and macerated in 10% KOH solution, washed in water and transferred to glycerin. Illustrations were made by eye using a Leica MZ 12.5 stereomicroscope. Multiple photographs were taken with a Leica D-lux 3 digital camera. Final digital images were compiled into Adobe Photoshop for labeling and plate composition. Specimens studied are deposited at the School of Life Sciences, Qufu Normal University, Qufu, China (**QFNU**) and the Institute of Entomology, Guizhou University, Guiyang, China (**GUGC**).

Key to known genera of Ledrinae from China

1	Tibia of hindfoot flat, foliaceous	**2**
–	Tibia of hindfoot, not foliaceous	**9**
2	Pronotum usually prominent, humped-like; with lateral extensions	**3**
–	Pronotum often declivous or weakly prominent; without extensions but lateral area concave	**4**
3	Lateral edge of pronotum laminately subangularly dilated	***Eleazara* Distant**
–	Lateral edge of pronotum straight	***Complanledra* Cai & He**
4	Lateral area of pronotum with ear shaped protrusions or longitudinal ridges	***Ledra* Fabricius**
–	Lateral area of pronotum without ear shaped protrusions	**5**
5	Crown elongate, middle length of crown greater than width between eyes	***Ledropsis* White**
–	Crown not significantly elongated, middle length of crown less than width between eyes	**6**
6	Crown ridge present	7
–	Crown without or weak ridge	***Confucius* Distant**
7	Forewing without a developed, sclerotized tubercle at first split of M vein	***Paraconfucius* Cai**
–	Forewing with a developed, sclerotized tubercle at first split of M vein	**8**

8 Crown with 2 window-like patches; bend at end of style with a small protuberance .... ***Funkikonia* Kato**
– Crown without window-like patch; bend at end of style without a small protuberance .... ***Kuohledra* Cai & He**
9 Forewing cells strongly depressed, forewing veins raised........ ***Dusuna* Distant**
– Forewing cells not strongly depressed, forewing veins raised not significantly **10**
10 Lateral edge of pronotum protrude in an angular shape **11**
– Lateral edge of pronotum not protrude in an angular shape........ **14**
11 Pronotal lateral extensions broad, with margins subtriangular **12**
– Pronotal lateral extensions broad, with margins rounded .... ***Thlasia* Germar**
12 Body large, length longer than 19 mm; style with long fine setae on inner edge .... ***Macrotrichia* Zhang, Sun & Dai**
– Body medium, length longer usually 10–15 mm; style without long fine setae on inner edge........ **13**
13 Lateral extensions of pronotum broad and well developed .... ***Tituria* Stål**
– Lateral extensions of pronotum narrow and not well developed .... ***Neotituria* Kato**
14 Body small, length 6–9 mm........ **15**
– Body moderate, longer than 9 mm **18**
15 Center of crown with a longitudinal groove .... ***Petalocephaloides* Kato**
– Center of crown with a longitudinally ridged or flat........ **16**
16 Center of crown flat; base of forewing A veins not raised **17**
– Center of crown with a longitudinally ridged; base of forewing A veins prominent .... ***Parapetalocephala* Kato**
17 Aedeagus longitudinally flat or slender, with ventral process........ **23**
– Aedeagus slender, without ventral process .... ***Arenoledra* Kuoh**
18 Body stout; style with an odontoid process on the outside of the bend near end **19**
– Body slender; style without odontoid process on the outside near end **20**
19 Forewing terminal venation reticulate; aedeagus slender........ ***Destinoides* Cai & He**
– Forewing terminal venation not reticulate; aedeagus longitudinally flattened .... ***Destinia* Nast**
20 Crown wider than the front of pronotum; pygofer posterior margin concave........ ***Laticorona* Cai**
– Crown narrower than pronotum; pygofer posterior margin not concave **21**
21 Crown broadly rounded; aedeagus slender, terminal with 2 pairs of processes........ ***Pachyledra* Schumacher**
– Crown parabolic; aedeagus without process or with 1 pair of processes **22**
22 Forewing A_1 vein prominent .... ***Platycephala* Kuoh**
– Forewing A_1 vein not prominent........ ***Petalocephala* Stål**
23 Aedeagus with paired ventral processes........ ***Midoria* Kato**
– Aedeagus with single ventral process .... ***Parathlasia* gen. nov.**

Taxonomy

Parathlasia **Li, Jiang, Li & Xing, gen. nov.**

https://zoobank.org/11D3E520-25B6-4311-9FDC-D652CB159CEF
Figures 1–3

Type species. *Parathlasia guizhouensis* Li, Jiang, Li & Xing, sp. nov.

Description. Medium-sized, 7.5–8.0 mm long (including tegmen); yellowish to sordid brown. Head (Fig. 1A, B) with crown declivous, in dorsal view nearly twice as long and five times wider than eye; median carina complete but weakly elevated, weakly concave either side of midline, with some granular protuberances; ocelli (Fig. 1A)

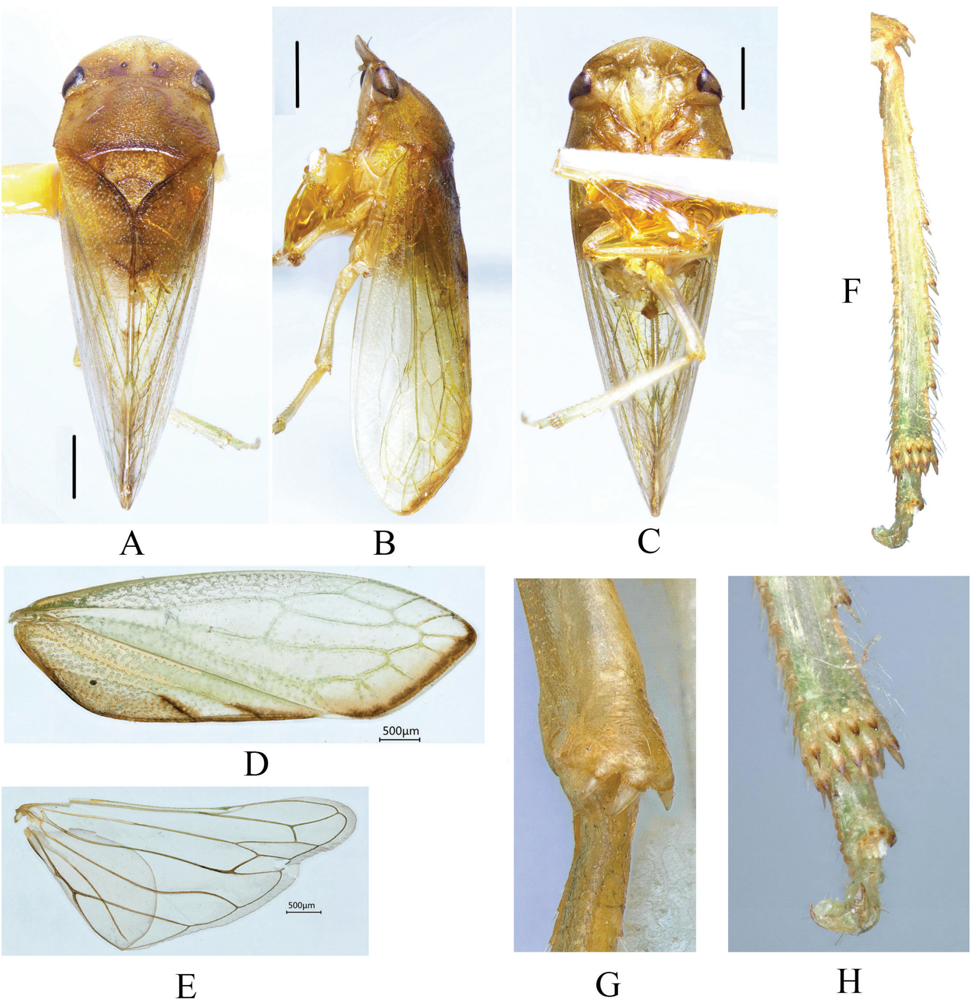

Figure 1. External morphology of *Parathlasia guizhouensis* sp. nov. **A** dorsal habitus **B** lateral habitus **C** ventral habitus **D** forewing **E** hindwing **F** hind tibia **G** apex of hind femora **H** apex of hind leg.

submarginal and close to posterior margin, closer to midline than corresponding eyes. Face (Fig. 1C) including eyes shorter than wide; frontoclypeus flattened. Pronotum slightly wider than head with anterior margin slightly convex, lateral margins oblique, slightly divergent posteriorly. Metanotum (Fig. 1A) two-thirds length of pronotum with distinct transverse depression. Forewing (Fig. 1A, B, D) with apical margin strongly oblique, three subapical cells, inner subapical open, middle subapical closed, extra apical cells present; appendix very narrow. Hind leg as in Fig. 1F, H.

Male pygofer (Fig. 2A, E) with long ventrocaudal process; with some small stout setae subapically. Xth segment very short. Subgenital plates (Fig. 2A, H) fused basally, elongate, inner margin with short spine-like setae. Aedeagus (Fig. 2B, C, F, I) with shaft somewhat elongate, tubular, curved dorsally with a ventral medial process, gonopore apical on ventral surface; basal apodeme distinct. Style (Fig. 2C, D, F, I) elongate, apophysis curved ventrally, apex truncate. Connective (Fig. 2C, F, I) T-shaped.

Female unknown.

Distribution. China (Guizhou) (Fig. 3).

Etymology. The name of the new genus refers to the similarity of the genus to *Thlasia* Germar externally.

Remarks. The new genus is similar in appearance to *Thlasia* Germar, *Midoria* Kato and *Yelahanka* Viraktamath, Webb & Yeshwanth in its relatively small size with a short head and with similar extra apical forewing veins but lacking accessory cross veins. In addition, the oblique forewing apex in *Parathlasia* is also found in some species of *Yelahanka* (see Viraktamath et al. 2021) and long ventrocaudal pygofer process is found also in some species of *Thlasia* (see Zhang et al. 2004). It differs from these and other Ledrinae in having the aedeagus with a single ventral medial process (Fig. 2B, F); *Midoria* has paired ventral processes on the aedeagus (Li and Li 2010, 2011).

The new genus also appears closely related to *Parapetalocephala* Kato. The main difference between *Parathlasia* and *Parapetalocephala* are the forewing veins which in the later genus are prominent (see Jones and Deitz 2009).

Parathlasia guizhouensis **Li, Jiang, Li & Xing, sp. nov.**

https://zoobank.org/9443BF3B-7115-49C6-8F7D-D387C3B90636
Figures 1–3

Description. Head (Fig. 1A) yellowish brown, base of crown with some darker brown marking, ocelli reddish brown. Thorax sordid brown; forewings (Fig. 1A, B, C, D) yellowish hyaline apically margined with brown.

Crown flat, more or less horizontal, surface punctate with median short ridge on posterior margin, about 0.4 times as long as wide between eyes. Ocelli not prominent, closer to each other than to adjacent eye. Pronotum shallowly foveate on either side of median line in anterior half, posterior half slightly gibbous, anterior margin slightly convex, posterior margin medially concave, lateral margin somewhat straight, about

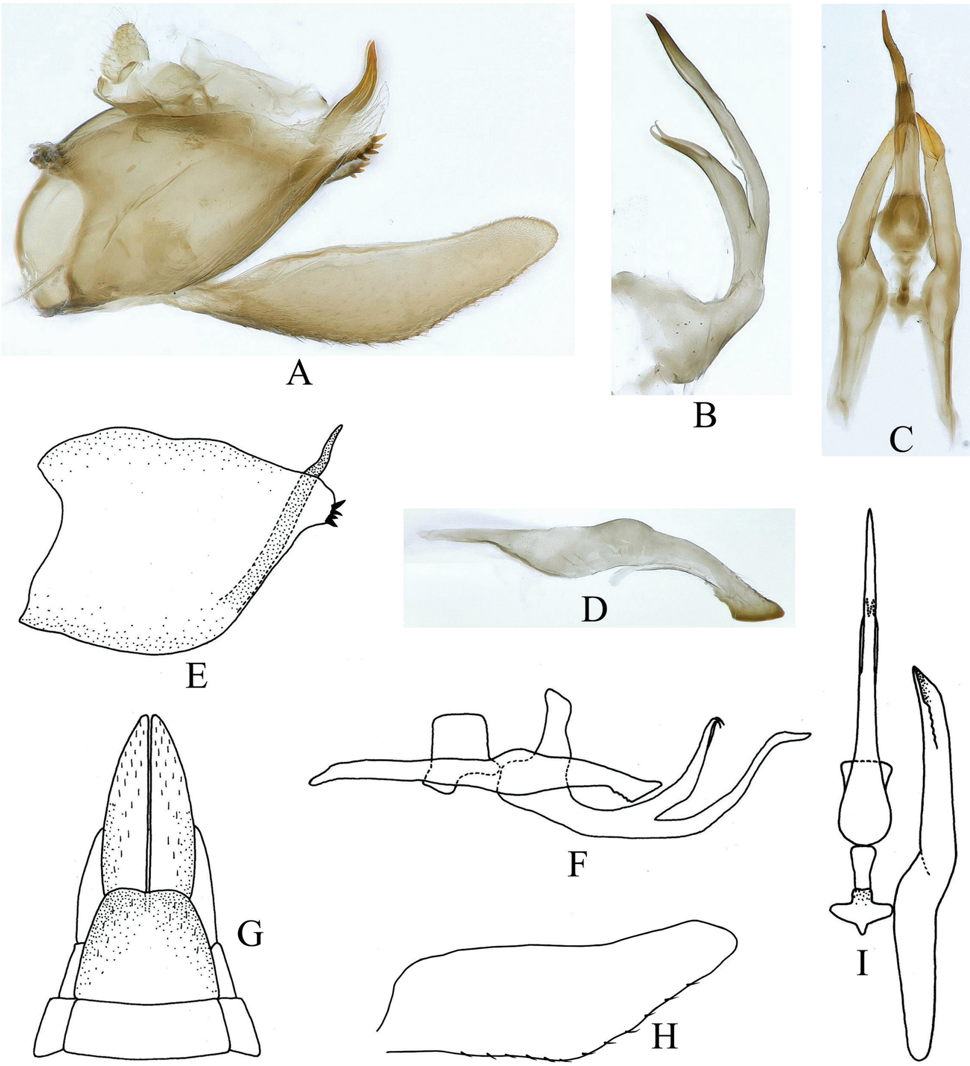

Figure 2. Male genitalia of *Parathlasia guizhouensis* sp. nov. **A** genital capsule, lateral view **B** aedeagus, lateral view **C** aedeagus, connective and style, ventral view **D** right style, lateral view **E** pygofer, lateral view **F** aedeagus, connective and style, lateral view **G** apex of abdomen, ventral view **H** subgenital plate **I** aedeagus, connective and style, ventral view.

1.85 times as long medially as crown. Mesonotum shorter than pronotum. Forewing claval region densely punctate, apical margin obliquely truncate.

Pygofer anterior margin deeply bilobed, posterior margin slightly sinuate, in lateral view about 1.2 times as long as height, ventro-cauadal process long, extending beyond dorsal pygofer margin, with some conical protrusions at end of ventral margin. Subgenital plate widest in mid-region tapering both anteriorly and posteriorly, apex acutely angled. Style broad in middle region, tapering forward and backward,

Figure 3. Distribution of *Parathlasia guizhouensis* sp. nov.

apophysis curved ventrally with axe shaped apex. Aedeagal shaft (Fig. 2B, C, F, I) bifurcate apically; ventral processes elongate, curved dorsally, longer than shaft. Other male genitalia characteristics as in Figs 1 and 2.

The characteristics of female are unknown.

Measurement. Length (including tegmen): ♂, 7.5–8.0 mm.

Type material. ***Holotype*:** ♂, China: Guizhou, Fanjingshan, Huguosi, 29 May 2002, coll. Li Zizhong (QFNU). ***Paratypes*:** 6♂♂, same data as holotype; 2♂♂, same data as holotype except 29 July 2001, coll. Yang Maofa (GUGC); 1♂, China: Guizhou, Leigonghan, Lianhuaping, 2 June 2005, coll. Li Zizhong and Zhang Bin (GUGC) (see Fig. 3 for geographic distributions of new species).

Host plant. Unknown.

Etymology. The species name is derived from the type locality.

Acknowledgements

We thank Mr M. D. Webb (Natural History Museum, London, UK) for suggestions to earlier manuscript and improve thoughtfully. We thank Dr J. Adilson Pinedo-Escatel (University of Illinois at Urbana-Champaign Champaign, USA) and an anonymous reviewer for reading the manuscript and making some suggestions. This project is supported by the Young Talents Invitation Program of Shandong Provincial Colleges and Universities (Grant No. 20190601).

References

Dietrich CH (2005) Keys to the families of Cicadomorpha and Subfamilies and Tribes of Cicadellidae (Hemiptera: Auchenorrhyncha). The Florida Entomologist 88(4): 10–15. https://doi.org/10.1653/0015-4040(2005)88[502:KTTFOC]2.0.CO;2

Jones JR, Deitz LL (2009) Phylogeny and systematics of the leafhopper subfamily Ledrinae (Hemiptera: Cicadellidae). Zootaxa 2186(1): 1–120. https://doi.org/10.11646/zootaxa.2186.1.1

Li YJ, Li ZZ (2008) Research Progress in Ledrinae Taxonomy. Guizhou Agricultural Sciences 36: 110–112.

Li YJ, Li ZZ (2010) A taxonomic study of the genus of *Midoria* Kato (Hemiptera: Cicadellidae: Ledrinae) with descriptions of two new species from China. Zootaxa 2451(1): 63–68. https://doi.org/10.11646/zootaxa.2451.1.5

Li YJ, Li ZZ (2011) Descriptions of six new species of *Midoria* Kato (Hemiptera: Cicadellidae: Ledrinae) from China with a key to the species of the genus. Zootaxa 2897(1): 57–63. https://doi.org/10.11646/zootaxa.2897.1.6

Viraktamath CA, Webb MD, Yeshwanth HM (2021) Leafhopper subfamily Ledrinae of the Indian subcontinent: 1, Description of *Yelahanka* gen. nov. (Hemiptera: Cicadellidae) with seven new species and new combinations. Zootaxa 4915(4): 451–480. https://doi.org/10.11646/zootaxa.4915.4.1

Zhang YL, Yang LH, Webb MD, Sun Q (2004) Type specimens of Jacobi's Fukien leafhoppers and description of three new species from China (Insecta: Auchenorrhyncha: Cicadellidae: Ledrinae: Penthimiinae). Entomologische Abhandluagen (Dresden) 62: 83–92.

ZooKeys 1138: 183–209 (2023)
doi: 10.3897/zookeys.1138.96201
https://zookeys.pensoft.net

RESEARCH ARTICLE

A peer-reviewed open-access journal
ZooKeys
Launched to accelerate biodiversity research

Three Loxocaudinae species (Ostracoda, Podocopida) from South Korea

Hyunsu Yoo[1*], Pham Thi Minh Huyen[2*], Jinho Chae[1], Ivana Karanovic[3,4*]

1 *Marine Environmental Research and Information Laboratory (MERIL), 17, Gosan-ro, 148 beon-gil, Gunpo-si, Gyoenggi-do, 15180, Republic of Korea* **2** *Department of Applied Chemistry and Biological Engineering, Graduate School Department of Molecular Science and Technology, Ajou University, Suwon, 16499, Republic of Korea* **3** *Department of Life Science, College of Natural Sciences, Hanyang University, Seoul, 04763, Republic of Korea* **4** *Research Institute for Convergence of Basic Science, Hanyang University, Seoul 04763, Republic of Korea*

Corresponding authors: Hyunsu Yoo (yhs@meril.co.kr), Ivana Karanovic (ivana@hanyang.ac.kr)

Academic editor: Sarah Gerken | Received 11 October 2022 | Accepted 16 December 2022 | Published 6 January 2023

https://zoobank.org/B7224B8C-4808-48B4-A2F7-DDF5EAF204E2

Citation: Yoo H, Huyen PTM, Chae J, Karanovic I (2023) Three Loxocaudinae species (Ostracoda, Podocopida) from South Korea. ZooKeys 1138: 183–209. https://doi.org/10.3897/zookeys.1138.96201

Abstract
For many ostracod groups in Korea, published records are missing or are very limited. Loxocaudinae is one such subfamily, with only one named species, *Loxocauda orientalis* Schornikov, 2011 reported from Korea. Having fewer than 50 species, this subfamily can be considered a small ostracod group, with most of the species known only by their shell morphology. The diagnoses of genera are based on the shell characters that are often homoplastic, and soft body appendages that are difficult to observe, such as the mandibular exopodite. Because of this, the validity of the entire subfamily and some of its genera have been questioned. Here three Loxocaudinae species were collected from the marine macrobenthic assemblages from Korea. Two are new and belong to the genus *Glacioloxoconcha* Hartmann, 1990, previously known only from Antarctica: *Glacioloxoconcha jeongokensis* **sp. nov.** and *Glacioloxoconcha jisepoensis* **sp. nov.** *Loxocauda orientalis* is briefly redescribed, with some of the populations having unusual morphological features. COI and 18S rRNA sequences of all three species are provided and the latter marker used to assess the position of the subfamily within the family Loxoconchidae and the superfamily Cytheroidea. The resulting tree shows that within the family Loxoconchidae, the genera *Glacioloxoconcha* and *Loxocauda* Schornikov, 1969 are the most closely related, with very shallow but well-supported branches. Polyphyletic and paraphyletic natures of several Cytheroidea families are discussed, inferred from the reconstructed phylogeny.

Keywords
Biodiversity, Cytheroidea, Loxoconchidae, phylogeny, taxonomy

* These authors contributed equally to this work.

Introduction

The subfamily Loxocaudinae was established by Schornikov (2011a) to encompass the following five genera: *Glacioloxoconcha* Hartmann, 1990; *Loxocauda* Schornikov, 1969; *Phlyctocythere* Keij, 1958; *Pseudoloxoconcha* Müller, 1894, and *Sarmatina* Stancheva, 1984. It is a relatively small group of ostracods, currently accounting for 34 described species, of which 20 belong to *Phlyctocythere*, ten to *Loxocauda*, two to *Pseudoloxoconcha*, and one each to *Glacioloxoconcha* and *Sarmatina*. Their most noticeable morphological characteristics are a prominent caudal process on the shell, an adont hinge, a compact naupliar eye (without eye tubercles), and a smooth shell (with a reduced lateral sculpture). The majority of species were described based on their shells only, and little is known about the soft parts morphology. Soft parts have been described only for one species of *Glacioloxoconcha*, four species of *Loxocauda*, and one each species for *Pseudoloxococnha* and *Phlyctocythere*. Consequently, some authors doubt the validity of a few genera, and the current systematic position of a number of species (Ikeya and Hanai 1982; Schornikov 2011a). Besides the lack of information regarding the soft parts morphology, the reason is also a high similarity in the shell morphology between species currently belonging to different Loxocaudinae genera.

The subfamily Loxocaudinae has a worldwide distribution and species inhabit marine and brackish waters (Brandão and Karanovic 2022). In South Korea, the subfamily is represented by 11 species (Schornikov 2011a), most of which are left in the open nomenclature. Only one of them, *L. orientalis* Schornikov, 2011, was described from the sea grass beds and it seems to be distributed across the northern part of the Far East region (Schornikov 2011b). Here we report two new *Glacioloxoconcha*, and briefly redescribe *L. orientalis*. The genus *Glacioloxoconcha* was originally described from Antarctica (Hartmann 1990) to include *G. suedshetlandensis* Hartmann, 1990, a small phytal species with a conspicuous morphology. In this species all the claws on appendages are weak, segments of antennula and antenna are slender, and male copulatory organ has strong frontal chitinous braces. The new Korean species have also been collected from algal and macrobenthic assemblages. We provide 18S rRNA and CO1 gene sequence data for the two new *Glacioloxoconcha* and *L. orientalis*. The aims of this paper are to provide additional details of the soft body morphology of Loxocaudinae, and reconstruct its phylogenetic position within Cytheroidea. As a result of the phylogenetic reconstruction, we briefly discuss the systematics of the superfamily Cytheroidea.

Materials and methods

Sampling methods and taxonomy

Macrobenthos attached to boat moorings were initially collected by scuba diving. When brought ashore it was washed and rinsed through a hand-net (mesh size is 63 μm) (Figs 1–3), and directly fixed in 99% ethanol on site. Sorting and dissecting were done under a stereomicroscope (Olympus SZX12) in the laboratory at Hanyang University. Soft parts are first used for the DNA extraction and after that dissected and mounted on slides in the CMC-10 Mounting Media (Masters Company, Inc.). The valves were mounted on SEM stubs and latter stored on micropaleontological slides. All drawings were prepared using a drawing tube, attached to the microscope ZEISS Axioskop 50. For observations under the scanning electron microscope (SEM), carapaces were coated with platinum. SEM photographs were taken at the National Institute of Biological Resources (**NIBR**) and at Hanyang University with JEOL JSM-6390 and COXEM EM-30 electron microscopes. All specimens are deposited either in the collections of the National Institute of Biological Research (**NIBR**) or in the National Marine Biodiversity Institute of Korea (**MABIK**).

DNA extraction and molecular data analysis

The extraction followed the HotSHOT method described in Pham et al. (2021). PCR reactions for 18S rRNA gene were carried out in 25 µl volume containing: 5 µl of

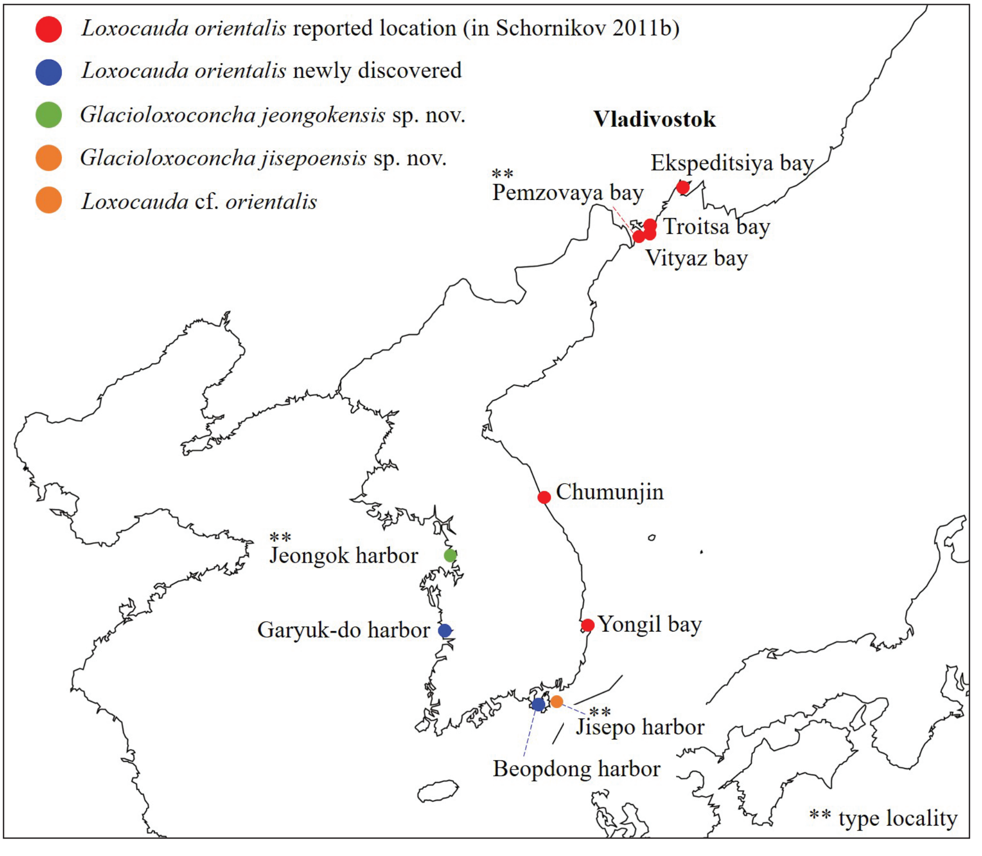

Figure 1. Map of sampling locations from Schornikov (2011b) and the newly collected samples.

Figure 2. Photographs of the mooring structure near various harbors **A** Jeongok harbor **B** Jisepo harbor **C** Beopdong harbor **D** Garyuk-do harbor.

diluted DNA template, 1 μl of 10 pmol/μl forward and reverse primers, 15 μl free RNA&DNA water and 5 μl AccuPower PCR premix (Bioneer Inc.). COI gene amplification reactions were carried out in 21 μl: 10 μl HotStar Taq mastermix (Qiagen), 5 μl water, 1 μl of each primer at 10 pmol/μl and 2 μl DNA template. Primers used in this study along with the PCR settings are listed in Suppl. material 1. COI primers were designed with the webtool PrimerDesign-M following Brodin et al. (2013) and Yoon and Leitner (2015). PCR products were electrophoresed (for 20 min at 100 V) on 1% agarose gels (0.5X TAE buffer dyed with GelRed Nucleic Acid Gel Stain) to determine the presence of target DNA bands. PCR products were purified for sequencing by ethanol precipitation and neutralized by sodium acetate (pH 5.5). Sequencing reactions were run for both strands to confirm sequence reliability using the Sanger method for dideoxy sequencing (Macrogen Inc. and Bionic Inc., Seoul, South Korea). All obtained sequences have been deposited in GenBank (Suppl. material 2).

Phylogenetic trees were constructed based on the alignment of 18S rRNA and COI genes. For 18S tree, in addition to the newly obtained sequences, we also included 47 sequences belonging to the sub-order Cytherocopina Baird, 1850 deposited on GenBank. Of all available sequences attributed to Cytherocopina we only used those that belong to individuals identified to the species level (see Suppl. material 2).

Figure 3. Photographs of a macrobenthos sample including algae (after rinsing).

We have chosen *Terrestricythere pratensis* Schornikov, 1980, as the outgroup to root the 18S tree, and *Krithe kamchatkaensis* Yoo, Tanaka, Lee, Brandão & Karanovic, 2019 as the outgroup to root the COI tree. Uncorrected p-distances between sequences were calculated in MEGA 7 (Kumar et al. 2016). The best fit evolutionary model was calculated based on the Akaike Information Criterion (AIC) as implemented in

ModelFinder (Kalyaanamoorthy et al. 2017). Bayesian Inference, implemented in BEAST v. 2.6.4 (Bouckaert et al. 2014), was used to estimate phylogenetic relationships. Settings included the best fit evolutionary model with four gamma categories and a strict molecular clock. The analysis run for 10,000,000 generations, sampling every 1,000 generations. Tracer v. 1.7.1 (Rambautet et al. 2014) was used to visualize the results of the analyses. The final phylogenetic trees were rooted and visualized by FigTree v. 1.4.3 (Rambaut 2010).

Abbreviations used in text and figures:

A1	Antennula;
A2	Antenna;
BO	Brushed organ;
GF	Genital field;
H	Height;
Hp	Hemipenis;
L	Length;
LV	Left valve;
L5–7	Leg 5–7;
Md	Mandibula;
Mxl	Maxillula;
RV	Right valve.

Results

Systematics

Order Podocopida Sars, 1866
Family Loxoconchidae Sars, 1925
Subfamily Loxocaudinae Schornikov, 2011
Genus *Glacioloxoconcha* Hartmann, 1990

Glacioloxoconcha jeongokensis **sp. nov.**
https://zoobank.org/E7DC6CA1-4CBE-4BCF-8735-2A5C3E3B3372
Figs 4–6

Material examined. ***Holotype***, male, dissected on one slide (NIBRIV0000882303) and shell on micropaleontological slide (NIBRIV0000882313); ***Allotype***, female, dissected on one slide (NIBRIV0000882309) and shell on micropaleontological slide (NIBRIV0000882311); ***Paratypes*****:** one male and one female dissected on each slide, and shell on micropaleontological slides; ~ 20 specimens kept in 2 ml vial in 99% alcohol.

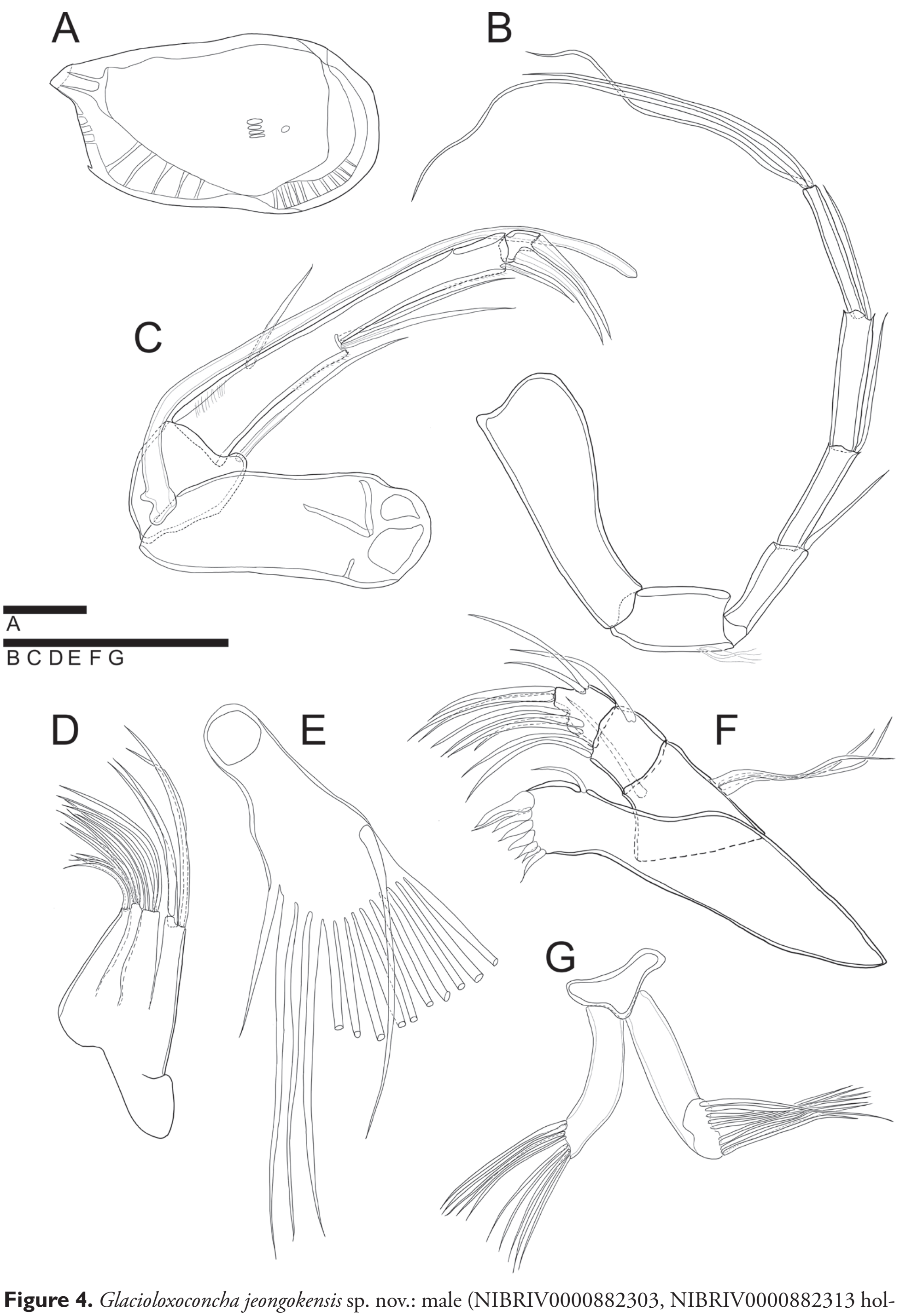

Figure 4. *Glacioloxoconcha jeongokensis* sp. nov.: male (NIBRIV0000882303, NIBRIV0000882313 holotype) **A** LV internal view **B** A1 **C** A2 **D** endopodite of Mxl **E** vibratory organ **F** Md **G** BO. Scale bars: 50 μm (**B–F**); 100 μm (**A**).

Type locality. South Korea, Gyeonggi-do, Hwaseong-si, Seosin-myeon, Jeongokhang-ro, Yacht mooring. 37°11.179'N, 126°39.024'E, 25 October 2019, leg. Hyunsu Yoo & Byung-jin Yoo.

Etymology. The species is named after the yacht mooring place from where it was collected.

Description. Male. ***Carapace*** (Figs 4A, 6). Relatively small, L ~ 356 μm, H ~ 189 μm. RV overlapping LV dorsally. Carapace subquadrate form in lateral view (Figs 4A, 6A). Anterior margin rounded; dorsal margin straight; postero-dorsal margin with extended caudal process; ventral margin almost straight and inclined gently toward posterior margin; postero-ventral margin with two small spines (Figs 4A, 6A, F). Postero-ventral and anterior margins strongly compressed (Fig. 6A). Greatest H situated in front of middle. Eye present. Surface ornamentation consisting of shallow reticulation on postero-dorsal margin, with few simple setae; few sieve-like pores also present (Fig. 6A, B). Marginal pore canals distributed on antero-ventral and posterior margins (Fig. 4A). Posterior inner lamella wider than anterior. Muscular scar imprints consisting of a row of four vertical scars and one frontal scar. Hinge adont (Fig. 4A).

A1 (Fig. 4B). Six-segmented. First segment without setulae and setae. Second segment with setulae on antero-distal margin. Third segment with one bare seta antero-distally, reaching end of fourth segment. Fourth and fifth segments each with one bare seta on anterior-distal margin, reaching end of next segment. Terminal segment with three long bare setae on distal margin, almost 2.5 × longer than terminal segment. L ratios between six segments 2.5: 1.1: 1: 1.2: 1.5: 1.4.

A2 (Fig. 4C). Four-segmented. Exopod transformed into spinneret seta. First endopodal segment without setulae and seta. Second segment with one bare seta postero-distally reaching 2/3 length of third segment. Third segment with setulae on antero-proximal, postero-medial, and postero-distal margins, and with one bare seta on antero-proximal margin, reaching 1/2 length of the same segment; two bare setae postero-medially, reaching end of the same segment; one bare seta postero-distally, almost 2 × longer than terminal segment. Terminal segment with two strong, bare claws on distal margin almost 3× longer than the same segment. L ratios between four segments 8.3: 3: 11.3: 1.

Md (Fig. 4F). Coxa with seven strong teeth and one thin, bare seta on distal margin, and one bare seta near anterior-distal margin. Exopod with three bare setae; endopod three-segmented. First endopodal segment with one bare seta antero-distally. Second segment with two bare setae antero-distally and one bare seta postero-distally. Terminal segment with nine setae, four of which arise from anterior margin, two from distal margin, and two from postero-distal margin. First segment almost 2× longer than terminal segment.

Mxl (Fig. 4D, E). Palp present. Two-segmented. Terminal segment with four bare setae distally. Exopodite with 1 reflexed seta and ~ 14 bare setae on branchial plate. Masticatory process with three endites, first and second endites each with four bare setae, third endite with two bare setae.

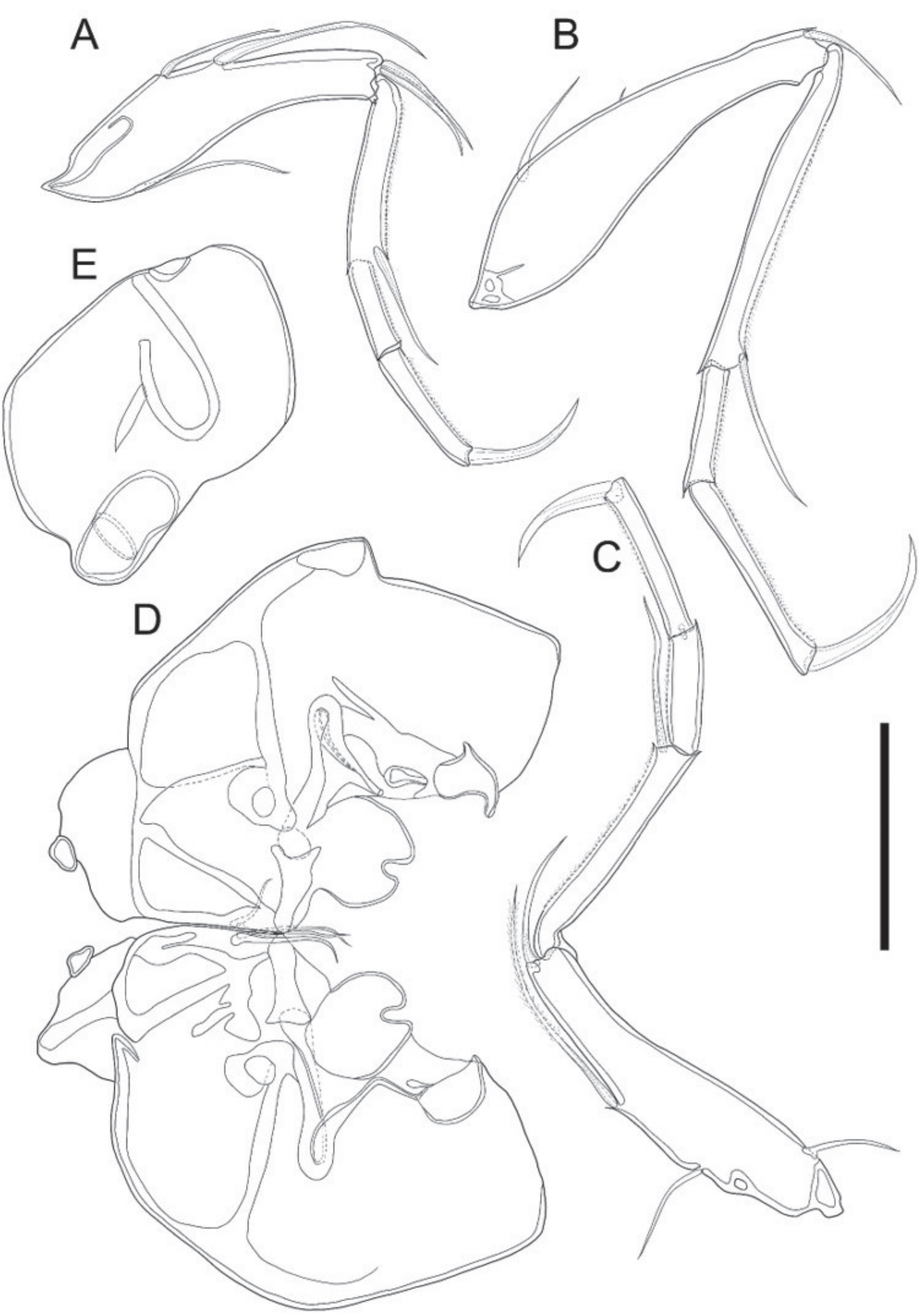

Figure 5. *Glacioloxoconcha jeongokensis* sp. nov.: male (NIBRIV0000882303 holotype) **A** L5 **B** L6 **C** L7 **D** Hp; female (NIBRIV0000882309 allotype) **E** GF. Scale bar: 50 µm.

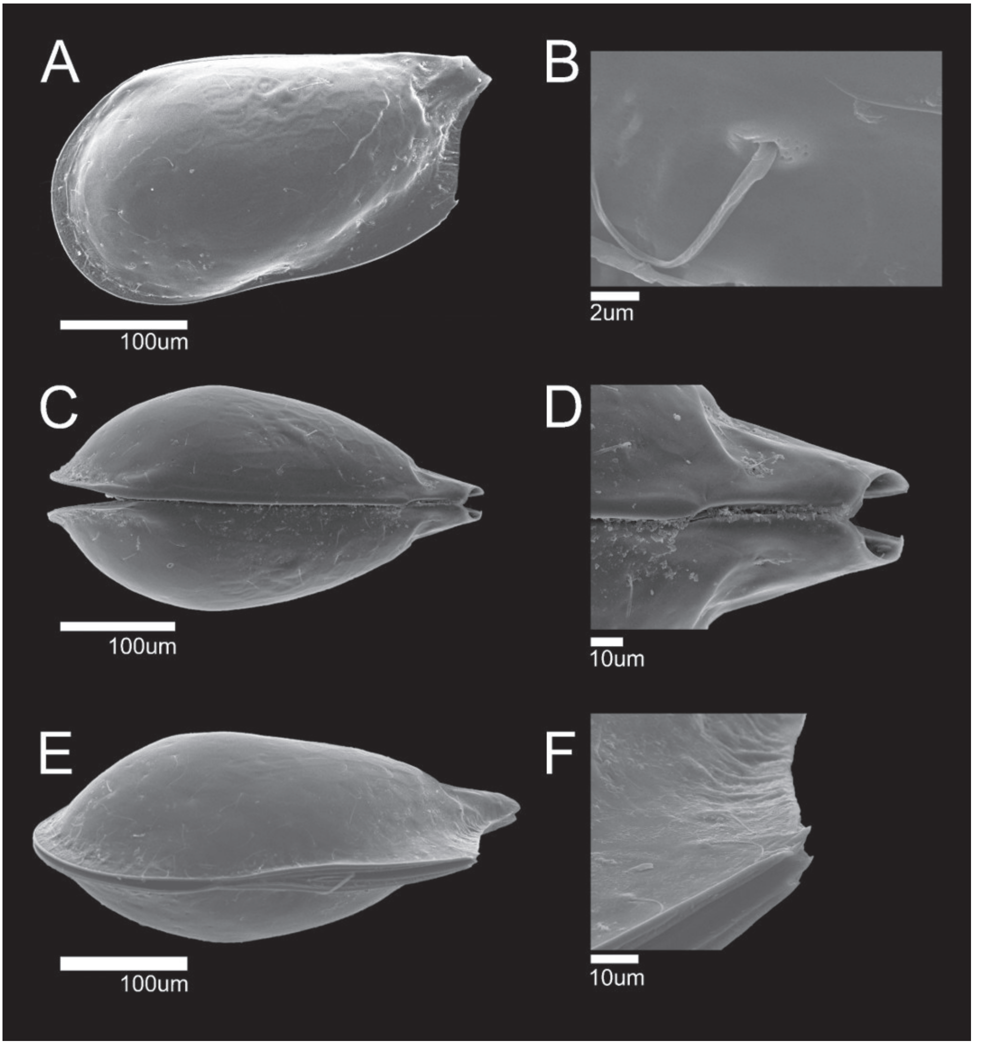

Figure 6. SEM photographs of *Glacioloxoconcha jeongokensis* sp. nov.: male (NIBRIV0000882313 holotype) **A** LV external view **B** Simple seta pore on external carapace; male (paratype) **C** dorsal view **D** posterior part of dorsal margin **E** ventral view **F** postero-ventral part of ventral margin.

L5 (Fig. 5A). Four-segmented. First segment with five bare setae, two antero-medially, one reaching and one not reaching end of the same segment; and two setae antero-distally, reaching 1/2 of second segment; and one postero-proximally, reaching 2/3 length of the same segment. Second segment with one bare seta antero-distally, reaching 1/3 length of the terminal segment. Penultimate segment without any seta. Terminal segment with one claw like seta on distal margin. Last three segments with setulae along anterior margin. L ratios between four segments 3.5: 1.9: 1: 1.4.

L6 (Fig. 5B). Four-segmented. First segment with three bare setae, one antero-proximally, reaching 1/2 length of the same segment; one tiny seta; and one antero-distally, reaching 1/5 length of second segment. Second segment with one bare seta antero-distally, reaching 1/3 length of terminal segment. Penultimate segment without any seta. Terminal segment with one claw-like seta on distal margin. Last three segments with setulae along anterior distal margin. L ratios between four segments 3.5: 2.8: 1: 1.8.

L7 (Fig. 5C). Four-segmented. First segment with four setae: one bare seta posterior-proximally, as long as 1/4 of the same segment; one bare seta on antero-proximally, as long as 1/4 of the same segment; one plumose seta antero-medially, reaching 1/4 length of second segment; one bare seta antero-distally, reaching 1/2 length of second segment. Second segment with one bare seta on anterior-distal margin, reaching 1/3 length of third segment. Third segment without seta. Terminal segment with one strong claw on distal margin, 1/2 as long as the segment. Last three segments with setulae along anterior margin. L ratios between four segments 3.2: 2: 1: 1.3. Compared with L5 and L6 segments, L7 is more elongated than L5, but similar to L6.

BO (Fig. 4G) With more than ten setae on distal margin. Positioned behind L7 and below Hp.

Hp (Fig. 5D). Basal plate sub-rectangular. Lobe rudimentary, shaped as a lotus leaf. CR fused with Hp and represented with two setae.

Female. *Carapace* (Fig. 13A). Slightly larger than males. L ~ 382 μm, H ~ 211 μm. Shape and all other morphological features similar to male.

GF (Fig. 5E). Basal part rectangular. CR setae not observed. Ovary sub-rectangular.

All other appendages same as in male.

Glacioloxoconcha jisepoensis **sp. nov.**
https://zoobank.org/FF235D4C-AEC4-4632-A800-53CA49E9CF10
Figs 7, 8

Material examined. *Holotype*, male, dissected on one slide (MABIKCR0025819); ***Allotype***, female, dissected on one slide (MABIKCR0025820); ***Paratypes*:** one male and female dissected on each slide, and shell on each micropaleontological slide and 5 specimens kept in 2 ml vial.

Type locality. South Korea, Gyeongsangnam-do, Geoje-si, Irun-myeon, Jisepo-haean-ro, Jisepo harbor. 34°49.919'N, 128°42.220'E, 19 May 2020, leg. Hyunsu Yoo & Byung-jin Yoo.

Etymology. The species is named after the harbor from where it was collected.

Description. Male. *Carapace* (Figs 7C, 8). Relatively small, L ~ 400 μm, H ~ 220 μm. RV overlapping LV dorsal margin (Fig. 8C). Carapace similar to that of *G. jeongokensis*. Some differences are that dorsal margin is slightly sloped (Fig. 8A, B), and the caudal process is slightly longer than that of *G. jeongokensis* (Fig. 8D). Anterior and posterior pore channel well developed (Fig. 7C). Muscular imprint same as *G. jeongokensis* (Figs 7C, 8B). Hinge adont (Fig. 7C).

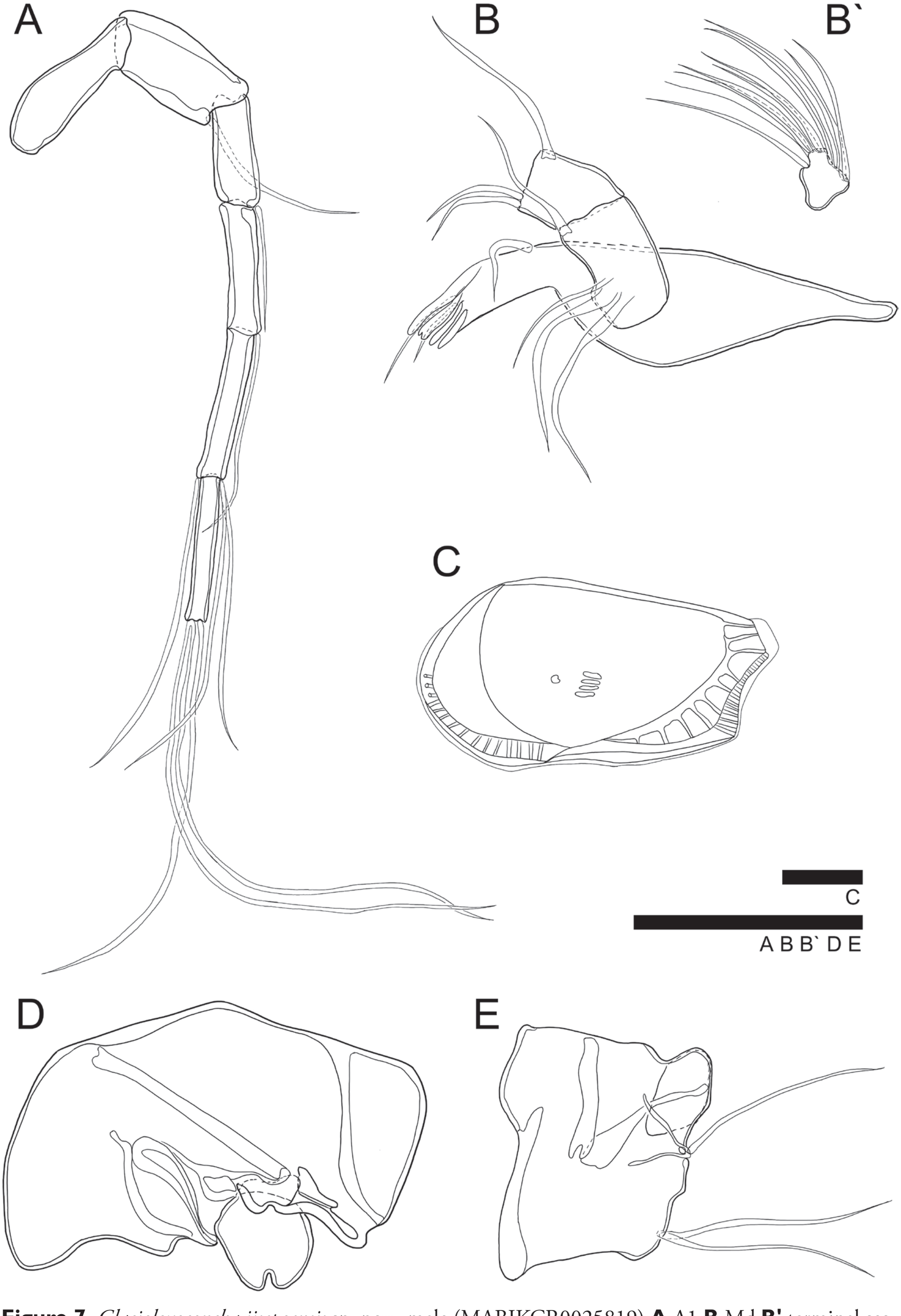

Figure 7. *Glacioloxoconcha jisepoensis* sp. nov.: male (MABIKCR0025819) **A** A1 **B** Md **B'** terminal segment of endopod **C** RV internal view **D** Hp, female (MABIKCR0025820) **E** GF. Scale bars: 50 μm (**A, B, B', D, E**); 100 μm (**C**).

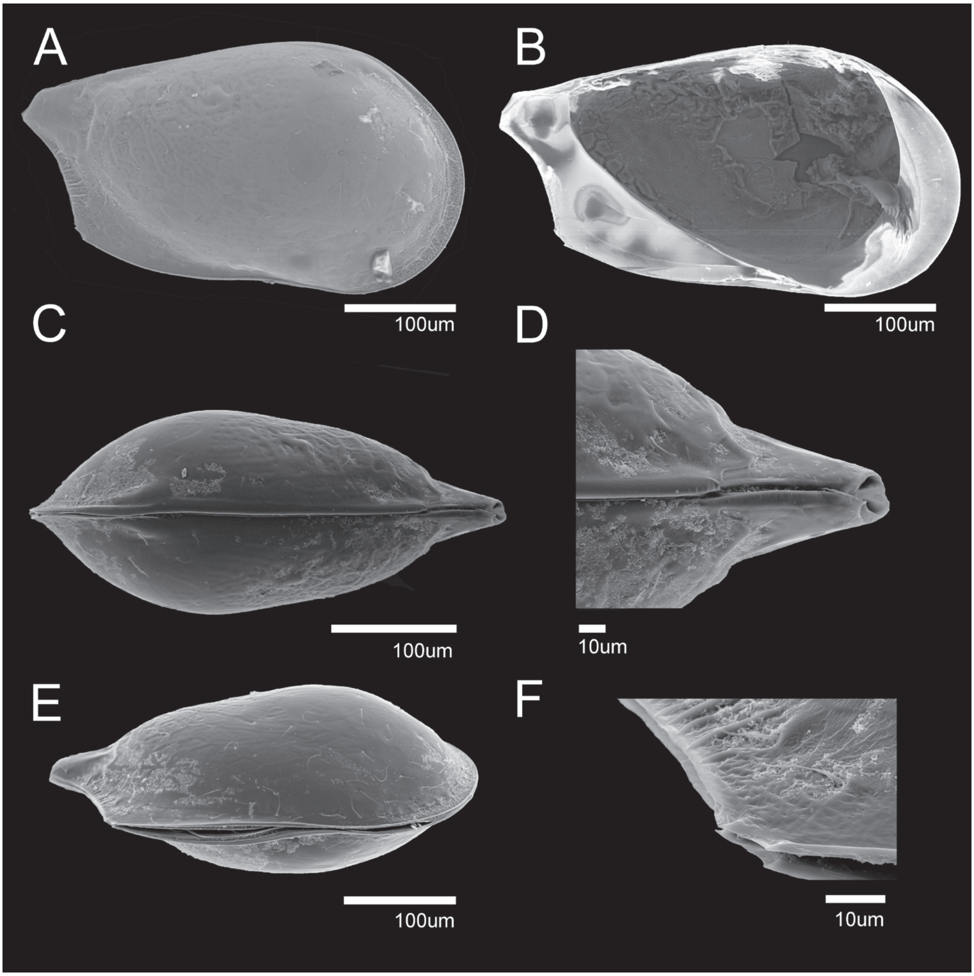

Figure 8. SEM photographs of *Glacioloxoconcha jisepoensis* sp. nov.: male (paratype) **A** RV external view **B** LV internal view, male (paratype) **C** dorsal view **D** postero dorsal margin **E** RV internal view **F** posterior ventral margin.

A1 (Fig. 4A). Six-segmented. First segment without setulae or setae. Second segment with one bare seta postero-distally reaching 1/2 length of fourth segment. Third segment with one bare seta antero-distally reaching end of fourth segment. Fourth segment with one bare seta antero-distally reaching 1/3 length of terminal segment. Fifth segment with two bare setae on anterior-distal margin almost 2 × longer than terminal segment, one bare seta postero-distally almost 2 × longer than terminal segment. Terminal segment with three long bare setae on distal margin, almost 3.5 × longer than terminal segment. L ratios between six segments 1.4:1.2:1:1.2:1.3:1.3.

Md (Fig. 7B, B'). Coxa slightly crushed shape with four strong teeth and two thin bare setae on distal margin and one bare seta near anterior distal margin. Exopod with three bare setae; endopod three-segmented. First segment with one bare seta antero-distally. Second segment with two bare setae antero-distally and one bare seta postero-distally. Terminal segment with ten setae, four of which arise from anterior margin, four from distal margin and two from postero-distal margin. First segment almost 2 × longer than terminal segment.

Hp (Fig. 7D). Similar to *G. jeongokensis* but smaller. CR lost.

Other appendages same as in *G. jeongokensis* sp. nov.

A2 Four-segmented. L ratios between four segments 10: 3.5: 12.3: 1.

L5 Four-segmented. L ratios between four segments 3.6: 2: 1: 1.4.

L6 Four-segmented. L ratios between four segments 3.4: 2.2: 1: 1.4.

L7 Four-segmented. L ratios between four segments 3.6: 2.9: 1: 1.8.

Female. Carapace broken.

GF (Fig. 5E). Basal part rectangular form. Three bare setae of CR observed. Ovary sub-rectangular.

All other appendages same as in male.

Genus *Loxocauda* Schornikov, 1969

Loxocauda orientalis Schornikov, 2011

Figs 9, 10

Loxocauda sp. – Schornikov 2006: 43; Zenina 2009: 307.
Loxocauda sp. 6 – Lee et al. 2000: 465.
Loxocauda sp. 9 – Lee et al. 2000: 466.
Loxocauda orientalis Schornikov, 2011: 100.

Material examined. One male, dissected on one slide and shell on micropaleontological slide from South Korea, Gyeongsangnam-do, Geoje-si, Geoje-myeon, Beopdongeogu-ro, Beopdong harbor. 34°49.252'N, 128°31.227'E, 5 Apr 2021, leg. Changgyun Yu & Byung-jin Yoo; two females, dissected on one slide each, and one male dissected on one slide, all shells on separate micropaleontological slides from South Korea, Jeollabuk-do, Buan-gun, Byeonsan-myeon, Saemangeum-ro, Garyuk-do harbor. 35°43.603'N, 126°31.770'E, 30 Apr 2021, leg. Hyunsu Yoo & Byung-jin Yoo.

Redescription. Male. *Carapace* (Figs 9A, 10). Larger than another *Glacioloxoconcha* species, L ~ 420 µm, H ~ 243 µm. RV overlapping LV dorsally. Carapace subquadrate in lateral view (Figs 9A, 10A, B). Anterior margin rounded, dorsal margin slightly arched and postero-dorsal margin with caudal process smaller than in *G. jeongokensis* sp. nov. (size almost 50 µm), ventral margin straight, postero-ventral margin with spine (Fig. 10E). Postero-ventral and anterior margins strongly compressed. Greatest H situated in front of middle. Surface smooth with few simple setae sporadically distributed (Fig. 10A). Marginal pore canals strongly developed and distributed from anterior to posterior margins (Fig. 9A). Fused zone situated medially on ventral margin, strongly developed. Muscular scar imprints consisting of a row of four vertical scars, one bent frontal scar, with two scars below it (Fig. 10F). Hinge adont (Fig. 9A).

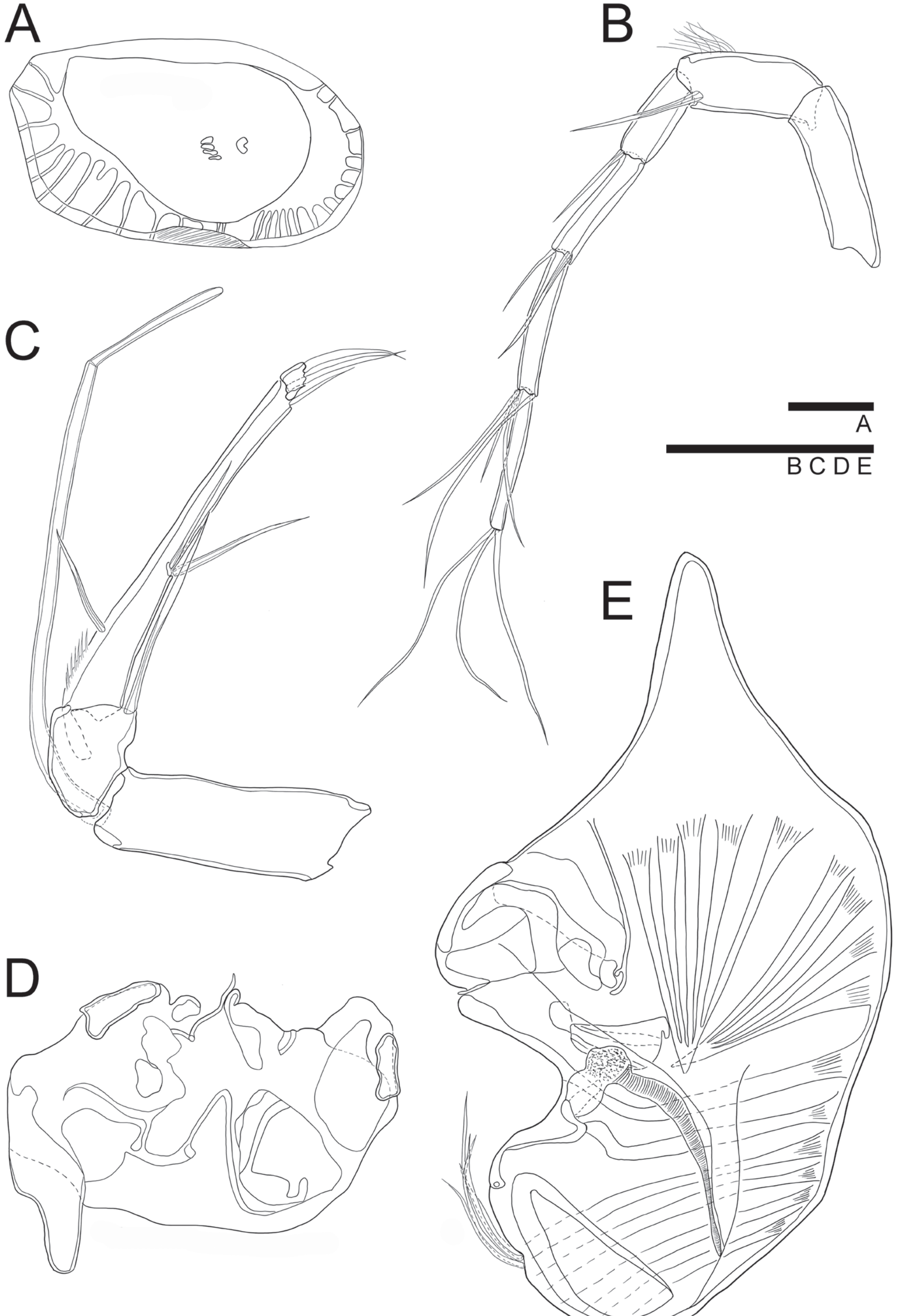

Figure 9. *Loxocauda orientalis* Schornikov, 2011: male **A** RV internal view **B** A1 **C** A2; female **D** GF; male **E** Hp. Scale bars: 50 μm (**B, C, D, E**); 100 μm (**A**).

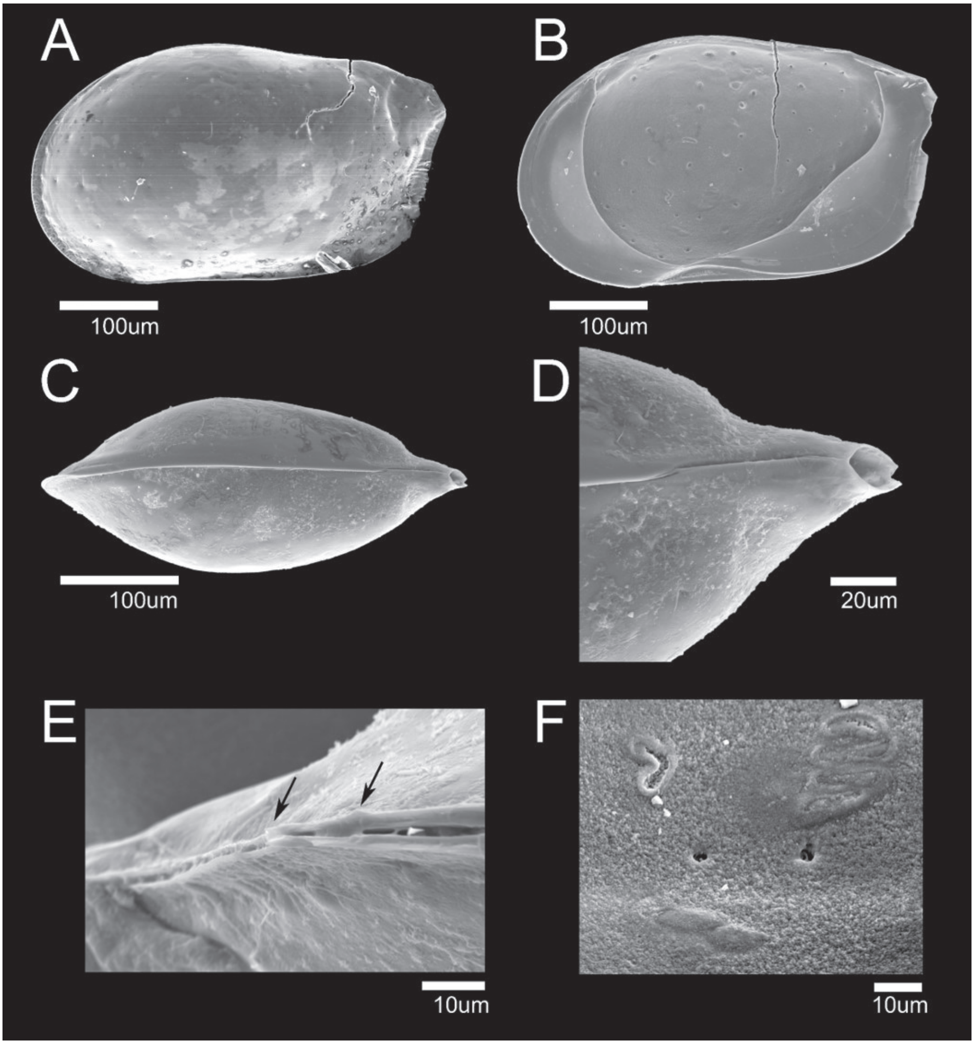

Figure 10. SEM photographs of *Loxocauda orientalis* Schornikov, 2011: male **A** LV external view **B** RV internal view; male **C** dorsal view **D** posterior part of dorsal margin **E** postero-ventral margin (black arrow point to spines) **F** muscular scar print.

A1 (Fig. 9B). Six-segmented. First segment without setulae and setae. Second segment with setulae on antero-distal and one bare seta on postero-distal margin, reaching 1/3 length of fourth segment. Third segment with one bare seta on antero-distally, reaching 3/4 length of fourth segment. Fourth segment with two bare setae, one antero-distally, reaching 1/2 length of next segment, another postero-distally, reaching 3/4 length of next segment. Penultimate segment with four bare setae, three setae antero-distally, and one on postero-distal margin, length of two setae on anteriorly reaching slightly over terminal segment, and one reaching 2/3 length of terminal segment, length of one seta on posteriorly over terminal segment. Terminal segment with three long, bare setae on distal margin, almost 1.5 × longer than terminal segment. L ratios between six segments 1.7: 1.3: 1: 1.2: 1.5: 1.6.

A2 (Fig. 9C). Four-segmented. Exopod transformed into two-segmented spinneret seta. First endopodal segment without setulae or seta. Second segment with one bare seta postero-distally reaching 2/3 of following segment. Third segment with setulae antero-proximally, and with one bare seta on antero-proximal margin, reaching 1/2 length of the same segment; two bare setae postero-medially, reaching 2/3 length of same segment, one bare seta postero-distally, almost 2.5 × longer than terminal segment, one bare seta on distal margin, almost 4 × longer than terminal segment. Terminal segment with one strong, bare claw on distal margin almost 4 × longer than same segment. L ratios between four segments: 7.1: 3: 11.4: 1.

Hp (Fig. 9E). Basal plate subquadrate with flection antero-medially, four bare setae antero-distally, and strong muscle keeping tension between central and peripheral parts. Distal lobe sub-triangular. Ejaculatory process densely coiled.

Female. Larger than males. L ~ 484 µm, H ~ 287 µm. Shape and all other morphological features similar to male. Fused zone with three simple setulae.

GF (Fig. 9D). Basal plate sub-rectangular and Ovary subquadrate. Without setulae and setae.

Loxocauda cf. *orientalis*

Figs 11, 12

Material examined. One male, dissected on one slide (NIBRIV0000882304), shell on micropaleontological slide (NIBRIV0000882314); one female, dissected on one slide (NIBRIV0000882310) and shell on micropaleontological slide (NIBRIV0000882312); one male and female dissected on slide each, and shells on micropaleontological slide each; South Korea, Gyeongsangnam-do, Geoje-si, Irun-myeon, Jisepohaean-ro, Jisepo harbor. 34°49.919'N, 128°42.220'E, 19 May 2020, leg. Hyunsu Yoo & Byung-jin Yoo.

Brief description. Male. Carapace same as in *L. orientalis* (Figs 11A, 12A, B). Differences include dorsal margin being straighter, and greatest H situated close medially. A2 (Fig. 11B) with well-developed setulae on second and third segments. Hp (Fig. 11C) with basal plate sub-rectangular and with three bare setae antero-distally. Lobe with sub-triangular form. No strong muscles present.

Other appendages same as in *L. orientalis* Schornikov, 2011

L ratios between segments as indicated below:

A1 Six-segmented. 2.4: 1.2: 1: 1.1: 1.4: 1.3.

A2 Four-segmented. 6.4: 2.9: 9.8: 1.

L5 Four-segmented. 3.5: 1.9: 1: 1.2.

L6 Four-segmented. 3.3: 2.4: 1: 1.3.

L7 Four-segmented. 2.4: 1.9: 1: 1.2.

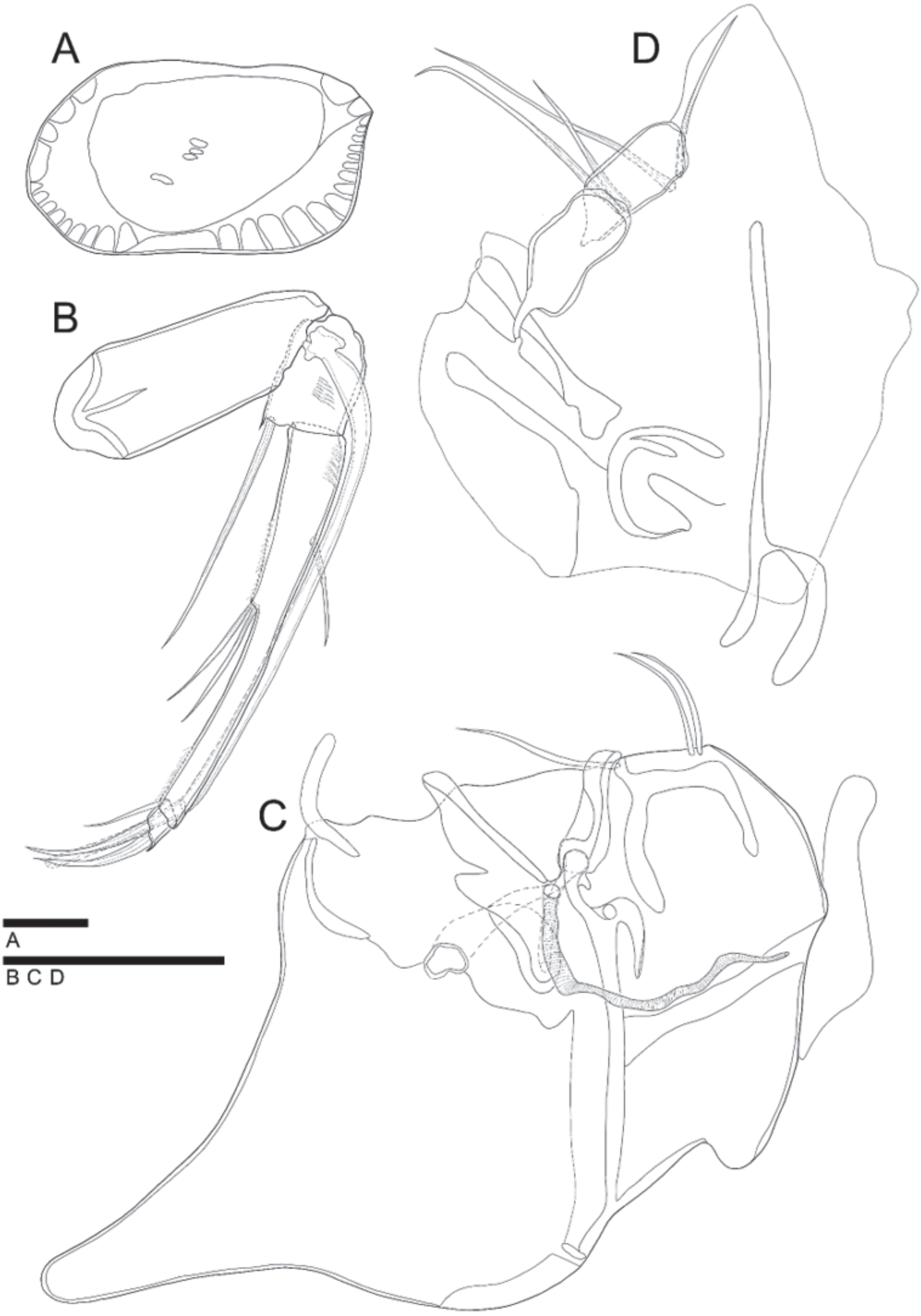

Figure 11. *Loxocauda* cf. *orientalis*: male (NIBRIV0000882304, NIBRIV0000882314) **A** RV internal view **B** A2 **C** Hp; female (NIBR0000882310) **D** GF. Scale bars: 50 µm (**B, C, D**); 100 µm (**A**).

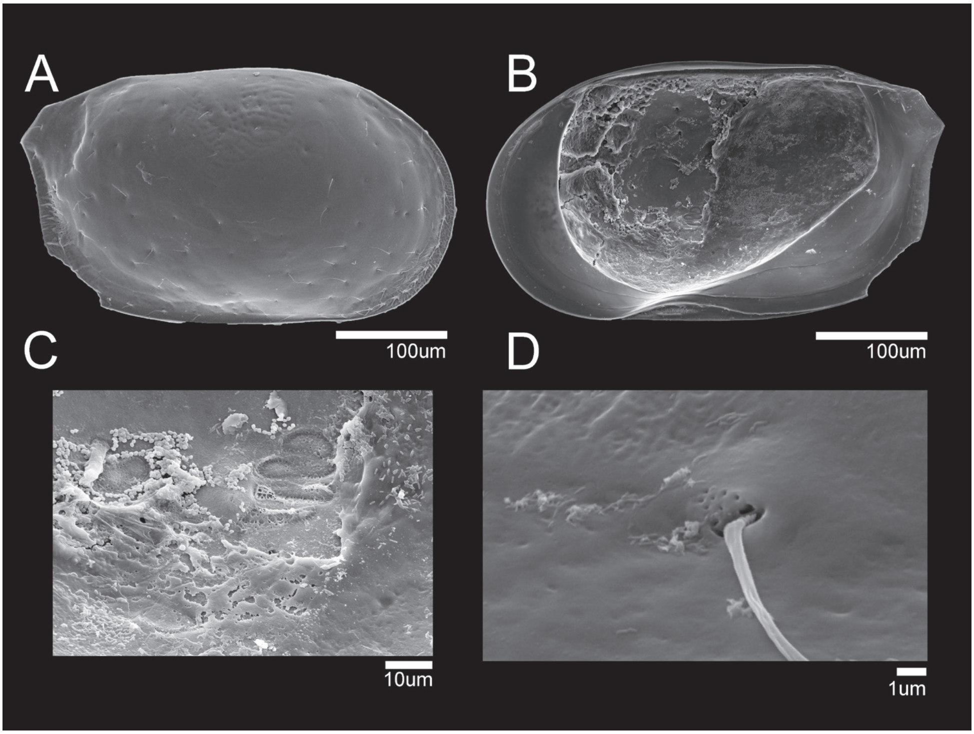

Figure 12. SEM photographs of *Loxocauda* cf. *orientalis*: male (NIBRIV0000882314) **A** RV external view **B** RV internal view **C** muscular scar print **D** simple seta pore on external carapace.

Female. Larger than male (Fig. 13B). L ~ 459 µm, H ~ 267 µm. Shape and all other morphological features similar to male. GF illustrated in Fig. 11D. Basal plate sub-triangular. Ovary subquadrate. With three bare setae on antero-medial margin. All other appendages same as in male.

Molecular analysis

Intraspecific pairwise distances (p-distances) of the COI sequences between specimens of *Glacioloxoconcha jeongokensis*, *G. jisepoensis*, and *Loxocauda orientalis* varied between 0 and 0.6% (Suppl. material 3). Interspecific p-distances between two new *Glacioloxoconcha* species were ~ 11%. Distances between COI sequences belonging to *Loxocauda orientalis* and to *Glacioloxoconcha* varied between 21.0% and 24.1%. The COI alignment was 707 base pairs long and TVM+F+I+G4 model (Kalyaanamoorthy et al. 2017) was chosen as the best fit. The number of constant sites and parsimony informative sites were 296 and 375, respectively.

Glacioloxoconcha and *Loxacauda* clustered separately on the tree (Fig. 14) and their respective branches received the maximum support. Similarly, two new *Glacioloxoconcha* species formed two well-supported clades.

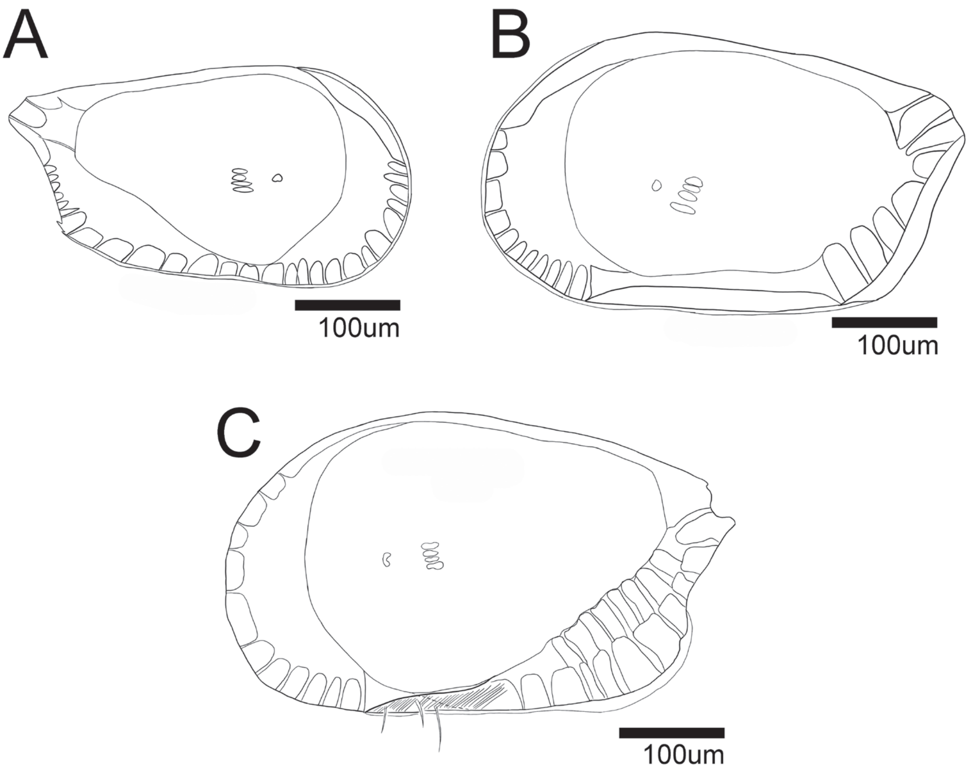

Figure 13. Internal view of female carapace **A** *Glacioloxoconcha jeongokensis* sp. nov. (NIBRIV0000882311 allotype) **B** *Loxocauda* cf. *orientalis* (NIBRIV0000882312) **C** *Loxocauda orientalis* Schornikov, 2011 (MABIKCR0025820).

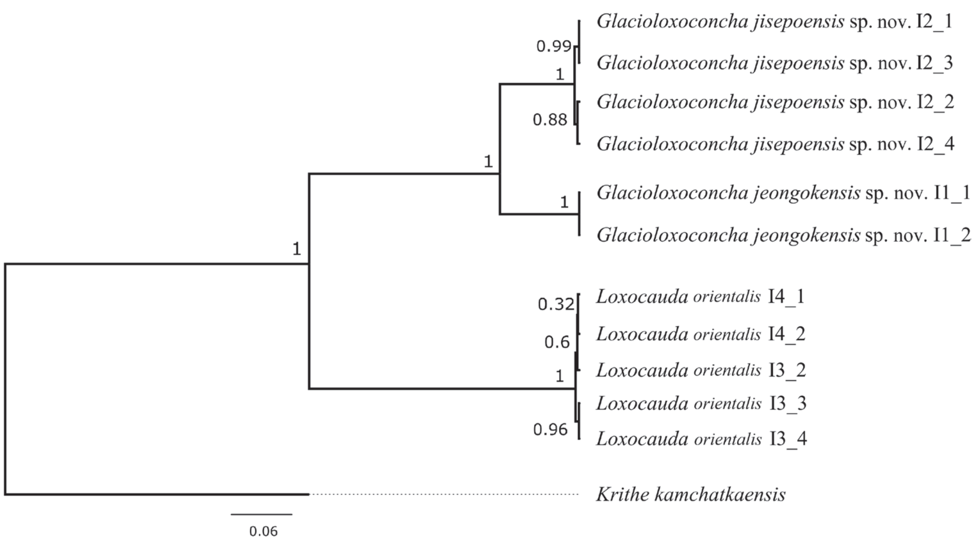

Figure 14. Bayesian inference rooted cladogram of three Loxocaudinae species constructed from the COI dataset. Numbers above branches represent posterior probabilities.

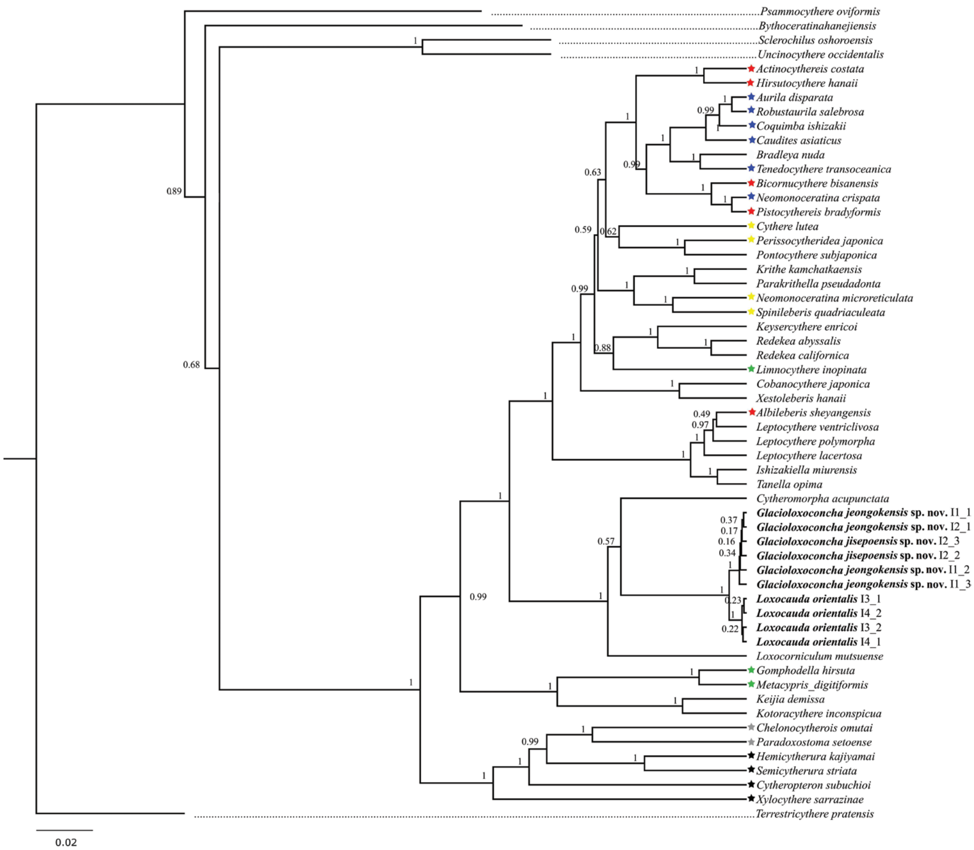

Figure 15. Bayesian inference rooted cladogram of the superfamily Cytheroidea constructed from the 18S rRNA dataset. Numbers above branches represent posterior probability. Stars indicate representatives of polyphyletic/paraphyletic families: red, Trachyleberididae; blue, Hemicytheridae, yellow, Cytheridae; green, Limnocytheridae; grey, Paradoxostomatidae; black, Cytheruridae.

The p-distances between *Loxocauda* and *Glacioloxoconcha* 18S rRNA sequences (Suppl. material 4) were much smaller and varied from 0.3% to 0.5%. Some differences (between 0.1% and 0.3%) were also recorded between two *Glacioloxoconcha* species, as well as between specimens belonging to the same species of this genus.

The final 18S alignment was 1972 base pairs long and it included the two new *Glacioloxoconcha* species and *L. orientalis*, in addition to 46 Cytherocopina taxa and an outgroup. The substitution model, TIM2+F+I+G4 (Kalyaanamoorthy et al. 2017) with gamma distribution was identified as the best fit for the evolutionary model. The number of constant sites was 1235 and the number of parsimony informative sites was 517.

The phylogenetic tree based on the 18S alignment (Fig. 15), strongly supports the monophyly of the family Loxoconchidae, which for this analysis only included one species each of *Cytheromorpha* Hirchmann, 1909, *Loxocorniculum* Benson & Coleman, 1963, and *Loxocauda*, as well as two new *Glacioloxoconcha* species. Our choice of the outgroup did not strongly support the monophyly of the ingroup taxa (Cytheroidea), as this branch had a posterior probability of only 0.89. The tree also indicates a polyphyletic and paraphyletic nature of several families (see discussion).

Discussion

In contrary to *Glacioloxoconcha suedshetlandensis*, the two new *Glacioloxoconcha* species from Korea have a distinct tail-like extension on each valve. Other differences include a more robust A2 in the new species, and the presence of three rays on the exopodite of the Md vs. one ray in *G. suedshetlandensis* (see Hartmann 1990; Schornikov 2011b). The chaetotaxy and the morphology of the Md exopodite has been widely used to distinguish cytheroid taxa on various systematic levels (Karanovic and Brandão 2015). Considering how delicate this part is and how easily it is lost or folded during dissection, it should not be the primary character used in cytheroids classification. All three *Glacioloxoconcha* species have a very similar hemipenis, which is the reason for placing the Korean species into a genus that has been known only from Antarctica. Such a wide distribution, especially of the cytheroid ostracods, seems to be relatively common (Brandão and Päplow 2011; Brandão and Karanovic 2015). For example, Yamaguchi (2000) examined the wide distribution of the genus *Ishizakiella* McKenzie & Sudijono, 1981, which has one species living in New Zealand and three in Japan and Korea (see Yoo et al. 2012), and suggested that the ancestor of the Japanese species colonized the islands before the Pleistocene glaciation, and subsequently diverged there. Tanaka et al. (2018) showed that some ostracod species endemic to Japan were transported across the Pacific on the tsunami debris from the 2011 earthquake. On the other hand, a wide geographic distribution of some taxa (especially species) should be taken with caution. Namely, recent studies showed that after the reexamination of the type material and various world records, a wide distribution is questionable (Brandão and Yasuhara 2013). The two new species are very similar, but *G. jeongokensis* has a slightly longer tail-like extension on the shell, a different chaetotaxy on the A1, and a larger hemipenis with a sinusoid ventral margin of the distal lobe. The two species also have high COI distances of ~ 11%, which has been suggested as good evidence for species delineation (da Silva et al. 2011; Léfebure et al. 2016). *Glacioloxoconcha* species are very closely related and seems to have allopatric distributions, which is supported by small morphological differences in all soft body parts, including the hemipenis. The character displacement phenomenon, where differences in sexual characters are enlarged in the case of overlapping distribution, was already noticed for the cytheroid ostracods (Tsukagoshi 1988).

Loxocauda orientalis and *L.* cf. *orientalis* are very similar both in the carapace and the soft body parts morphologies and differ only in few details. *Loxocauda* cf. *orientalis* does not have strong muscles on the hemipenis and has a slightly different shape of the female CR and genital lobe. Study of the ontogeny of another Loxoconchidae member, *Loxoconcha japonica* Ishizaki, 1968, does not mention any changes in the development of the hemipenis musculature after the last molt. But, as Yamada et al. (2014) showed, several morphological changes do occur in the development of the Zenker organ of a Candonidae ostracod after reaching the adult stage. The function of the Zenker organ in Cypridoidea is to pump the sperm, a role that is in Cytheroidea taken up by the hemipenis (see Meisch 2000). There are also some subtle differences in the dorsal margins of the male valves: in the *L.* cf. *orientalis* this margin is slightly flatter than in *L. orientalis*. Unfortunately, COI could not be successfully amplified for *L.* cf. *orientalis* to support our decision, and more material is needed.

The similarities and character overlap between *Glacioloxoconcha*, *Loxocauda*, and *Loxoconcha* Sars, 1926 question not only the validity of the subfamily Loxocaudinae within Loxoconchidae, but also the validity of *Glacioloxoconcha* and *Loxocauda*. On our reconstructed phylogenetic tree of Cytheroidea, the two genera are separated, but together form a well-supported clade. In addition, their respective branches are very short, especially in comparison to other two Loxoconchidae genera included in the analysis. One of them, *Loxocorniculum* Benson & Coleman, 1963 is currently accepted as a subgenus of *Loxoconcha* (see Bate et al. 1981). The phylogenetic tree does not include two 18S sequences attributed to *Loxoconcha* sp. (GenBank accession numbers AY191447 and AY455769) because of the incomplete identification, and also because our attempt to include them resulted in *Loxoconcha* clustering with sequences belonging to *Aurila* sp., *Pistocythereis* sp., *Limnocythere* sp.1, *Neomonoceratina* sp., and *Bicornucythere* sp. This indicates a potential misidentification not only of *Loxoconcha* but other unrelated genera.

Polyphyletic and/or paraphyletic nature of several families on the phylogenetic tree can partially be explained by misidentification. For example, *Albileberis sheyangensis* Chen in Hou, Chen, Yang, Ho, Zhou & Tian, 1982, a species belonging to the family Trachyleberididae, clusters within the family Leptocytheridae (Fig. 15). The two families have many prominent morphological differences in both the soft part and the shell morphologies and the position of a Trachyleberididae species within Leptocytheridae can only be a result of misidentification. On the other hand, polyphyly of the families Cytheridae, Hemicytheridae, Trachyleberididae, and Limnocytheridae on the tree (see different star colors on the tree, Fig. 15) is the result of unstable systematics and indicates the necessity for revisions. Trachyleberididae is a very diverse Mesozoic taxon, and a recent revision of the *Trachyleberis* Brady, 1898 type species (Brandão et al. 2013) contributed to a better understanding not only of this genus' systematics, but also of the family. Tanaka et al. (2021) studied a deep-sea member of the family Keysercytheridae, and their phylogenetic reconstruction showed that Limnocytheridae as well as Paradoxostomatidae are polyphyletic and proposed some systematic changes for the latter family. On our tree Paradoxostomatidae clusters with Cytheruridae (grey star on the tree, Fig. 15). However, *Xylocythere sarrazinae* Tanaka, Lelièvre & Yasuhara, 2019, a member of the family Cytheruridae, is a sister taxon to both Cytheruridae and Paradoxostomatidae, rendering the former family paraphyletic.

From both our and previous studies it is clear that several families belonging to Cytheroidea need a revision, which should combine morphology of both shell and soft parts (Karanovic and Brandão 2015). However, such revision is difficult as most cytheroids ostracods are known from the fossil record only and this would only partially resolve the problems. Nevertheless, Recent taxa could provide an insight into the morphological evolution of Cytheroidea and offer some solution, especially if geometric morphometrics of the shell are used as an aid in this revision.

Acknowledgements

We are thankful to the Korea Sciences Diving Technology team (Byung-jin Yoo) and Changgyun Yu for collecting samples. This work was supported by two National Institute of Biological Resources (NIBR) grants (NIBR202002110), (NIBR202203105) from the Ministry of Environment of Republic of Korea, and National Research Foundation grant (NRF, 2020R1A6A1A06046728). This work is also supported by 'Improvement of management strategies on marine disturbing and harmful organisms' funded by the Ministry of Oceans and Fisheries, Korea and by the National Marine Biodiversity Institute of Korea (MABIK), grant number 2022M01100.

References

Bate RH, Whittaker JE, Mayes CA (1981) Marine Ostracoda of the Galapogos Islands and Ecuador. Zoological Journal of the Linnean Society 73(1): 1–79. https://doi.org/10.1111/j.1096-3642.1981.tb01579.x

Bouckaert R, Heled J, Kühnert D, Vaughan T, Wu CH, Xie D, Drummond AJ (2014) BEAST 2: A Software Platform for Bayesian Evolutionary Analysis. PLoS Computational Biology 10(4): e1003537. https://doi.org/10.1371/journal.pcbi.1003537

Brandão SN, Karanovic I (2015) Biogeography of deep-sea wood fall, cold seep and hydrothermal vent Ostracoda (Crustacea), with the description of a new family and a taxonomic key to living Cytheroidea. Deep sea Research Part II: Topical Studies in Oceanography 111: 76–94. https://doi.org/10.1016/j.dsr2.2014.09.008

Brandão SN, Karanovic I (2022) World Ostracoda Database. [Accessed on 2021-10-06] http://www.marinespecies.org/ostracoda [Retrieved October 3, 2022]

Brandão SN, Päplow O (2011) New species and occurrences of *Bradleya* Benson, 1972, *Harleya* Jellinek & Swanson, 2003 and *Poseidonamicus* Benson, 1972 (Ostracoda: Cytheroidea) from the Atlantic Sector of the Southern Ocean. Journal of Micropalaeontology 30(2): 141–166. https://doi.org/10.1144/0262-821X10-017

Brandão SN, Yasuhara M (2013) Challenging deep-sea cosmopolitanism: Taxonomic re-evaluation and biogeography of '*Cythere dasyderma* Brady, 1880' (Ostracoda). Journal of Micropalaeontology 32(2): 109–122. https://doi.org/10.1144/jmpaleo2012-009

Brandão SN, Yasuhara M, Irizuki T, Horne DJ (2013) The ostracod genus *Trachyleberis* (Crustacea; Ostracoda) and its type species. Marine Biodiversity 43(4): 363–405. https://doi.org/10.1007/s12526-013-0163-6

Brodin J, Mohan K, Gayathri A, Will F, Peter H, Cheryl G, Thomas L (2013) A multiple-alignment based primer design algorithm for genetically highly variable DNA targets. BMC Bioinformatics 14(1): 1–9. https://doi.org/10.1186/1471-2105-14-255

da Silva JM, Creer S, dos Santos A, Costa AC, Cunha MR, Costa FO, Carvalho GR (2011) Systematic and evolutionary insights derived from mtDNA COI barcode diversity in the Decapoda (Crustacea: Malacostraca). PLoS ONE 6(5): e19449. https://doi.org/10.1371/journal.pone.0019449

Hartmann G (1990) Antarkritsche benthische Ostracoden VI Auswertung der Reise der "Polarstern" Ant. VI-2 (1. Teil, Meiofauna und Zehnerserien) Sowie Versuch einer vorläufigen Auswertung aller bislang vorliegenden Daten. Mitteilungen aus dem Hamburgischen Zoologischen Museum und Institut 87: 191–245.

Ikeya N, Hanai T (1982) Ecology of recent ostracods in the Hamana-ko region, the Pacific coast of Japan. Bulletin University Museum University of Tokyo 20: 15–59. https://eurekamag.com/research/020/912/020912477.php

Kalyaanamoorthy S, Minh BQ, Wong TKF, Von Haeseler A, Jermiin LS (2017) ModelFinder: Fast model selection for accurate phylogenetic estimates. Nature Methods 14(6): 587–589. https://doi.org/10.1038/nmeth.4285

Karanovic I, Brandão SN (2015) Biogeography of deep-sea wood fall, cold seep and hydrothermal vent Ostracoda (Crustacea), with the description of a new family and a taxonomic key to living Cytheroidea. Deep-sea Research. Part II, Topical Studies in Oceanography 111: 76–94. https://doi.org/10.1016/j.dsr2.2014.09.008

Kumar S, Stecher G, Tamura K (2016) MEGA7: Molecular Evolutionary Genetics Analysis Version 7.0 for Bigger Datasets. Molecular Biology and Evolution 33(7): 1870–1874. https://doi.org/10.1093/molbev/msw054

Léfebure A, Paarlberg AJ, Winter C (2016) Results of analysis and model simulation of the bed profiles. Pangaea. https://doi.org/10.1594/PANGAEA.863505

Meisch C (2000) Freshwater Ostracoda of Western and Central Europe. Spektrum Akademischer Verlag, Heidelberg, 522 pp.

Pham T, Jöst AB, Karanovic I (2021) Phylogenetic position of *Xenoleberis* Kornicker, 1994 within Cylindroleberidinae (Ostracoda : Myodocopa) with descriptions of three new species and one new genus from the Northwestern Pacific Ocean. Marine Biodiversity 51(6): 51–86. https://doi.org/10.1007/s12526-021-01223-7

Rambaut A (2010) FigTree v. 1.3.1. Institute of evolutionary biology, University of Edinburgh, Edinburgh. http://tree.bio.ed.ac.uk/software/figtree/

Rambaut A, Suchard MA, Xie D, Drummond AJ (2014) Tracer v. 1.6. [Retrieved from:] http://beast.bio.ed.ac.uk/Tracer

Schornikov EI (2011a) Loxocaudinae: A new subfamily in the Ostracod family Loxoconchidae. Zoology of Invertebrates 37(3): 185–192. https://doi.org/10.1134/S1063074011030102

Schornikov EI (2011b) *Loxocauda orientalis* sp. n. (Ostracoda: Loxoconchidae) from the Sea of Japan. Zoology of Invertebrates 37(2): 98–103. https://doi.org/10.1134/S1063074011020106

Tanaka H, Yasuhara M, Carlton JT (2018) Transoceanic transport of living marine Ostracoda (Crustacea) on tsunami debris from the 2011 Great East Japan Earthquake. Aquatic Invasions 13(1): 125–135. https://doi.org/10.3391/ai.2018.13.1.10

Tanaka H, Yoo H, Pham TMH, Karanovic I (2021) Two new xylophile cytheroid ostracods (Crustacea) from Kuril-Kamchatka Trench, with remarks on the systematics and phylogeny of the family Keysercytheridae, Limnocytheridae, and Paradoxostomatidae. Arthropod Systematics & Phylogeny 79: 171–188. https://doi.org/10.3897/asp.79.e62282

Tsukagoshi A (1988) Reproductive character displacement in the Ostracod genus *Cythere*. Journal of Crustacean Biology 8(4): 563–575. https://doi.org/10.2307/1548693

Yamada S, Matzke-Karasz R, Martin H (2014) How is a giant sperm ejaculator formed? Development of the Zenker organ the last moult in *Pseudocandona marchica* (Crustacea, Ostracoda, Candonidae). Zoologischer Anzeiger 253(6): 449–460. https://doi.org/10.1016/j.jcz.2014.05.002

Yamaguchi S (2000) Phylogenetic and biogeographical history of the genus *Ishizakiella* (Ostracoda) inferred from mitochondrial COI gene sequences. Journal of Crustacean Biology 20(2): 357–384. https://doi.org/10.1163/20021975-99990047

Yoo H, Karanovic I, Lee W (2012) First record of *Ishizakiella supralittoralis* (Ostracoda, Cytheroidea, Leptocytheridae) from South Korea with a key to species of the genus. Journal of Species Research 1(1): 68–77. https://doi.org/10.12651/JSR.2012.1.1.068

Yoon H, Leitner T (2015) PrimerDesign-M: A multiple-alignment based multiple-primer design tool for walking across variable genomes. Bioinformatics (Oxford, England) 31(9): 1472–1474. https://doi.org/10.1093/bioinformatics/btu832

Supplementary material 1

List of primers and PCR conditions

Authors: Hyunsu Yoo, Pham Thi Minh Huyen, Jinho Chae, Ivana Karanovic

Data type: table (word document)

Link: https://doi.org/10.3897/zookeys.1138.96201.suppl1

Supplementary material 2

List of 18S and COI sequences used for phylogenetic analysis

Authors: Hyunsu Yoo, Pham Thi Minh Huyen, Jinho Chae, Ivana Karanovic

Data type: table (word document)

Link: https://doi.org/10.3897/zookeys.1138.96201.suppl2

Supplementary material 3

Pairwise p-distances among COI sequences of three new Loxocaudinae species

Authors: Hyunsu Yoo, Pham Thi Minh Huyen, Jinho Chae, Ivana Karanovic

Data type: table (word document)

Link: https://doi.org/10.3897/zookeys.1138.96201.suppl3

Supplementary material 4

Pairwise p-distances among 18S sequences of three new Loxocaudinae species

Authors: Hyunsu Yoo, Pham Thi Minh Huyen, Jinho Chae, Ivana Karanovic

Data type: table (word document)

Link: https://doi.org/10.3897/zookeys.1138.96201.suppl4